

Limitations, **I**mprovements, **A**lternatives

for the

Silt **D**ensity **I**ndex

The research presented in this thesis was financed by Vitens and Norit/X-Flow B.V. Part of this work is carried out in the framework of the InnoWATOR subsidy regulation of the Dutch Ministry of Economic Affairs (project IWA08006 ‘Zero Chemical UF/RO System for Desalination’).

Promotion committee

prof.dr. G. van der Steenhoven (chairman)	University of Twente
prof. dr. Ir. W.G.J. van der Meer (promotor)	University of Twente
dr. ir. A.J.B Kemperman (assistant promotor)	University of Twente
prof. dr. Ir. J.C. Schippers	UNESCO-IHE
prof. dr. G Mul	University of Twente
prof. dr. ir. A. Nijmeijer	University of Twente
prof. ir. J.C. van Dijk	Delft University of Technology
prof. dr. MSc. S.K Hong	Korea University (South Korea)

Limitations, Improvements, Alternatives for the Silt Density Index

ISBN: 978-90-365-3157-3

DOI: <http://dx.doi.org/10.3990/1.9789036531573>.

Printed by Gildeprint Drukkerijen

© 2011 Abdulsalam M.M. Al-hadidi, Enschede, The Netherlands

LIMITATIONS, IMPROVEMENTS, ALTERNATIVES
FOR THE
SILT DENSITY INDEX

DISSERTATION

to obtain

the degree of doctor at the University of Twente,

on the authority of the rector magnificus,

prof. Dr. H. Brinksma,

on account of the decision of the graduation committee,

to be publicly defended

on Friday the 25th of February, 2011, at 16:45

by

Abdulsalam Mohammed Mohammed Al-hadidi

born on December 12th, 1975

in Sana'a, Yemen

This thesis has been approved by:

prof. dr. ir. W.G.J. van der Meer (promotor)

dr. ir. A.J.B Kemperman (assistant promotor)

محددات و تطوير و بدائل

لـ

مؤشر كثافة الطمي في أنظمة التناضح العكسي

ألاطروحة مقدمة

لنيل درجة الدكتوراة من جامعة توننا/انسخدي/مملكة هولندا

بالاعتماد على سلطة رئيس الجامعة

prof. Dr. H. Brinksm,

وبالاعتماد على قرار لجنة التخرج

ليتم مناقشتها علنا

يوم الجمعة 25 فبراير 2011

في تمام الساعة 16:45

من قبل المرشح لنيل الدرجة

عبدالسلام محمد محمد الحديد

المولود في 12 ديسمبر 1975

صنعاء/ الجمهورية اليمنية

Contents

Chapter 1	Introduction	1
1.1	Quality control and misguided senses	3
1.2	SDI in desalination	4
1.3	Problem definition	5
1.4	Research objective and scope	5
	1.4.1 Objective	5
	1.4.2 Scope	5
1.5	Scientific and practical relevance	6
1.6	Thesis structure	6
	Reference	8
Chapter 2	Background of fouling indices	9
2.1.	Membranes in water desalination	11
2.2.	Silt Density Index SDI	13
2.3.	Modified fouling index MFI	14
2.4.	Alternatives fouling indices	16
2.5.	Membranes	17
2.6.	Fouling model	17
2.7.	Measured, calculated, normalized and theory SDI values	19
2.8.	Need for a reliable and sample fouling index	20
2.9.	SDI equipment and procedure	20
2.10.	Colloidal suspension as model feed water	22
2.11.	Definition of the reference testing conditions	23
	Reference	25
Chapter 3	The influence of membrane properties on the Silt Density Index	29
3.1	Introduction	31
3.2	Theory and background	32
	3.2.1 Pore size and pore shape	32
	3.2.2 Membrane bulk porosity and surface porosity	33
	3.2.3 Membrane thickness	34
	3.2.4 Membrane surface roughness	34
	3.2.5 Membranes surface charges	35
	3.2.6 Membrane hydrophilicity	35
3.3	Experimental	36
	3.3.1 Membrane Characterization	36
	3.3.2 Filter holders	38
	3.3.3 Model water	39
	3.3.4 Clean water membrane resistance	39
3.4	Results	39
	3.4.1 Variation in the membrane properties of the different membranes	39
	3.4.2 Meeting the ASTM standard	54
	3.4.3 Variation of membrane properties within one batch	55
	3.4.4 SDI of an AKP-15 model solution	57
3.5	Conclusions	60
	References	61

Chapter 4	Silt density index and modified fouling index relation, and effect of pressure, temperature and membrane resistance	63
4.1.	Introduction	65
4.2.	Theory and background	66
4.2.1	Mathematical relation between SDI and MFI _{0.45}	66
4.3.	Results and discussion	69
4.3.1.	Relation between the SDI and concentration of a colloidal suspension	69
4.3.2.	Effect of applied pressure	71
4.3.3.	Effect of temperature	72
4.3.4.	Effect of the membrane resistance	74
4.3.5.	Equivalent MFI _{0.45} value for SDI ₁₅ =3	76
4.3.6.	Normalizing SDI	77
4.4.	Conclusion	79
	References	80
Chapter 5	Effect of testing conditions and filtration mechanisms on SDI	81
5.1	Introduction	83
5.2	Theory and background	84
5.2.1	Fouling model	84
5.3	Results and discussion	85
5.3.1	Mathematical model	85
5.3.2	Calculating SDI	85
5.3.3	Theoretical SDI sensitivity	87
5.3.4	Experimental results	93
5.3.5	Fouling load	95
5.3.6	Shortcomings of the model	96
5.4	Conclusions	98
	References	99
Chapter 6	Sensitivity of SDI for experimental errors	101
6.1	Introduction	103
6.2	Theory and background	103
6.2.1	Sensitivity and Error Analysis	103
6.2.2	Influence of water salinity and acidity	105
6.2.3	Modeling input data	107
6.3	Results and discussion	108
6.3.1	Deviation ± 0.1 at SDI ₀ =3	108
6.3.2	Equipment accuracy and uncertainty	109
6.3.3	Systematic errors	120
6.3.4	Artifacts	122
6.3.5	Personal experience	124
6.3.6	Commercial SDI devices	126
6.3.7	Summary of the effects of accuracy errors on SDI=3	126
6.4	Conclusions	127
	Annex 1	128
	References	130

Chapter 7	SDI normalization and alternatives	131
7.1.	Introduction	133
7.2.	Results and discussion	134
	7.2.1. Determining the sample volume	134
	7.2.2. Calculating SDI when t_f equals 15 minutes	135
	7.2.3. Normalized SDI under a cake filtration mechanism (SDI ⁺)	137
	7.2.4. Normalizing SDI under different fouling mechanisms (SDI ⁺)	142
	7.2.5. Alternatives for SDI	144
7.3.	Conclusions	155
	References	156
Chapter 8	Evaluating the fouling challenge in a UF/RO desalination plant using the SDI, SDI⁺ and MFI	157
8.1	Introduction	159
	8.1.1 Plant description	159
	8.1.2 Raw water characteristics	161
8.2	Results and discussion	162
	8.2.1 Evides UF/RO plant operation	162
	8.2.2 SDI determination using different membranes	165
	8.2.3 Model validation	166
	8.2.4 UF performance under different operation regimes	168
	8.2.5 Fouling potential at different locations in the plant	172
	8.2.6 Reduction in SDI values and MFI _{0.45}	174
	8.2.7 Total resistance at different sampling points	175
8.3	Conclusions	177
	References	178
Chapter 9	Summary & Outlook	181
9.1	Summary English	183
9.2	Outlook	186
9.3	خلاصة	188
9.4	Nederlandse samenvatting	190
	Nomenclature	195
	Acknowledgments شكر و عرفان	197

CHAPTER 1

INTRODUCTION

1.1 Quality control and misguided senses

Quality control is a process that entails the review of a product's quality during its production. The product should be checked precisely, therefore, with the correct tools or tests to guarantee that it is of satisfactory quality. In our daily life, our senses are the physiological capacities within the human body that provide the input of our observations. At one time, human senses controlled the quality of items such as food, perfumes and clothes. Our human senses, however, can be easily confused which results in misguided observations and, consequently, incorrect decisions. For example, our sight cannot determine how tasty food is. Even a mouthwatering dish from a famous restaurant can appear delicious and yet prove to be too salty or spicy once tasted. What we need is to use the right senses under the right conditions to achieve the right objective.

In scientific practice, the tools that control quality can be defined as senses as well. One such tool is the ASTM standard Silt Density Index (SDI) test used to determine pretreated water's fouling potential. The fouling problem in Reverse Osmosis (RO) systems is a particularly good example of this combination of quality control and misguided senses. In most cases, the RO feed passes the pretreatment process such as UF in order to improve the feed quality and decrease its fouling potential. The quality control for an RO feed is usually done by the SDI test. The SDI test, similar to a misguided sense, can mislead the operators or the designers in appreciating the fouling potential of the RO feed. Observations based on SDI values might be attributed to deficiencies of the SDI test, e.g. the test is not corrected for variations in pressure, temperature, and pore size and membrane resistance of the used filters [1-3]. Moreover, the test is not based on any filtration mechanism and as a consequence there is no linear relation between SDI and the particulate matter concentration. Due to the difference between the SDI test and the RO system in terms of the pore size of the used membranes and the hydraulic system (dead-end vs. cross-flow), the SDI value may have no strong correlation with RO fouling. Such misleading values of the SDI have been observed several times in the field; in fact, high SDI values do not necessary mean high RO fouling. The opposite can also be true. Even a low SDI value can indicate that the RO can have a fouling problem [4, 5].

An ideal fouling index should have a linear relationship with the relevant particle concentration in the feed water and should not be sensitive to the testing condition parameters nor the membrane resistance. Predicting RO problems and fouling remains a great challenge. However,

the right way to appreciate the RO feed fouling potential is by operating a pilot plant in the field for a sufficient testing period that “can last for years”.

1.2 SDI in desalination

Reverse osmosis, nanofiltration, ultra- and microfiltration are well-established membrane technologies that are rapidly expanding. Nevertheless, these technologies are still hindered in their smooth operation by fouling phenomena. Fouling due to suspended and colloidal matter (particulate fouling) is one of the reasons for this hindrance [6]. Particulates tend to foul the membrane surface (covering the surface and blocking pores), plug the spacer in spiral-wound elements, and plug the hollow fibre bundles in reverse osmosis and nanofiltration.

Fouling of the membrane itself results in an increase in membrane resistance and, as a result, a higher feed water pressure is required to maintain the capacity of the RO/NF plant. In addition, the salt passage is expected to increase due to enhanced concentration polarization in the fouling layer. Plugging of the spacer initially leads to an unequal flow distribution and, as a result, concentration polarization increases. An increase in head loss across the spacer of a spiral-wound element occurs as well, which might eventually seriously damage the element. To control the effects of fouling, frequent physical and chemical cleaning might be necessary, which negatively affects the robustness of this technology, shortens its lifetime and generates direct and indirect extra operational costs.

Estimating the fouling potential is a prerequisite to successfully controlling membrane fouling. For this purpose, the SDI test is used. The SDI is an empirical test initially developed by Dupont Permasep to characterize the fouling potential of their hollow fine fiber elements [7]. In SDI tests, membranes with pores of 0.45 μm are used to measure the rate of flux decline at constant pressure. The SDI test has been applied worldwide for many years because it is cheap and simple and, hence, executed on a routine basis by operators.

To overcome the SDI deficiencies the MFI0.45 has been developed. This test is based on the occurrence of cake filtration during a substantial part of the test, has a linear relation with particulate matter content, and is corrected for pressure and temperature. However the manual procedure of measuring an MFI0.45 is more complicated and for this reason less suitable for application on a routine basis in practice by the operators. Fully automated equipment, measuring SDI and MFI0.45 at the same time is on the market[8, 9].

1.3 Problem definition

The SDI test is a simple test to perform and does not require professional skills. This test has some disadvantages which make it unreliable. The question of reliability of SDI can be observed several times, for example, when pre-treated seawater passed through a 0.02 μm UF membrane gives a high and unexpected SDI result >3 . Contrary to what one would expect, the pre-treated water does not meet the RO requirement of $\text{SDI} < 3$ [7]. It is difficult to explain the reasons behind this phenomenon. Even with good UF performance, this problem could happen due to the SDI test conditions and the MF membrane used.

The SDI test has another disadvantage that no linear relationship exists between SDI and the colloidal concentration in the water. Besides that, SDI is not based on a filtration model, nor is it corrected for temperature. Many parameters play a fundamental role in determining the results of a SDI test.

1.4 Research objective and scope

1.4.1 Objective

The objective of this research is to investigate the limits of the SDI test, improve its protocol and propose an SDI test alternative to test the UF performance. This includes:

- Obtaining a very clear picture of the deficiencies of the current SDI test. This includes the formulation of restrictive conditions with regard to guaranteeing the performance of the UF plants, e.g. testing condition parameters, type of membranes used for the test etc.
- Improving the protocol for measuring SDI and excluding deficiencies in the test, e.g. those due to variations in membrane characteristics/performance and artifacts. In addition, creating international support so that this protocol becomes accepted worldwide.
- Obtaining sufficient evidence to propose an alternative test for judging the performance of UF installations and predicting the rate of fouling in RO/NF membrane plants due to particles

1.4.2 Scope

The scope of this thesis is limited to the study of the variation of the MF membranes used in the SDI test. Eight MF commercial membranes with pore size 0.45 μm were chosen according to

the ASTM-D4189-95 standard (reproved in 2002). The new ASTM-D4189-07 standard from 2008 was considered in this work. The chosen membranes were made from different polymers. The variation of the membrane characteristics in SDI test was studied and the following parameters were measured: pore size and pore shape, pore size distribution, roughness, Zeta potential, hydrophilicity, surface porosity and bulk porosity, membrane resistance and the variations in characteristics between batches and within batches of membranes. The bubble point is not considered due to the unclear description for this property in the ASTM standard. In this work, the SDI was modeled under four different fouling mechanisms. The effect of cake compression is out of the scope for this work, as are the influences of the testing condition parameters on the membrane properties. By assuming cake filtration and 100 % particle retention, a mathematical relationship between the SDI and the MFI_{0.45} was built.

1.5 Scientific and practical relevance

This work contributes to building a better understanding of the theoretical and practical background for the SDI based on different fouling mechanisms. The influence of the membrane properties and testing condition parameters are demonstrated mathematically and experimentally. Different tools and charts were proposed in this work to normalize the SDI for the influence of the membrane resistance, temperature and applied pressure. The normalized values (SDI⁺) can be then compared for different water qualities tested under different conditions. A new fouling index, named the Volume Based Silt Density Index (SDI_v), was developed within this work. The SDI_v is a more reliable fouling index due to the fact that it is naturalized to the effects of the membrane resistance and the testing parameters.

1.6 Thesis structure

Chapter2: Provides the theoretical background information regarding RO fouling and fouling indices. The experimental setup used during this work is described.

Chapter3: Studies the variation in the membrane properties of eight MF membranes available in the market made from different materials and within one batch of membrane. It describes the influence of the membrane properties on the SDI.

Chapter 4: Deriving a mathematical relationship between SDI and MFI_{0.45}. This mathematical relation is used to study the influence of the membrane resistance and the testing parameters on SDI assuming cake filtration. The theoretical model was verified experimentally in this chapter.

Chapter 5: Mathematically investigates the influences of the membrane resistance and the testing conditions on SDI assuming different filtration mechanisms. Experimentally the effect of the membrane resistance on SDI was verified.

Chapter 6: Mathematically and experimentally studies the sensitivity of SDI for errors due to the equipments accuracy, systematic error, artifacts and human experience.

Chapter 7: Normalization formula, charts and tools are developed. An alternative fouling test SDI_v is proposed in this chapter.

Chapter 8: Presents the SDI/MFI0.45 results obtained in a case study at the UF/RO desalination plant.

Reference

- [1] A. Alhadidi, A.J.B. Kemperman, J.C. Schippers, M. Wessling, W.G.J. van der Meer, The influence of membrane properties on the Silt Density Index, To be submitted (2010).
- [2] A. Alhadidi, B. Blankert, A.J.B. Kemperman, J.C. Schippers, M. Wessling, W.G.J. van der Meer, Sensitivity of SDI for the error in measuring the testing parameters, To be submitted (2010).
- [3] A. Alhadidi, A.J.B. Kemperman, J.C. Schippers, M. Wessling, W.G.J. van der Meer, Silt density index and modified fouling index relation, and effect of pressure, temperature and membrane resistance, Desalination, In press (2010).
- [4] E.A. Moelwyn-Hughes, Physical Chemistry, 2ed ed., Pregamon Press Ltd., London, 1965.
- [5] N.R.G. Walton, Some observations on the considerable variability of silt density index results due to equipment, filter and operator variables, Desalination, 61 (1987) 201-210.
- [6] S. Lee, J. Cho, M. Elimelech, Combined influence of natural organic matter (NOM) and colloidal particles on nanofiltration membrane fouling, J. Membr. Sci., 262 (2005) 27-41.
- [7] R. Nagel, Seawater desalination with polyamide hollow fiber modules at DROP, Desalination, 63 (1987) 225-246.
- [8] M. Mulder, Basic principles of membrane technology, 2 ed., Kluwer Academic Publishers, Dordrecht, The Netherlands, 2003.
- [9] K. Hong, S. Lee, S. Choi, Y. Yu, S. Hong, J. Moon, J. Sohn, J. Yang, Assessment of various membrane fouling indexes under seawater conditions, Desalination, 247 (2009) 247-259.

CHAPTER 2

BACKGROUND OF FOULING INDICES

2.1. Membranes in water desalination

Increasing water demand is a global problem. Only 2.5 % (35 million km³) of the water on our planet is fresh water, of which two-thirds is unavailable for human consumption (glaciers, ice, snow, permafrost) [1]. In many parts of the world local demand is exceeding conventional resources. It is estimated that in 2025 1,800 million people live in countries with absolute water scarcity. Two-thirds of the population will be under severe stress conditions concerning water supply [2]. More economical use of water, reducing distribution losses and increased use of recycle water can help alleviating this problem. If there is still a shortfall, desalination of seawater or brackish water is the an important technology to provide sufficient fresh water.

Sea water contains a high concentration of total dissolved solids (15,000 to 50,000 mg/L TDS), while the TDS in brackish water is lower ranging from 1,500 to 15,000 mg/L TDS [3]. Water with a TDS of 1,000 mg/L generally is unpalatable to most people due to the high sodium and chloride contents. By desalination, salts are removed from sea and brackish water, lowering the TDS to potable water quality 500 mg/L [4]. During the last 50 years there has been a steady growth of desalination plants. The first interest in membrane filtration for drinking water production started in the 1980s [5]. Most of this growth has been in the Middle East and is based on distillation technology and reverse osmosis technology using membranes (RO) [3].

The principles of membrane filtration for the separation of liquids had been known for long time, and the introduction of the asymmetric membrane in 1961 was the most important impulse for the development of membrane technology. Since 1961, research has resulted in many new and improved membrane materials. Duo to this development membrane filtration has become one of the most significant modern separation technologies, also for water treatment and purification. There are very few drinking water contaminates that cannot be removed economically by membrane processes and many examples of the use of membranes have been described in textbooks on water treatment.

Membrane processes with the greatest immediate application potential to water treatment are reverse osmosis (RO), nanofiltration (NF), electro-dialysis (ED), ultrafiltration (UF) and microfiltration (MF). The size range of membrane processes is shown in Figure 2.1.

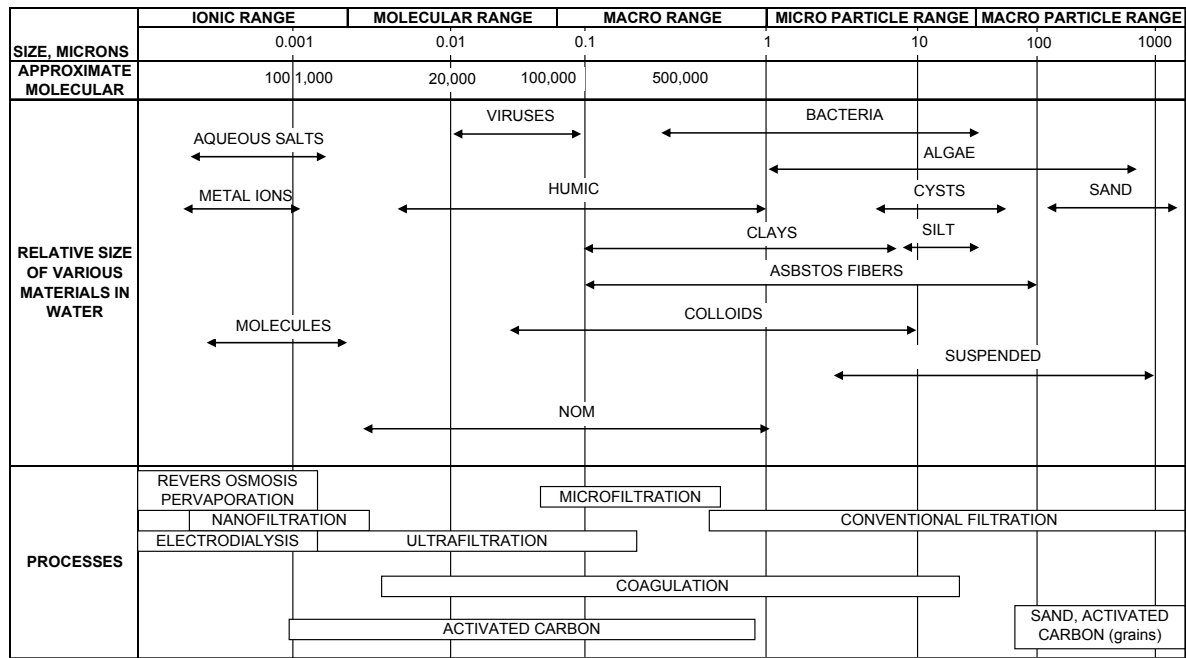


Figure 2.1. Size range of solutes and membrane processes (redrawn from [6]).

An alternative for conventional desalination methods like distillation and ion exchange is reverse osmosis, which is used to separate dissolved solutes from brackish water and seawater. RO is also capable of a very high rejection of microorganisms and synthetic organic compounds (SOCs). RO processes show a significant rejection for microorganisms, SOCs and inorganic compounds (IOCs), because the exclusion limit of this membrane is so small that many of these compounds cannot pass or their permeation is diffusion limit. RO is more energetically favorable compared to thermal distillation as no phase transformation is required, but only electrical energy to drive the high pressure pumps to overcome the osmotic pressure of the seawater.

Fouling is a major problem facing salt separation from water by reverse osmosis systems. Several types of fouling in RO can occur in the membrane system, e.g. inorganic fouling or scaling, particulate and colloidal fouling, organic fouling and finally biological fouling or biofouling.

Cleaning frequency, pretreatment requirement, operating condition, cost and system performance are affected by membrane fouling.

Ultrafiltration often is applied as pre-treatment step for reverse osmosis. The first milestone in UF technology began in the mid-1960s. UF became an industrial process in the late 1960s when user realized the importancy membrane fouling management [4]. Hollow fiber ultrafiltration is widely accepted today for municipal water treatment applications including production of drinking water from surface water and water reuse applications. UF is also used for industrial water treatment including pretreatment to spiral-wound reverse osmosis and nanofiltration

membranes for production of high purity water, and coupled in several cases with coagulation [7-11]. Because of the increasing awareness of the need for adequate pretreatment, there has been significant interest in UF as pretreatment for RO for municipal applications in brackish and seawater desalination plants. Depending on the feed water quality, extensive pretreatment may be needed to provide water that is suitable for RO feed, because the RO membrane is susceptible to colloidal plugging. UF provides excellent pretreatment to RO because it can consistently deliver filtrate with very low turbidity, regardless of feed water quality. Conventional pretreatment such as sand filters may not reliably produce consistent, high quality water, especially when the feed water changes in composition and properties. In addition, compared to conventional water treatment technologies, UF systems require less space and often have lower operating costs.

Estimating the fouling potential of RO feed water is a prerequisite to control membrane fouling successfully and to evaluate the quality of the pretreatment. For this purpose two different tests are mostly used in the field, i.e. the Silt Density Index (SDI) and the Modified Fouling Index (MFI0.45) [12]. In both tests microfiltration membranes with pores of 0.45 μm are used and measure the rate of flux decline at constant pressure. In principle these tests can be done by making use of the same equipment [13-14].

2.2. Silt Density Index SDI

To determine the SDI, the rate of plugging of a membrane filter with pores of 0.45 μm at 207 kPa is measured. The measurement is done as follows:

- a) The time t_1 is determined which is required to filter the first 500 mL.
- b) 15 minutes (t_f) after the start of this measurement time t_2 is measured which is required to filter 500 mL.
- c) The index is calculated with the following formula:

$$SDI = \frac{100\%}{t_f} \left(1 - \frac{t_1}{t_2} \right) = \frac{\%P}{t_f} \quad (2.1)$$

Where SDI is the Silt Density Index (%/min), t_f is the elapsed filtration time (min) after the start of collecting the first 500 mL, t_1 is the time required to collect the first 500 mL and t_2 is the time required to collect the second 500 mL after 15 minutes (or less). If the plugging ratio %P is exceeding 75 %, a shorter period t_f has to be taken e.g. 10, 5 or 2 minutes. By rearranging the

equation it can be shown easily that the SDI measures the decline in filtration rate expressed as “percentage” per minute [15].

The SDI is an empirical test initially developed by Dupont Permasep to characterize the fouling potential of their hollow fine fiber RO elements [16]. A pretreatment method such as UF has to guarantee an fine hollow fiber RO feed water with an SDI <3. An SDI test is one of the criteria in designing new desalination plants and has to be performed on the RO feed water [17-18]. The SDI is a useful tool to monitor the efficiency of the RO pretreatment in removing the particles presents in the raw water [19].

Manufacturers of spiral wound RO membrane recommend that the SDI should not exceed 4 or 5 and set limits of membrane productivity depending on the SDI [20]. Different RO manufacturers use different limits for the feed water SDI, depending on their experiences and the RO membrane instructions [21-24]:

- Toyobo recommended for all theirs RO products (HR, HM, HB, HJ, HL series) a maximum SDI 4;
- DOW (RO FILMTEC™ Membranes) recommended a maximum SDI 5;
- Hydranautics (ESPA, LFC, ESNA1LF, SWC, and CPA) recommended maximum SDI 5. For ESNA1LF2 a maximum SDI 4 is recommended;
- Koch recommended a maximum SDI 5 for all theirs RO products (TFC: SS, HF, HR, XR, ULP and ROGA HR).

In the most recent ASTM International ‘Standard Test Method for Silt Density Index (SDI) of Water’ [25] the following membrane properties are recommended to be used in the test:

Membrane white hydrophilic, mixed cellulose nitrate (50–75 %) and cellulose acetate (MCE); Mean Pore Size 0.45 μm . Diameter 47 mm nominal, plain; size 25 mm or 90 mm diameter also can be used. Thickness is between 115 and 180 μm . Pure Water Flow Time 25–50 seconds for 500 mL under applied pressure difference 91.4–94.7 kPa. Bubble Point 179–248 kPa; Use only filters that are packaged in the same orientation.

2.3. Modified fouling index MFI

The Modified Fouling Index (MFI_{0.45}), was derived by Schippers and Verdouw in 1980 from the SDI [26] by assuming a cake filtration mechanism. It aimed at measuring the fouling potential of feed water for reverse osmosis installations. For determination of the MFI_{0.45}, the flow through the membrane filter is measured as a function of time.

These data are processed with Eqn. (2.2) which follows from the theory of cake filtration:

$$\frac{t}{V} = \frac{\mu \cdot R_M}{dP \cdot A_M} + \frac{\mu \cdot I}{2 \cdot \Delta P \cdot A_M^2} \cdot V \quad (2.2)$$

Where t is the time [s], V is the accumulated filtrate volume [L or m³], μ is the water viscosity [Pa.s], R_M is the clean membrane resistance [m⁻¹], dP is the applied pressure [Pa], A_M is the membrane area [m²], and I is the fouling potential index [m⁻²].

The MFI0.45 is derived from the slope in the relation of t/V versus V , as given by Eqn. (2.3):

$$tg\alpha = \frac{\mu \cdot I}{2 \cdot dP \cdot A_M^2} \quad (2.3)$$

This slope $tg\alpha$ is by definition equal to MFI0.45 when it has its minimum and under the conditions that the temperature is 20 °C, the pressure is 30 psi (207 kPa) and the membrane surface area equals 13.8×10⁻⁴ m² (47 mm diameter). The MFI0.45 is corrected for T and P using Eqn. (2.4) and is therefore independent of temperature and pressure:

$$MFI = tg\alpha \times \frac{\mu_{20}}{\mu} \times \frac{dP}{dP_o} \times \left(\frac{A_M}{A_{M_o}} \right)^2 \quad (2.4)$$

Where μ_{20} is the water viscosity at 20 °C [Pa.s], A_{M_o} is the reference membrane area 13.8×10⁻⁴ [m²] and dP_o is the reference surface area of membrane 2.07×10⁵[Pa]. The water viscosity at a temperature T [°C] is calculated using the following empirical equation [27-29]

$$\mu = 0.497 \times (T + 42.5)^{-1.5} \quad (2.5)$$

Where T is the temperature [°C].

The minimum value for $tg\alpha$ is by definition MFI0.45, since at the start the filtration mechanism is frequently pore blocking resulting in a high slope. Subsequently cake filtration starts and becomes gradually the governing mechanism until cake compression starts, resulting in an increasing slope. Figure 2.2(a) shows how $tg\alpha$ is calculated out of the t/V versus V curve. Figure 2.2(b) shows that the fouling index $tg\alpha$ is dependent on time, and that the minimum value of $tg\alpha$ equals the MFI . The MFI0.45 is expressed in s/L² to get values which are in the same order of magnitude as SDI.

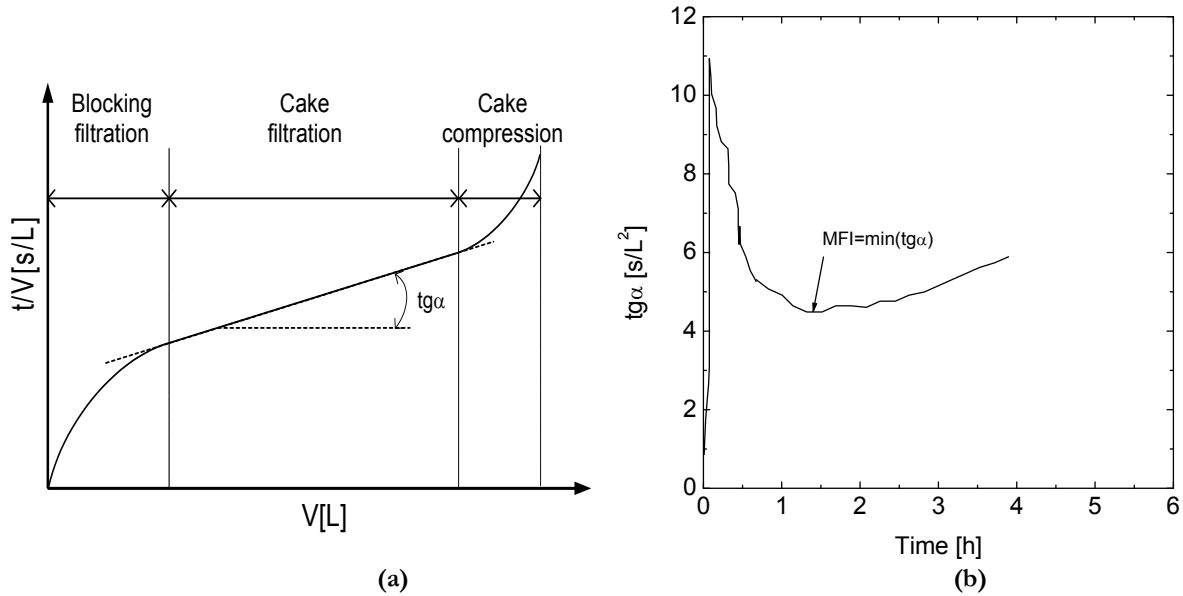


Figure 2.2. (a) $\tan \alpha$ calculated out of the t/V vs. V curve, (b) fouling potential index I curve. Redrawn from [30].

Measurements needed for determining the MFI0.45 are less simple than for the SDI test, which is the reason why MFI0.45 measurements are usually not done by operators in the field.

2.4. Alternatives fouling indices

Since the 0.45 μm MF membrane used for SDI and MFI0.45 determination is unable to capture particles smaller than 0.45 μm , new fouling indices were developed based on the MFI definition using membranes with smaller pore sizes (MFI-UF, MFI-NF), different filtration systems (MFI-UF constant pressure, MFI-UF constant flux) and different hydraulic systems (dead-end MFI, crossflow Sampler CFS-MFI_{UF}) [31-34]. However, the manual procedures of measuring those alternatives indices are more complicated comparing to SDI. For this reason MFI-UF, MFI-NF and CFS-MFI_{UF} are less suitable for application on a routine basis in practice. MFI-UF can be used for predicting the RO fouling by estimating the deposit factor [31]. However, the salinity of the RO concentrate is affecting the particle nature and by that the MFI-UF results. Moreover, concentration polarization is a limiting parameter for the MFI-NF productivity. This lead to the search for other approaches that better estimate the membrane fouling potential [14, 35]

2.5. Membranes

Eight different 0.45 μm MF membranes were used in this study, including membrane filters meeting the ASTM standards Table 2.1.

Table 2.1 Microfiltration membranes used in this work. Pore size as given by manufacturer. R_M is the measured average clean water resistance [36]

Code	Material	Nominal Pore size [μm]	Manufacture	Manufacture Code
M1	PVDF	0.45	Millipore	HVLP
M2	PTFE	0.45	Millipore	FHUP
M3	Acrylic Polymer	0.45	Pall	Versapor®
M4	Nitro Cellulose*	0.45	Millipore	HAWP
M5	Nylon6,6	0.45	Pall	NBS5BXFB05
M6	Cellulose Acetate*	0.45	Sartorius	11106
M7	Cellulose Acetate*	0.45	SterliTech	CA045
M8	Polycarbonate	0.45	Whatman	Nuclepore® (PC)

* ASTM standard material.

2.6. Fouling model

Hermia [37] described four empirical models that corresponded to four basic types of fouling: complete blocking, intermediate blocking, standard blocking and cake layer formation. These empirical models are known as the blocking laws:

- a. **Cake filtration:** In this case, a cake layer forms on the membrane surface. As in the case of the pore blocking model, solute particles are larger than the membrane pores and do not penetrate inside them.
- b. **Intermediate blocking:** As well as the complete blocking model (see d), this model assumes that the particles block the pore when it approaches an open membrane pore. The intermediate blocking model is less restrictive because it states that some particles may deposit on other particles previously settled. This means that not every particle that arrives to the membrane surface blocks a complete membrane pore. This model examines the probability of a particle to block a membrane pore.
- c. **Standard blocking:** This model states that particles deposit at the pore walls. As a result, the volume of membrane pores decreases proportionally to the filtered permeate volume.

- d. **Complete blocking:** According to the filtration model, every particle that reaches the membrane surface completely blocks the entrance of the membrane pores. Moreover, a particle never settles on another particle that has previously deposited on the membrane surface.

The parameters considered by these models have a physical meaning and contribute to the comprehension of the mechanisms of membrane fouling. These models were developed for dead-end filtration and are based on constant pressure filtration laws. The four fouling models are summarized in Table 2.2, where: [11]

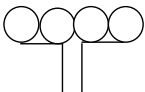
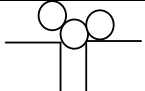
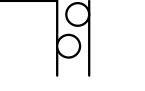
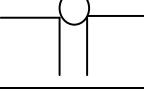
w_R : represents the specific cake resistance and is defined as the volume of feed water per unit area for which the cake resistance is equal to the membrane resistance.

w_A : represents the pore blocking potential and is defined as the volume of feed water per unit area that contains enough particles to block the pores completely.

w_V : represents the pore filling potential and is defined as the amount of feed water per unit area that contains enough particles to fill the pores completely.

Based on the definitions given above, the fouling parameters $w_{(R,A,V)}$, are inversely proportional to the particle concentration. For example, one will need half amount of feed water if the amount of particles in the feed water is doubled to block all the pores or to build up a cake layer.

Table 2.2 Definition of the four fouling mechanisms. The parameters C and m are depending on the fouling mechanisms and particle concentration. The total resistance R is a function of filtration state w [11].

Mechanism	Definitions	m	C	Resistance equation $R(w)$
Cake filtration		0	$\frac{R_M}{w_R}$	$R_M \left(1 + \frac{w}{w_R} \right)$
Intermediate blocking		1	$\frac{1}{w_A}$	$R_M \cdot e^{\frac{w}{w_A}}$
Standard blocking		1.5	$\frac{2}{w_V R_M^{0.5}}$	$R_M \left(1 - \frac{w}{w_V} \right)^{-2}$
Complete blocking		2	$\frac{1}{w_A R_M}$	$R_M \left(1 - \frac{w}{w_A} \right)^{-1}$

2.7. Measured, calculated, normalized and theory SDI values

During the SDI test, the filtration data t and V will be collected. The times t_1 and t_2 for collecting the samples V_1 and V_2 will be measured. Furthermore, the testing condition parameters (T, dP, R_M) will be recorded during the SDI test. The *SDI-measured* will be determined using Eqn.(2.1). The fouling potential index I will be estimated from the curve of t/V versus V . The *SDI-calculated* then can be determined using the fouling model which will be developed in section 4.2.1. The fouling potential index I will be used to calculate *SDI-normalized* using the fouling model or specially developed charts. To determine the theoretical SDI values for different particle concentrations, the following procedure was applied. Assuming that cake filtration is the dominating fouling mechanism during the SDI measurements, w_R values obtained from the experimental data were plotted versus the particle concentration. Theoretically, the relation between w_R and the particle concentration is linear. However, the experimental w_R values show some deviations from this linearity. Therefore, a linear equation was fitted to the experimental data and w_R values were recalculated for each concentration (w_R theory') using this linear least square fitting equation. Subsequently, the ' w_R theory' values were used to determine the *SDI-theory*. Figure 2.3 schematically shows the procedure to determine the four SDI values. More details will be concluded in Chapters 4 and 5.

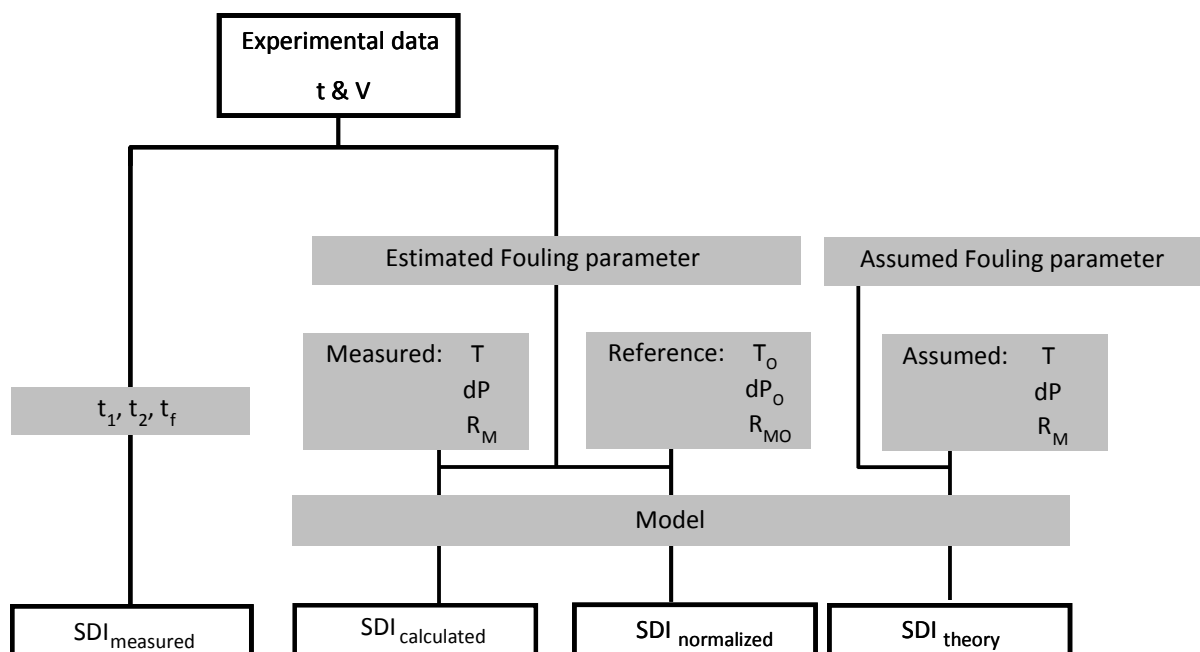


Figure 2.3. Diagram showing the calculation of the measured, calculated, normalized and theory SDI values.

2.8. Need for a reliable and sample fouling index

Although the SDI test is widely used, there is growing doubt about the significance of the SDI test as a predictive tool for RO membrane fouling [20, 26, 38]. These doubts consist of two factors: 1) the relation between the SDI value and the performance of the RO unit, and 2) the reproducibility and accuracy of the SDI test.

Due to the inability to capture fine colloids, fouling rates predicted from the SDI and MFI0.45 as measured for RO feed water were far too low [30, 33]. It was, therefore, hypothesized that smaller colloidal particles were responsible for the observed flux decline rates in RO [34]. RO, using membranes with no distinct pores, operates with a cross-flow system and uses spacers to separate the membranes whereas the SDI and MFI0.45 tests use a 0.45 μm MF membrane in a dead-end filtration experiment. Particles much smaller than 0.45 μm easily can foul the RO membrane and the spacers. Since the 0.45 μm MF membrane used for SDI determination is unable to capture particles smaller than 0.45 μm , the SDI value may have no strong correlation with RO fouling. The SDI deficiencies affect the reliability, reproducibility, and/or operational usefulness of the SDI test.

Besides the colloid nature and the water properties [20, 39-41], other factors influence the measured SDI value, as there are [26, 42]:

- MF membrane properties such as pore size, porosity, hydrophilicity, zeta potential and surface roughness [43-49],
- Testing conditions like feed temperature and applied pressure [49-53];
- Artifacts parameters such as air bubbles in the set-up, equipment material suitable for high salinity water and shear force affecting the physical particle properties;
- Operator errors.

Despite its deficiencies, the SDI remains the most applied tool to simulate and predict the fouling in RO installations [54]. Therefore, in the most recent standard (D 4189-07) ASTM mentioned that SDI is not applicable for the effluents from most RO and UF systems.

2.9. SDI equipment and procedure

The procedure for measuring the SDI has been standardized by the ASTM [25]. The apparatus was assembled as shown in Figure 2.4. The applied pressure was maintained either by the feed pump in the automatic setup or by pressurized N_2 in the manual set-up. The feed pump

was automatically controlled to provide a constant feed pressure of 207 ± 7 kPa (30 ± 1 psi). Before installing the membrane filter, the water to be tested was flushed through the apparatus in order to remove entrained contaminants. The water temperature was measured and kept constant throughout the test. A $0.45 \mu\text{m}$ MF membrane filter (25 mm in diameter) was placed on the support plate of the holder. The membrane filter was touched only with tweezers to avoid puncturing or contamination. It was checked whether the O-ring was in a good condition and properly placed. The trapped air was bleed out through a relief air valve in the filter holder. The flow rate was measured using the flow meter (connected to a PC). The time to collect the first sample t_1 and the second sample t_2 was determined experimentally using the collected filtration data (time vs. volume). The SDI was calculated using Eqn (2.1).

From the raw filtration data obtained from the SDI setup, the resistance and filtered volume were calculated. Subsequently C , m and R_M were determined by least-squares curve fitting [55], minimizing the following error criterion:

$$\min \sum_{i=0}^n (f(w_i, R_M, C, m) - R_i)^2 \quad (2.6)$$

Where n is the number of data points, w_i is the accumulated filtrated volume per unit area, C is the scaling factor proportional to the foulants concentration, m is the Fouling mechanism parameter R_i is the total resistance at data point i .

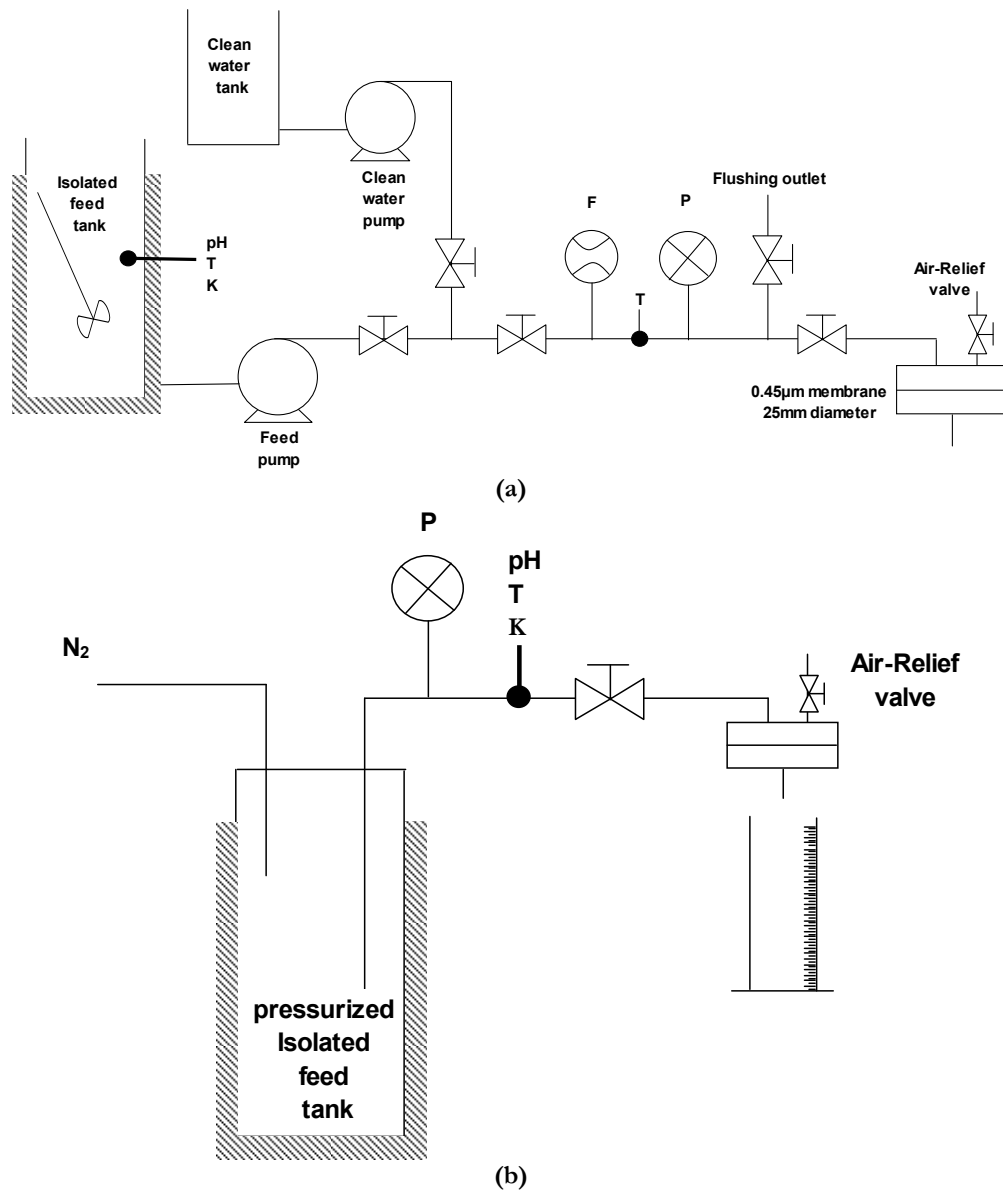


Figure 2.4. Flowsheet of the SDI setup. (a) Automated SDI setup using a feed gear pump. (b) Manual SDI setup using a feed tank pressurized with N_2 . Feed tank is shown. pH, Temperature (T) and conductivity (K) are measured in the feed tank. Pressure (P), flow rate (F) and temperature (T) are measured in the feed line.

2.10. Colloidal suspension as model feed water

To prepare the model feed water, hydrophilic α -Alumina particles (AKP-15, Sumitomo Chemical, Tokyo, Japan) with a core particle size of $0.6 \mu\text{m}$ and an isoelectric point (IEP) at pH 9 [56] were used. The AKP-15 particle has a narrow size distribution curve. The feed solution was prepared by adding 4 mg/L AKP-15 to demineralized water, purified by an Ultra-Pure system from Millipore (Synergy SYNS). The solution was well mixed using a mechanical mixer in the feed tank.

Malvern Instruments' Zetasizer range with Dynamic Light Scattering (DLS) was used to measure the α -Alumina particle size distribution. To avoid the agglomeration of the particles, the pH was adjusted to 4.1 by adding HNO_3 .

2.11. Definition of the reference testing conditions

Membrane resistance, feed temperature, applied pressure and membrane area are the main testing parameters in this study. In order to study the effect of each parameter independently, the following reference testing parameters were defined (Table 2.3).

- a. The membrane resistance R_M :

In the updated version of the ASTM standard 2007, the membrane filter was specified. The pure water flow time should be 25-50 s/500mL under applied pressure 91.4-94.7kPa. These water flows imply the membrane resistance R_M should be in the range $0.86 \times 10^{10} - 1.72 \times 10^{10} \text{ m}^{-1}$. An average value $R_{MO} = 1.29 \times 10^{10} \text{ m}^{-1}$ is defined as the reference membrane resistance.

- b. Feed temperature T :

The lab temperature (20 °C) was taken as the reference feed temperature T_O .

- c. Applied pressure dP :

The standard pressure to be applied (207 kPa) was defined in this study as the reference pressure dP_O .

- d. Membrane area A_M :

A membrane with diameter 47 mm is the standard SDI membrane size, and therefore the reference membrane area A_{MO} is equal to $13.8 \times 10^{-4} \text{ m}^2$

- e. SDI:

The commonly applied SDI limitation for the RO feed water $\text{SDI}_O = 3$ was defined as a target value.

- f. $w_{R,A,V}$

The fouling potentials (cake filtration, intermediate, standard and complete blocking) of the feed water correspond to were calculated using the previously defined R_{MO} , T_O , dP_O , A_{MO} and SDI_O .

Table 2.3.

Reference parameters.	
Parameter	Reference value
R_{MO}	$1.29 \times 10^{10} \text{ m}^{-1}$
T_O	20 °C
dP_O	207 kPa
A_{MO}	$13.4 \times 10^{-4} \text{ m}^2$
SDI _O	3
w_{RO} (Cake filtration)	12.2
w_{AO} (Intermediate pore blocking)	17.5
w_{VO} (Standard pore blocking)	40.5
w_{AO} (Complete pore blocking)	24.3

Reference

- [1] M. Black, J. King, *The Atlas of Water*, 2 ed., University of California Press, Berkeley, Los Angeles, 2010.
- [2] WHO, World Health Organization: 10 facts about water scarcity, <http://www.who.int/features/factfiles/water/en/>, 2010 (March 2009).
- [3] C. Fritzmann, J. Löwenberg, T. Wintgens, T. Melin, State-of-the-art of reverse osmosis desalination, *Desalination*, 216 (2007) 1-76.
- [4] H.K. Lonsdale, The growth of membrane technology, *J. Membr. Sci.*, 10 (1982) 81-181.
- [5] J. Crittenden, R. Trussell, D. Hand, K. Howe, G. Tchobanoglous, *Water treatment: Principles and Design*, 2ed edition ed., Jhon Wiley & Sons, New Jersey, 2005.
- [6] L.D. Benefield, J.M. Morgan, J.S. Taylor, M. Wiesner, *Water quality and treatment*, 5th edition ed., McGraw-Hill, Boston, 1999.
- [7] F. Knops, S. van Hoof, H. Futselaar, L. Broens, Economic evaluation of a new ultrafiltration membrane for pretreatment of seawater reverse osmosis, *Desalination*, 203 (2007) 300-306.
- [8] J.-J. Qin, M.H. Oo, H. Lee, R. Kolkman, Dead-end ultrafiltration for pretreatment of RO in reclamation of municipal wastewater effluent, *J. Membr. Sci.*, 243 (2004) 107-113.
- [9] S.C.J.M. van Hoof, A. Hashim, A.J. Kordes, The effect of ultrafiltration as pretreatment to reverse osmosis in wastewater reuse and seawater desalination applications, *Desalination*, 124 (1999) 231-242.
- [10] N. Uzal, L. Yilmaz, U. Yetis, Microfiltration/ultrafiltration as pretreatment for reclamation of rinsing waters of indigo dyeing, *Desalination*, 240 (2009) 198-208.
- [11] B. Blankert, B.H.L. Betlem, B. Roffel, Dynamic optimization of a dead-end filtration trajectory: Blocking filtration laws, *J. Membr. Sci.*, 285 (2006) 90-95.
- [12] M.H.V. Mulder, *polrization phenomena and membrane fouling in membrane separation technology, principles and applications*, Elsevier, Amstrdam, 1993.
- [13] M. Mulder, *Basic principles of membrane technology*, 2 ed., Kluwer Academic Publishers, Dordrecht, The Netherlands, 2003.
- [14] K. Hong, S. Lee, S. Choi, Y. Yu, S. Hong, J. Moon, J. Sohn, J. Yang, Assessment of various membrane fouling indexes under seawater conditions, *Desalination*, 247 (2009) 247-259.
- [15] J.C. Schippers, *Course on Pre-treatment, membrane fouling and scaling*, Genoa, 2010.
- [16] R. Nagel, Seawater desalination with polyamide hollow fiber modules at DROP, *Desalination*, 63 (1987) 225-246.
- [17] D. Vial, G. Doussau, The use of microfiltration membranes for seawater pre-treatment prior to reverse osmosis membranes, *Desalination*, 153 (2002) 141-147.
- [18] D. Vial, G. Doussau, R. Galindob, Comparison of three pilot studies using Microza membranes for Mediterranean seawater pre-treatment, *Desalination*, 156 (2003) 43-50.
- [19] S. Lueck, Reducing RO Operating Costs with Automated Monitoring Technology, in: *International Water Conference, IWC*, Pittsburgh, 1999.
- [20] S.G. Yiantsios, A.J. Karabelas, An assessment of the Silt Density Index based on RO membrane colloidal fouling experiments with iron oxide particles, *Desalination*, 151 (2003) 229-238.
- [21] Toyobo, HR, HM, HB and HL Series Seawater desalination, <http://www.toyobo.co.jp/e/seihin/ro/index.htm>, (2010).
- [22] Koch, RO Spiral Elements, http://www.kochmembrane.com/support_ro_lit.html (2010).
- [23] Dow, FILMTEC SW Seawater Reverse Osmosis Element, <http://www.dowwaterandprocess.com/products/ronf.htm>, (2010).
- [24] Hydranautics, ESPA, LFC, CPA ESNA and SWC RO Seawater Element, <http://www.membranes.com/pdf/HYDRABrochure.pdf>, (2010).

- [25] ASTM Standard (D 4189 – 07): Standard Test Method for Silt Density Index (SDI) of Water, D19.08 on Membranes and Ion Exchange Materials, (2007).
- [26] J.C. Schippers, J. Verdouw, The modified fouling index, a method of determining the fouling characteristics of water, *Desalination*, 32 (1980) 137-148.
- [27] W.J.C.v.d. Ven, Towards optimal saving in membrane operation, The development of process inspection and feedwater characterization tools, in: MTG/TNW, University of Twente, Enschede, 2008.
- [28] J.H. Roorda, J.H.J.M.v.d. Graaf, New parameter for monitoring fouling during ultrafiltration of WWTP effluent, IWA Publishing, 2001.
- [29] P. van den Brink, A. Zwijnenburg, G. Smith, H. Temmink, M. van Loosdrecht, Effect of free calcium concentration and ionic strength on alginate fouling in cross-flow membrane filtration, *J. Membr. Sci.*, 345 (2009) 207-216.
- [30] S.F.E. Boerlage, M.D. Kennedy, M.P. Aniye, E.M. Abogrean, G. Galjaard, J.C. Schippers, Monitoring particulate fouling in membrane systems, *Desalination*, 118 (1998) 131-142.
- [31] S.F.E. Boerlage, M. Kennedy, M.P. Aniye, J.C. Schippers, Applications of the MFI-UF to measure and predict particulate fouling in RO systems, *J. Membr. Sci.*, 220 (2003) 97-116.
- [32] S.F.E. Boerlage, M.D. Kennedy, M.P. Aniye, E. Abogrean, Z.S. Tarawneh, J.C. Schippers, The MFI-UF as a water quality test and monitor, *J. Membr. Sci.*, 211 (2003) 271-289.
- [33] L.N. Sim, Y. Ye, V. Chen, A.G. Fane, Crossflow Sampler Modified Fouling Index Ultrafiltration (CFS-MFIUF)--An alternative Fouling Index, *J. Membr. Sci.*, 360 (2010) 174-184.
- [34] S. Khirani, R. Ben Aim, M.-H. Manero, Improving the measurement of the Modified Fouling Index using nanofiltration membranes (NF-MFI), *Desalination*, 191 (2006) 1-7.
- [35] J.-S. Choi, T.-M. Hwang, S. Lee, S. Hong, A systematic approach to determine the fouling index for a RO/NF membrane process, *Desalination*, 238 (2009) 117-127.
- [36] A. Alhadidi, A.J.B. Kemperman, J.C. Schippers, M. Wessling, W.G.J. van der Meer, The influence of membrane properties on the Silt Density Index, To be submitted (2010).
- [37] J. Hermia, Constant pressure blocking filtration Laws - Application to power-low non-newtonian fluids, *Trans IChemE*, 60 (1982) 183-187.
- [38] A. Mosset, V. Bonnelye, M. Petry, M.A. Sanz, The sensitivity of SDI analysis: from RO feed water to raw water, *Desalination*, 222 (2008) 17-23.
- [39] Y. Zhao, J. Taylor, S. Hong, Combined influence of membrane surface properties and feed water qualities on RO/NF mass transfer, a pilot study, *Water Research*, 39 (2005) 1233-1244.
- [40] S.G. Yiantsios, D. Sioutopoulos, A.J. Karabelas, Colloidal fouling of RO membranes: an overview of key issues and efforts to develop improved prediction techniques, *Desalination*, 183 (2005) 257-272.
- [41] M. Manttari, A. Pihajamaki, M. Nystrom, Effect of pH on hydrophilicity and charge and their effect on the filtration efficiency of NF membrane at different pH, *J. Membr. Sci.*, 280 (2006) 311-320.
- [42] N.R.G. Walton, Some observations on the considerable variability of silt density index results due to equipment, filter and operator variables, *Desalination*, 61 (1987) 201-210.
- [43] Y. Zahao, J. S. Taylor, Assessment of ASTM 4516 for evaluation of reverse osmosis membrane performance, *Desalination*, 180 (2005) 231-244.
- [44] E.M. Vrijenhoek, S. Hong, M. Elimelech, Influence of membrane surface properties on initial rate of colloidal fouling of reverse osmosis and nanofiltration membranes, *J. Membr. Sci.*, 188 (2001) 115-128.
- [45] M. Nystrom, A. Pihlajamiiki, N. Ehsani, Characterization of ultrafiltration membranes by simultaneous streaming potential and flux measurements, *J. Membr. Sci.*, 87 (1994) 245-256.
- [46] M. Elimelech, A.E. Childress, Zeta Potential of Reverse Osmosis Membranes: Implications for Membrane Performance, in: *Water Treatment Technology Program Report No. 10*, Department of Civil and Environmental Engineering/University of California, Los Angeles, 1996.

- [47] M. Elimelech, W.H. Chen, J.J. Waypa, Measuring the zeta (electrokinetic) potential of reverse osmosis membranes by a streaming potential analyzer, *Desalination*, 95 (1994) 269-286.
- [48] R. Ziel, A. Haus, A. Tulke, Quantification of the pore size distribution (porosity profiles) in microfiltration membranes by SEM, TEM and computer image analysis, *J. Membr. Sci.*, 323 (2008) 241-246.
- [49] M. Chandler, A. Zydney, Effects of membrane pore geometry on fouling behavior during yeast cell microfiltration, *J. Membr. Sci.*, 285 (2006) 334-342.
- [50] J.C. Schippers, J.H. Hanemaayer, C.A. Smolders, A. Kostense, Predicting flux decline of reverse osmosis membranes, *Desalination*, 38 (1981) 339.
- [51] S.F.E. Boerlage, M.D. Kennedy, P.A.C. Bonne, G. Galjaard, J.C. Schippers, Prediction of flux decline in membrane systems due to particulate fouling, *Desalination*, 113 (1997) 231-233.
- [52] S.S. Kremen, M. Tanner, Silt density indices (SDI), percent plugging factor (%PF): their relation to actual foulant deposition, *Desalination*, 119 (1998) 259-262.
- [53] R. Bryant, Chemtrac Systems, An Alternative to Silt Density Index (SDI) Continuous Particle Counting, in: <http://www.chemtrac.com>, 2005.
- [54] M.A. Javeed, K. Chinu, H.K. Shon, S. Vigneswaran, Effect of pre-treatment on fouling propensity of feed as depicted by the modified fouling index (MFI) and cross-flow sampler-modified fouling index (CFS-MFI), *Desalination*, 238 (2009) 98-108.
- [55] C.R. Rao, H. Toutenburg, A. Fieger, C. Heumann, T. Nittner, S. Scheid, *Linear models: least squares and alternatives*, Springer, New York, 1999.
- [56] F. Rossignol, A.L. Penard, F.H.S. Nagaraja, C. Pagnoux, T. Chartier, Dispersion of alpha-alumina ultrafine powders using 2-phosphonobutane-1,2,4-tricarboxylic acid for the implementation of a DCC process, *European Ceramic Society*, 25 (2005) 1109-1118.

CHAPTER 3

**THE INFLUENCE OF MEMBRANE PROPERTIES ON
THE SILT DENSITY INDEX**

THIS CHAPTER HAS BEEN SUBMITTED TO PUBLICATION:

A. Al-hadidi, A.J.B. Kemperman, J. C. Schippers, M. Wessling, W.G.J. van der Meer, The influence of membrane properties on the Silt Density Index, J. Membr. Sci.

In this Chapter, the influence of membrane properties on the SDI value is investigated. Eight commercial '0.45 μm ' membrane types made of different materials (PVDF, PTFE, Acrylic copolymer, Nitro Cellulose, Cellulose Acetate, Nylon 6,6, and Polycarbonate) were used to measure the SDI.

Three samples were randomly chosen from each membrane type (same lot), and several membrane properties were studied (pore size distribution, pore shape, surface and bulk porosity, thickness, surface charge, contact angle and surface roughness). SDI values for an artificial feed, composed of a solution of α – Alumina particles of 0.6 μm diameter, were determined. The characterization of these membranes shows variation between the membranes used in this study (M1-M8), and within a batch of one membrane type. Substantial differences were found in the SDI values for the different types of membrane filters used.

Pore size, porosity and thickness are the most important membrane properties and determine the membrane resistance. Using a membrane with high a membrane resistance results in a low SDI value. The variations in measured SDI values between batches and within a batch are large and explain, at least partly, the problems encountered in practice with unacceptable variations in SDI values. These observed differences make the test unreliable. The variations are attributed to differences in properties of the membranes used. In order to make the SDI a reliable fouling index, there is a very strong need for membrane filters with uniform and constant properties.

3.1 Introduction

Many parameters may play a role in the final results of an SDI test and can be potential sources of error such as: variation in the membrane properties (as revealed in R_M , the membrane resistance), operator experience, feed water properties (pH and salinity) testing condition parameters (T and dp), artifacts (filter holder, air bubbles) and accuracy of the SDI equipment. In this Chapter, the variation in properties of commercial MF membranes and their influence on the SDI results will be investigated.

Mosset et al. [1] compared the SDI values as measured with hydrophobic and hydrophilic membranes. Higher values were obtained for hydrophobic membranes compared to hydrophilic membranes. Mosset et al. also observed differences between 2 batches of identical membrane types of the same manufacturer. As a consequence, a verification of the SDI measurement must always be performed with a new membrane batch.

To clearly demonstrate the relation between membrane characteristics and resulting performance in SDI tests, several structural and foulant-membrane interaction parameters affecting MF membrane fouling could be taken into consideration: (1) pore size and pore shape [2], (2) bulk porosity and surface porosity [3] (3) thickness and cross section morphology, (4) surface roughness [4], (3) zeta potential [5], (4) hydrophilicity [6], and (5) variations in membrane characteristics between different batches and within one single batch of the same membrane type.

In this Chapter, variations in membrane properties were studied for a large number of membranes which can be used for SDI tests. In addition, SDI measurements were carried out for a model feed water. The objective of our work is to link the variations in membrane properties to the SDI results.

3.2 Theory and background

The effects of the physicochemical properties of the used membrane on the SDI test will be discussed in this section such as Pore size, porosity, thickness, surface roughness, surface charges and hydrophilicity

3.2.1 Pore size and pore shape

Membrane fouling by cake layer formation is affected by physicochemical properties of the membrane surface (surface charge, roughness, and hydrophobicity), characteristics of the colloidal material (particle size and charge), solution chemistry (solution pH and ionic strength), and system hydrodynamics (cross-flow velocity and transmembrane pressure) [7].

The effect of membrane pore size on cake layer fouling in track-etched membranes was investigated by Hwang et al. [8] who found that the use of membrane with a larger pore size resulted in a lower filtration flux. This was due to more severe membrane blocking occurring in the larger membrane pores. In addition the filtration flux increases by decreasing the particles concentration, because of less particle accumulation during a fixed time interval. Theoretically, the Hagen–Poiseuille and Kozeny-Carman equations describe the relation between the pore diameter and the membrane flux.

1- Hagen-Poiseuille equation

The Hagen-Poiseuille equation assumes that the membrane consists of a number of uniform parallel, straight and cylindrical pores parallel or oblique to the membrane surface. The flux J through these pores is given Eqn. (3.1)

$$J = \frac{\varepsilon \times r^2}{8 \times \eta \times \tau} \frac{dP}{dx} \quad (3.1)$$

Where: J is the flux [$\text{m}^3/\text{m}^2 \text{ s}$], ε is the surface porosity [%], r is the pore radius [m], μ is the water viscosity [Pa.s], τ is the tortuosity [-], dP is the transmembrane pressure [Pa] and dx is the membrane thickness [m]

2- Kozeny-Carman

Hagen-Poiseuille equation limited for the uniform straight and cylindrical pores. The Kozeny-Carman equation is corrected the pore shape and can be used for membranes which consist of closely packed spheres Eqn. (3.2).

$$J = \left(\frac{\varepsilon^3}{K \times \eta \times S^2 \times (1 - \varepsilon)^2} \right) \left(\frac{dP}{dx} \right) \quad (3.2)$$

Where: S is the pore internal surface area/unit volume [m^{-1}] and K is the Kozeny-Carman constant [-]

The flux increases exponentially with the pore radius. Consequently, the amount of particles arriving to the membrane pores will increase with an increase in flux and pore size. The blocking index for membrane with larger pore size is larger than that for smaller pore size [8].

The influence of the pore shape can be explained as follows: an irregularly shaped pore has more selectivity against a particle with certain dimensions comparing to a regularly shaped pore with same area. Therefore, the regular pore allows bigger particles to penetrate through the membrane. Based on experimental and modeling work, a study by Chandler et al. [9] shows that the initial rate of flux decline is slower for the membrane with stretched or slotted pores compared to the membrane with circular pores. This clearly demonstrates that pore geometry can have a significant effect on membrane fouling.

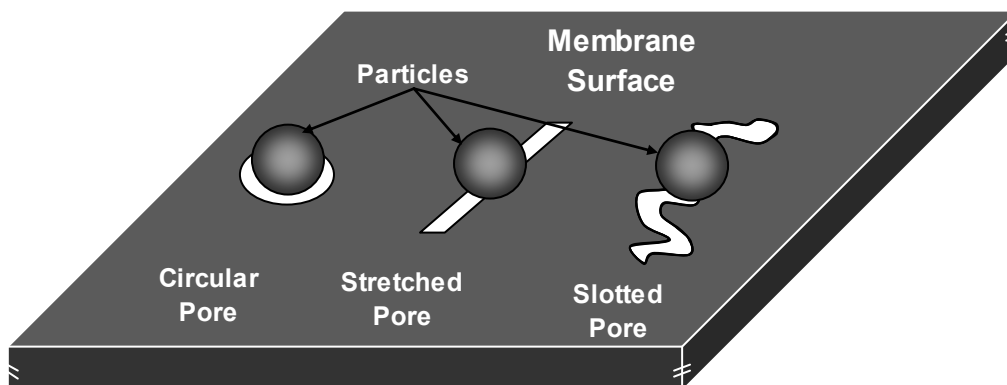


Figure 3.1. The effect of the pore shape on the particle rejection. Particles deposit on circular, rectangular and irregular membrane pore shape.

3.2.2 Membrane bulk porosity and surface porosity

Transport properties of membranes are closely related to morphological properties like surface porosity and variation of their inner pore structure [10]. For water transport, only the active pores are important for the final water flux. The membrane bulk density describes how much empty space the membrane has inside including non-active pores, while the surface porosity describes the fraction of pores at the surface of the membrane including non-active pores. Active pores are those pores connecting the feed side to the permeate side. Eqn (3.1)

shows that the flux is proportional to the surface porosity. A number of studies show the influence of the membrane pore connectivity and structure on fouling rate [9]. Under constant pressure, the more active pores the membrane has, the more water is filtered per time unit across the same membrane area. Consequently, more particles are transported to the membrane surface which results in a higher fouling load and a larger SDI value.

3.2.3 Membrane thickness

Flux and membrane thickness are inversely related. An increase in membrane thickness leads to an increase in the distance that the water need to cross to arrive at the permeate side of the membrane. This leads to an increase in pressure drop across the membrane. Therefore, a larger membrane thickness causes an increase in the membrane resistance (when pore size and shape are identical). Darcy's law gives the relation between the flux and the membrane resistance:

$$J = \frac{dP}{\eta \times R_M} \quad (3.3)$$

Combining equations (3.1) and (3.3) leads to the following relation:

$$R_M = \frac{8 \times \tau}{\varepsilon \times r^2} dx \quad (3.4)$$

In equation (3.4), the membrane resistance R_M increases proportionally with increasing membrane thickness, and is inversely proportional to the membrane surface porosity and to the square of the pore radius.

3.2.4 Membrane surface roughness

A certain amount of fouling will distribute on a larger surface area in the case of a rough surface than when the surface is smooth. Consequently, with the same amount of fouling as at smooth surface, a rough membrane produces a looser surface fouling layer having a lower flow resistance per unit foulant thickness than a smooth membrane surface. This will cause a higher flux across the rough membrane than across the smooth membrane.

On the other hand, more particles can deposit on rough membranes than on smooth membranes when all test conditions are held constant. Surface roughness increases membrane fouling by increasing the rate of colloid attachment onto the membrane surface [11].

When the particle size is comparable to the membrane roughness, the particles can find locations on the membrane where the contact area between the particle and the membrane is much larger than the corresponding contact area between a particle and the smooth surface [12]. In this case,

particles preferentially accumulate in the “valleys” of rough membranes, resulting in “valley clogging” which causes more severe flux decline than in smooth membranes [13-17]. Clearly, colloidal fouling of RO membranes is markedly influenced by membrane surface morphology.

3.2.5 Membranes surface charges

Polymeric membranes acquire a surface charge when brought into contact with an aqueous solution. The surface charge is compensated by counterions in the solution close to the surface, forming the so-called electrical double layer. The zeta potential can be defined as the potential at the plane of shear between the surface and solution where relative motion occurs between them. Several techniques can be used to determine the zeta potential of surfaces. Among these techniques, the streaming potential technique is most the applied for membrane surfaces. The streaming potential is the potential induced when an electrolyte solution flows across a stationary, charged surface. The streaming potential quantifies an electrokinetic effect which reflects the properties of the surface, the flow characteristics, and the chemistry and thermodynamics of the electrolyte solution in the experiment [18-19].

The zeta potential of the membrane is important because of the interaction between the nanoparticles and the membrane surface due to charge effects: repulsion in the case of similar charges, and attraction in the case of opposite charges. The membrane zeta potential is influenced by solution ionic strength and pH [19]. The ionic strength has a significant effect on colloidal fouling in membrane processes [20].

3.2.6 Membrane hydrophilicity

Membranes have an attractive or repulsive response to water. The material composition of the membrane and its corresponding surface chemistry determine this interaction with water. A hydrophilic membrane exhibits an affinity for water. It possesses a high surface tension value and has the ability to form hydrogen-bonds with water. The extent of flux reduction by foulants also is affected by the hydrophilicity of the membrane material [21]. Adsorption of foulants on the membrane plays an important role in membrane fouling. Hydrophobic membranes in general have a large tendency to foul, especially in the case of proteins.

Contact angle measurements have been widely used to estimate the surface energy of membranes. Such measurements are severely limited with regard to substrate surfaces that exhibit surface restructuring, that are contaminated, and/or are porous. In order to study the

hydrophilicity of the membrane surface, the captive air bubble technique can be used. The captive air bubble technique was described by Zhang and Hallstrom [22].

3.3 Experimental

The techniques which will be used to characterize the used membrane in the SDI test will be described. The equipments which will be used to perform the clean membrane resistance experiments and SDI tests using different membrane material will be specified in his section.

3.3.1 Membrane Characterization

The membranes used in the SDI test were characterized using the following techniques.

3.3.1.1 Pore size distribution

The pore size distribution was measured using a Coulter Porometer II (Coulter Electronics Ltd.) with pore wetting liquid Profil3. The capillary constant was set to the European System ($\tau_o=1$). Coulter results were compared those obtained with another Porometer, the Capillary Flow Porometer (PMI) from PMI porous material Inc. To study the effect of the capillary constant τ_o on the pore size distribution, the Capillary Flow Porometer (PMI) was manually set at $\tau_o=1$ or 0.715 (EU and USA systems, respectively) with Profil3 as wetting liquid. The pore size distribution was calculated out of the wet and dry flows using the Laplace equation. The mean flow pore size (MFP) was determined at the cross point of the wet curve with the average differential line. The largest pore was determined at the bubble point, while the smallest pore was determined at the point where the wet and the dry curve cross each other.

3.3.1.2 Thickness and SEM images

Membrane thicknesses were measured for 3 samples of each membrane type (M1-M8) using a Mitutoyo digital micrometer at ten different position across the membrane surface. For surface SEM images, a dry sample was sputtered with a very thin gold layer (SCD040, Blazers Union). Cross section SEM images samples were prepared by fracturing a fresh sample (wetted with 50%-50% water/ethanol) in liquid nitrogen. Before SEM imaging, the samples were dried over night in a 30 °C oven under vacuum. After drying the samples were sputtered with a gold layer. SEM images were taken using a Jeol JSM-5600 LV scanning electron microscope.

3.3.1.3 Bulk porosity and surface porosity

Bulk porosities of the membranes were determined using a helium Pycnometer from Micromeritics (AccuPyc 1330). Randomly, three samples were chosen from each type of membranes. The diameter, thickness and weight of each sample were measured in order to calculate the total membrane volume. The volume of the solid part of the membrane (polymer), was estimated using the Pycnometer. The bulk porosity was defined as the ratio of the empty space volume to the total volume. The surface porosity of the membranes in this work was qualitatively studied using the SEM surface images.

3.3.1.4 Membrane surface roughness

A Veeco multi mode scanning Atomic Force Microscopy (AFM) was used to determine the membrane surface roughness. Three new membrane samples were chosen randomly from the same lot of each type (M1-M8). The samples were cut in 50×50 mm size pieces and flushed with ultra-pure water. After that, the samples were dried in an oven over night under vacuum at 30 °C. AFM images of three sizes (20×20, 40×40, and 60×60 μm) at 3 different positions were scanned by in-tapping mode. The membrane roughness is given as the rms roughness R_q .

3.3.1.5 Contact angle

The membrane contact angle typically is measured with a liquid (usually ultra-pure water) drop on the surface membrane surface. The contact angle is defined as the angle at which a liquid interface meets a surface. Most of membrane used in this study have large pores in which the water can penetrate by gravity only. Water penetration through the pores causes an unstable volume of the drop during the contact angle measurement, especially with hydrophilic membranes. The captive air bubble is an alternative technique for measuring the contact angle. Contact angle measurements using the captive Air Bubble technique were carried out using a Contact angle system OCA20 (DataPhysics GmbH). Fresh and dry membrane samples (2 ×3.5 cm) were fixed with double side adhesive tape on a glass microscope slide. The membrane samples were submerged in the water bath (ultra-pure water), and the static captive air bubble contact angle was measured using the OCA20 system. The membrane was considered as hydrophilic at a contact angle $\geq 90^\circ$ and hydrophobic at a contact angle $< 90^\circ$ [23].

3.3.1.6 Surface charges

Membranes surface charges were measured as a function of the pH using an Electro Kinetic Analyzer EKA or the updated version SurPass (Anton Parr), and calculated according to Stern's (tangential) electric double layer model [18]. The measurements were carried out using a 10 mM KCl electrolyte solution, where the pH was adjusted using 1 M of HNO₃ and NaOH to low and high values, respectively. The zeta potential was calculated using the Fairbrother-Mastin equation in order to correct the zeta potential for the part of the back current flows over the surface which may not be desirable [24].

$$\zeta = \frac{E_s}{\Delta P} \frac{\mu}{\varepsilon_r \times \varepsilon_0} \frac{K^h \times R^h}{R} \quad (3.5)$$

Where:

ζ	zeta potential [mV]
μ	liquid viscosity [Pa.s]
ε_r	relative permittivity of the electrolyte
ε_0	permittivity of free space (vacuum) [F/m]
E_s / dp	slope of streaming potential versus pressure difference curve [mV/Pa]
R	resistance measured when the cell is filled with the measurement electrolyte [ohm]
R^h	ohmic resistance across the capillary [ohm]
K^h	conductivity of the electrolyte [S/m]; R^K and K^h can be considered to be the cell constant

3.3.2 Filter holders

Different filter holders can be used for SDI tests. In this work, the test was performed with a 25 mm polycarbonate filter holder from Sartorius. The original support plate in this filter holder has thick edges which can block part of the membrane and in this way decrease the effective membrane area during filtration. In order to avoid the effect of the support, the support plate was replaced with a 60 μ m pore size sintered metal fiber filtration sheet. Membrane pores can be clogged by trapped air in the feed stream. A relief valve was added to the top cover of the filter holder in order to get rid of the air bubbles on the membrane surface. The relief valve was used also to perform clean water flux measurements before each SDI test. The membrane surface was

flushed with the feed water through the relief valve to remove residual clean water and guarantee equal starting conditions at the beginning of the SDI test.

3.3.3 Model water

The model feed solution contained 4 mg/L AKP-15 in ultra-pure water, purified by a ultra-pure system from Millipore (Synergy SYNS). The solution was well mixed mechanically in the feed tank.

3.3.4 Clean water membrane resistance

Clean water flux experiments (CWF) were performed before each SDI experiment. The CWF measurements were performed with ultra-pure water under constant pressure. The clean water resistances of the membranes R_M were calculated using Darcy's law in Eqn. (3.3).

3.4 Results

The used membrane in the SDI test will be characterized and compared. The clean membrane resistance will be tested and SDI tests using different membrane material will be performed in this section using model water of AKP-15 solution.

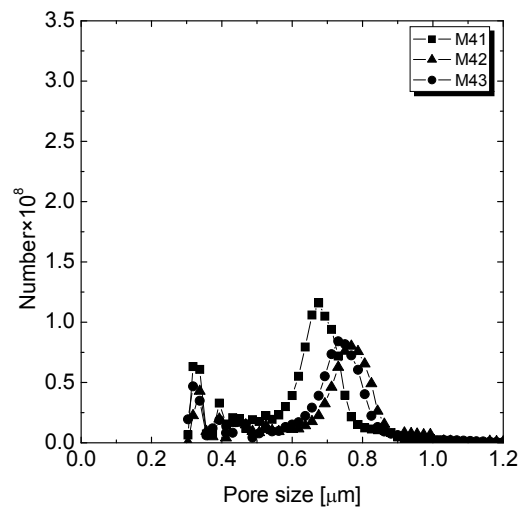
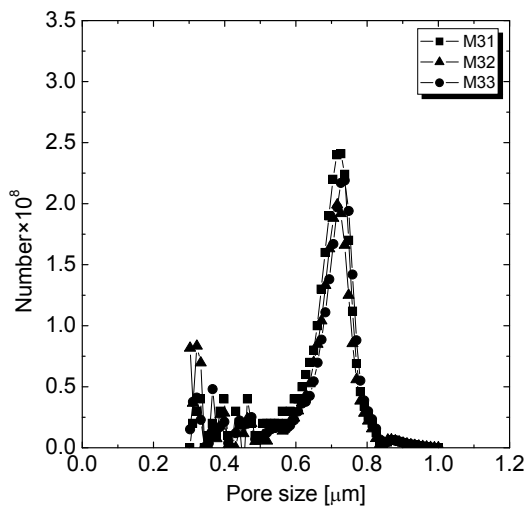
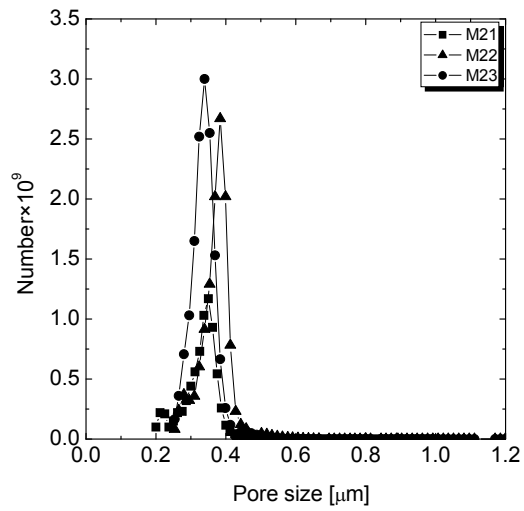
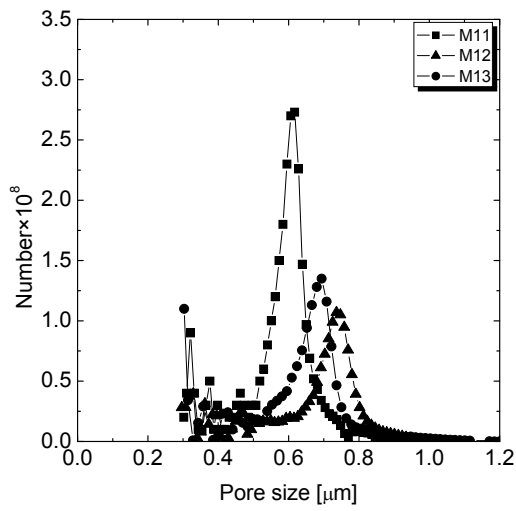
3.4.1 Variation in the membrane properties of the different membranes

The fouling of the membrane depends, amongst others, on the chemical and physical properties of the membrane and the particles. The variation in membrane properties such as pore size, pore shape, membrane thickness, bulk/surface porosity, surface roughness, contact angle, and the surface charge over the membrane were measured and compared. In addition, the clean water membrane resistances were determined.

3.4.2.1 Pore size and pore shape

To investigate the influence of the pore size on the SDI results, pore size distributions for all membranes used were determined. For each membrane type, three samples were chosen randomly from the same lot, taken from the top, middle and bottom of the package. The mean flow pore size (MFP) and the minimum and maximum pore sizes were determined using the Coulter Porometer II for each sample. The final pore size distribution curves for the membranes, each measured in triplicate, are shown in Figure 3.2. The noise in the PSD curve at

high pressures/small pore sizes is due to experimental difficulties with the flowmeter of the Porometer device.



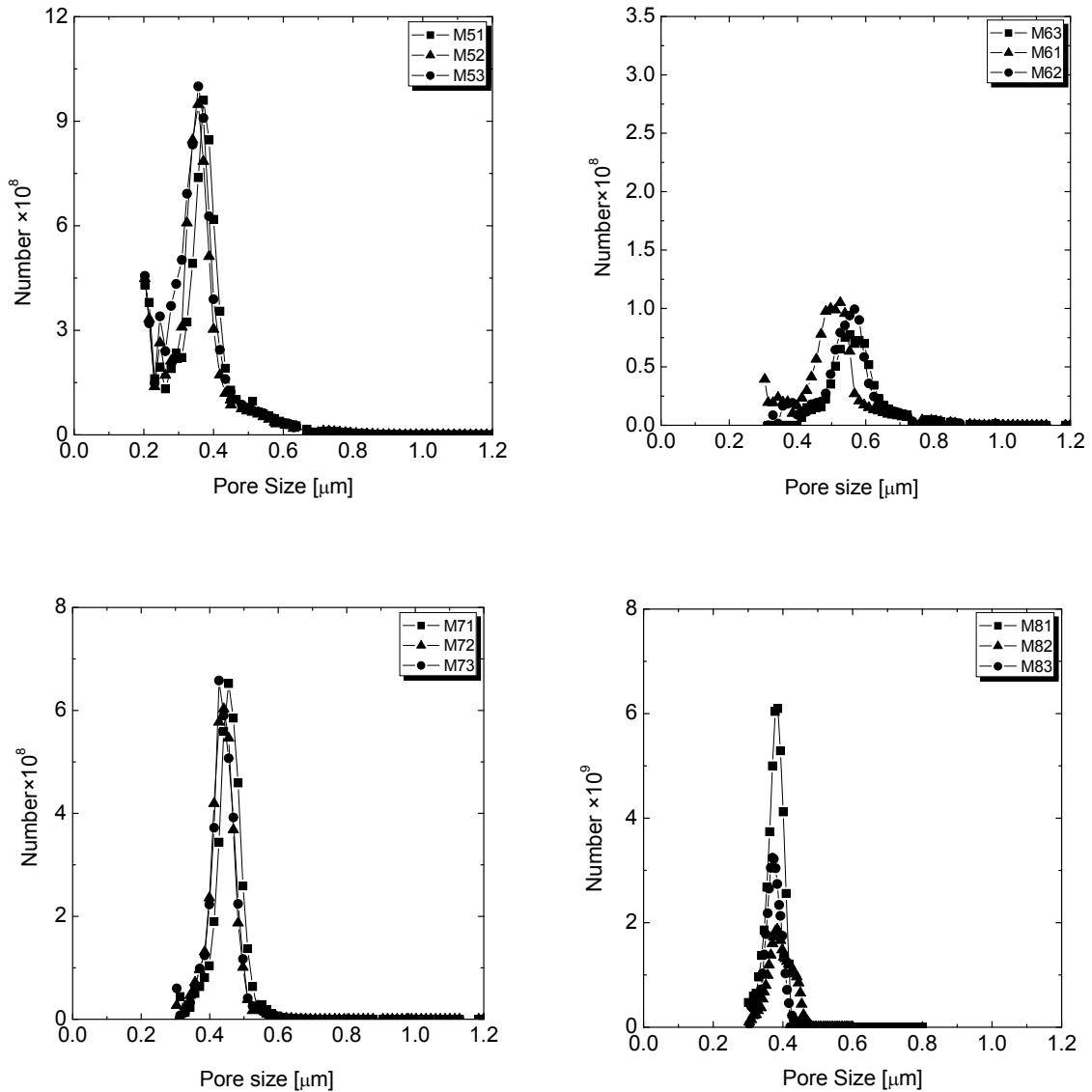


Figure 3.2. Pore size distribution curves (PSD) for membranes M1-M8 as measured in triplicate with the Coulter Porometer.

The maximum pore size varies from one membrane type to the other. Furthermore, Figure 3.2 shows clearly the variation in the smallest pores and the peaks in the PSD. Membranes M2, M5, M7 and M8 have narrow PSD curves, while membranes M1, M3, M4 and M6 show broader PSD curves. In addition, in Figure 3.3 the MFP, maximum and minimum pore sizes for each membrane type (M1-M8) were plotted. Some membranes show a clear difference between the measured and the manufacturer nominal pore size of 0.45 μm. The manufacturer’s pore size might have been determined with a different technique, which explains (part of) the difference. M2 has the smallest MFP of 0.37 μm, while membranes M1, M4 and M3 have a MFP > 0.7 μm. Figure 3.3 shows that the membranes M5, M7 and M8 have an MFP close to 0.45 μm.

Membrane M4 deviates the most from the ASTM standard requirement size of $0.45\ \mu\text{m}$ (almost 71% larger pore size) and has a broad pore size distribution. M7 on the contrary deviates only +1.2% from the $0.45\ \mu\text{m}$ guideline and has a narrow pore size distribution.

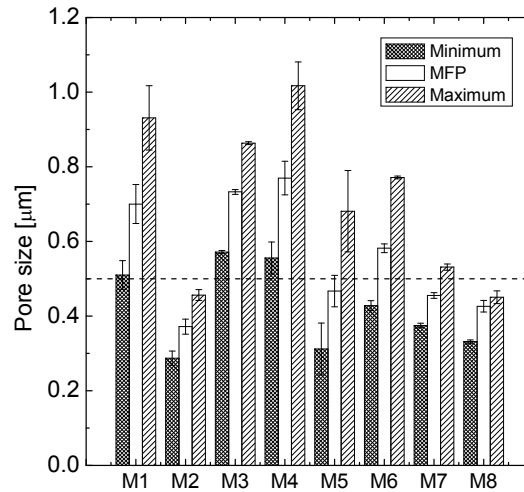


Figure 3.3. MFP, max, and min pore size for membranes M1-M8

The pore size results obtained with the Coulter Porometer were compared to the PMI results. Two capillary constants (τ) were used for the PMI device (1 and 0.715) for calculating the pore size. The capillary constant is defined as the change in the size (pore diameter) along the pore. The ASTM F-316-86 [25] standard sets the capillary constant at a value of 0.715. However, this value was not mentioned in the new version of the standard ASTM F-316-03 [26]. According to the manufacturer's instruction, PMI calls $\tau = 1$ the EU system, while $\tau = 0.715$ is USA system.

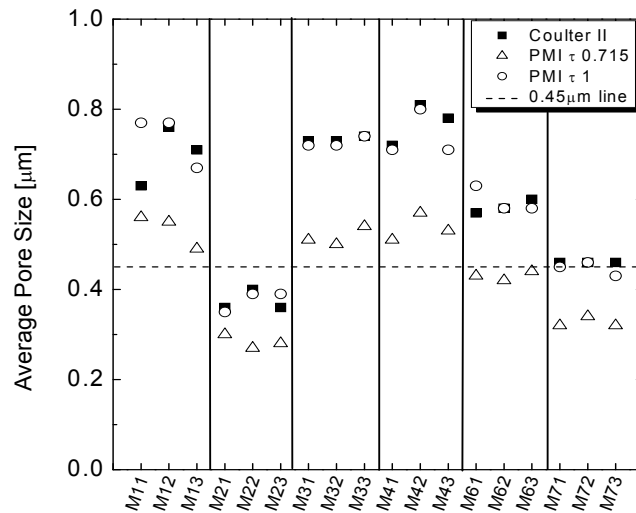


Figure 3.4. Overall average pore size for the membranes used M1-M8 as function of the capillary constant τ .

The influence of τ on the average pore size distribution is shown in Figure 3.4 for membranes M1-M4, M6 and M7. The average pore sizes of M1, M3, M4 and M6 were lower when τ was decreased from 1 to 0.715. However, the average pore sizes of M7 determined with both Coulter II as well as with the PMI equipment with a capillary constant of 1 give a pore size of 0.45 μm . M6 has a pore size of 0.45 μm only when 0.715 is used as capillary constant.

Top view images of the surfaces of the membranes were made using SEM. SEM surface images are shown in Figure 3.5. A difference was noticed between the top side of M1 ('M1_T') and the bottom side of the same membrane M1 ('M1_B'), where top and bottom are referring to the orientation of the membrane in the original packaging.

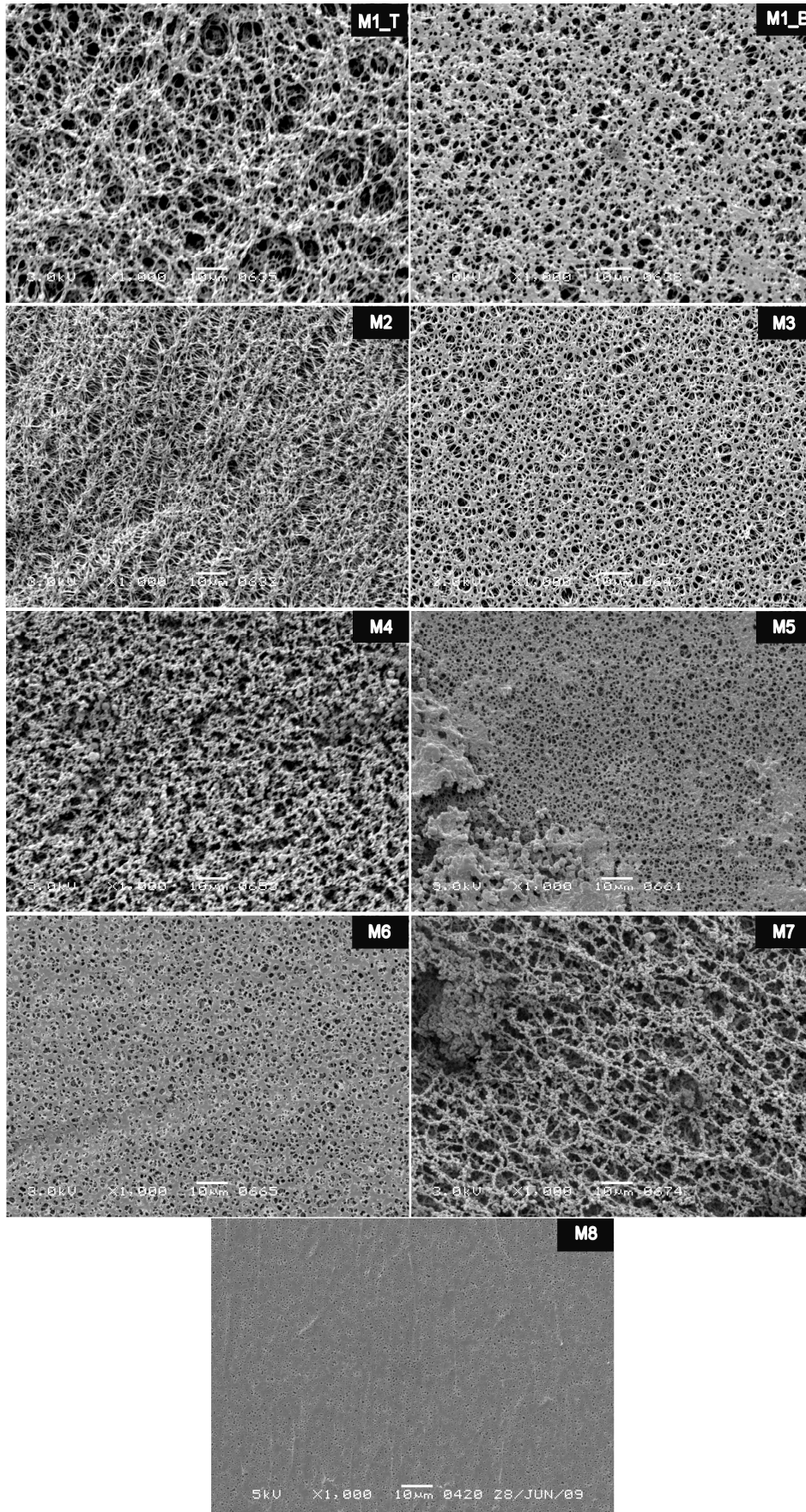


Figure 3.5. SEM surface images of membranes M1-M8 (magnification x1,000).

The membranes used in this work are made out of different polymers and are prepared by the manufacturers using different techniques by the manufactures. M6 and M7 both are cellulose acetate membranes from two different manufacturers. Figure 3.5 shows differences in the pore morphology between M6 and M7. M1_B with the smooth surface has different a pore shape compared to the rougher top surface M1_T. Moreover, M2 has a stretched pore shape, whereas M3 and M8 have a well-defined circular pore shape. M7 has an irregular pore shape. In general, we can conclude that the membranes used in this work all have different pore shapes at the surface.

3.4.2.2 Bulk and surface porosity

a. Bulk porosity

The bulk porosity (pore volume to total volume ratio) was estimated for the membranes used in this study (M1-M8). The bulk porosity was determined for each type using three fresh samples. The average bulk porosities of the membranes used are plotted in Figure 3.6. There is a large variation in the bulk porosities between the 8 membranes tested Membranes M2 and M4 show the largest average bulk porosity (around 80 %), while membrane M8 only has 40 % bulk porosity. The other membranes used show porosities around 60 %.

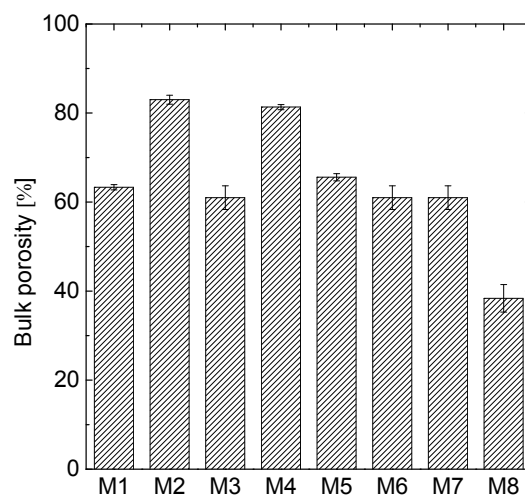


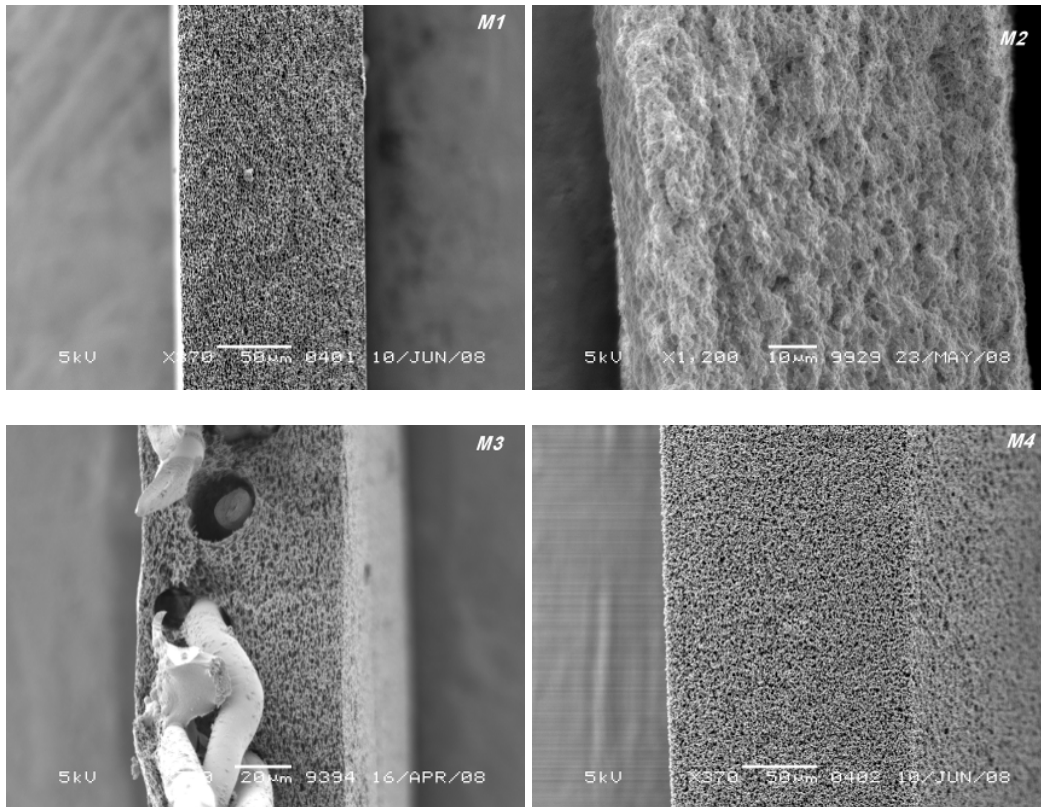
Figure 3.6. Bulk porosity for membranes M1-M8.

b. Surface porosity

Beside the bulk porosity, the surface porosity was determined qualitatively from SEM images for each type of membrane used. In Figure 3.5 SEM surface images (magnification x1,000) are shown. Membrane M8 (track-etched membrane) shows a very low surface porosity. The top and back sides of M1 have different surface porosities. The top side of M1 shows higher surface porosity than the back side.

3.4.2.3 Thickness and cross-sectional morphology

Cross sectional SEM images of the membrane used are shown in Figure 3.7. Membranes M1, M2, M4 and M6 are symmetric, spongy membranes. On the other hand, M3, M5 and M7 are asymmetric, spongy and reinforced membranes.



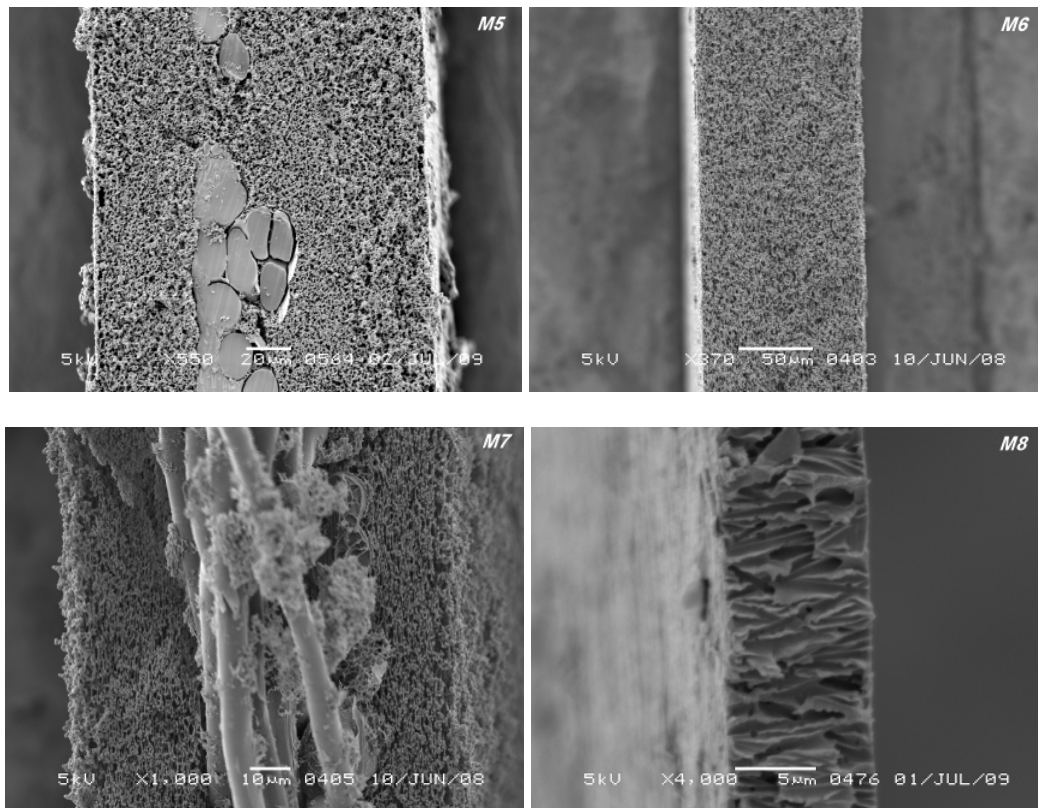


Figure 3.7. SEM cross section image pictures of membranes M1-M8

The pores in membrane M8 are cylindrical and non-parallel channels. Some pores are not located perpendicular towards the membrane surface, but are intersecting deeply into the membrane. The schematic pore structure of membrane M8 is shown in Figure 3.8. At the crossing of two intersecting pores a larger pore is present, and consequently the pore size distribution is broader compared to the situation where only vertical pores are present.

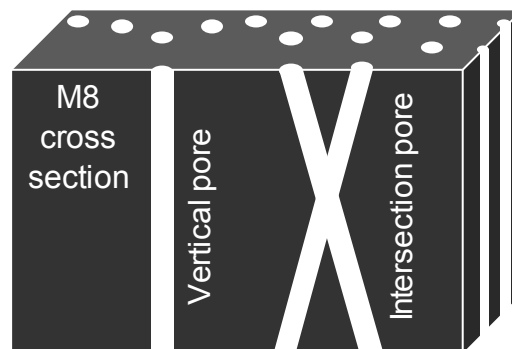


Figure 3.8. Schematic representation of vertical and intersecting pores in M8.

Membrane thicknesses were measured using a digital micrometer. The measurement was carried out for three samples for each membrane types and in ten different positions across the

membrane surface. The average thicknesses were plotted in Figure 3.9. The membrane thicknesses were measured ten times in different position across the membrane surface. The nitro-cellulose membranes M4 and M5 were the thickest membranes (150 μm), while the track-etched membrane M8 was the thinnest membrane (12 μm). Membranes M1, M6, and M7 have comparable thicknesses (100-120 μm).

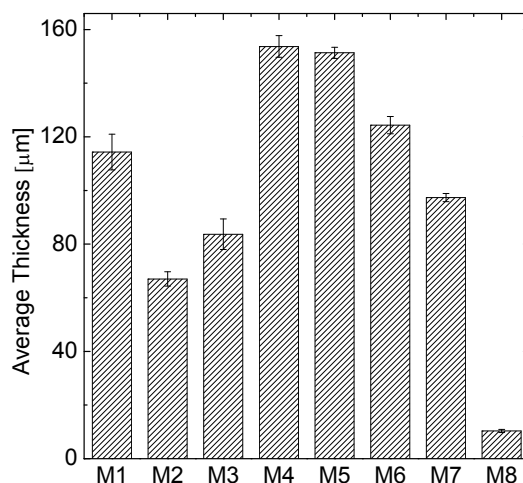


Figure 3.9. Average thicknesses of the membranes used, measured ten time across the membrane surface with a digital micrometer.

3.4.2.4 Surface roughness

For each sample the surface roughness was examined using the AFM 3D images shown in Figure 3.10. Three membrane samples were taken from same lot for each membrane type. Several AFM 3D images were scanned at different positions on the membranes surface with surface dimensions (20 \times 20, 40 \times 40 and 60 \times 60 μm). For PVDF membrane M1, the surface roughnesses of both sides were determined. Membranes M2, M3, M6 and M8 have smooth surfaces. Obviously, the back side of M1 (M1_B) has a smooth surface. Some agglomerated polymers were observed on the surface of M5 (Nylon 6,6 membrane) which makes the membrane surface rough and non-homogenous.

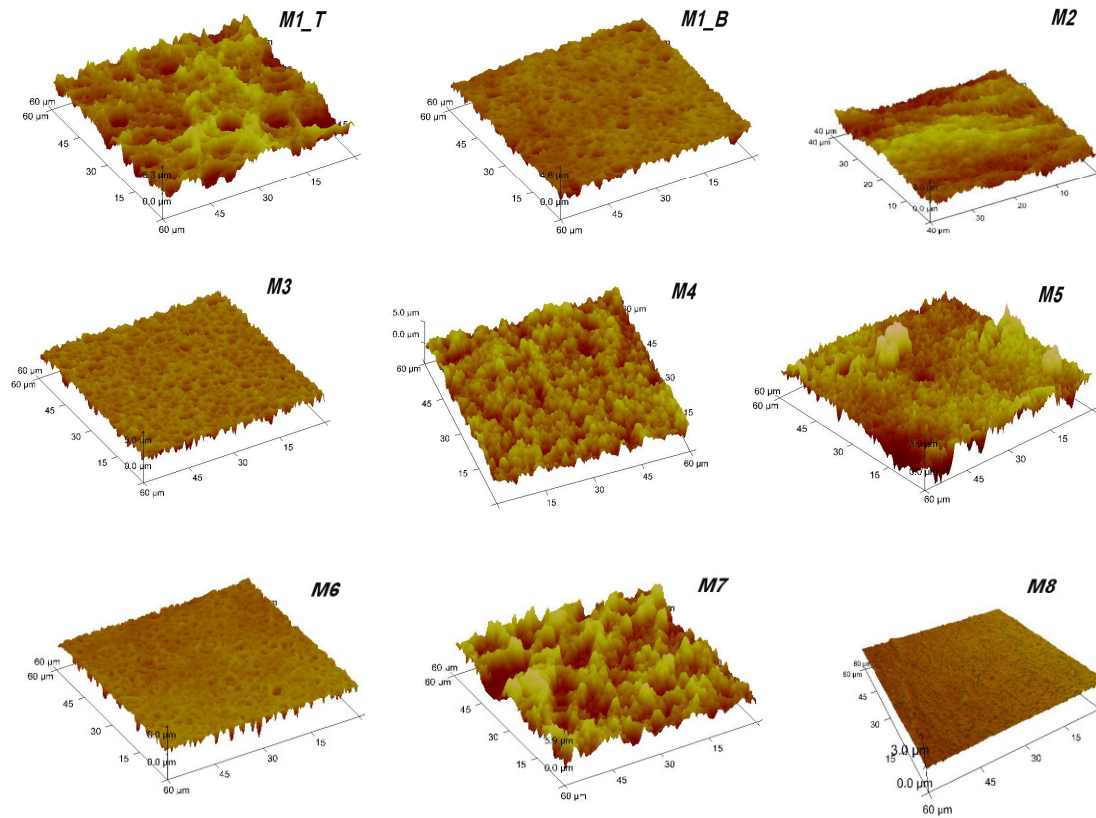


Figure 3.10. AFM topographic images of membranes M1-M8.

Figure 3.11 shows the surface roughness (R_q) in the Z direction (vertical dimension) between the references markers over the length L of the profile of the membranes. Membrane M8 has the smoothest surface (R_q equals 75 nm in average). On the other hand, membrane M7 has a very rough surface (R_q 1200 nm in average). Membranes M2, M3, M5 and M6 have a roughness between 300 to 400 nm.

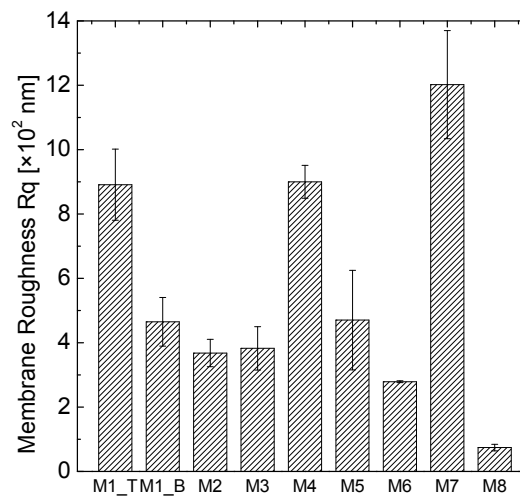


Figure 3.11. Surface roughness (R_q) of membranes M1-M8.

3.4.2.5 Membranes surface charges

Figure 3.12 shows the measured zeta potentials for each membrane type as a function of the pH.

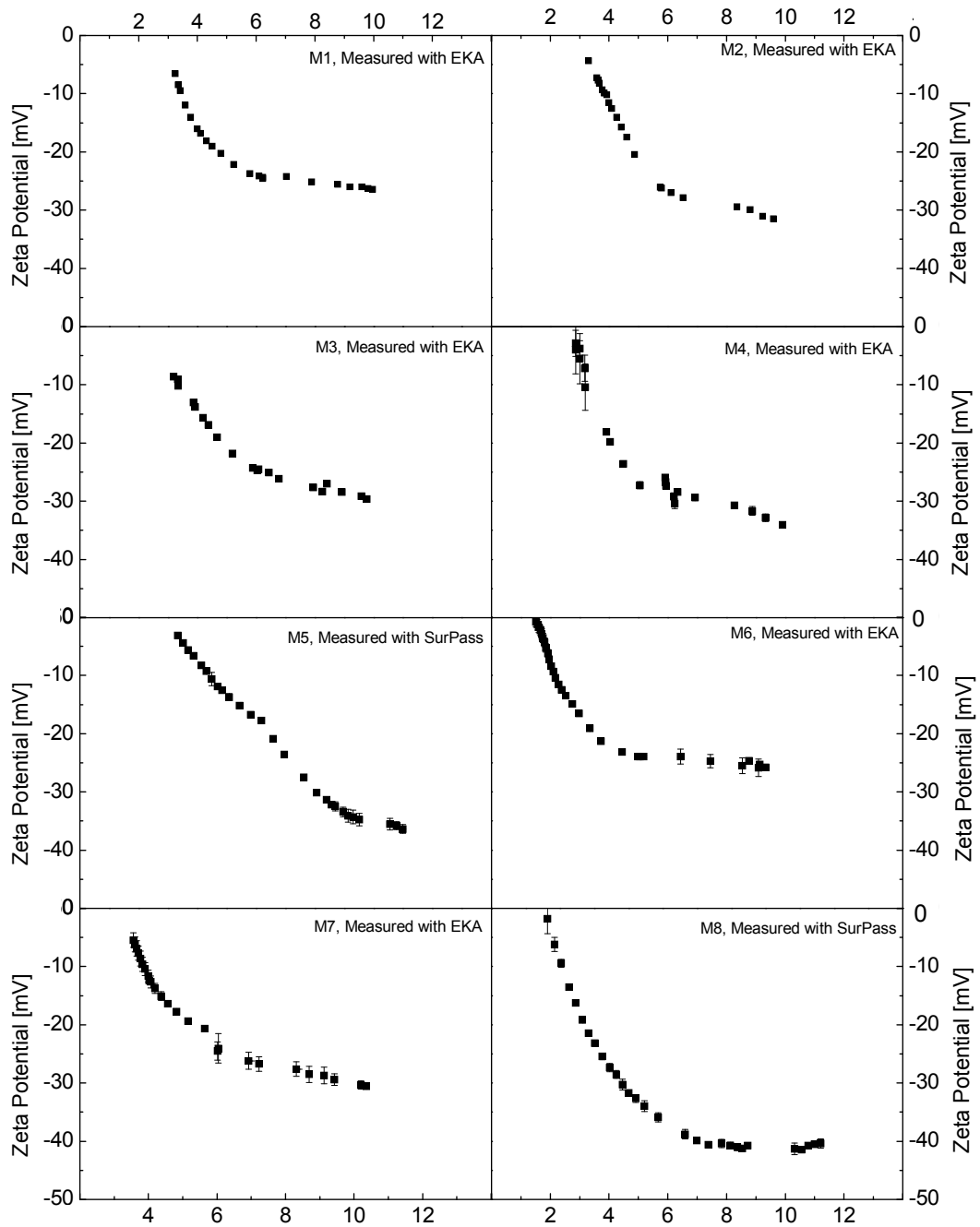


Figure 3.12. Zeta potential of membranes M1-M8 using 10mM KCl electrolyte solution.

In general, all the membranes were negatively charged at pH 7. The isoelectric points (IEP) is defined as the pH which the membrane surface carries no charge (zeta potential=0 mV). For the membranes M1, M2, M3, M5 and M7, the isoelectric points (IEP) were determined by interpolated the zeta potential curves to the intersect point with the zero line in Figure 3.12. The isoelectric points (IEP) were in between 2 and 3.3 for the membranes studied. The zeta potential values for the membranes at pH 7 are plotted in Figure 3.13. Membrane M8 has the most negative surface charge at pH 7 (-38mV), whereas M6 has the smallest surface charge (-22.5 mV).

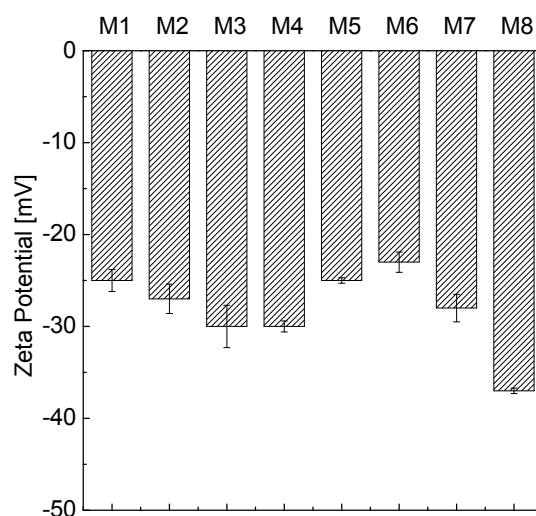


Figure 3.13. Membrane zeta potential at pH 7.

3.4.2.6 Hydrophilicity

Three samples were taken from each membrane material. For each sample the contact angle was measured using the captive air bubble technique. Figure 3.14 shows the average contact angles for each membrane material. All of the membranes were hydrophilic except M2 which is a hydrophobic membrane.

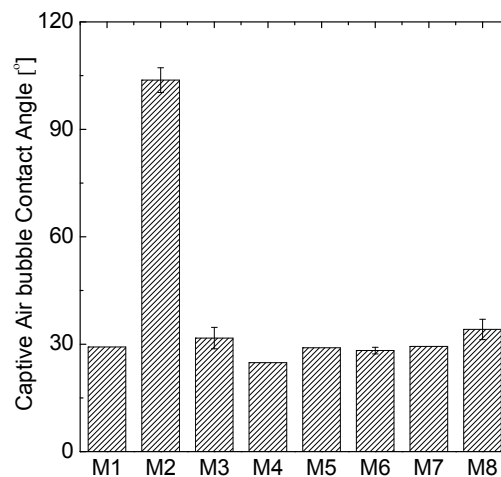


Figure 3.14. Contact angle of M1-M7 measured using the Captive air bubble technique.

3.4.2.7 Membrane resistance

In this work the membrane resistance was determined by performing clean water flux (CWF) experiment with ultra-pure water. The membrane resistance can be used as an overall indicator for the membrane properties, including e.g. membrane porosity, pore size and thickness.

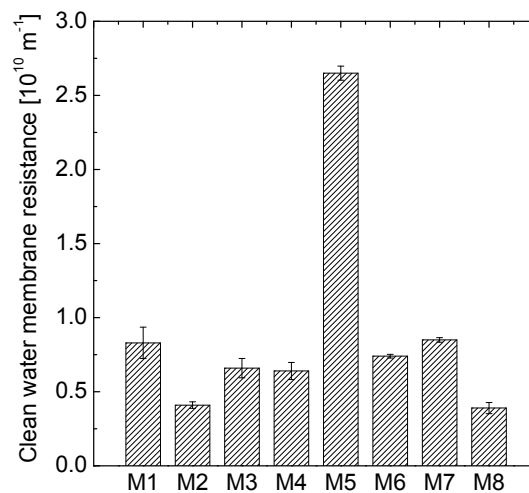


Figure 3.15. Clean membrane resistances R_M of membranes M1-M8, based on CWF experiments.

Figure 3.15 shows the clean membrane resistances for the membranes used. M5 has the highest resistance ($2.65 \times 10^{10} \text{ m}^{-1}$), while M8 has the lowest resistance ($0.39 \times 10^{10} \text{ m}^{-1}$).

The average membrane resistances for the other membranes were around $0.6\text{-}0.8 \times 10^{10} \text{ m}^{-1}$. The membrane resistance R_M of M1 varies 23 % within the same batch of membranes, while M7 has

only 7 % variation in the membrane resistance R_M . The ASTM (D4189-07) standard for the SDI test requires that the pure water flow time is 25-50 s for 500 mL at a pressure of 91.4-94.7 kPa and a membrane diameter of 47mm. No temperature correction is mentioned in the ASTM standard for the SDI test. The ASTM requirement of the pure water flow can be translated into clean membrane resistance limits: $0.86 \times 10^{10} \text{ m}^{-1} < R_M < 1.72 \times 10^{10} \text{ m}^{-1}$ at 20°C.

Table 3.1 shows the average clean membrane resistance R_M for the used membrane M1-M8.

Table 3.1 The measured average clean water resistance R_M for the used membrane M1-M8.

Code	Material	Nominal Pore size [μm]	R_M [$\times 10^{10} \text{ m}^{-1}$]
M1	PVDF	0.45	0.83
M2	PTFE	0.45	0.41
M3	Acrylic Polymer	0.45	0.66
M4	Nitro Cellulose*	0.45	0.64
M5	Nylon6,6	0.45	2.65
M6	Cellulose Acetate*	0.45	0.74
M7	Cellulose Acetate*	0.45	0.85
M8	Polycarbonate	0.45	0.39

* ASTM standard material.

3.4.2 Meeting the ASTM standard

The work in this project was started in 2006, one year before the most recent version of ASM in 2007. However, the standard ASTM (D4189-97) did not require a specific polymer material for the membrane used in the SDI test and only requires a hydrophilic membrane. Therefore, a number of commercial MF membranes were randomly chosen for comparison and tested. Besides that, a track-etched and hydrophobic membrane were used in this work for comparison to the ASTM requirements.

Based on the characterization results and with regard to the ASTM (D4189-07) standard, Table 3.2 shows where the membranes do not meet the new ASTM (D4189-07) requirements:

- M1, M2, M3, M5 and M8 not cellulose acetate or cellulose nitrate material
- M1, M2, M3, M4, M6 and M8 average pore size $\neq 0.45 \mu\text{m}$
- M2, M3 and M8 membrane thickness $< 115 \mu\text{m}$
- M5 (high resistance) pure water flow time $R_M > 1.72 \times 10^{10} \text{ m}^{-1}$ ASTM limit

- M8 (low resistance) pure water flow time $R_M < 0.86 \times 10^{10} \text{ m}^{-1}$ ASTM limit

Table 3.2. Meeting the ASTM requirements by the membranes.

Code	Material	Pore size	Thickness	Membrane resistance
M1	-	-	√	√
M2	-	-	-	√
M4	√	-	√	√
M3	-	-	-	√
M5	-	-	√	-
M6	√	-	√	√
M7	√	√	√	√
M8	-	-	-	-

√ The membrane property meets the requirement

- The membrane property does not meet the requirement

3.4.3 Variation of membrane properties within one batch

In order to investigate the variation of the membrane properties within a batch, three samples were randomly chosen from a pile of membranes (top, middle, and bottom of the packaging) for each type. The variations in the average pore size, surface roughness, contact angle, total porosity and membrane thickness within the same lot were studied for each membrane type. In order to be able to compare the variation of the properties for the different membranes, the variations were calculated for each type as a percentage (relative standard deviation $\sigma_{rel} = \text{SD}/\text{Avg. } \%$). σ_{rel} was calculated for each property out of at least three single measurements for each membrane.

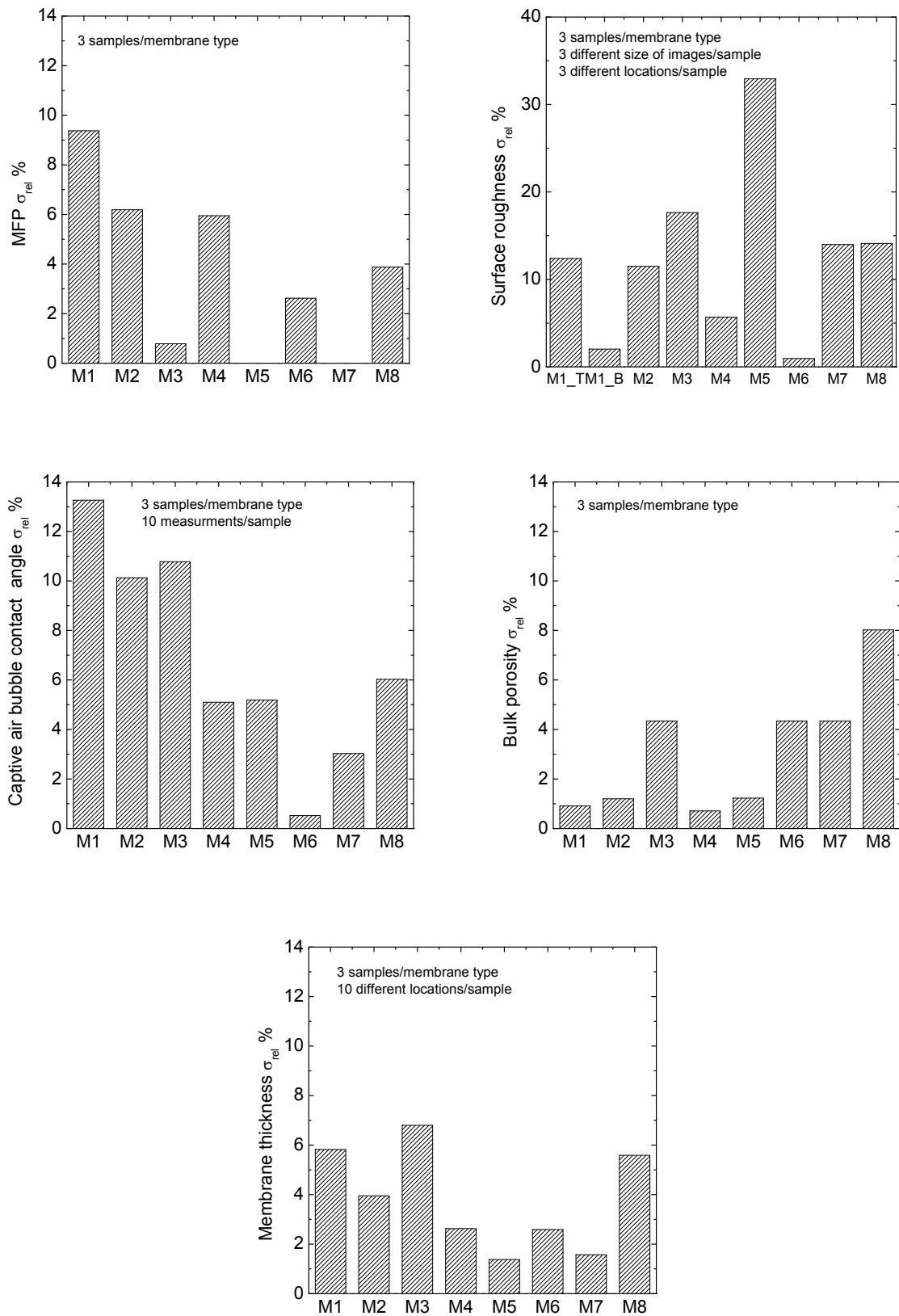


Figure 3.16. Variations in mean flow pore size (MFP), surface roughness, contact angle, total porosity and membrane thickness within a membrane batch.

Figure 3.16 shows the variation in the membrane properties within one batch of each membrane type. The membranes used in this study (M1-M8) have a variation $<10\%$ in the MFP, membrane thickness and the total porosity. Membrane M5 has a rough surface with 33% variation within one batch of membrane, while membranes M1_B, M4, and M6 have a minor variation $<10\%$. Concerning the contact angle M1, M2 and M3 have $>10\%$ variation in the results. The top side of M1 (M1_T) shows a larger variation than the back side (M1_B) in the membrane surface roughness.

The total variation in membrane pore size, bulk and surface porosity and membrane thickness are important for the variation in the clean membrane resistance. Consequently, these parameters also are important for variations in the SDI values since they influence the initial flow rate at the beginning of the SDI test. For each membrane type the total variation is calculated by summing up the individual variations in the membrane properties. Figure 3.17 shows that membrane M6 has the lowest overall variation ($<10\%$). Membranes M1_T, M3, M5 and M8 show much larger overall variations above 40% .

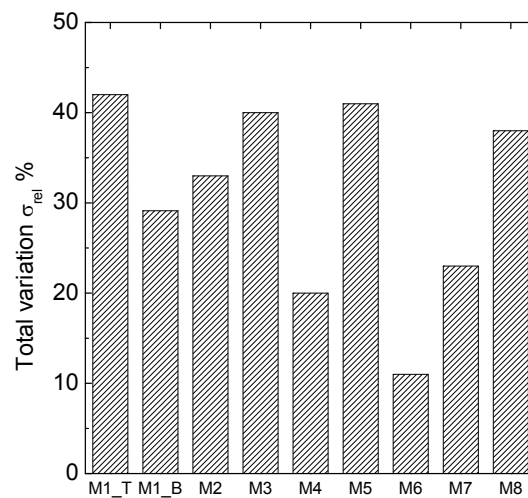


Figure 3.17. Total variation in membranes properties within each membrane batch.

3.4.4 SDI of an AKP-15 model solution

AKP-15 particles with pore size $0.6\ \mu\text{m}$ have a narrow particle size distribution, with an average size larger than that of the membrane pores. For this reason a $4\ \text{mg/L}$ solution of AKP-15 in ultrapure water was chosen as model foulant solution with reproducible properties. Three samples out of each membrane batch were randomly chosen for the SDI test. As prescribed by

the ASTM standard, the SDI was measured using a 25 mm diameter cell and the volumetric samples size was adjusted to 141 mL. Constant feed water quality during the SDI tests was ensured by using a large stirred feed tank (2×60 L).

Figure 3.18 gives the SDI values as determined for membranes M1-M8. When the back side of M1 is directed towards the feed, a 0.3 higher SDI value is measured compared to the situation where the top side is facing the feed. Membrane M5 shows the lowest SDI value (2.0 ± 0.23), while membrane M8 results in the highest SDI value (4.6 ± 0.24). Membrane M2 shows the highest variation in the SDI value 3.8 ± 0.5 . The variation in the SDI results of M2 can be explained by the pre-wetting with ethanol. During the filtration step, the feed water flushes the ethanol out of the pores and part of the membrane become dry and inactive to water transport, which lowers the flow rate and results in an increase of the SDI value. The dried areas in M2 were frequently observed when the holder was opened directly after the SDI test. Membranes M1_T, M1_B, M3, M4, and M6 show less variation in the SDI values (between 0.21 and 0.25).

In the SDI test, the time between the two measurements is fixed and the total volume that is filtered in that time depends on the flow rate. Thus, any effect that increases the flow rate through the membrane will increase the fouling load of the membrane and consequently the measured SDI will be higher. This explains our observation that the SDI increases with decreasing membrane resistance due to an increasing pore size, increasing bulk and surface porosities, decreasing membrane thickness and/or increasing surface roughness of the membrane. This relation is confirmed when plotting the SDI results as a function of the clean membrane resistance R_M in Figure 3.19. A decrease in the SDI with an increasing the membrane resistance R_M was observed experimentally. Furthermore, the surface charge and hydrophilicity of both the membrane surface and the foulants affect the SDI value by influencing the membrane adsorption for the foulants (membrane-foulants interaction).

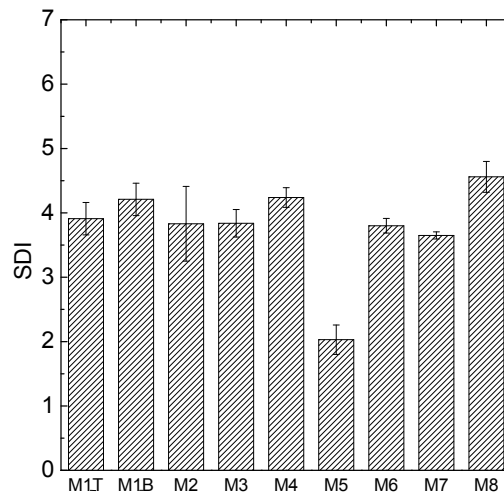


Figure 3.18. SDI results using a 4 mg/L AKP-15 model feed for the different membranes.

The initial flow rate plays an important role in the SDI value since it affects the fouling load and thus the amount of particles carried to the membrane surface. Membrane pore size, porosity and thickness affect the initial flow rate of the membrane and defined the clean membrane resistance R_M .

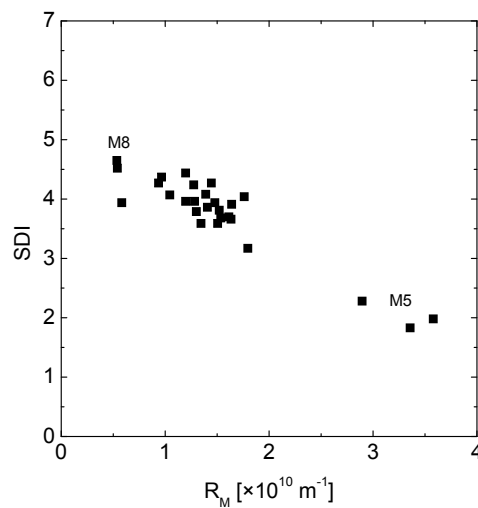


Figure 3.19. SDI as a function of the membrane resistance for a 4 mg/L AKP-15 model feed solution.

3.5 Conclusions

Three samples were randomly chosen from a set of 8 different 0.45 μm membranes to study the effect of the variation in the membrane properties on the SDI value. Significant variation was observed in the membrane properties within a membrane batch and between the different membrane types.

The pore size, porosity and thickness are the most important membrane properties, which can be measured as one parameter, the clean membrane resistance. The use of membranes with a high clean membrane resistance results in a higher fouling load and therefore in a low SDI value and vice versa. The membrane resistance increases with increasing pore size, increasing bulk and surface porosities, decreasing membrane thickness and/or increasing surface roughness of the membrane. Furthermore, the surface charge and hydrophilicity of both the membrane and the foulants affect the SDI values by influencing the adsorptive fouling.

Variations in measured SDI values between different membrane types and within a batch of one membrane type are large and explain at least partly the problems encountered in practice with unacceptable variations in the final SDI results. These observed differences make the SDI test unreliable. These differences are attributed to differences in properties of the membranes used. For a reliable SDI determination in the field, there is a very strong need for standardized membrane filters having uniform and constant properties.

References

- [1] A. Mosset, V. Bonnelye, M. Petry, M.A. Sanz, The sensitivity of SDI analysis: from RO feed water to raw water, *Desalination*, 222 (2008) 17-23.
- [2] Y. Wyart, G. Georges, C. Deumie, C. Amra, P. Moulin, Membrane characterization by microscopic methods: Multiscale structure, *J. Membr. Sci.*, 315 (2008) 82-92.
- [3] A. Drews, C.-H. Leeb, M. Kraume, Membrane fouling – a review on the role of EPS, *Desalination*, 200 (2006) 186-188.
- [4] K. Riedl, B. Girard, R.W. Lencki, Influence of membrane structure on fouling layer morphology during apple juice clarification, *J. Membr. Sci.*, 139 (1998) 155-166.
- [5] M. Elimelech, W.H. Chen, J.J. Waypa, Measuring the zeta (electrokinetic) potential of reverse osmosis membranes by a streaming potential analyzer, *Desalination*, 95 (1994) 269-286.
- [6] M. Nystrom, A. Pihlajamiiki, N. Ehsani, Characterization of ultrafiltration membranes by simultaneous streaming potential and flux measurements, *J. Membr. Sci.*, 87 (1994) 245-256.
- [7] Q. Li, M. Elimelech, Synergistic effects in combined fouling of a loose nanofiltration membrane by colloidal materials and natural organic matter, *J. Membr. Sci.*, 278 (2006) 72-82.
- [8] K.-J. Hwang, Chien-Yao, L.-L. Tung, Effect of membrane pore size on the particle fouling in membrane filtration, *Desalination*, 234 (2008) 16-23.
- [9] M. Chandler, A. Zydney, Effects of membrane pore geometry on fouling behavior during yeast cell microfiltration, *J. Membr. Sci.*, 285 (2006) 334-342.
- [10] R. Ziel, A. Haus, A. Tulke, Quantification of the pore size distribution (porosity profiles) in microfiltration membranes by SEM, TEM and computer image analysis, *J. Membr. Sci.*, 323 (2008) 241-246.
- [11] M. Elimelech, X. Zhu, A.E. Childress, S. Hong, Role of membrane surface morphology in colloidal fouling of cellulose acetate and composite aromatic polyamide reverse osmosis membranes, *J. Membr. Sci.*, 127 (1997) 101-109.
- [12] T. Rizwan, Colloidal particle deposition onto charge-heterogeneous substrates, in: *Mechanical Engineering*, Alberta, 2009.
- [13] K.C. Khulbe, C.Y. Feng, T. Matsuura, *Synthetic Polymeric Membranes*, Springer, Berlin Heidelberg, 2008.
- [14] K. Boussu, B. Van der Bruggen, A. Volodin, C. Van Haesendonck, J.A. Delcour, P. Van der Meeren, C. Vandecasteele, Characterization of commercial nanofiltration membranes and comparison with self-made polyethersulfone membranes, *Desalination*, 191 (2006) 245-253.
- [15] A.S. Al-Amoudi, Factors affecting natural organic matter (NOM) and scaling fouling in NF membranes: A review, *Desalination*, 259 (2010) 1-10.
- [16] E.M. Vrijenhoek, S. Hong, M. Elimelech, Influence of membrane surface properties on initial rate of colloidal fouling of reverse osmosis and nanofiltration membranes, *J. Membr. Sci.*, 188 (2001) 115-128.
- [17] Y. He, P. Xu, C. Li, B. Zhang, High-concentration food wastewater treatment by an anaerobic membrane bioreactor, *Water Research*, 39 (2005) 4110-4118
- [18] M. Elimelech, A.E. Childress, Zeta Potential of Reverse Osmosis Membranes: Implications for Membrane Performance, in: *Water Treatment Technology Program Report No. 10*, Department of Civil and Environmental Engineering/University of California, Los Angeles, 1996.
- [19] M. Ernst, A. Bismarck, J. Springer, M. Jekel, Zeta-potential and rejection rates of a polyethersulfone nanofiltration membrane in single salt solutions, *J. Membr. Sci.*, 165 (2000) 251-259.
- [20] G. Singh, L. Song, Experimental correlations of pH and ionic strength effects on the colloidal fouling potential of silica nanoparticles in crossflow ultrafiltration, *J. Membr. Sci.*, 303 (2007) 112-118.

- [21] C. Jonsson, A.-S. Jonsson, Influence of the membrane material on the adsorptive fouling of ultrafiltration membranes, *J. Membr. Sci.*, 108 (1995) 79-87.
- [22] W. Zhang, B. Hallstrom, Membrane Characterization Using the Contact Angle Technique I. Methodology of the Captive Bubble Technique, *Desalination*, 79 (1990) 1-12.
- [23] M.J. Rosa, M.N. de Pinho, Membrane surface characterisation by contact angle measurements using the immersed method, *J. Membr. Sci.*, 131 (1997) 167-180.
- [24] D. Mockel, E. Staude, M. Dal-Cin, K. Darcovich, M. Guiver, Tangential flow streaming potential measurements: Hydrodynamic cell characterization and zeta potentials of carboxylated polysulfone membranes, *J. Membr. Sci.*, 145 (1998) 211-222.
- [25] ASTM Standard (F-316-86): Standard Test Methods for Pore Size Characteristics of Membrane Filters by Bubble Point and Mean Flow Pore Test, (1986).
- [26] ASTM Standard (F-316-03): Standard Test Methods for Pore Size Characteristics of Membrane Filters by Bubble Point and Mean Flow Pore Test, (2003).

CHAPTER 4

**SILT DENSITY INDEX AND MODIFIED FOULING INDEX
RELATION, AND EFFECT OF PRESSURE, TEMPERATURE
AND MEMBRANE RESISTANCE**

THIS CHAPTER HAS BEEN PUBLISHED:

A. Al-hadidi, A.J.B. Kemperman, , B. Blankert , J. C. Schippers, M. Wessling, W.G.J. van der Meer, Silt density index and modified fouling index relation, and effect of pressure, temperature and membrane resistance, *Desalination* (2010), doi:10.1016/j.desal.2010.11.031

In this chapter a mathematical relation between SDI and MFI0.45 has been successfully developed, assuming that cake filtration is the dominant filtration mechanism during the tests. Based on the developed mathematical relation and experiments with an artificial colloidal suspension of aluminium oxide spheres (0.6 μm) as model water, it could be demonstrated that the SDI depends on pressure, temperature and membrane resistance. The effect of temperature and membrane resistance explains to a large extent the erratic results from the field. It is recommended to correct SDI for temperature and membrane resistance and/or to making the guideline formulated by ASTM for the allowable range of membrane resistances much more stringent.

4.1. Introduction

The SDI test is applied for many years because it is cheap and simple, which explains that this test is done a routine basis by operators. However, there are growing doubts about the reliability of this test e.g. several manufacturers of micro-and ultrafiltration membranes UF are frequently confronted with the phenomenon that the filtered water does not meet the requirement and that the SDI should be lower than 3 [1]. From a theoretical point of view it is hard to explain that water filtered through membranes with pores smaller than $0.02 \mu\text{m}$ has an SDI higher than 3.

These observations might be attributed to deficiencies of the SDI test described in Chapter 2. Due to the SDI deficiencies, in the most recent standard (D 4189-07) ASTM mentioned that SDI is not applicable for the effluents from most RO and UF systems.

To overcome the main deficiencies of the SDI, the MFI0.45 has been developed by Schippers et al. This test is based on cake filtration, and is corrected for pressure and temperature [2-5]. Measurements needed for determining MFI0.45 are less simple than for the SDI test that is why MFI0.45 measurements are usually not done by operators. By definition the MFI should be corrected for the testing conditions (T , dP , A_M). The membrane resistance correction for MFI was initially proposed with an empirical equation by Heijman et al. [6]. Fully automated equipment measuring SDI and MFI0.45 at the same time is on the market.

The aim of this chapter is to reveal potential reasons for the erratic results in measuring the SDI, obtained in practice when characterizing the fouling potential of water pre-treated with ultra- and microfiltration plants. Objectives are:

- 1) to develop a mathematical relation between SDI and MFI0.45 to make it possible to demonstrate the effect of pressure, temperature and membrane resistance on SDI. In addition, such a relation might be useful in practice to convert the MFI0.45 values into SDI values;
- 2) to measure the effect of pressure, temperature and membrane resistance on the SDI with a colloidal suspension of aluminum oxide particles;

This work was performed with an α -Alumina suspension as model water. The proposed SDI/MFI relation was proven to be valid on real seawater too, as will be discussed in Chapter 7.

4.2. Theory and background

In this section the mathematical relation between SDI and MFI0.45 will be built.

4.2.1 Mathematical relation between SDI and MFI0.45

The development of the mathematical relation between SDI and MFI0.45 is based on the assumption that only cake filtration occurs during the whole test. To determine the SDI from a model, two functions are needed: a function describing the volume filtered in a certain time period: $V(t)$ and a function describing the time required to filter a certain volume: $t(V)$.

The starting point is Eqn. 2.1 which is used to calculate the SDI. In this equation t_1 and t_2 need to be determined, while t_f can be chosen. The relation between the different parameters is given below:

$$\begin{aligned} t_1 &= t_1(V_1) \\ V_f &= V(t_f) \\ t_{total} &= t_{total}(V_f + V_2) \\ t_2 &= t(V_f + V_2) - t(V_f) \end{aligned} \quad (4.1)$$

Where:

t_1 is the time to collect the volume V_1 ;

t_2 is the time to collect the volume V_2 which is equal to V_1 ; it is called V_c which is the collected filtrate volume in time t_1 or t_2 ;

V_f is volume collected in t_f ;

t_{total} is time to collect the volume $V_f + V_2$;

The parameters mentioned above are derived from Eqns. 2.1 and 2.2 according to the following steps.

1. t_1 follows from Eqn. (4.2):

$$t(V) = \frac{\mu \cdot R_M}{dP \cdot A_M} \cdot V + \frac{\mu \cdot I}{2 \cdot dP \cdot A_M^2} V^2 \quad (4.2)$$

2. Since t_2 can not be determined directly, a couple of steps are needed.

3. For calculating t_2 , first an equation has been derived from Eqn. 2.2 to obtain V as a function of t :

$$V(t) = \frac{-\mu \cdot R_M + \sqrt{\mu^2 \cdot R_M^2 + 2 \cdot I \cdot dP \cdot t}}{I \cdot \mu} \cdot A_M \quad (4.3)$$

$V_{total} = V_f + V_2$ (V_{total} , V_f and V_2 are the volumes filtered in respectively t_{total} , t_f and t_2)

4. By substitution of t_f for t in Eqn. (4.3) one obtains V_f ;
5. Substitution of V_f in Eqn. (4.2) gives t_f ;
6. t_2 follows from $t_2 = t_{total} - t_f$;
7. Substitution of t_1 and t_2 in Eqn. 2.1 results in Eqn. (4.4):

$$SDI = \frac{100}{t_r(\text{min})} \left(1 - \frac{\frac{\mu \cdot R_M}{dP \cdot A_M} \cdot V_c + \frac{1}{2} \cdot \frac{\mu \cdot I \cdot V_c^2}{dP \cdot A_M^2}}{\frac{\mu \cdot R_M}{dP \cdot A_M} \left(V_c + \frac{(-\mu \cdot R_M + \sqrt{\mu^2 \cdot R_M^2 + 2 \cdot \mu \cdot I \cdot dP \cdot A_M \cdot t_f}) \cdot A_M}{\mu \cdot I} \right) + \frac{1}{2} \cdot \frac{\mu \cdot I}{dP \cdot A_M^2} \left(V_c + \frac{(-\mu \cdot R_M + \sqrt{\mu^2 \cdot R_M^2 + 2 \cdot \mu \cdot I \cdot dP \cdot A_M \cdot t_f}) \cdot A_M}{\mu \cdot I} \right)^2} \right) - t_f \quad (4.4)$$

Where:

- I fouling potential index [m^{-2}]
- V_c volume of the first and second sample $V_c = V_1 = V_2$ [m^3]
- A_M membrane area [m^2]
- t_f elapsed filtration time (15 [min] or 900 [s])
- dP applied pressure [Pa]
- μ water viscosity [Pa.s]

Eqn. (4.4) can be used to model the SDI results, however, this relation is limited to the cake filtration mechanism and 100 % particle rejection. Eqn. (4.4) is not valid in case of cake compression.

Figure 4.1 illustrates schematically the determination steps for SDI from a time-volume curve.

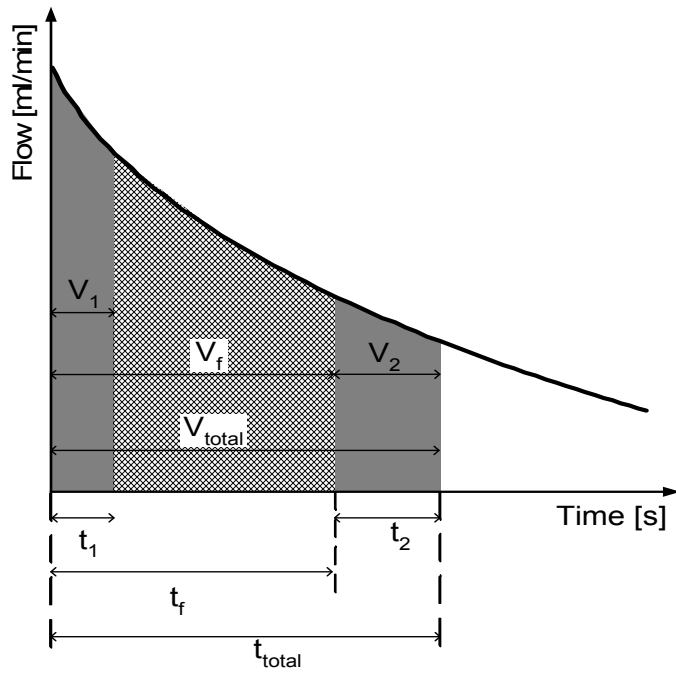


Figure 4.1. Schematic filtration diagram for calculation of the SDI out of the measured flow-time curve. V_1 and V_2 are the shaded areas under the curve.

This equation demonstrates that SDI depends on pressure, temperature and membrane resistance. SDI/MFI0.45 relation can be demonstrated by substitute Eqn. 2.3 and 2.4 in Eqn. (4.4).

4.3. Results and discussion

In this section, the modeling and the experimental results of the effect of the testing conditions and membrane resistance on the SDI results will be presented. The variation of SDI due to the range of membrane resistance that is allowed by ASTM and the available membrane in the market will be studied. Moreover, equivalent values of MFI0.45 for SDI=3 will be mathematically calculated.

4.3.1. Relation between the SDI and concentration of a colloidal suspension

The MFI0.45 has a linear relation with particle concentrations as proved by Schippers and Verdouw [2]. On the contrary SDI has a non-linear relation with the particle concentration as demonstrated in Figure 4.2 (a). In this figure the results of nine SDI test are shown, which were performed at a constant temperature of 21.5°C and a constant pressure of (207kPa) for three AKP-15 particle concentrations: 2, 4 and 8 mg/L. Three SDI test for each concentration were performed using the cellulose acetate membrane (M7) diameter 25mm.

The linear relationship between MFI0.45 with the particle concentration was confirmed by Schippers and Verdouw [2]. However, in Figure 4.2 (b) the relation between MFI0.45 and particle concentration is not a perfect linear relationship, which might be due to a particle rejection unequal to 100 %.

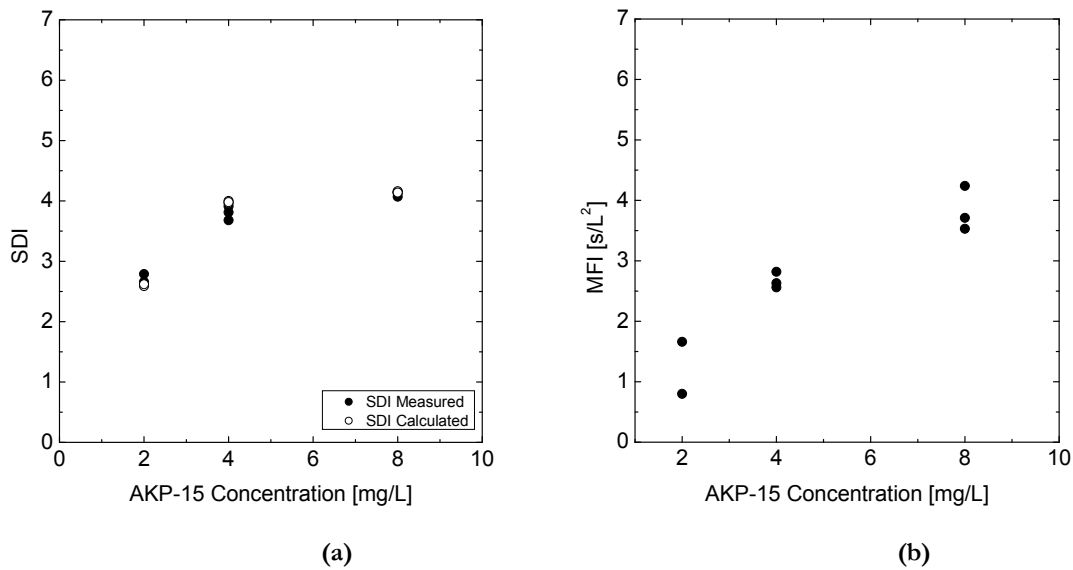


Figure 4.2. (a) Experimental and theoretical SDI (SDI-measured and SDI-calculated) results (b) MFI_{0.45} for three colloidal suspensions (2, 4 and 8 mg/L) of α -Alumina particles (AKP-15) with 0.6 μm size. The filtration experiments were carried out using cellulose acetate membrane M7 (25 mm diameter).

The difference between the SDI-measured and SDI-calculated is marginal and indicates that cake filtration is dominant. This conclusion is supported by Figure 4.3 showing t/V versus V , having an almost linear relation. The effect of different fouling mechanisms on the SDI will be presented in a future article [7].

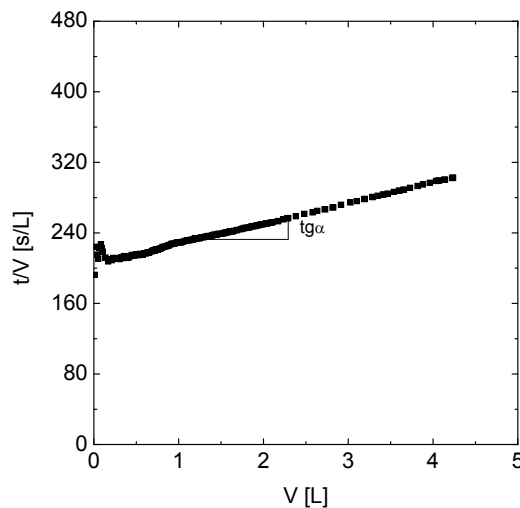


Figure 4.3. $\text{tg}\alpha$ calculated out of the t/V versus V curve. Filtration test of 4 mg/L AKP-15 particle solution in ultra-pure water using M7 (25 mm diameter). The test was under a constant pressure difference (dP) of 207 kPa and a temperature (T) of 20 $^{\circ}\text{C}$.

4.3.2. Effect of applied pressure

The ASTM procedure requires a constant pressure difference over the membrane of 207 kPa (± 7 kPa) during the SDI test. To demonstrate the theoretical effect of different applied pressures, Eqn. (4.4) was used at different values of MFI0.45 (0.2-10 s/L²). The reference parameters assumed were: feed temperature 20 °C, membrane resistance R_{MO} 1.29×10^{10} m⁻¹ and membrane area A_M 13.8×10^{-4} m².

Table 4.1 shows that the ASTM allowable range of dP (± 7 kPa) results in an SDI deviation of $\approx \pm 0.04$ at SDI₀=3.

Table 4.1 The deviation in SDI value due to ± 7 kPa variation in dP_0 for different SDI levels.

$SDI(dP_0 \text{ kPa})$	$SDI(dP_0 + 7 \text{ kPa})$	$SDI(dP_0 - 7 \text{ kPa})$
1	1.03	0.98
2	2.04	1.97
3	3.04	2.96
4	4.04	3.96

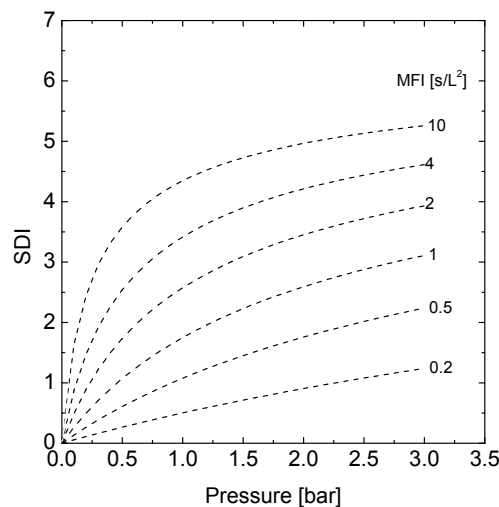


Figure 4.4. Theoretical SDI results for different applied pressures (dP) and different MFI0.45 values (0.2-10 s/L²). The calculation was performed with reference conditions membrane resistance (R_M) 1.29×10^{10} m⁻¹, membrane area (A_M) 13.8×10^{-4} m² and feed temperature 20 °C.

Figure 4.4 shows the results of the calculated SDI as a function of the pressure. The higher the pressure, the higher the SDI. At low MFI0.45 (i.e. a low particle concentration), the influence of the applied pressure in SDI is higher (higher slope).

To verify the results of these calculations the effect of pressure was measured experimentally. For this purpose SDI tests were carried out using membrane M7 and a suspension of α -Alumina particles (AKP15) at various pressures: 0.5, 2.07 and 3 bar (50, 207 and 300 kPa). All the experiments were performed at room temperature (20 °C).

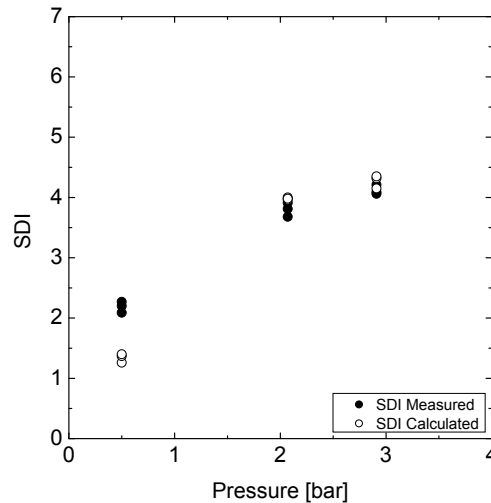


Figure 4.5. SDI theoretical and experimental results for different applied pressure (50, 207 and 300kPa) with an AKP-15 particle concentrations of 4mg/L.

Figure 4.5. shows that the experimental results are in good agreement with the theoretical predictions at 207 and 300 kPa. At 50 kPa however, the results are lower than the experimental results. Figure 4.4 shows that the slope of the SDI/dP relation decreases with increase dP . Therefore, the deviation between the measured and calculated SDI might be attributed to the high sensitivity of SDI for error at low SDI values. Furthermore, at low dP the fouling load arrived to the membrane surfaces lower than high dP case. This relaxation affects the cake formation time and density which influence SDI value as well.

4.3.3. Effect of temperature

Based on Eqn. (4.4) the effect of temperature on SDI was studied for assumed MFI0.45 values at a membrane resistance R_{MO} of $1.29 \times 10^{10} \text{ m}^{-1}$, a membrane area A_{MO} of $13.8 \times 10^{-4} \text{ m}^2$ and constant pressure difference dP_O of 207 kPa. Figure 4.6 demonstrates that the SDI increases with increasing temperature. This effect is because of the temperature dependency of the viscosity

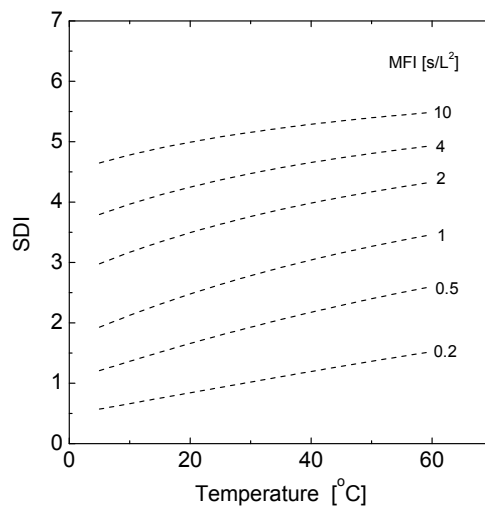


Figure 4.6. Theoretical SDI results for different temperatures (T) and different MFI0.45 values (0.2-10 s/L²). The calculation is carried out with the following reference conditions: a membrane resistance (R_{MO}) of 1.29×10^{10} m⁻¹, a membrane area (A_{MO}) of 13.8×10^{-4} m² and a constant applied pressure difference (dP_O) of 207kPa.

In the desalination field, RO plants might operate either in hot areas (e.g. in the Middle East up to 40°C) as well as in cold areas (e.g. in Europe down to 5 °C). Consequently, the SDI results need to be corrected for the feed water temperature in order to compare them.

To verify the predicted results experimentally, the SDI of a colloidal suspension of 4 mg/L α -Alumina particles (AKP-15) has been measured using membrane M7 at different feed temperatures (8, 22, and 38 °C). Three SDI tests were carried out for each temperature. The results of these experiments and the theoretical prediction of the SDI are shown in Figure 4.7.

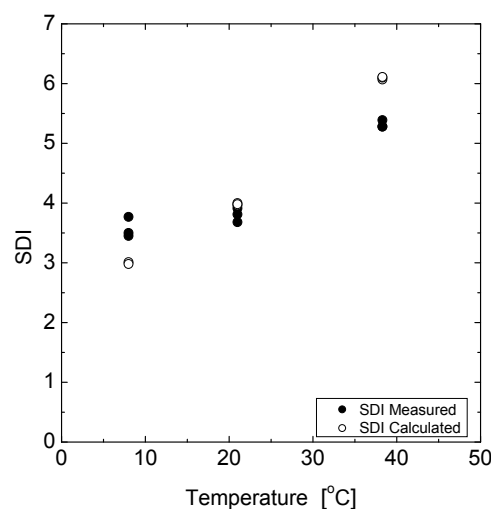


Figure 4.7. Calculated and measured SDI values for different 8, 22 and 38 °C of a colloidal suspension of 4 mg/L of AKP-15.

Theoretical results are in good agreement at 22 °C. However, at 8 °C and 38 °C the theoretical results deviate from the experimental results. The artifacts that happened during the test affect the SDI value. The sensitivity for error is higher at low T than high T . However, the foulants-foulants and foulants-membrane interaction was not cooperated in the modeling calculation for SDI

4.3.4. Effect of the membrane resistance

4.3.4.1 ASTM Allowable range for R_M

In order to demonstrate the effect of the membrane resistance on SDI, the following reference testing conditions were set: A_{MO} 13.8×10^{-4} m², T 20 °C and dP 207 kPa. The SDI/MFI0.45 relation is shown in Figure 4.8 (a) for different membrane resistances: the ASTM allowable range $0.86 - 1.72 \times 10^{10}$ m⁻¹, and the range for what is available in the market $0.39 - 2.65 \times 10^{10}$ m⁻¹. Figure 4.8 (a) demonstrates a very pronounced effect of membrane resistance on the SDI value. As a consequence the SDI value for water with a fouling potential of MFI0.45 = 2 might vary between 1.7 and 5.6 depending on a membrane resistance between 0.86×10^{10} and 1.72×10^{10} m⁻¹ (the ASTM standard). The pure water flow guidelines set by the ASTM, indirectly for the resistance of the used membranes, are much too broad to ensure correct and comparable SDI values.

Table 4.2 The deviation in SDI value due to the ASTM range and $\pm 10\%$, $\pm 20\%$ variation in R_{MO} .

$SDI(R_{MO})$	$SDI(R_{MO} \pm 10\%)$	$SDI(R_{MO} \pm 20\%)$	$SDI(R_{MO} \text{ ASTM range})$
1	0.86 – 1.18	0.71 – 1.40	0.60 – 1.81
2	1.79 – 2.26	1.60 – 2.65	1.38 – 3.00
3	2.76 – 3.26	2.54 – 3.55	2.29 – 3.98
4	3.79 – 4.23	3.59 – 4.46	3.34 – 4.78

The ASTM wide range of allowable membrane resistances explains at least at part of the frequently reported erratic results in practice. Table 4.2 shows the influences of $\pm 10\%$ and $\pm 20\%$ on the SDI results. From a practical point of view, the influence of 10% in R_M results in SDI deviation with $\approx \pm 0.26$ at SDI = 3 is acceptable. Therefore, to avoid the SDI deficiency of the SDI it is recommended to narrow the allowable range to the reference R_{MO} value 1.29×10^{10} m⁻¹ $\pm 10\%$.

Figure 4.8 (b) shows the deviation in SDI values as result of ASTM range, available range in the market, 10 % and 20 % variation in R_{MO} .

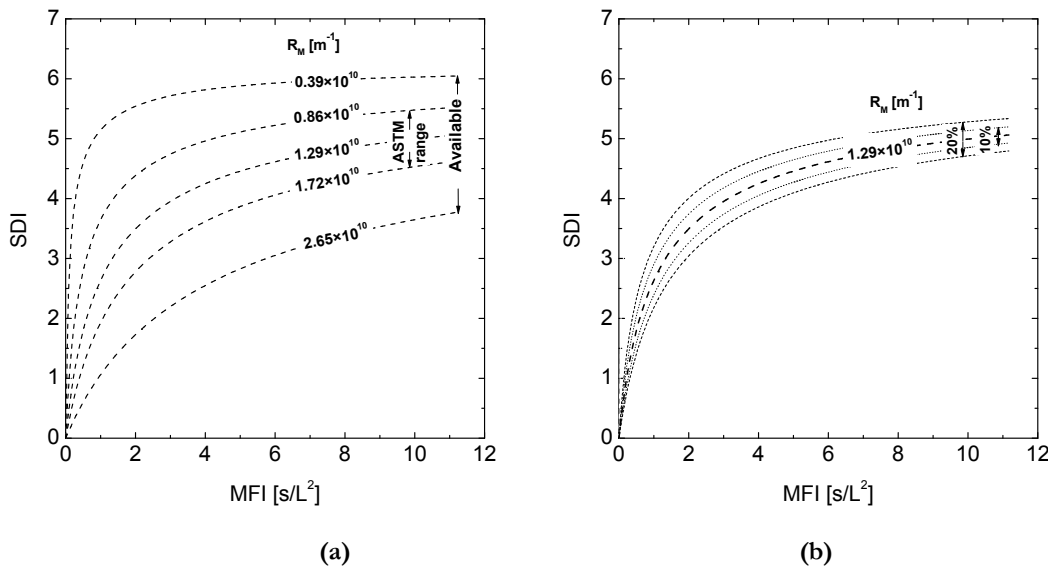


Figure 4.8. The mathematical relation between SDI and MFI0.45 as a function of the membrane resistance.
 (a): ASTM range: 0.86×10^{10} to 1.72×10^{10} . Range of what is available in the market: 0.39×10^{10} to 2.65×10^{10} m⁻¹.
 (b): (Suggested allowable range: $\pm 10\%$, $\pm 20\%$ of R_{MO} 1.29×10^{10} m⁻¹).
 Reference conditions assumed: a membrane area (A_{MO}) of 13.8×10^{-4} m², a temperature of T_O 20 °C and a pressure difference (dP_O) of 207kPa

4.3.4.2 Experimentally determined effect of membrane resistance

To demonstrate experimentally the effect of the membrane resistance on SDI, different membranes made of different materials and by different manufactures were used Table 3.1. In the tests a colloidal suspension of 4 mg/L α -Alumina particles (AKP-15) was applied. The temperature was 21 °C and the pressure was 207 kPa. The measured SDI results were plotted vs. the clean membrane resistance in Figure 4.9. Besides that, the fouling potential index I was calculated for each experiment Subsequently Eqn. (4.4) was used to calculate the theoretical SDI values for each experiment.

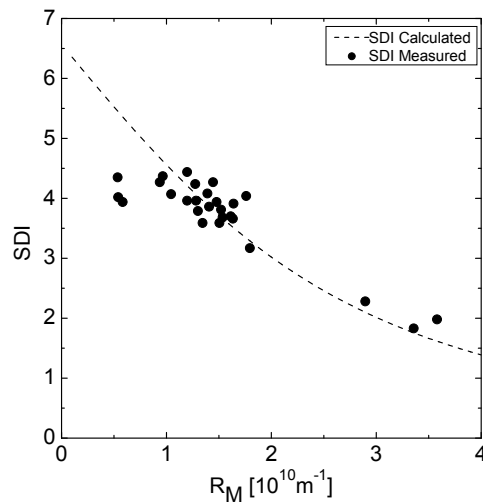


Figure 4.9. SDI experimental and theoretical results as a function of the membrane resistance for different membranes Table 3.1. The experiments were carried out using a particles concentration of 4 mg/L AKP-15 and a pressure difference of 207 kPa.

The theoretically and experimentally determined relation between membrane resistance with SDI are in good agreement and show a strong dependency of the membrane resistance, e.g. increasing the membrane resistance from $0.5 \times 10^{10} \text{ m}^{-1}$ to $3.5 \times 10^{10} \text{ m}^{-1}$ results in a reduction of the SDI from 4.5 to 2 for the same water quality. At low R_M , the measured SDI values that deviate from the calculated SDI may be due to the SDI sensitivity for error and artifacts.

This tremendous effect has to be attributed to the fact that the rate of filtration, and consequently the fouling load, depends on the resistance of the membrane used.

In the SDI test is the time between the two measurements is fixed and the volume that is filtered in that time depends on the flow rate. Thus, any effect that increases the flow through the membrane will increase the fouling load of the membrane incrementally and consequently the measured SDI. This explains our observation that the SDI increases with increasing temperature (decreasing viscosity so increasing flow), increasing pressure and decreasing membrane resistance.

4.3.5. Equivalent MFI0.45 value for $SDI_{15}=3$

In practice it is commonly accepted that the SDI of RO feed water preferably should be lower than 3. Taking into account the deficiencies in the SDI method, the MFI0.45 method is to be preferred. Besides the less simple procedure, the other hurdle needs to be taken is defining a similar guideline like $SDI < 3$ for MFI0.45.

In principle this guideline can be simply derived for e.g. $SDI = 3$ by making use of Eqn. (4.4). However doing so it will turn out that it is not possible to get one distinct guideline value. The reason is that the SDI strongly depends on the membrane resistance. This effect is illustrated in Figure 4.5 showing the calculated MFI0.45 values for $SDI = 3$. This means that a wide range of MFI0.45 values are equivalent to $SDI = 3$. Limiting the range of allowable membrane resistances according to ASTM reduces the equivalent MFI0.45 guideline to the range of 0.6 to 2.4 s/L². This situation again clearly demonstrates the need of narrowing down the allowable range of resistances of the applied membranes.

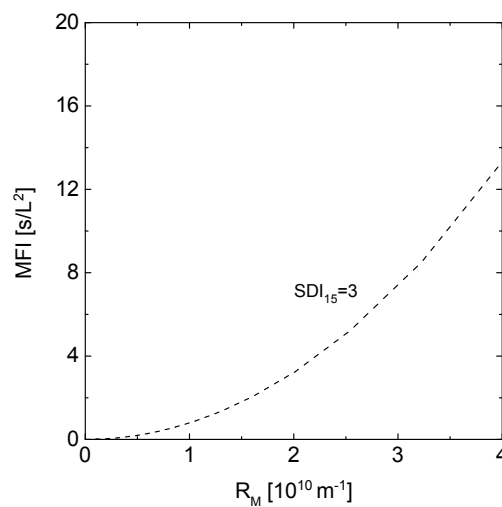


Figure 4.10. Equivalent MFI0.45 values for $SDI=3$ for different membrane resistances (R_M). The calculations were performed with the following reference conditions: an applied pressure difference of 207 kPa, a feed temperature of 20 °C and a membrane area of $13.8 \times 10^{-4} \text{ m}^2$.

4.3.6. Normalizing SDI

Large deviations might occur in measuring the SDI, due to differences in membrane resistance, temperature and pressure. These observed variations are unacceptably large. So it is recommended to reduce these variations by normalizing the obtained results. The mathematical bridge SDI/MFI0.45 in model Eqn. (4.4) gives can be used for this purpose. Normalizing needs to define reference values for the testing conditions. The reference conditions are listed in Table 2.3.

The proposed correction is based on the assumption that cake filtration occurs and effects of variations in rejection can be neglected. However it is well known that during the SDI test, initially pore blocking occurs. The length of these periods varies with the type of particulate

matter e.g. particle size distribution. Furthermore it is known that particles smaller than 0.45 μm are passing at least partly the membrane filters. During filtration a part of these particles might be rejected, due to narrowing of the pores and/or formation of the cake. This means that the proposed normalization will improve the accuracy and reproducibility of the SDI, but that the proposed corrections are not fully covering reality.

Reducing the allowable range of the membrane resistance might be useful to eliminate at least the dramatic effect of variations in the membrane properties. From a practical point of view, it is reasonable to use a membrane with a resistance of $1.29 \times 10^{10} \text{ m}^{-1}$ and allowing variations of $\pm 10\%$ and acceptable variation in SDI ± 0.25 at a level of SDI=3. Additional studies on normalizing SDI are ongoing and will be published in Chapter 7.

4.4. Conclusion

A mathematical relation between SDI and MFI_{0.45} has been developed. This relation is valid under the conditions that cake filtration occurs during the whole filtration test and variations in rejection have no effect on the SDI/MFI_{0.45} results.

Based on this relation and experiments the following can be concluded:

- The SDI depends on pressure, the higher the pressure the higher the SDI;
- A pronounced effect of temperature exists;
- The membrane resistance has a very dominant effect on the SDI.

A higher membrane resistance results into dramatically lower SDI values. The indirectly formulated guideline by ASTM for an acceptable range for membrane resistance R_M (between $0.86 \times 10^{10} < R_M < 1.72 \times 10^{10} \text{ m}^{-1}$) is far from adequate. The allowable variations in membrane resistance are responsible for values of the SDI between 2.29 and 3.98 at a level of $\text{SDI}_O=3$.

It is therefore recommended:

- 1) to narrow the resistance range to e.g. $1.29 \times 10^{10} \text{ m}^{-1} \pm 10 \%$ ($1.16 \times 10^{10} < R_M < 1.42 \times 10^{10}$); this range results in deviations of ± 0.25 in SDI value (at $\text{SDI} = 3$);
- 2) to correct the SDI for temperature and membrane resistance.

The effects of temperature and variations in membrane resistance on SDI explain to a large extent the erratic results reported in practice. Therefore, there is a strong need for normalization. This work was performed with a model water consisting of an α -Alumina suspension. However, the proposed SDI/MFI relation was proven to be valid for real seawater too as will be presented in Chapter 8 [8]. The effect of different fouling mechanisms on the SDI will be shown in Chapter 5 [7].

References

- [1] R. Nagel, Seawater desalination with polyamide hollow fiber modules at DROP, *Desalination*, 63 (1987) 225-246.
- [2] J.C. Schippers, J. Verdouw, The modified fouling index, a method of determining the fouling characteristics of water, *Desalination*, 32 (1980) 137-148.
- [3] S.F.E. Boerlage, M.D. Kennedy, P.A.C. Bonne, G. Galjaard, J.C. Schippers, Prediction of flux decline in membrane systems due to particulate fouling, *Desalination*, 113 (1997) 231-233.
- [4] S.F.E. Boerlage, M.D. Kennedy, M.R. Dickson, D.E.Y. El-Hodali, J.C. Schippers, The modified fouling index using ultrafiltration membranes (MFI-UF): characterisation, filtration mechanisms and proposed reference membrane, *J. Membr. Sci.*, 197 (2002) 1-21.
- [5] M.A. Javeed, K. Chinu, H.K. Shon, S. Vigneswaran, Effect of pre-treatment on fouling propensity of feed as depicted by the modified fouling index (MFI) and cross-flow sampler-modified fouling index (CFS-MFI), *Desalination*, 238 (2009) 98-108.
- [6] B. Heijman, E.V.D. Baan, G.V.D. Haar, Betrouwbaarheid Membraan-Filtratie-Index kan aanzienlijk vergroot worden, *H₂O - Tijdschrift voor watervoorziening en waterbeheer* 12 (2000) 21-23.
- [7] A. Alhadidi, B. Blankert, A.J.B. Kemperman, J.C. Schippers, M. Wessling, W.G.J. van der Meer, Effect of testing conditions and filtration mechanisms on SDI, Submitted to *J. Membr. Sci.*, (2010).
- [8] A. Alhadidi, A.J.B. Kemperman, J.C. Schippers, M. Wessling, W.G.J. van der Meer, Evaluate the fouling challenge in a RO/UF desalination plant using SDI, SDI⁺ and MFI, Submitted to *Desalination*, (2010).

CHAPTER 5

EFFECT OF TESTING CONDITIONS AND FILTRATION MECHANISMS ON SDI

THIS CHAPTER HAS BEEN SUBMITTED TO PUBLICATION:

A. Al-hadidi, A.J.B. Kemperman, B. Blankert, J. C. Schippers, M. Wessling, W.G.J. van der Meer,
Effect of testing conditions and filtration mechanisms on SDI, J. Membr. Sci.

To identify opportunities for improvements, mathematical models were developed in this Chapter to study the effect of temperature, applied pressure and membrane resistance on the SDI value under four different fouling mechanisms. Significant variations in SDI values are observed mathematically as a result of differences in temperature and membrane resistance for the same water quality. The fouling mechanisms are described by the relationship between the filtrated volume w and the total resistance R . The sensitivity of the SDI for variations in the testing parameters theoretically increases when the relation between w and R is stronger.

The SDI increases with an increase in the feed temperature and the applied pressure. The SDI value decreases when membranes with a high resistance are used.

Temperature has a substantial effect on SDI. As a consequence it is not recommended to compare of SDI values measured at different temperatures. To achieve a more reliable SDI, the use of a standardized membrane with constant properties, in particular having a narrow range of resistance, is recommended.

5.1 Introduction

Membrane fouling may manifest in deposition/growth on membrane surface and/or spacers in spiral wound RO membrane elements. Remedial actions are commonly taken e.g. regular chemical cleaning of the membrane elements. However frequent cleaning will shorten the life time of the membranes.

SDI is commonly used to judge the performance of pre-treatment systems – including micro- and ultrafiltration – as well.

Besides the reported poor reproducibility, doubts are growing about the predictive value of the SDI. These doubts are based on the inability to capture small particles, which might foul RO membranes, having much smaller pores than $0.45\ \mu\text{m}$. For this purpose the MFI (0.05) and MFI-UF and MFI-NF has been developed [1-7]. The applicability of these tests in predicting fouling of RO membranes will not be discussed.

Four main fouling mechanisms commonly encountered in membrane filtration can be categorized to:

- cake filtration;
- intermediate blocking;
- standard blocking;
- complete blocking;

In the cake filtration, the particles precipitated on the membrane surface. The pore blocking occurs when large particle seal the pore mouth. The small particle adsorbed in side the pores results in narrowing the pore. The four fouling mechanisms can be used to study and predict the fouling membrane behavior. In this Chapter, the four fouling mechanisms will be used to study the effects of the testing conditions on the SDI results.

The objective of this Chapter is to investigate the influence of temperature, pressure and membrane resistance on SDI, assuming four different fouling mechanisms namely.

For this purpose theoretical models are developed and applied to simulate different test conditions. The results of these simulations are compared with experimental tests, making use of aluminum oxide particles ($0.6\ \mu\text{m}$) as model colloid.

5.2 Theory and background

In this section the four fouling models will be discussed.

5.2.1 Fouling model

Assuming constant retention, for dead-end filtration and an initially clean membrane, the fouling state is defined by:

$$\frac{dw}{dt} = J \quad (5.1)$$

In which J is the filtration flux and w is the filtration state (filtrated volume per unit area).

Blankert et al. [8] generalized the relations between the total resistance and the filtrated volume for each of the four fouling mechanisms, by writing the equations in a common form:

$$\frac{dR}{dw} = C \cdot R^m \quad (5.2)$$

R is the total resistance, and C and m are constants depending on the filtration mechanisms. Table 3.1 shows the resulting resistance R as a function of the filtration state w , the membrane resistance R_M and the fouling potential of the feed.

The resistance R is calculated using Darcy's law Eqn. (3.3) [9]:

$$R = \frac{dP}{\mu \times J} \quad (5.3)$$

The relative difficulty of operation (γ) due to membrane fouling was introduced by Blankert et al. [8]. Conceptually, the difficulty of operation is the ratio between the total resistance and the membrane resistance:

$$\gamma = \frac{R}{R_M} \quad (5.4)$$

Where R is the total resistance and R_M is the membrane resistance.

The trajectory of this variable can be calculated from the fouling model parameters (C and m) and the operating strategy parameter s . The values for s equal to 0, 1 and 0.5 define constant flux, constant pressure and constant power filtration, respectively. The relative difficulty of operation in time is given by [8]:

$$\gamma(t) = \begin{cases} (1 + (s - m + 1)K_o \cdot t)^{1/(s-m+1)} & s - m + 1 \neq 0 \\ e^{K_o \cdot t} & s - m + 1 = 0 \end{cases} \quad (5.5)$$

Where the parameter K_o is defined as:

$$K_o = C \cdot J_o \cdot R_M^{m-1} = \frac{C \cdot dP \cdot R_M^{m-2}}{\mu} \quad (5.6)$$

With J_o as the initial flux and μ as the water viscosity.

The state trajectory may be given by:

$$w(t) = \begin{cases} \frac{1}{C} \frac{R_M^{1-m}}{1-m} (\gamma^{1-m} - 1) & 1-m \neq 0 \\ \frac{1}{C} \ln(\gamma) & 1-m = 0 \end{cases} \quad (5.7)$$

5.3 Results and discussion

The SDI sensitivity for the variation in the particle concentration and the testing parameters will be described in this section. The theoretical results will be confirmed experimentally using a AKP-15 model feed water.

5.3.1 Mathematical model

Based on Eqn. (5.7), the accumulated volume can be defined as $V(t) = w(t) \times A_M$. The SDI is determined under constant pressure, and therefore s is equal to 1. The filtrated volume V can be calculated by substituting Eqn. (5.6) and Eqn. (5.5) into Eqn. (5.7) and results in Eqn. (5.8):

$$V(t) = \begin{cases} \frac{A_M \cdot R_M^{1-m}}{C \cdot (1-m)} \left(\left(1 + \frac{(2-m) \cdot C \cdot dP \cdot R_M^{m-2} t}{\mu} \right)^{\frac{1-m}{2-m}} - 1 \right) & m \neq 1,2 \\ A_M \cdot w_A \ln \left(1 + \frac{dP \cdot t}{w_A \cdot \mu \cdot R_M} \right) & m = 1 \\ A_M w_A \left(1 - e^{-\frac{dP t}{w_A \mu R_M}} \right) & m = 2 \end{cases} \quad (5.8)$$

The time t to collect filtration volume V can be calculated by inverting Eqn. (5.8):

$$t(V) = \begin{cases} \frac{\mu}{(2-m) \cdot C \cdot dP \cdot R_M^{m-2}} \left(\left(\frac{V \cdot C \cdot (1-m)}{R_M^{1-m} \cdot A_M} + 1 \right)^{\frac{2-m}{1-m}} - 1 \right) & m \neq 1,2 \\ \left(e^{\frac{V}{w_R \cdot A_M}} - 1 \right) \cdot \frac{R_M \cdot w_R \cdot \mu}{dP} & m = 1 \\ \ln \left(\frac{A_M \cdot w_A}{A_M \cdot w_A - v} \right) \cdot \frac{R_M \cdot w_A \cdot \mu}{dP} & m = 2 \end{cases} \quad (5.9)$$

5.3.2 Calculating SDI

Eqns. (5.8)&(5.9) can be combined to give the analytical expression for the SDI.

With the functions $t(V)$ and $V(t)$, t_1 and t_2 can be determined which are needed to calculate the

SDI in Eqn (2.1):

$$\begin{aligned}
 t_1 &= t(V_1) \\
 V_{15} &= V(t_{15}) \\
 t_{total} &= t(V_{15} + V_2) \\
 t_2 &= t(V_{15} + V_2) - t(V_{15})
 \end{aligned}
 \tag{5.10}$$

These parameters are derived from Eqns. (5.8) & (5.9) using the following steps;

1. t_1 follows from Eqn. (5.9)
2. t_2 can not be determined directly and as a consequence a couple of steps are needed.
3. $V_{total} = V_f + V_2$ (V_{total} , V_f and V_2 are the volumes filtered in respectively t_{total} , t_f and t_2)
4. Substitution of t_f for t in Eqn. (5.8) obtains V_f
5. Substitution of V_t in Eqn. (5.9) gives t_f
6. t_2 follows from $t_2 = t_{total} - t_f$
7. The SDI is calculated by substitution of t_1 and t_2 in Eqn. (2.1)

The filtrated volume as function of time (V vs. t) can plotted in a typical fouling curve as schematically presented in Figure 5.1. Additionally, Figure 5.1 illustrates schematically the determination steps for SDI from a time-volume curve.

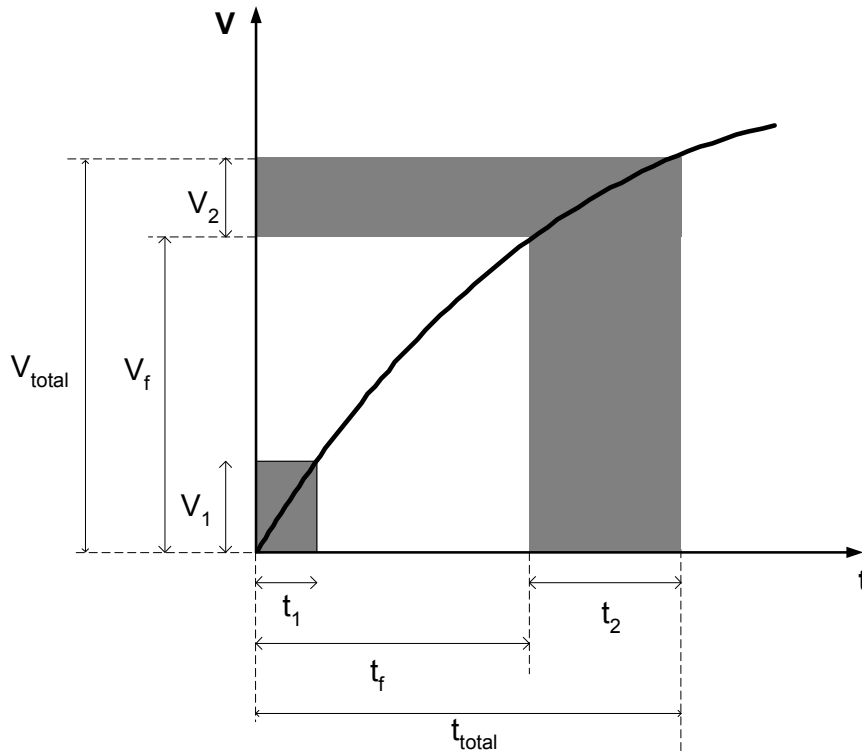


Figure 5.1. Theoretical diagram showing the filtrated volume as function of time and the variables used to determine SDI.

5.3.3 Theoretical SDI sensitivity

An ideal fouling index should have a linear relationship with the relevant particle concentration in the feed water and should not be sensitive for the testing condition parameters nor the membrane resistance. The sensitivity of the SDI results for particle concentration and testing parameters such as feed water viscosity (μ), membrane area A_M , applied pressure dP and membrane resistance R_M will be investigated in this section. Eqns. (5.8) & (5.9) were used in this study by fixing the defined reference testing conditions and varying the target parameters one by one.

5.3.3.1 Fouling potential and particle concentration

The effects of different fouling mechanisms on the SDI will be demonstrated. Besides that, the influence of the main four fouling mechanisms on SDI results will be compared using Eqn. (5.8) & (5.9). The value of parameter m (0, 1, 1.5 or 2) indicates the fouling mechanism. For each fouling mechanism (or m value), the feed fouling potentials $w_{(R,A,V)}$ were determined for $SDI =$

3. Table 5.1 shows the $w_{(R,A,V)}$ values for each of the four fouling mechanisms corresponds to $SDI_0=3$.

Table 5.1 $w_{(R,A,P)}$ values for each fouling mechanism.

Details	m	Fouling potential	$w_{(R,A,V)}$ [m] values for $SDI=3$
Cake filtration	0	w_{RO}^*	12.2
Intermediate blocking	1	w_{AO}	17.5
Standard blocking	1.5	w_{VO}	40.5
Complete blocking	2	w_{AO}	24.3

* Corresponding to $R_C = 1.056 \times 10^9 \text{ m}^{-2}$

The sensitivity of the SDI to the feed fouling potential was studied as follows. By assuming $w_{(RO,AO,VO)}$ in Table 5.1 are the 100 % values, the $w_{(RO,AO,VO)}$ values were varied in small steps between 40 % to 180 % of this value. Subsequently the ratios of the $w_{(R,A,V)}$ to $w_{(RO,AO,VO)}$ values were plotted in Figure 5.2(a,b), which shows the sensitivity of SDI for $w_{(R,A,V)}$ and particle concentration for the different m values. $w_{(R,A,V)}$ by definition is inversely proportional to particle concentration.

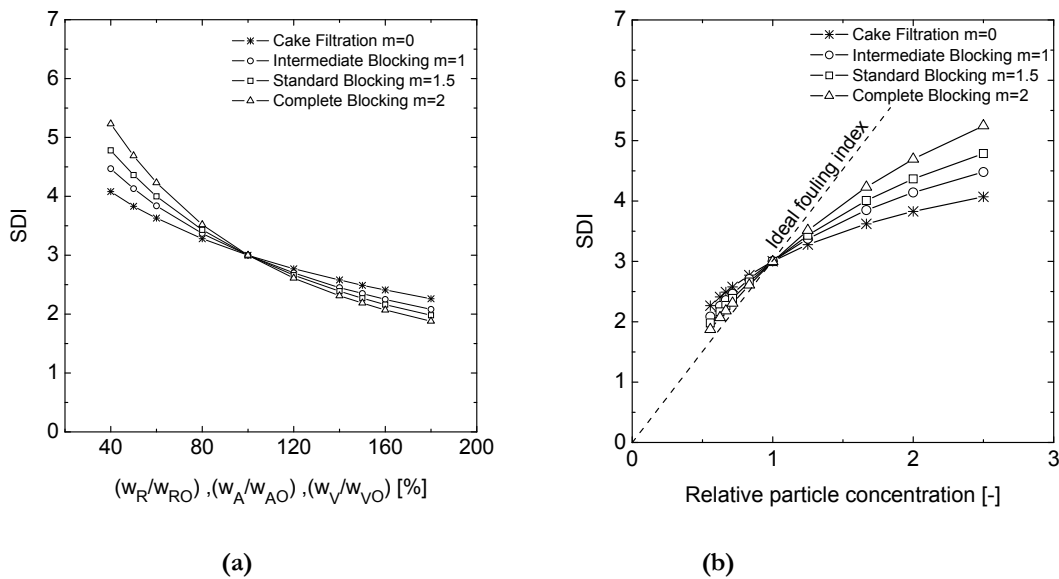


Figure 5.2. The effect of different fouling mechanisms on the SDI. (a) SDI as a function of w_R , w_A and w_V . (b) SDI as a function of the particle concentration. Assuming the reference testing conditions, Eqn. (5.8) & (5.9) were used for calculating the SDI values for different fouling potentials and different fouling mechanisms.

As expected, the fouling potential $w_{(R,A,V)}$ is inversely related to the SDI: the lower the fouling potential $w_{(R,A,V)}$, the higher the SDI. The particle concentration is non-linearly related to the

SDI shown in Figure 3b. However, the ideal fouling index should have a linear relationship to the particle concentration. The SDI sensitivity due to an increase in the fouling potential is higher if the complete blocking dominates the fouling mechanism. SDI is less sensitive if cake filtration is the main fouling mechanism.

5.3.3.2 Feed water viscosity (μ):

To investigate the sensitivity of the SDI for feed water viscosity, the feed temperature was varied between 5 and 50 °C. By changing the feed temperature, the feed water viscosity is affected. The effect of the temperature on the membrane properties (pore size etc.) was neglected. In practice, the feed water temperature in desalination plants does not exceed 45 °C. Figure 5.3 (a) and (b) show the effect of the feed water viscosity and feed water temperature on SDI results. The figures shows that the temperature clearly influences the SDI value. The sensitivity of the SDI for temperature is higher under a pore blocking mechanism than with cake filtration.

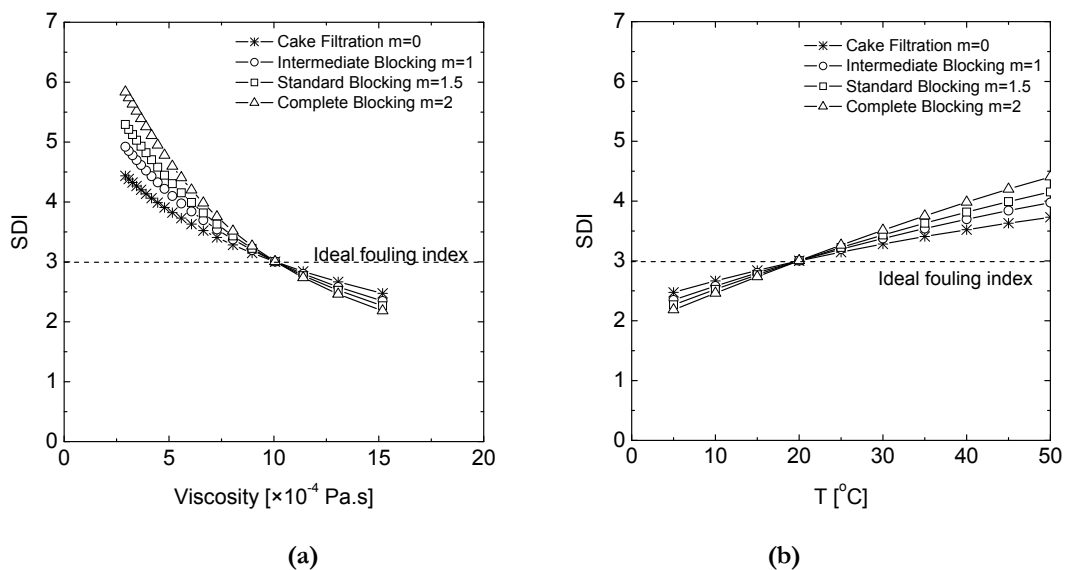


Figure 5.3. The effect of the feed viscosity on SDI results. (a) SDI as a function of feed water viscosity, (b) SDI as a function of feed water temperature. Assuming the reference testing conditions, Eqn. (5.8) & (5.9) were used to calculate SDI values for different fouling mechanisms. The viscosity was varied between $(2.5 \text{ to } 15) \times 10^{-4} \text{ Pa.s}$ by varying the feed temperature between 5 and 50 °C.

5.3.3.3 Membrane area (A_M):

A diameter of 47 mm was defined as standard filter size by the ASTM to be used for the SDI test with a sample volume of 500 mL. However, diameters of 25 or 90 mm may be used as well according to the ASTM protocol. The sample volume should be adjusted in direct proportion with the filter area. In this work, the effect of membrane area A_M on SDI was studied using Eqns. (5.8) & (5.9). In accordance with the note in the ASTM standard, Figure 5.4 proves that the membrane area A_M has no influence on the SDI results. In other words, the SDI can be obtained using any membrane size as far as the sample volume is adjusted in direct proportion to the membrane area.

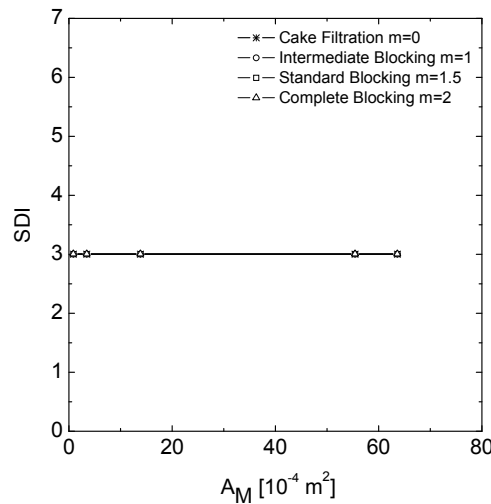


Figure 5.4. The effect of the membrane area on SDI result. Assuming the reference testing conditions, Eqn. (5.8) & (5.9) were used to calculate SDI values for different fouling mechanisms. The membrane area was varied from 10×10^{-4} to $65 \times 10^{-4} \text{ m}^2$.

5.3.3.4 Applied pressure (dP):

The applied pressure is the driving force during the SDI test. According to the ASTM standard, SDI tests require an applied constant pressure $207 \pm 7 \text{ kPa}$. Eqns. (5.8) & (5.9) were used to study the effect of the applied pressure on SDI results. Standard reference conditions in Table 2.3 were assumed and the applied pressure was varied between 0 and $4 \times 10^5 \text{ Pa}$ (0 to 4 bar). The calculated SDI was plotted versus the assumed applied pressure in Figure 5.5. The figure shows that the applied pressure influences the SDI measurement. SDI is more sensitive

for a change in the applied pressure under the pore blocking mechanism than under the cake filtration mechanism.

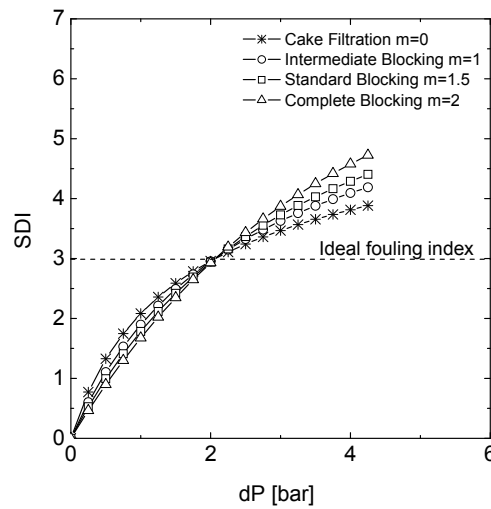


Figure 5.5. The effect of the applied pressure on SDI results. Assuming the reference conditions, Eqn. (5.8) & (5.9) were used to calculate SDI values for different fouling mechanisms. The applied pressure was varied from 0 to 4×10^5 Pa (0 to 4 bar).

5.3.3.5 Membrane resistance (R_M):

The membrane resistance is a membrane constant which does not depend on the feed composition nor on the applied pressure. Eqn. (5.8) & (5.9) together with the defined reference conditions and $w_{(R,A,V)}$ values in Table 5.1 were used to calculate the SDI as a function of the membrane resistance. In Figure 5.6, the calculated SDI results were plotted for different membrane resistances. The figure shows that for all 4 fouling mechanisms with increasing membrane resistance the measured SDI value decreases.

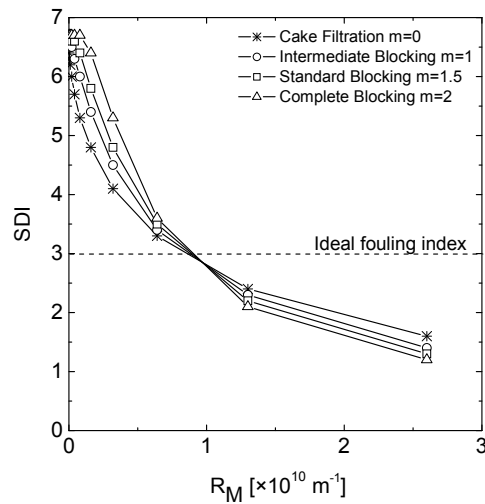


Figure 5.6. The effect of the membrane resistance on SDI results. Assuming the reference conditions, Eqn. (5.8) & (5.9) were used to calculate SDI values for different fouling mechanisms. The membrane resistance was varied from 0 to $2.75 \times 10^{10} \text{ m}^{-1}$.

The clean membrane resistance R_M is, amongst others, dependent on the pore size distribution, number of pores, pore length, tortuosity and hydrophilicity. Fouling is a result of interaction between the membrane and feed water. Thus, membrane resistance is in practice hard to vary independently.

If it is assumed that the retention does not change, the specific cake resistance is not affected by the membrane properties. One should be careful however, since w_R is defined relative to the membrane resistance as follow:

$$w_R = \frac{R_M}{R_C} \quad (5.11)$$

Where R_M is the membrane resistance and R_C is the specific cake resistance.

The pore blocking mechanisms (complete, intermediate, standard) are directly related to the pore volume and pore area. If it is assumed that the membrane resistance can be varied without changing the volume and area of the pores, it follows that $w_{A,V}$ are independent parameters of the clean membrane resistance effect.

5.3.4 Experimental results

To validate the model, SDI tests are performed for model feed waters with different AKP-15 particle concentrations. The experimental results will be compared to the modeling results. In this way, the limitations of the modeling will be studied.

Different concentrations of α -Alumina (AKP-15) particles in ultra-pure water were prepared (0, 2, 4, 6, 8 and 10 mg/L). Three SDI tests were carried out for each concentration using the cellulose acetate MF membrane M7. In order to determine the parameters C , m and R_M , the best fits were calculated for the raw data (w and R) assuming one single fouling mechanism. The mathematical Eqn. (5.8) & (5.9) and the measured testing parameters (T , dP and R_M) were used to calculate t_1 , t_2 and the SDI.

To determine the theoretical SDI values for different particle concentrations, the following procedure was applied. Assuming that cake filtration is the dominating fouling mechanism during the SDI measurements, w_R values obtained from the experimental data were plotted versus the particle concentration in Figure 5.7. Theoretically, the relation between w_R and the particle concentration is linear. However, the experimental w_R values show some deviations from this linearity. Therefore, a linear equation was fitted to the experimental data and w_R values were recalculated for each concentration (' w_R theory') using this linear least square fitting equation. Subsequently, the ' w_R theory' values were used to determine the theoretical SDI.

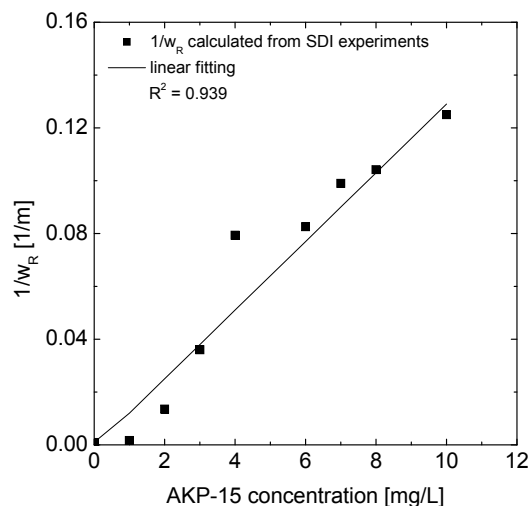


Figure 5.7. w_R calculated from the SDI test and least square linear fitting. The fitting values of w_R are used in Eqns. (5.8) & (5.9) to determine the theoretical SDI values.

The measured values for t_1 , t_2 and the SDI were compared with the mathematically calculated values in Figure 5.8 and Figure 5.9. The maximum deviation between the calculated and measured values of t_1 and t_2 is indicated by dotted lines in Figure 5.9.

The time required for collecting the first sample t_1 and the second sample t_2 were measured experimentally and estimated mathematically for each SDI test. In Figure 5.8, the calculated t_1 and t_2 values are in good agreement with the measured values. There is some deviation due to the limitations of the model, which will be discussed in section 5.3.6. The SDI test was performed for feed water prepared with different AKP-15 particle concentrations between 0 and 10 mg/L. The SDI as experimentally measured and the SDI values calculated using Eqn. (5.8) & (5.9) were plotted in Figure 5.9.

The fouling potential of the feed water increases with increasing particle concentration. Since the particle retention in our work is 100%, the SDI increases exponentially when the particle concentration is higher [10]. In Figure 5.9, the SDI has negative values at very low particle concentrations, which can be explained by the high sensitivity of the SDI for measurement errors in this region. Deviations between the calculated and the measured SDI values can be explained by the limitations of the model as will be discussed in section 5.3.6.

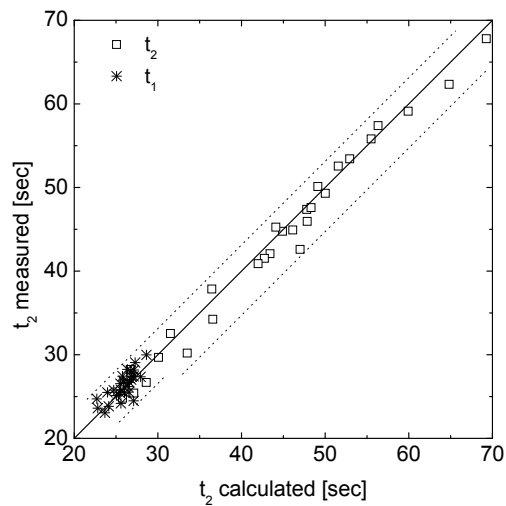


Figure 5.8. Calculated and measured (t_1) and (t_2) the time to collect the first and the second samples for different particle concentration. Calculated t_1 and t_2 were determined using Eqns. (5.8) & (5.9) and the measured testing parameters T , A_M , dP and R_M . Measured t_1 and t_2 were determined according to the ASTM standard protocol.

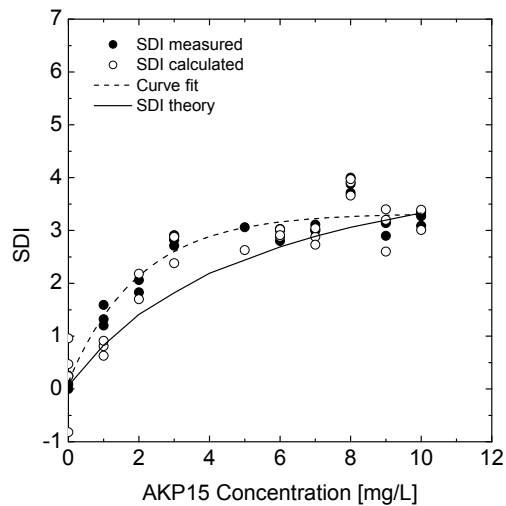


Figure 5.9. Calculated, measured and theoretical SDI values. Calculated SDI results were determined using Eqns. (5.8) & (5.9) and the measured parameters T , A_M , dP and R_M . Theoretical SDI values were calculated assuming cake filtration and the expected C and m values for AKP-15. Measured SDI values were determined according to the ASTM standard.

5.3.5 Fouling load

The SDI test essentially determines the average flow during filtration of a reference volume. The change in average flow between the two measurements (represented by t_1 and t_2) is a measure for the change in the fouling state of the test membrane. In the fouling models the fouling state of the membrane is related to the filtered volume. However, in the SDI test the

time between the two measurements is fixed and the total volume that is filtered in that time depends on the flow rate. Thus, any effect that increases the flow through the membrane will increase the fouling load of the membrane incrementally and consequently the measured SDI will be higher. This explains our observation that the SDI increases with increasing temperature (decreasing viscosity implies increased flow), increasing pressure and decreasing membrane resistance.

The plugging ratio is corresponding to the change in the resistance during the SDI test. Eqn. (5.2) shows that the relation between the filtered volume and the fouling resistance and thus the flow decline is non-linear. The sensitivity of the fouling resistance due to the change in the filtrated volume is increased with increasing m value (0, 1, 1.5 and 2). Hence, when this relation is convex, a moderate increment in filtered volume can result in a relatively large increase in the fouling resistance. As a result, the sensitivity for factors that increase flow is also relatively large. This explains our observation that the cake filtration mechanism (lowest m value) is the least sensitive for the testing conditions, followed by intermediate blocking, standard blocking and complete blocking. Consequently, the sensitivity of the SDI increases in the same order: cake filtration < intermediate blocking < standard blocking < complete blocking.

5.3.6 Shortcomings of the model

The deviations between the measured and calculated SDI values can be explained in different ways. The commercial 0.45 μm membranes which are used for SDI test actually have a broad pore size distribution (Figure 5.10). Furthermore, Figure 5.10 shows that the α -Alumina particles have a particle size distribution between 200 and 800 nm with an average size of 600 nm. During the SDI test, the smaller particles either will deposit deeply in the pores and cause pore blocking, or will pass to permeate side. The cake layer formation will start when enough large particles arrived to the membrane surface. So, one or more fouling mechanisms can occur during the SDI test in parallel or successively. Flux decline can be consistent with one or more pore blocking mechanisms during the earlier stages and with the cake filtration mechanism during the latest stages of filtration [11].

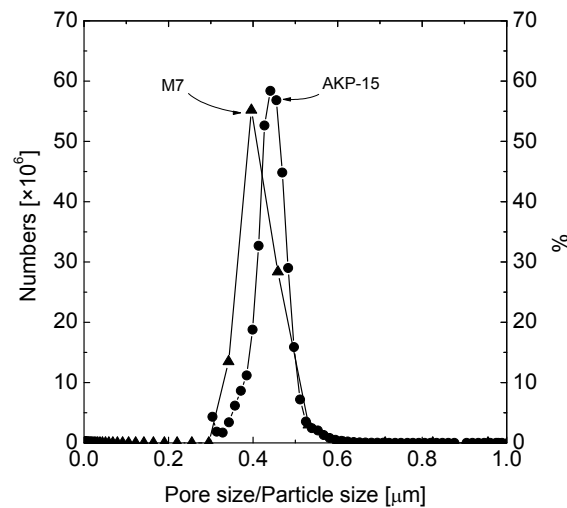


Figure 5.10. α -Alumina (AKP-15) particle size distribution (4 mg/L particles in ultra-pure water at pH 4.1 and T 20 °C well mixed) determined using a Malvern Zetasizer. The pore size distribution for membrane M7 is measured using the Coulter Porometer II with Profil3 as pore filling liquid.

- 1- Feed water properties such as pH and salinity influence the foulant-foulant and foulant-membrane interactions by affecting the surface charge of both particle and membrane. The change in the surface charge can influence the membrane adsorption for particles (standard pore blocking) as well as the cake layer density. The fouling rate will be influenced too and that is reflected by the SDI value. The feed water temperature can influence the SDI by a change in the water viscosity. In Eqn. (5.8) & (5.9) the effect/s of the feed temperature on the membrane physical properties was neglected.
- 2- A particle rejection of 100 % was assumed in the modeling. However, small particles were noticed in the permeate, indicating that the particle rejection is below 100 %

5.4 Conclusions

The SDI measurement initially is designed to measure the fouling potential of feed water for RO membranes. However, the measured values will also depend on several testing parameters. In this paper a model was developed, based on blocking laws, which is able to explain this dependency and shows why a reproducible determination of the SDI is difficult.

An increase in testing parameters such as T , dP or R_M affect the fouling load, which leads to a different SDI value. The sensitivity of the SDI for small variations in the testing parameters increases when the relation between w and R is stronger, so in the order cake filtration < intermediate blocking < standard blocking < complete blocking.

An increase of the feed water viscosity or the membrane resistance leads to a decrease in the SDI, while an increase of the applied pressure or the feed temperature leads to an exponential increase of the SDI. The membrane area has no effect on SDI as far as the sample volume is adjusted proportionally to the membrane area

The relation between the particle concentration and the SDI is a function of the fouling mechanism parameter m . Therefore, for the same amount of particles in the feed, the SDI can vary depending on the fouling mechanisms occurring during the test.

The experimental and calculated SDI values are in good agreement with the results of Eqn. (5.8) & (5.9). The final conclusion of this work is that the SDI is not an ideal fouling index due to the effects of the membrane resistance and the testing condition parameters on the measured values. Therefore, there is a strong need for normalization of the SDI which compensates for variations in these parameters.

5.5 References

- [1] J.C. Schippers, J. Verdouw, The modified fouling index, a method of determining the fouling characteristics of water, *Desalination*, 32 (1980) 137-148.
- [2] J.C. Schippers, J.H. Hanemaayer, C.A. Smolders, A. Kostense, Predicting flux decline of reverse osmosis membranes, *Desalination*, 38 (1981) 339.
- [3] S.F.E. Boerlage, M.D. Kennedy, P.A.C. Bonne, G. Galjaard, J.C. Schippers, Prediction of flux decline in membrane systems due to particulate fouling, *Desalination*, 113 (1997) 231-233.
- [4] S.F.E. Boerlage, M.D. Kennedy, M.P. Aniyé, E.M. Abogrean, G. Galjaard, J.C. Schippers, Monitoring particulate fouling in membrane systems, *Desalination*, 118 (1998) 131-142.
- [5] S.F.E. Boerlage, M. Kennedy, M.P. Aniyé, J.C. Schippers, Applications of the MFI-UF to measure and predict particulate fouling in RO systems, *J. Membr. Sci.*, 220 (2003) 97-116.
- [6] S.F.E. Boerlage, M.D. Kennedy, M.P. Aniyé, E. Abogrean, Z.S. Tarawneh, J.C. Schippers, The MFI-UF as a water quality test and monitor, *J. Membr. Sci.*, 211 (2003) 271-289.
- [7] S. Khirani, R. Ben Aim, M.-H. Manero, Improving the measurement of the Modified Fouling Index using nanofiltration membranes (NF-MFI), *Desalination*, 191 (2006) 1-7.
- [8] B. Blankert, B.H.L. Betlem, B. Roffel, Dynamic optimization of a dead-end filtration trajectory: Blocking filtration laws, *J. Membr. Sci.*, 285 (2006) 90-95.
- [9] M. Mulder, Basic principles of membrane technology, 2 ed., Kluwer Academic Publishers, Dordrecht, The Netherlands, 2003.
- [10] L.F. Greenlee, D.F. Lawler, B.D. Freeman, B. Marrot, P. Moulin, Reverse osmosis desalination: Water sources, technology, and today's challenges, *Water Research*, 43 (2009) 2317-2348
- [11] F. Wang, V.V. Tarabara, Pore blocking mechanisms during early stages of membrane fouling by colloids, *Journal of Colloid and Interface Science*, 328 (2008) 464.

CHAPTER 6

SENSITIVITY OF SDI FOR EXPERIMENTAL ERRORS

THIS CHAPTER HAS BEEN SUBMITTED TO PUBLICATION:

A. Al-hadidi, A.J.B. Kemperman, B. Blankert, J. C. Schippers, M. Wessling, W.G.J. van der Meer, Sensitivity of SDI for experimental errors, Desalination and Water Treatment

In this Chapter, mathematical models were developed to investigate the sensitivity of SDI for the following types of errors: errors due to inaccurate lab or field equipment, systematic errors, and errors resulting from artifacts and personal observations and experience. The mathematical results were verified experimentally.

6.1 Introduction

Both the mathematical models and experimental results show that the membrane resistance R_M has the highest impact on the SDI results. The allowable ASTM variation in R_M is responsible for a deviation in SDI between 2.29 and 3.98 at a level of SDI=3. Besides that, a 1 second error in measuring the time to collect the second sample t_2 results in ± 0.07 at SDI_O=3. The artifacts and personal experience also influence the SDI results. The total error in measuring SDI was estimated to be equal to ± 2.11 in the field and only ± 0.4 in the lab in level of SDI_O=3. Furthermore, several recommendations are mentioned based on these theoretical results and our personal experience.

This study demonstrates the sensitivity of the SDI for errors in R_M and the accuracy of the equipments, and explains the difficulties in reproducing SDI results for the same water.

6.2 Theory and background

A mathematical model was developed to describe the relation between SDI, particle concentration, and the test conditions under different fouling mechanisms. This developed model was used to study the influence of the membrane resistance and test conditions on the SDI values.

6.2.1 Sensitivity and Error Analysis

The following types of errors for SDI were investigated: errors due to inaccurate lab or field equipment, systematic errors, and errors resulting from artifacts and personal observations and experience.

6.2.1.1 Equipment accuracy and uncertainty

Accuracy of equipment is how close the measured value is to the true or actual value, while the error is the difference between these two values. Inaccuracy in the equipment leads to an error in the obtained SDI values. The error in SDI due to the inaccuracy in the equipment is calculated as follows:

$$\Delta SDI = \frac{\partial SDI}{\partial (\text{parameter})} \times \Delta (\text{Equipment Accuracy}) \quad (6.1)$$

Where:

ΔSDI is the error in SDI,

$\frac{\partial SDI}{\partial(\text{parameter})}$ is the change in SDI due to the variation in the testing parameter

$\Delta(\text{Equipment Accuracy})$ is the accuracy of the equipment used to measure the testing parameter.

The equipment used in the lab SDI setups (see Figure 2.4 (a) and (b)) have a limited guaranteed accuracy in measuring the testing condition parameters. The equipment inaccuracy is a result of the accuracy of the manufactured equipment and the operator's accuracy in using the equipment and monitoring the test conditions. The accuracy of the flow meter, thermometer, beaker, pressure sensor and the stopwatch are mentioned in the products' brochures. Lack of operator experience causes additional errors in the measurement of temperature, sample volumes, the times t_1 and t_2 , and the time to start collecting the second sample t_f . The temperature in the field can easily vary from morning to night with $\pm 5^\circ\text{C}$ causing differences in SDI for the same feed water.

The equipment accuracy, operator error and the testing conditions are shown in Table 6.1. The operator errors are estimations based on our practical experience.

Table 6.1 Equipment used for the SDI test accuracy in the lab and in the field

Equipment uncertainty	Variation	
	Lab equipment	Field equipment
Equipment accuracy		
Flow meter	0.1 L/hr	
Thermometer	0.1 °C	0.1 °C
Volumetric flask	0.25 mL/500 mL	
Pressure sensor	0.07 bar	0.1 bar
Stopwatch	0.01 s	0.01 s
Operator experience		
Thermometer	1 °C	1 °C
Beaker	5 mL/500 mL	50 mL/500 mL
Stopwatch in measuring t_1, t_2	2×0.5 s	2×2.5 s
Stopwatch in measuring t_{15}	10 s	15 s
Testing conditions		
Thermometer	1	5 °C

In the field, fairly inaccurate equipment results in erratic SDI results. The error in V and t are relatively large for the field tests. This is caused by the fact that the operator has to start/stop the

collection of permeate and start/stop the stopwatch at the same moment. Although according to the ASTM standard the water temperature T should remain constant (± 1 °C) throughout the test, in fact the SDI should be measured at a standard temperature. Mathematical and experimental results show that SDI value is very dependent on temperature. During field tests, a difference of 5 °C is not unusual, depending on for example at what time during the day the SDI was performed.

6.2.1.2 Systematic error

Systematic errors in SDI test observations usually originate from unknown measuring equipment errors such as the support plate in the filter holder, height difference between the pressure gauge and the membrane, contamination in the membrane upstream, and errors in calculating the effective membrane area. Systematic errors can be difficult to identify and correct. Given a particular experimental procedure and setup, it does not matter how many times the experiment is repeated; the systematic error remains unchanged. No statistical analysis of the data set eliminates a systematic error, nor alerts us to its presence. A systematic error can be located and minimized with careful analysis and design of the test conditions and procedures, by comparing the results to other results obtained independently, or by using different equipment or techniques.

6.2.1.3 Artifacts

Errors appear in the SDI results which are not a true feature of the testing parameters, but instead are a result of experimental or observational mistakes. There are numerous examples of this. Gas bubbles can appear in the feed water which interrupt the filtration process and cause a high SDI value. The feed pump and the valves placed before the membrane can affect the particle size due to the shear force they exert on the particles. Carbon particles can be introduced in the feed solution originating from the graphite gear of the gear pump.

6.2.2 Influence of water salinity and acidity

SDI as a fouling index is related to the interaction between particles and the membrane, which is influenced by the water salinity and acidity. The initial rate of particle deposition depends on the colloidal interaction forces between particles and membrane surfaces, among which double layer forces are the most important. The double layer forces between particles, and

between the membrane surface and the fouling are determined by the zeta potentials of particles and membranes, and by solution chemistry.

The AKP-15 particle which was used to prepare the model water has an iso-electric point (IEP) at pH 9 [1], while test membrane M7 has an IEP at pH 2.5-3 [2]. Therefore, the particles and membranes are oppositely charged in the range of pH 2.5-9.

The particles deposit on the membrane surface as a cake or are adsorbed on the internal pore surface causing pore blocking. At $SDI_o=3$, cake filtration dominates the fouling mechanisms and most of the particles are deposited on the membrane surface. At high ionic strength, the repulsive double-layer forces between the particles and the membrane surface are small because of double layer compression. As a result, particles, which are transported to the membrane surface by the inherent permeation drag, deposit onto the membrane or inside the pore. No significant lateral repulsion occurs between deposited particles, so their density on the membrane surface is relatively high. Because the particles are unstable at a high ionic strength, the deposition of suspended particles onto previously retained particles is also favorable. This deposition behavior results in a thick fouling layer and extensive fouling. Therefore, a high ionic strength of the test water may result in increasing SDI values.

At low ionic-strength, the initial deposition of particles onto the oppositely charged membrane surface is favorable. Because of the low ionic strength, strong lateral double-layer repulsion exists between retained particles, and the initial density of surface coverage is not too high. Under these conditions, strong double layer repulsion also exists between retained particles and approaching suspended particles. In this case, the extent of colloidal fouling is postulated to depend on the interplay between double-layer repulsion and permeation drag [3-6].

The effect of pH on SDI for seawater was discussed by Mosset et al. [7]. Their SDI results as function of pH are plotted in Figure 6.1.

Figure 6.1 shows SDI values increasing from 4 to 6 when the pH is increased from 7 to 8. Mosset et al. stated that this is mainly due to dissolved substances (Ca, Mg,...) which precipitate with increasing pH. Moreover, the pH influences the double-layer forces between particles and the membrane surface.

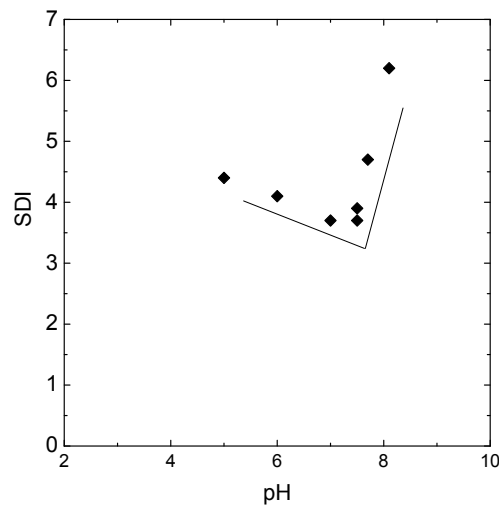


Figure 6.1 SDI values versus pH of UF seawater. Redrawn from [7].

6.2.3 Modeling input data

The following input data were used to mathematically study the sensitivity of SDI for errors.

Parameter	Reference value	Variation range to be studied
R_M	$1.29 \times 10^{10} \text{ m}^{-1}$	$0.39 \times 10^{10} - 2.65 \times 10^{10} \text{ m}^{-1}$
dP	$2.07 \times 10^5 \text{ Pa}$	50 – 400 kPa (0.5 – 4 bar)
A_M	$13.4 \times 10^{-4} \text{ m}^2$	
$V_{1,2}$	500 mL	
t_f	15 min	
T	20 °C	5 – 70 °C
MFI		0-3.5 s/L ²

The water viscosity was calculated using the following empirical equation[8, 9]:

$$\mu = 0.497 \times (T + 42.5)^{-1.5} \quad (6.2)$$

Where T is the water temperature (°C).

6.3 Results and discussion

6.3.1 Deviation ± 0.1 at $SDI_0=3$

There is no allowable error mentioned for the SDI test in the ASTM standard or in other literature. From a practical point of view and based on our experience, a deviation of 0.1 in the SDI result can be acceptable. Assuming cake filtration and the reference testing conditions mentioned in Table 2.3, the variations of several testing parameters resulting in a deviation of ± 0.1 at $SDI_0=3$ are calculated. Table 6.3 shows this variation for each testing condition (T , dP , R_M , A_M and the times t_1 , t_2 and t_f).

Table 6.3 shows that an error of ± 0.6 s in measuring the time to collect the first sample (t_1) results in a ± 0.1 variation of the SDI value. However, the variation in measuring the time to collect the second sample t_2 for obtaining an identical ± 0.1 variation in SDI value is twice that in t_1 , ± 1.18 s. Under cake filtration, the relationship between the total resistance R and the filtrated volume V is linear. Due to the linearity between R and V , the error in measuring the membrane area results in an increase in both sampling time t_1 and t_2 with almost same ratio. Thus, an increase in the membrane area A_M does not have an effect on the SDI value, whereas decreasing A_M has a small effect and SDI remains almost constant. Collecting the second sample should start after an elapsed filtration time t_f of 15 min. However, the collection of the second sample can be earlier or later due to an error in measuring the 15 minutes. An error of +30 or -70 s in measuring t_f causes a ± 0.1 deviation in the measured SDI value. From Table 6.3, we conclude that SDI is more sensitive for errors in measuring t_1 and t_2 , while SDI is hardly sensitive for inaccuracies in the membrane area A_M in the case of a cake filtration mechanism.

Table 6.3 Variation range in the testing parameters resulting in a deviation $SDI_0=3 \pm 0.1$ for a cake filtration mechanism.

Parameter	SDI=3	SDI=3 ± 0.1
T [$^{\circ}$ C]	20	23.36-16.84
dP [kPa]	207	224-192
R_M [m^{-1}]	1.29×10^{10}	1.19×10^{10} - 1.40×10^{10}
A_M [m^2]	1.39×10^{-3}	$> 2.63 \times 10^{-4}$
t_1 [s]	22.96	22.33-23.58
t_2 [s]	41.74	42.92-40.60
t_f [min]	15 min (900 s)	871.2 s-931.2 s

6.3.2 Equipment accuracy and uncertainty

Errors due to inaccuracies in the equipment readouts can result in erratic SDI results. There is a large variation of equipment on the market which can be used for SDI testing in terms of quality and price. The manual equipment selected for field use is most likely to be lower in accuracy and price compared to lab equipment. Besides that, a wide range of commercial membranes with a pore size of 0.45 μm are available which can be used for the SDI test. The errors in the SDI results due to the variation in the testing conditions due to the inaccuracy of the used equipments and the membrane resistance are discussed in this work.

6.3.2.1 Different fouling mechanisms

The sensitivity of SDI for errors in measuring temperature, applied pressure and membrane resistance were studied for the four different fouling mechanisms. The effect of the equipment accuracy and errors on the SDI value was calculated by substituting the mathematical SDI model (Eqns. (5.8) & (5.9)) in Eqn. (6.1).

The accuracy values in Table 6.1 for lab equipment were used to compare the SDI sensitivity for errors for the four different fouling mechanisms. The ASTM standard allows a ± 7 kPa error in the applied pressure and a variation of 1 $^{\circ}\text{C}$ in the temperature [10]. The error in the membrane resistance was estimated to be $0.1 \times 10^{10} \text{ m}^{-1}$. Figure 6.2 shows the errors in the SDI due to the inaccuracy of the equipment in measuring T and dP and the membrane resistance R_M . For cake filtration mechanisms, the fouling potential index I was assumed to be equal to $1.056 \times 10^9 \text{ m}^{-2}$, corresponding to $\text{SDI}_0=3$. In Figure 6.2 the variation in the SDI results due to the variation in each parameter for the four fouling mechanisms are presented by the error bars.

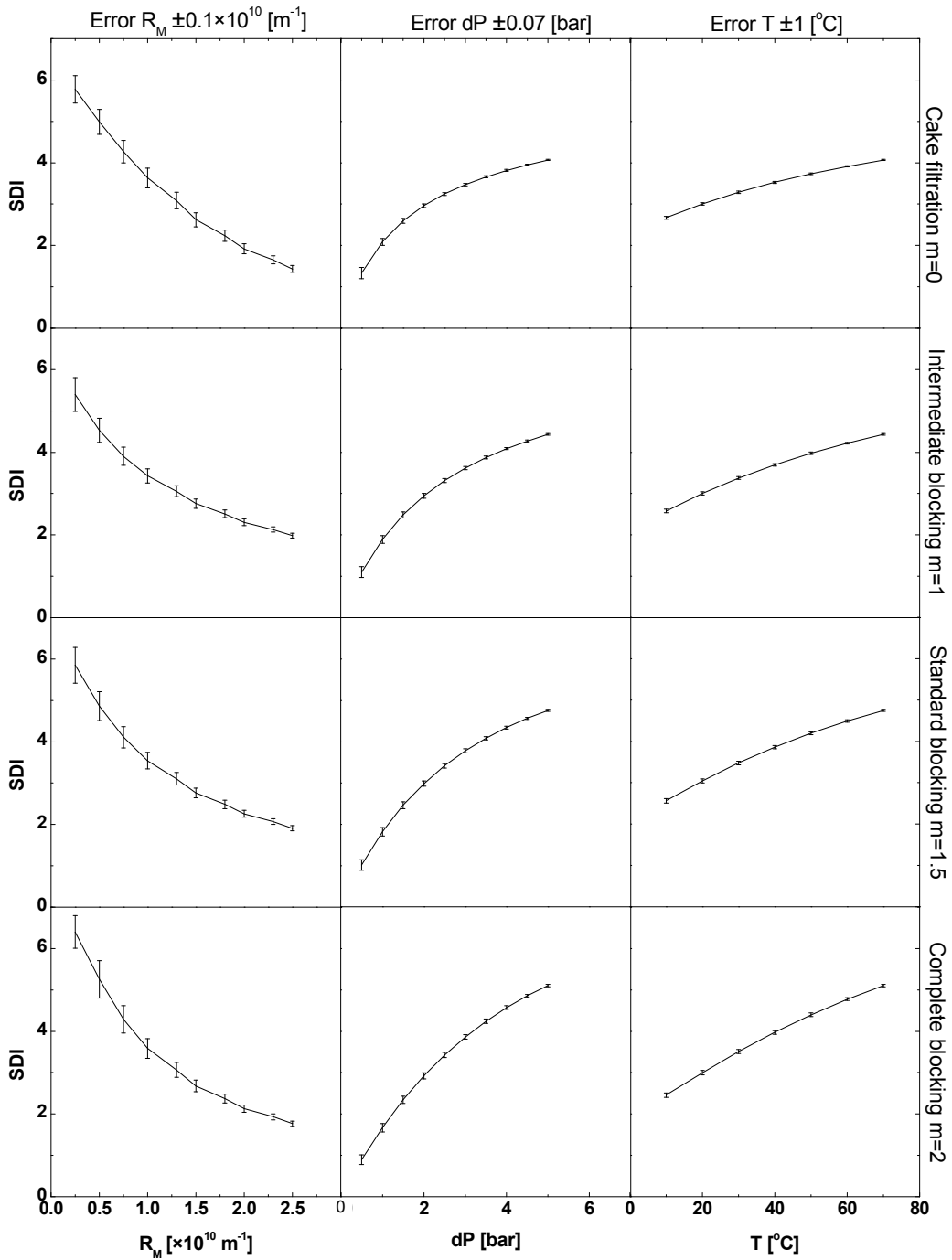


Figure 6.2 Accuracy errors in equipment and membrane resistance under different fouling mechanisms.

The effects of a variation in the different testing conditions on the SDI can be studied in Figure 6.2 by comparing the graphs horizontally. Figure 6.2 shows that the SDI is more sensitive for errors in the membrane resistance than for errors in the temperature and the applied pressure. The SDI is more sensitive for errors during the test when a membrane with a low resistance is used, when a lower pressure is applied, or when the test is performed at a low temperature. By

comparing the graphs in Figure 6.2 vertically, we can conclude that the effects of different fouling mechanisms on SDI sensitivity are negligible. As simplification for the calculations, in the next sections therefore a cake filtration mechanism is assumed.

6.3.2.2 Accuracy of the SDI equipment

The minimal requirements for the accuracy of SDI equipment are not specified at all in the ASTM standard. As a result, equipment with a low accuracy is often used to measure the SDI, and this, in turn, leads to erratic SDI results. In this section, the different components of the SDI equipment are examined for their inaccuracy and their effect on the SDI results.

Feed Temperature (Thermometer)

In the most recently ASTM standard, no reference temperature was suggested for measuring or correcting SDI. The flow rate through the membrane is affected by variations in the feed water temperature. SDI values obtained at different feed water temperatures may not necessarily be comparable [10]. An inaccuracy in the thermometer of ± 1 °C is estimated for the calculations. In Figure 6.3, SDI values were plotted as a function of the specific cake resistance to simulate varying particle concentrations, and assuming a feed temperature of 20 ± 1 °C. The SDI sensitivity for errors in measuring the temperatures is calculated by substituting the mathematical SDI model of Eqns. (5.8) & (5.9) in Eqn.(6.1). From Figure 6.3 we can conclude that the effect of a ± 1 °C error in measuring the temperature only has a very small effect on the SDI results.

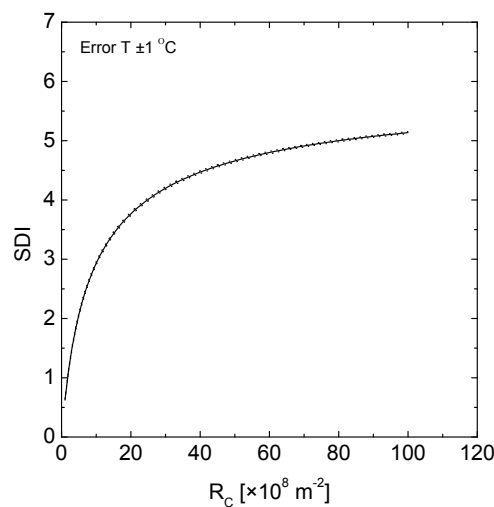


Figure 6.3 Effect of an accuracy error in T on the SDI variation (dotted lines) under cake filtration at 20 ± 1 °C as a function of the specific cake resistance.

Applied pressure “Pressure Gauge”

ASTM allowed a variation of ± 0.07 bar (1 psi) in measuring the applied pressure during the SDI test. Two pressure indicators with an accuracy of ± 0.07 bar and ± 0.1 bar were used in the error calculations for the lab and field measurements, respectively. The SDI values were plotted in Figure 6.4 (a,b) as a function of the specific cake resistance assuming applied pressures of 207 ± 7 kPa and 207 ± 10 kPa. The effect of the error in measuring the applied pressure was calculated by substituting the SDI model described by Eqns. (5.8) & (5.9) in Eqn. (6.1). The effect of a ± 0.07 bar and ± 0.1 bar error on the SDI results was small and negligible.

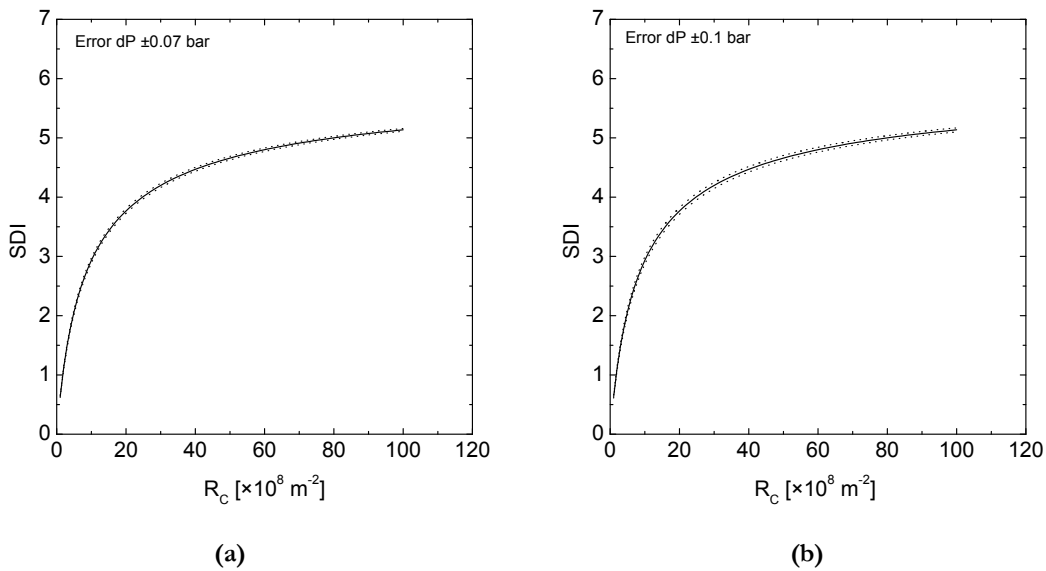


Figure 6.4 Effect of an accuracy error in dP determination on the SDI variation (dotted lines) under cake filtration at 207 kPa as a function of the specific cake resistance. (a): ± 7 kPa; (b) ± 10 kPa.

Membrane area A_M

The O-ring in the filter holder covers part of the membrane surface. The covered part of the membrane is inactive for filtration. The error in measuring the membrane diameter for different types of filter holders was experienced to be ± 2 mm and ± 4 mm for a 47 mm membrane diameter for the lab and field equipment, respectively. This causes an error in the membrane area A_M of ± 8.3 % and ± 16.3 %. The specific cake resistance R_C was varied between 0.01 and $1 \times 10^{10} \text{ m}^{-2}$. The effect of ± 8 % and ± 16.3 % errors in the membrane area on the SDI results was determined by using Eqns. (5.8) & (5.9) - (6.1) and assuming cake filtration. The results are shown in Figure 6.5 (a,b). The influence of ± 8.3 % and ± 16.3 % errors in calculating the

membrane area are close to zero. The sensitivity of SDI for an error in measuring A_M therefore is negligible.

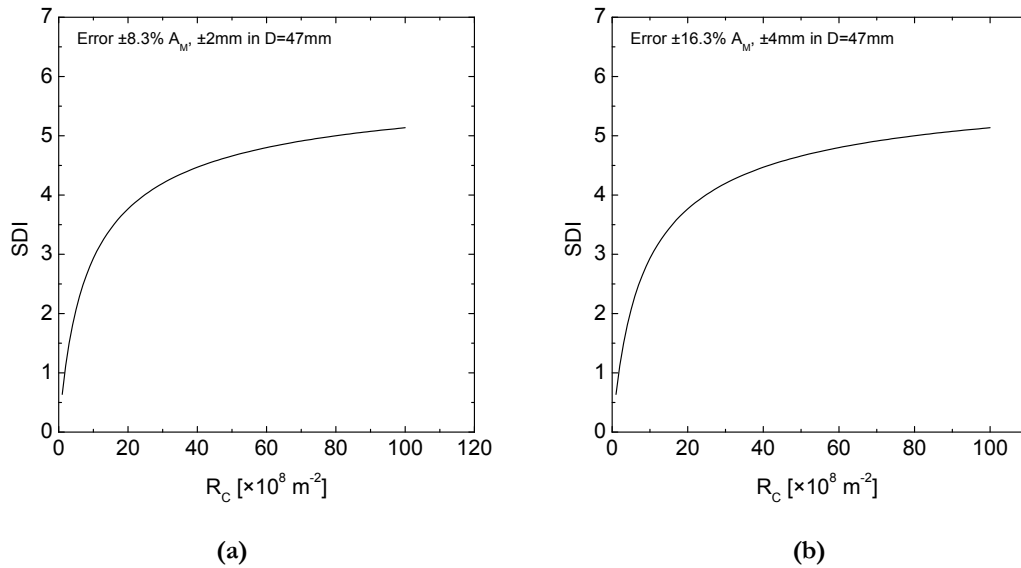


Figure 6.5 The effect of (a) 8.3% and (b) 16.3% error in the membrane area on SDI as a function of R_c , under a cake filtration mechanism.

Timing (stopwatch)

An error in the stopwatch will have an effect on the determination of t_1 , t_2 and t_f and consequently in the calculation of SDI using Eqn. (6.1). To study this effect, as an illustrative example the following assumptions were made: the errors in t_1 were ± 1 s and ± 5 s (lab and field equipments), t_1 varied between 20 and 200 s, and t_2 was 200 s. SDI results and the effect of ± 1 s and ± 5 s errors in t_1 are presented in Figure 6.6. The first derivative of Eqn. (2.1) with respect to t_1 describes the change in the SDI due to an error in t_1 as shown in Eqn. (6.3).

$$\Delta SDI = \pm \left(\frac{100}{t_2 \times t_f} \times \Delta t_1 \right) \quad (6.3)$$

Where, $t_f = 15$ min, $t_2 = 200$ s, Δt_1 error in measuring $t_1 = 1$ or 5 s. The SDI variation is not influenced by the value of t_1 , and ΔSDI is equal to ± 0.03 and ± 0.17 respectively.

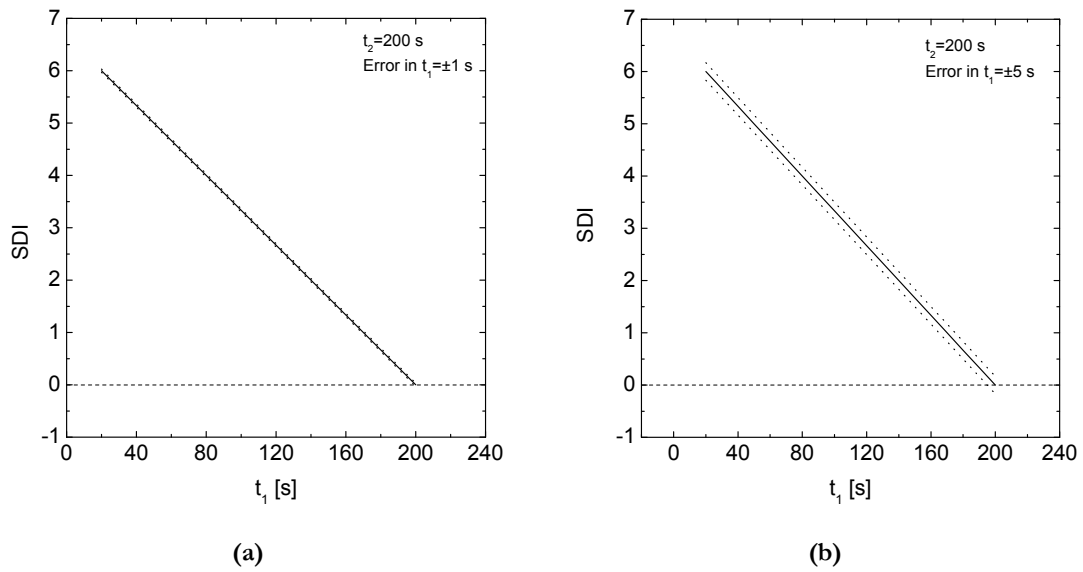


Figure 6.6 The effect of an accuracy error in t_1 on the SDI variation (dotted lines) under cake filtration for $t_2 = 200$ s as a function of t_1 . (a) ± 1 s; (b) ± 5 s.

The effect of an error in measuring t_2 on the SDI results was studied assuming the errors in t_2 to be ± 1 s and ± 5 s (lab and field equipment, respectively) for t_2 between 20 to 200 s, and t_1 equal to 20 s. The first derivative of Eqn. (2.1) with respect to t_2 describes the effect of the t_2 error on the SDI as shown in Eqn. (6.4).

$$\Delta SDI = \pm \left(100 \times \frac{t_1}{t_f \times t_2^2} \times \Delta t_2 \right) \quad (6.4)$$

Where, $t_f = 15$ min, $t_1 = 20$ s, Δt_2 error in measuring $t_2 = 1$ or 5 s. The SDI results and the effect of ± 1 s and ± 5 s errors on t_2 are shown in Figure 6.7.

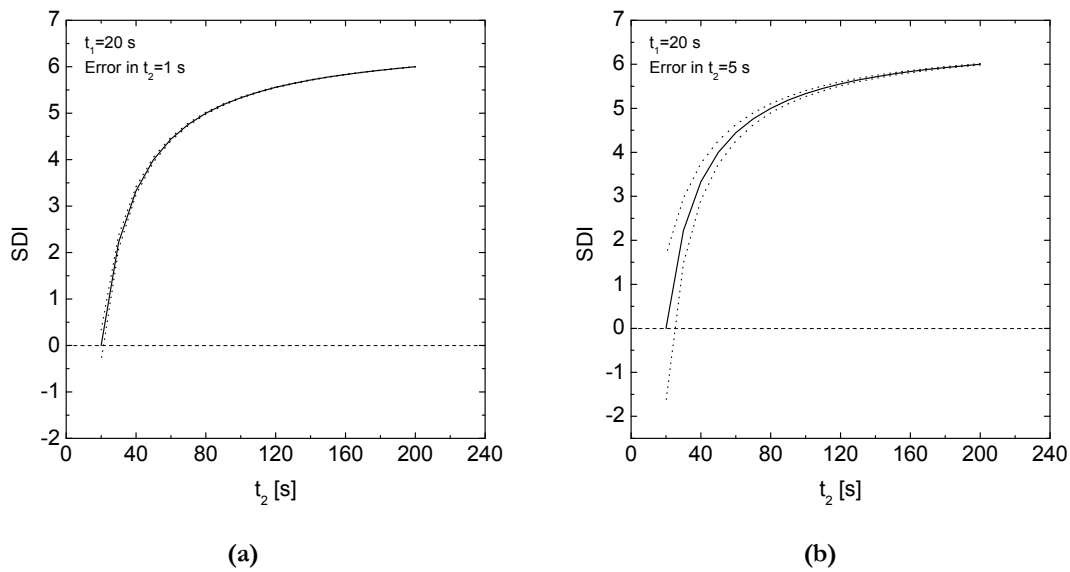


Figure 6.7 The effect of an accuracy error in t_2 determination on the SDI variation (dotted lines) for $t_1 = 20$ s as a function of t_2 assuming cake filtration. (a) ± 1 s; (b) ± 5 s.

The sensitivity of the SDI for errors in measuring t_2 is increasing with decreasing SDI. The SDI can even have a negative value due to an error in measuring t_2 , as shown by the SDI values between -1.5 to 1.8 due to a 5 s error in measuring t_2 when t_1 equals 20 s. The effect of 1 s and 5 s errors on the SDI variation resulted in a ΔSDI decreasing from ± 0.33 and ± 1.7 down to zero, respectively, with increasing SDI (increasing t_2). The SDI sensitivity for errors in t_2 was significant and the larger the error in t_2 and the lower the SDI, the more sensitive the SDI is.

The error in the elapsed filtration time t_f after starting the measurement (usually 15 min) was experienced to be ± 10 s to ± 15 s. The feed water quality was changed by varying the specific cake resistance R_C between 0.01 and 10^{10} m⁻². The effect of the ± 10 s and ± 15 s errors on the variation of the SDI was calculated using Eqn. (6.5).

$$\Delta SDI = \pm \left(\frac{100}{t_f^2} \times \left(1 - \frac{t_1}{t_2} \right) \times \Delta t_2 \right) \quad (6.5)$$

Where, $t_1 = 20$ s, $t_2 = 200$ s, Δt_f error in measuring $t_f = 10$ or 15 s. The results were plotted in Figure 6.8. The assumed errors in t_f have a maximum effect on the SDI of ± 0.05 and ± 0.07 , respectively.

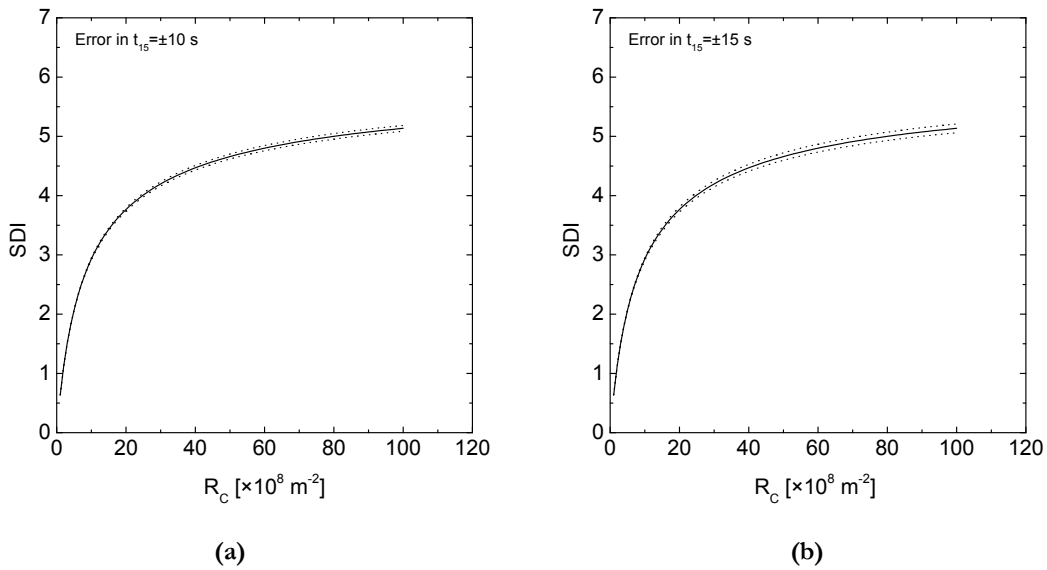


Figure 6.8 The effect of an accuracy error in t_f on the SDI variation (dotted lines) under cake filtration for $t_1 = 20$ s and $t_2 = 200$ s as a function of R_c . (a) ± 10 s; (b) ± 15 s.

Sample volume determination (volumetric flask)

The 500 mL sample volume was based on using a 47 mm diameter membrane. In the lab, a volumetric flask was used to measure the sample volumes V_1 and V_2 . We experienced that the flask manufacturing accuracy and operator errors together in the lab and field can sum up to ± 5 mL/500 mL and ± 50 mL/500 mL per volume measurement respectively. The effect of the flasks errors on ΔSDI were calculated using Eqn. (6.6) and plotted in Figure 6.9 as a function of the specific cake resistance. The maximum SDI sensitivity for 5 mL/500 mL and 50 mL/500 mL errors in the sample volume were ± 0.003 and ± 0.6 , respectively.

$$\Delta SDI = \frac{\partial SDI}{\partial V_1} \times \Delta V + \frac{\partial SDI}{\partial V_2} \times \Delta V \quad (6.6)$$

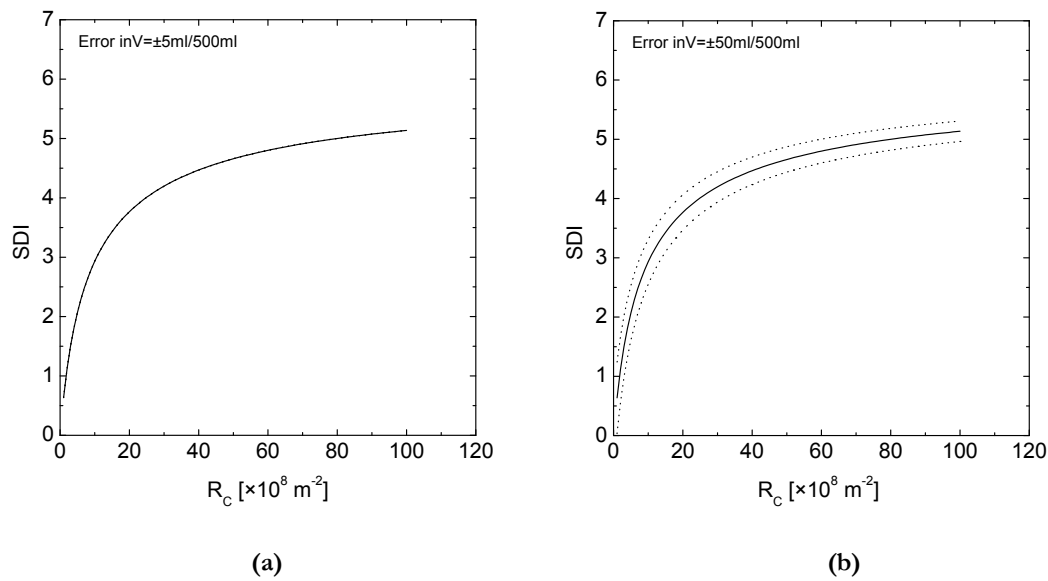


Figure 6.9 The effect of an accuracy error in the determination of V on the SDI variation (dotted lines) under cake filtration as a function of R_c for $V = 500$ mL. (a) ± 5 mL; (b) ± 50 mL.

6.3.2.3 Membrane resistance

The membranes M1-M8 previously tested show a wide range of membrane resistances R_M (0.39×10^{10} - 2.65×10^{10} m^{-1}) [11]. The requirement of the ASTM standard is $0.86 \times 10^{10} < R_M < 1.72 \times 10^{10}$. This broad range of allowable membrane resistances explains, at least partly, the frequently reported erratic SDI results. The effect of a variation in the membrane resistance on the SDI results was calculated using Eqns (5.8) & (5.9)-(6.1) assuming the reference testing conditions in Table 2.3. The error in the reference membrane resistance R_{MO} was estimated to be $\pm 10\%$. The SDI results were plotted in Figure 6.10.

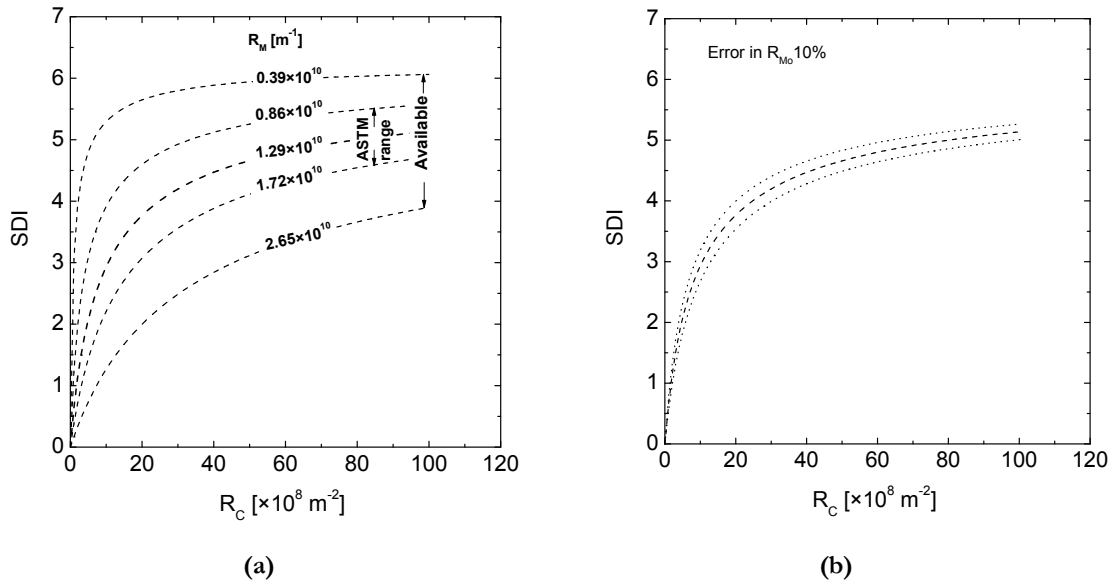


Figure 6.10. The effect of the membrane resistance on SDI as a function of R_C , assuming a membrane area (A_M) 13.8×10^{-4} m², temperature (T) 20 °C and pressure (dP) 207 kPa.
 (a) ASTM range: 0.86×10^{10} to 1.72×10^{10} . Tested range M1-M8: 0.39×10^{10} to 2.65×10^{10} m⁻¹;
 (b) the effect of $\pm 10\%$ variation in R_{M0} (1.29×10^{10} m⁻¹).

Figure 6.10 shows that the guidelines indirectly set by ASTM for the resistance of the used membranes are much too broad resulting in a maximum variation of 2.29 – 3.98 at $SDI = 3$ for a membrane with a resistance R_{M0} (1.29×10^{10} m⁻¹). To avoid this deficiency of the SDI test, it is recommended to narrow the allowable range to 10 % of the R_{M0} value 1.29×10^{10} m⁻¹ which reduces the error to only ± 0.25 at $SDI_0 = 3$.

To experimentally demonstrate the influence of the membrane resistance on SDI, eight different membranes with different clean water resistances as described in Table 3.1 were used. The feed solution of 4 mg/L α -Alumina particles (AKP-15) was prepared in a big feed tank to maintain a constant feed water quality during all experiments. SDI tests were performed at a temperature of 20 °C. The applied pressure was kept constant at 207 kPa. SDI results were plotted vs. the membrane resistance in Figure 6.11.

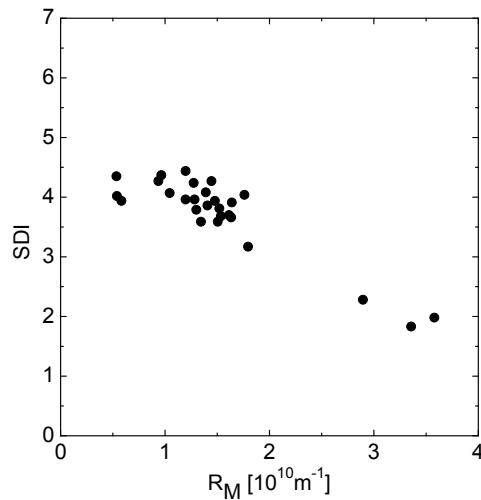


Figure 6.11. SDI results for 0.45 μm membranes from different manufacturers. The experiments were performed using a particle concentration of 4 mg/L of AKP-15 and a pressure of 207 kPa [2].

The experimental results show that the SDI decreases with an increase in the membrane resistance R_M . An increase of the membrane resistance from $0.5 \times 10^{10} \text{ m}^{-1}$ to $3.5 \times 10^{10} \text{ m}^{-1}$ leads to a decrease in SDI from 4.5 to 2 for the same water quality.

6.3.2.4 Total error in the SDI due to inaccuracies

The total error in the SDI due to the inaccuracy in the equipment that can be used to measure SDI is the sum of all individual errors. The total error can be calculated by substituting the SDI model built with Eqns. (5.8) & (5.9) in Eqn. (6.1) for each individual parameter:

$$\begin{aligned}
 \text{Total Error} = & \left(\frac{\partial \text{SDI}}{\partial V_1} \times \Delta V \right) + \left(\frac{\partial \text{SDI}}{\partial V_2} \times \Delta V \right) + \left(\frac{\partial \text{SDI}}{\partial t_f} \times \Delta t \right) + \left(\frac{\partial \text{SDI}}{\partial A_M} \times \Delta A_M \right) + \left(\frac{\partial \text{SDI}}{\partial P} \times \Delta P \right) + \\
 & \left(\frac{\partial \text{SDI}}{\partial T} \times \Delta T \right) + \left(\frac{\partial \text{SDI}}{\partial R_M} \times \Delta R_M \right) + \left(\frac{\partial \text{SDI}}{\partial t_1} \times \Delta t \right) + \left(\frac{\partial \text{SDI}}{\partial t_2} \times \Delta t \right) + \left(\frac{\partial \text{SDI}}{\partial t_f} \times \Delta t \right)
 \end{aligned} \quad (6.7)$$

By substituting the variations mentioned in sections 6.3.2.2. and 6.3.2.3. into Eqn.(6.7), it can be concluded that for the lab equipment the SDI can vary with ± 0.40 , and for the field equipment with ± 2.11 .

6.3.2.5 Effect of a variation in membrane properties within a batch

Two membranes from two different manufacturers were tested to show the influence of variations in membrane properties within a batch on the SDI. The variations in the membrane resistances were 23 % and 7 % within one batch for M1 and M7, respectively [11]. Assuming the

reference testing conditions listed in Table 2.3, the SDI sensitivity for the variation in membrane resistance were calculated by substituting the SDI model described by Eqns. (5.8) & (5.9) in Eqn. (6.1). The SDI sensitivity is plotted in Figure 6.12 as a function of the specific cake resistance.

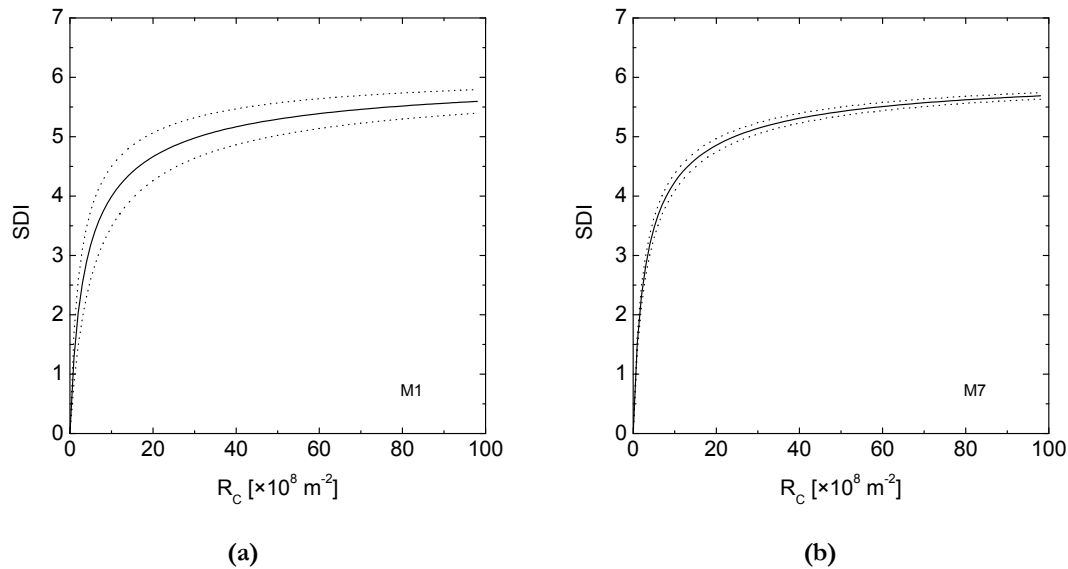


Figure 6.12 The influence of the variation in R_M within a batch of membranes (a) M1 and (b) M7 on SDI. M1 clean membrane resistance $R_M 0.85 \times 10^{10} \text{ m}^{-1}$ with a variation of 23%. M7 clean membrane resistance $R_M 0.74 \times 10^{10} \text{ m}^{-1}$ with a variation of 7%.

At $\text{SDI}=3$ for membrane M1, the SDI varied between 3.58 and 2.42 due to the variation in membrane resistance within one batch. This again illustrates the difficulties in reproducing the SDI in the field due to variations in the membrane resistance within one batch of the same test membrane.

6.3.3 Systematic errors

In this section the experienced practical errors, such as the effects of the pump and filter holder support plate, will be transformed into an error in the SDI results. Systematic errors in the SDI test were difficult to identify, separate and correct. Personal experience and mistakes during the duration of this project lead to the discovery of error sources, such as the filter holder, cleanliness of the setup, and level difference between the filter and the pressure gauge. The change in SDI due to the systematic errors was mathematically estimated using the SDI model built with Eqns. (5.8) & (5.9) and the reference testing conditions.

The filter holder components are the inlet, top cover, O-ring, support plate, and outlet. All of these components can be a source for errors. Some big objects in the feed water can partially

block the holder inlet. The pressure gauge is located in the holder upstream. Therefore, additional resistance in the holder inlet leads to an error in the gauge readout and in the measured SDI. Assume $SDI=3$, and that an error of 0.1 bar due to the blocking in the holder inlet was observed. As a result, the mathematically calculated SDI value varied between 3.06 and 2.94 assuming cake filtration.

The color of the membrane surface changes because of the deposit of foulants. An abnormal concentration of the deposited foulants can be observed as more intense color on the membrane surface. The support plate, located underneath the membrane to hold and support the membrane, can seal part of the membrane and lower the water flow. The effective membrane area in this case is smaller and the filtrated sample volume should be adjusted. When not corrected, this systematic error affects the SDI value since it is obtained with the wrong sample volume. Practically, up to 53% of a membrane surface area can be sealed by the support bulge (see Annex 1-4). Assuming that 53% of the pores will be also sealed in that case, the difference between the real effective membrane area and the assumed area causes an SDI drop from 3 to 2.98. To avoid the effect of the support plate, the use of a filter paper under the membrane is recommended.

Another error source influencing the estimation of the effective area is the O-ring. The O-ring is placed on the top of the membrane to seal the membrane in the cell. The O-ring minimizes the effectiveness of the membrane area as well. The thickness of the O-ring determines the covered area.

System cleanliness and contamination are one of the major sources of systematic errors in measuring an SDI. The SDI limit ($SDI=3$) can be easily obtained with 4 mg/L particles (0.08 g particles in 20 L ultra-pure water with membrane M7). However, any small contamination present in the upstream leads to an increase in the SDI value. A 10 % increase in the particle concentration (w_p decreases from 12.17 to 11.06), causes already an increase in SDI from 3 to 3.13.

The pressure gauge and the filter holder should be at the same level. A difference in level causes an additional pressure difference over the membrane. A level difference of 1 m between the pressure gauge and the filter holder, increases the SDI from 3 to 3.06.

The calculated effects of each of the above mentioned individual errors on SDI are very minimal. However, the accumulated effect of all the errors can have a larger impact on SDI.

6.3.4 Artifacts

During the SDI test, pressurized gas can be used to build up the driving force (pressure) in the feed tank. At the required pressure of 207 kPa, the feed water is super-saturated with gas compared to water at atmospheric pressure, and gas bubbles form during filtration. These gas bubbles obstruct the membrane pores and prevent the water from permeation through the membrane which decreases the flow through the membrane. Consequently, the fouling rate increases and SDI is higher. The effect of entrapped air on the MFI results was mentioned before by Dillon et al. [12].

In order to demonstrate the effect of gas bubbles on the SDI value, two SDI tests were performed using M7, the membrane with lowest variation in its properties. Sufficient feed solution containing 4 mg/L of AKP-15 particles was prepared and divided for two SDI tests. The first SDI test was performed in the morning. The feed solution for the second SDI test was stored under 400 kPa pressure overnight, resulting in an over-saturated feed solution. The next morning, the second SDI test was performed with new membrane out of the same M7 batch. In the second SDI test, gas bubbles clearly were observed upstream of the membrane and on the membrane surface as well. The SDI value increased from 3.31 to 3.80 solely due to the effect of the gas bubbles present in the feed water.

Particle size and nature might change due to the shear forces during mixing in the feed tank, and shear forces caused by the feed pump, flow meter and valves. Three samples were taken from the feed tank (top, middle and bottom of the tank). Three samples (triplicate) were also taken directly at the following positions: the feed pump, the flow meter, the valve and the membrane. The results of the average measured particle size are presented in Figure 6.13.

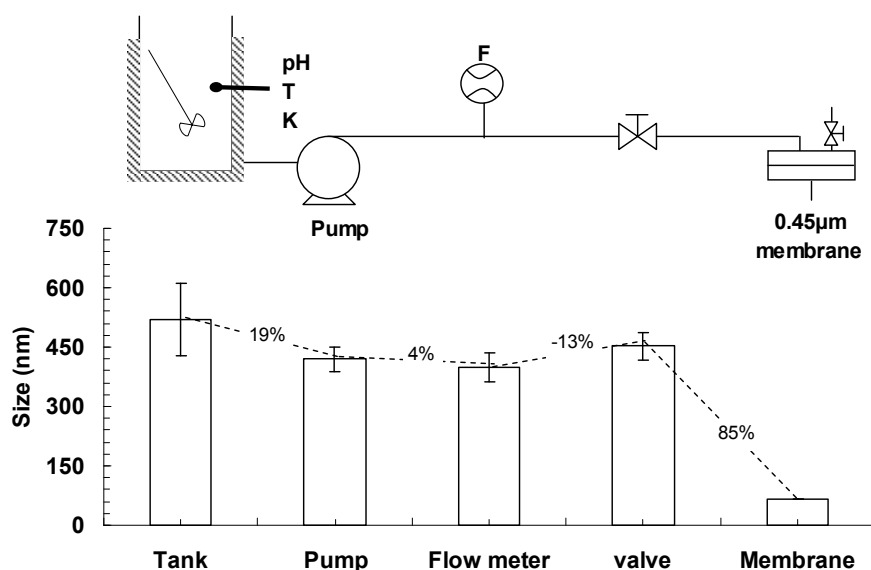


Figure 6.13 Average particle size along the SDI setup. pH (5.6), temperature (T 20 °C) and conductivity (K 180 μ S/cm) were measured in the feed tank. The flow rate measured with online flow meter (F). Membrane M7 was used in the filter holder.

The particle size in the feed tank varied between 440 and 620 nm. The shear force in the feed pump lowered the particle size by 19%. Due to particle agglomeration caused by the shear force in the valve, the average particle size increased with 13 %. At the membrane permeate side the average particle size was 100 nm. We can conclude that for this model water, the particle size in the membrane cell is the same as in the feed tank, within the error margins. These agglomeration/separation processes of course are dependent on the particle properties and the pH of the water, so this conclusion can not be generalized.

Cavitations of the pump were experienced in the membrane fouling experiments of Dillon et al. [12]. Another pump effect is that wear of the gear pump can be a source for particles that arrive to the membrane surface. SDI tests with ultrapure water were performed using two gear pumps made of different material (graphite and PTFE). SEM images (top surface) of the used M7 membranes were taken after the SDI tests, as well as that of a virgin M7.

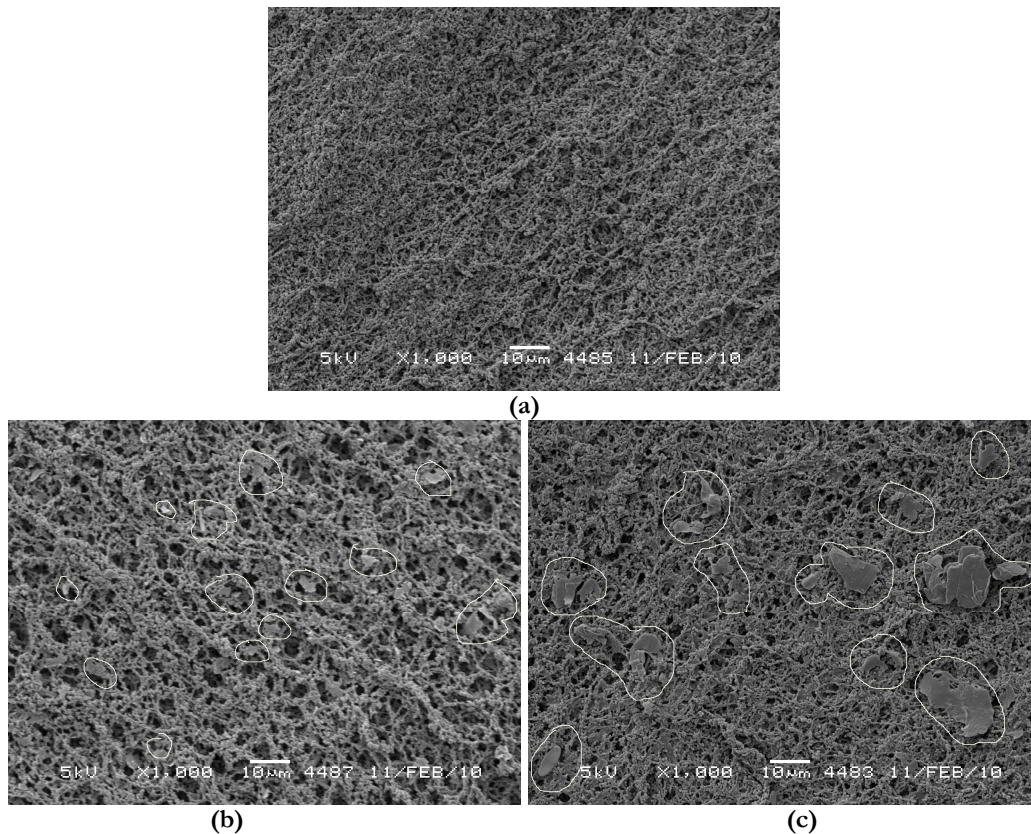


Figure 6.14 a: Virgin membrane M7. b: Ultrapure water filtered through M7 using a graphite gear pump. c: Ultrapure water filtered through M7 using a PTFE gear pump. Wear of the gear pump can be source for contamination by particles in the SDI setup.

The SEM images in Figure 6.14 (a,b,c) show the top surface of the membrane and the deposited particles. The SEM images show that carbon particles introduced by the graphite gear were deposited on the membrane surface. Figure 6.14 also shows that larger particles ($>2 \mu\text{m}$) deposited on the membrane surface, originating from the PTFE gear pump. The SDI for particle free, ultrapure water should be zero. However, SDI values were 0.31 and 0.24 for ultrapure water using the graphite and PTFE pump gears, respectively. Mathematically, this increase in the SDI values is equivalent to specific cake resistance R_C $4.5 \times 10^7 \text{ m}^{-2}$ and $3.4 \times 10^7 \text{ m}^{-2}$, respectively (estimated using Eqns. (5.8) & (5.9)).

6.3.5 Personal experience

Two non-experienced volunteers (persons A and B) were each asked to independently perform the SDI tests manually. The ASTM standard was handed out one week in advance to the volunteers. The SDI setup was assembled as shown in Figure 2.4(b) and membranes M1 and M7 were available for the test. Sufficient feed solution consisting of 4 mg/L of AKP-15 particles

was prepared in a big tank for three SDI tests (person A, person B and an experienced test person using the automated SDI setup shown in Figure 2.4(a)). The SDI results of persons A and B were compared to the SDI results obtained using the automated setup in Table 6.4.

Person A

Person A chose to do the SDI test using the membrane M1. He checked the pore size mentioned on the membrane batch by the manufacturer. Person A did not check the O-ring condition nor the membrane polymer material.

Person B

Person B was more precise in performing the SDI test. She checked the O-ring condition, membrane polymer material and the precision of the stopwatch. She repeated the test two times due to a damage visually observed on the membrane. She faced a difficulty in maintaining a constant and stable pressure of 207 kPa. She was worried about the setup contamination and cleaning.

Both Persons A and B:

- had no doubt that the membranes properties met the ASTM requirements;
- faced difficulties in using two stopwatches, opening the valves and maintaining the pressure at the same time;
- were confused by the t_f starting point: was it $t=0$ or $t=t_1$;
- flushed the system before the SDI test;
- chose a graduated cylinder;
- monitored the temperature accurately throughout the test.

Table 6.4 SDI results obtained by two non-experienced volunteers and one with the automatic SDI setup

	SDI value	$t_1(s) / t_2(s)$	Normalized SDI for R_M (SDI ⁺)
A	4.8	29.9/107.6	-
B	4.4	27/78	-
Automatic SDI setup	4.1	27.6/72.1	4.4

From Table 6.4 we can conclude that apparently different persons who got the same procedure and setup came to different SDI values as a result of differences in personal experience. Due to the fact that in the case of using the automated setup R_M was determined, the SDI could be

normalized for the effect of the membrane resistance to SDI^+ . Moreover, the automated SDI setup is more accurate in measuring t_1 and t_2 .

6.3.6 Commercial SDI devices

Several SDI devices are commercially available (Annex 1-5). The biggest advantage of the automated SDI devices is that the human error is less compared to manual devices. However, the SDI obtained from the commercial devices is not corrected for temperature, pressure and membrane properties. The commercial SDI devices do not consider the effect of the variation in the membrane properties. Most of the commercial SDI devices use a feed pump (or booster pump) which can be a source for additional particles. The feed pump requires time to maintain a constant and stable pressure in the beginning, which affects the final SDI result. The accuracy of the equipment and the SDI results are not mentioned in the instruction manuals of most devices. The pressure gauge and the flow meter need regular calibration which often is not done. The regular calibration is not mentioned in the manuals of the available commercial SDI devices.

6.3.7 Summary of the effects of accuracy errors on $SDI=3$

Table 6.5 shows the effects of errors due to the accuracy of the equipment in the lab and the field at $SDI_0=3$, assuming cake filtration, the reference testing conditions in Table 2.3 different equipment inaccuracies and the experienced errors.

Table 6.5 The effects of accuracy errors of the Lab and Field equipment on $SDI_0=3$.

Parameter	Lab		Field	
	Error \pm	Influence $SDI_0=3\pm$	Error \pm	Influence $SDI_0=3\pm$
T	1 [°C]	0.03	5 [°C]	0.15
dP	7 [kPa]	0.05	10 [kPa]	0.06
R_M	0.1×10^{10} [m^{-1}]	0.20	0.2×10^{10} [m^{-1}]	0.39
A_M [D=47 mm]	2 [mm]	0.00	4 [mm]	0.00
t_1	1 [s]	0.03	5 [s]	0.17
t_2	1 [s]	0.07	5[s]	0.57
t_{15}	10[s]	0.02	15[s]	0.03
V_1	5 [mL/500mL]	0.00	50 [mL/500mL]	0.37
V_2	5 [mL/500mL]	0.00	50 [mL/500mL]	0.37
Total error		0.40		2.11

6.4 Conclusions

The SDI is sensitive for errors due to a low accuracy of equipment, different membrane properties, and variations in the testing parameters. Both mathematical models as well as experimental results show that a variation in the membrane resistance R_M has the highest impact on the SDI results. A 10 % error in R_{M0} results in a ± 0.25 variation for $\text{SDI}_0=3$. The variation in R_M the ASTM standard allows is responsible for an SDI range of 2.29-3.98 at the level of $\text{SDI}=3$. In addition, a 1 s error in measuring the time to collect the second sample t_2 results in a variation ± 0.07 at $\text{SDI}=3$. Artifacts and personal experience also influence SDI results.

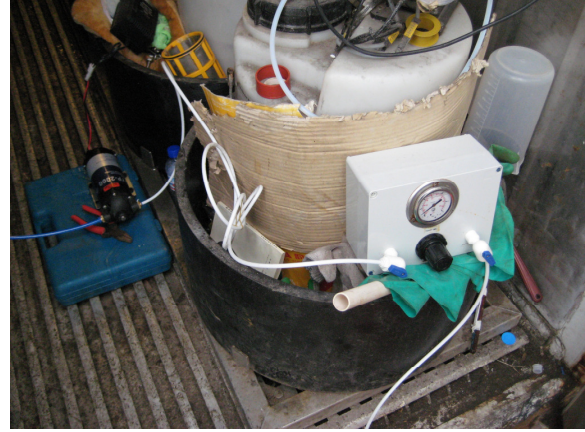
The total error in measuring the SDI can sum up to ± 2.11 in the field and ± 0.4 in the lab at the level of $\text{SDI}_0=3$. This large error in the SDI values might have large consequences for pretreatment evaluation at desalination plants.

The following advices and recommendations are based on the theoretical results and personal experience. Besides the ASTM protocol, we believe that these recommendations are important for reliable and reproducible SDI result and should be mentioned in an updated version of the ASTM standard.

It is strongly recommended to use fresh SDI feed water. The SDI feed water should not be stored close to a heat source. The SDI setup should be cleaned and flushed well with clean water (RO production) before the test. After that, the SDI setup should be flushed with the SDI feed water to remove the residual clean water and guarantee a constant feed water quality from $t=0$ on. The pressure gauge and the filter holder should be positioned at the same level. Accurate equipment is needed for reliable SDI results. The membrane should not be touched with the experimenter's hands; tweezers should be used. The support plate has to contain delicate bulges and have a low resistance. It is recommended to use an adjusted filter holder with a relief air valve. It is recommended to place filter paper under the membrane. t_0 for the test membrane should be between 25-50 s, where t_0 is the time to collect 500 mL of clean water under a pressure difference of 91.4-94.7 kPa. Preferably, new membranes should be used which should be stored in a dry and covered place. Last but not least, the SDI should be corrected for temperature, pressure and membrane resistance. For normalizing SDI for the testing conditions, available charts and tools can be used [13].

Annex 1

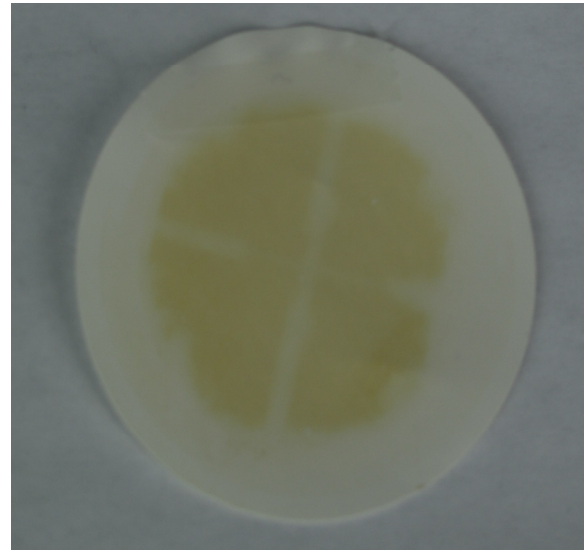
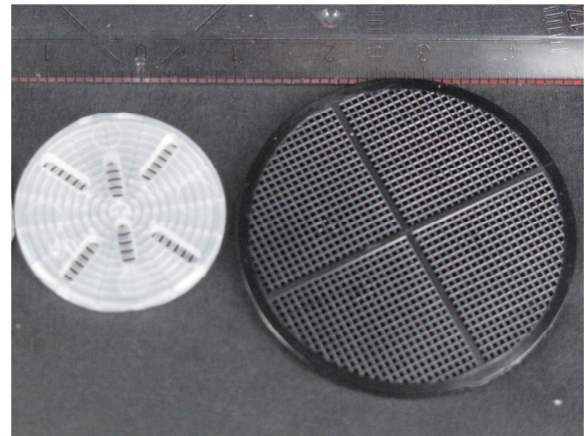
1. Field apparatus



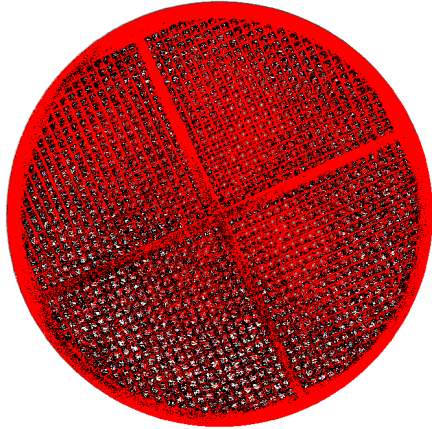
2. Filter holder, different sizes and material



3. Filter holder, support plates



4. Support plate, active area estimated using Image J software



5. Automatic SDI device



References

- [1] F. Rossignol, A.L. Penard, F.H.S. Nagaraja, C. Pagnoux, T. Chartier, Dispersion of alpha-alumina ultrafine powders using 2-phosphonobutane-1,2,4-tricarboxylic acid for the implementation of a DCC process, *European Ceramic Society*, 25 (2005) 1109-1118.
- [2] A. Alhadidi, A.J.B. Kemperman, J.C. Schippers, M. Wessling, W.G.J. van der Meer, Silt density index and modified fouling index relation, and effect of pressure, temperature and membrane resistance, *Desalination*, In press (2010).
- [3] M. Elimelech, J. Gregory, X. Jia, W. R.A, *Particle Deposition and Aggregation - Measurement, Modelling and Simulation*, in, Elsevier, 1995.
- [4] V. Privman, H.L. Fr'isch, N. Ryde, E. Matijevic, Particle Adhesion in Model Systems. Part 13: Theory of Multilayer Deposition, *Journal of Chemical Society Faraday Transactions*, 87 (1991) 1371-1375.
- [5] L. Song, M. Elimelech, Dynamics of Colloid Deposition in Porous Media: Modeling the Role of Retained Particles, *Colloids and Surfaces A*, 73 (1993) 49-63.
- [6] L. Song, M. Elimelech, Particle Deposition onto a Permeable Surface in Laminar Flow, *Journal of Colloid and Interface Science*, 173 (1995) 165-180.
- [7] A. Mosset, V. Bonnelye, M. Petry, M.A. Sanz, The sensitivity of SDI analysis: from RO feed water to raw water, *Desalination*, 222 (2008) 17-23.
- [8] J.H. Roorda, J.H.J.M.v.d. Graaf, *New parameter for monitoring fouling during ultrafiltration of WWTP effluent*, IWA Publishing, 2001.
- [9] P. van den Brink, A. Zwijnenburg, G. Smith, H. Temmink, M. van Loosdrecht, Effect of free calcium concentration and ionic strength on alginate fouling in cross-flow membrane filtration, *J. Membr. Sci.*, 345 (2009) 207-216.
- [10] ASTM Standard (D 4189 – 07): Standard Test Method for Silt Density Index (SDI) of Water, D19.08 on Membranes and Ion Exchange Materials, (2007).
- [11] A. Alhadidi, A.J.B. Kemperman, J.C. Schippers, M. Wessling, W.G.J. van der Meer, The influence of membrane properties on the Silt Density Index, Submitted to *J. Membr. Sci.*, (2010).
- [12] P. Dillon, P. Pavelic, G. Massmann, K. Barry, R. Correll, Enhancement of the membrane filtration index (MFI) method for determining the clogging potential of turbid urban stormwater and reclaimed water used for aquifer storage and recovery, *Desalination*, 140 (2001) 153-165.
- [13] A. Alhadidi, A.J.B. Kemperman, J.C. Schippers, M. Wessling, W.G.J. van der Meer, SDI normalization and alternatives, To be submitted (2010).

CHAPTER 7

SDI NORMALIZATION AND ALTERNATIVES

THIS CHAPTER HAS BEEN SUBMITTED TO PUBLICATION:

A. Al-hadidi, A.J.B. Kemperman, J. C. Schippers, M. Wessling, W.G.J. van der Meer, SDI normalization and alternatives, Desalination

This chapter introduces practical tools to resolve the SDI testing disadvantages. The SDI can be normalized to the SDI^+ based on a mathematical model developed before. From the mathematical relations, a line chart and slide wheel charts are developed to normalize SDI to SDI^+ for the testing conditions and the membrane resistance. A new fouling index was introduced to estimate the reverse osmosis (RO) feed fouling potential (SDI_v). SDI_v is the second fouling index developed at the University of Twente, 30 years after the MFI0.45.

7.1. Introduction

This chapter introduces practical tools to resolve these testing disadvantages of SDI. Based on the SDI definition, a slide tool was developed to calculate the SDI from the measured times for the collection of the first and second sample (t_1 and t_2) after 15 minutes (t_f). The 500 mL volume sample to be collected is based on a membrane diameter of 47 mm. Different membrane diameters such as 25 or 90 mm can also be used and the adjusted sample volume can be calculated in the field with another specially developed tool.

Assuming cake filtration and 100 % particle rejection, the SDI can be normalized to the SDI^+ based on a mathematical model developed before. From the mathematical relations, a line chart and slide wheel charts are developed to normalize SDI to SDI^+ for the testing conditions and the membrane resistance.

A new fouling index is introduced to estimate the reverse osmosis (RO) feed fouling potential. The volume based SDI, SDI_v , compares the initial flow rate to the flow rate after filtering the standard volume V_f using MF membranes with an average pore size of 0.45 μm . SDI_v has a linear relationship to the particle concentration if complete blocking mechanism is dominant during the test. The mathematical model shows that SDI_v is independent of the testing parameters and membrane resistance. The mathematical model and the experimental results show that SDI_v eliminates most of the above mentioned SDI disadvantages. SDI_v is the second fouling index developed at the University of Twente, 30 years after the MFI0.45.

7.2. Results and discussion

Four new tools to calculate or correct the SDI will be introduced. For determining the sample volume for different membrane diameters (25, 47 and 90 mm) a small circular chart can be used. Based on the ASTM definition of the SDI, a tool is developed to be used in calculating the SDI based on the measured t_1 and t_2 values. Line and wheel slide charts were developed to normalize the measured SDI for the testing conditions (T , dP , and R_M) based on the SDI/MFI0.45 relation by assuming cake filtration as well as 100% particle retention. For different fouling mechanisms, four different charts can be used for normalizing the SDI to eliminate the influence of the testing parameters on the SDI.

7.2.1. Determining the sample volume

In the ASTM standard, the volumes to be collected are 500 mL which is based on a 47 mm membrane diameter. However, the sample volumes change in direct proportion to the membrane area:

$$V_{1,2} = V_o \times \frac{A_M}{A_{M0}} \quad (7.1)$$

Where

$V_{1,2}$ sample volume 1 and 2 [mL]

V_o reference standard sample volume [500 mL]

A_{M0} reference membrane area [$13.8 \times 10^{-4} \text{ m}^2$]

A_M membrane area [m^2]

The ASTM includes the use of three standard membrane diameters of 47, 25 and 90 mm. The sample volumes for those standard diameters are 500, 141.5 and 1833.4 mL, respectively, which were calculated using Eqn. (7.1).

Figure 7.1 is a tool which was used to determine the sample volumes V_1 and V_2 for the different membrane diameters 25, 47 and 90 mm.

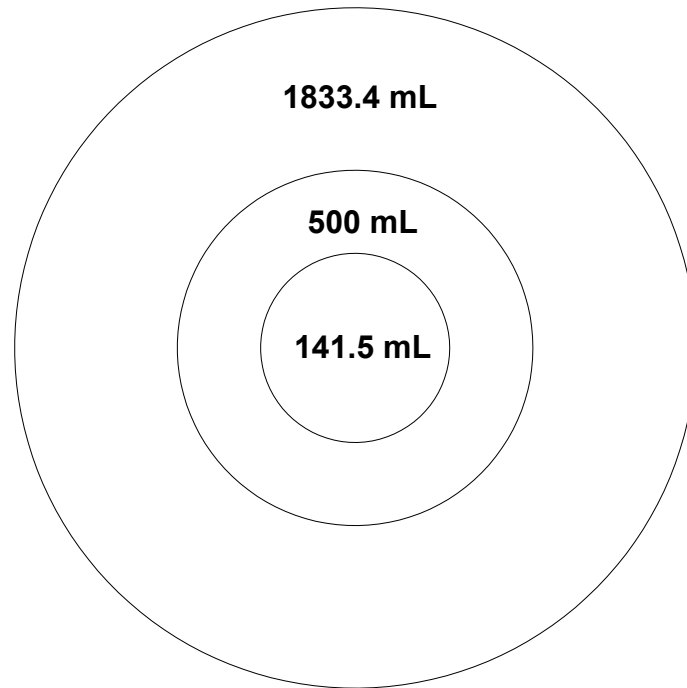


Figure 7.1. Determining the sample volume $V_{1,2}$ for different membrane diameters 25, 47 and 90mm.

Figure 7.1 is a useful tool for operators in the field and should be produced as a chart in the right scale according to the membrane diameter. The used membrane can be placed on the chart. The operator can then read directly the correct sample volume for that membrane.

7.2.2. Calculating SDI when t_f equals 15 minutes

Since the SDI test might be performed by non-professionals in the field, they may make mistakes in calculating the SDI using a calculator. Figure 7.2 presents a new tool (slide chart) for calculating the SDI based on the measured t_1 , t_2 , and $t_f = 15$ min. The new tool was designed for the range of times t_1 and t_2 between 10 s – 100 s and calculates the SDI using Eqn. (2.1).

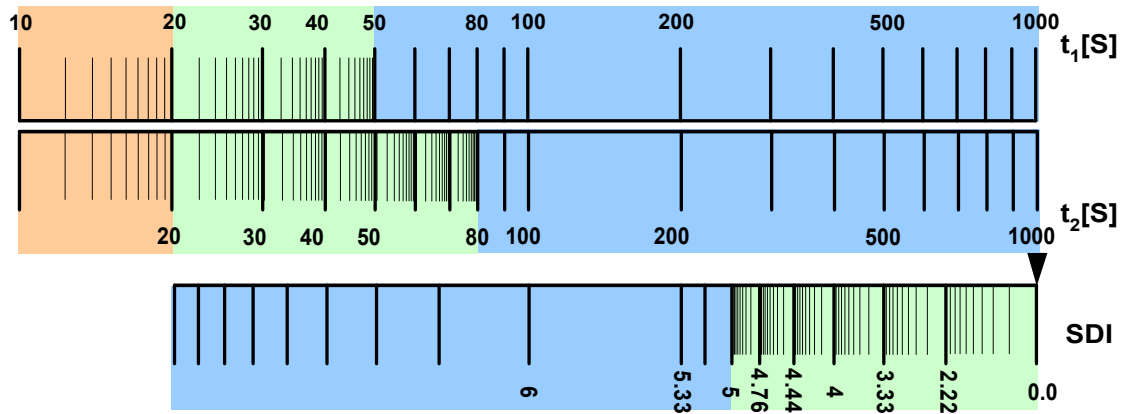


Figure 7.2. Tool for calculating SDI for t_1 and t_2 and $t_f = 15$ min.

The top and central rulers indicate t_1 and t_2 in seconds, while the bottom ruler indicates the calculated SDI value for t_f equaling 15 minutes. The chart in Figure 7.2 is used as follows: after determining t_1 and t_2 , the central ruler moves to the left until the value of t_1 in the top ruler is placed on top of the value of t_2 on the central ruler. In this way, the value directly below the arrow on the central ruler indicates the SDI value for $t_f = 15$ min. Figure 7.3 shows an example of how to use the presented slide chart. In this case, the slide rule indicates the SDI value for $t_1 = 20$ s and $t_2 = 30$ s at $t_f = 15$ min as $SDI = 2.22$.

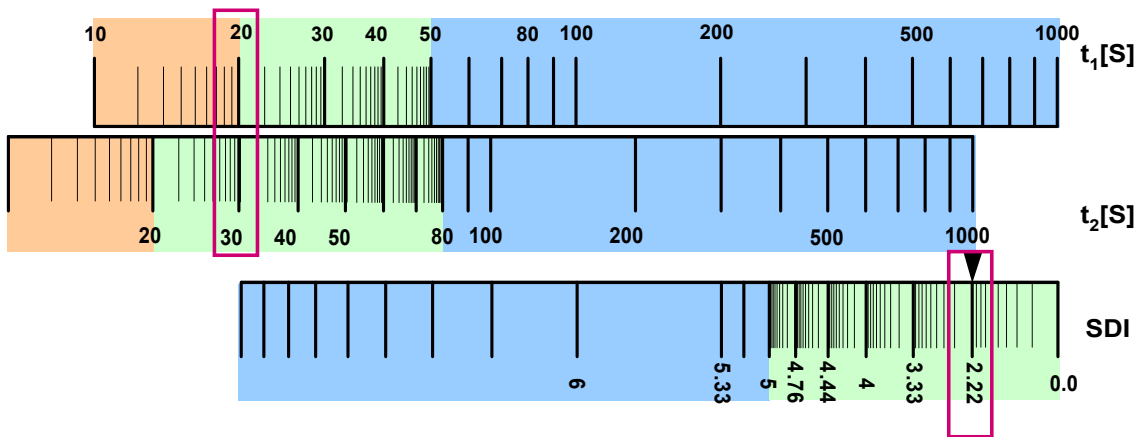


Figure 7.3. Example indicating $SDI = 2.22$ when $t_1 = 20$ s, $t_2 = 30$ s and $t_f = 15$ min.

7.2.3. Normalized SDI under a cake filtration mechanism (SDI⁺)

By assuming only cake filtration occurs during the SDI test, the SDI/MFI0.45 relation was used to normalize the SDI based on the reference testing conditions as defined in Table 2.3. In this way, the SDI⁺ is obtained by assuming the cake filtration mechanism as well as a 100 % particle rejection. For practical reasons in the field, line chart and slide wheel charts were developed to normalize SDI to SDI⁺ based on the SDI/MFI0.45 relation.

t_0 is defined as the required time in seconds for the 0.45 μm membrane used in the SDI test to collect a sample volume V_0 of an RO permeate (500 mL for a diameter of 47 mm) at constant applied pressure 207 kPa (2.07 bar) at 20 °C. The sample volume V_0 should be adjusted in direct proportion to the membrane area using Eqn. (7.1). This time t_0 is a measure for the membrane resistance R_M . At least one measurement of t_0 for each membrane batch is recommended. The relation between R_M and t_0 is described by Darcy's law in Eqn. (7.2) [1]:

$$R_M = \frac{dP}{\mu \times J} = \frac{dP}{\mu \times \frac{V_0}{A_M \times t_0}} = \text{const} \times t_0 \quad (7.2)$$

Where J is the flux [$\text{m}^3/\text{m}^2 \text{ s}$], μ is the water viscosity = 0.001 Pa.s, $dP = 207 \text{ kPa}$, $A_M = 13.8 \times 10^{-4} \text{ m}^2$ and $V_0 = 500 \text{ mL}$. Therefore, the membrane resistance $R_M [\text{m}^{-1}]$ can be converted to $t_0 [\text{s}]$ with Eqn.(7.3).

$$R_M = 0.57 \times 10^9 \times t_0 \quad (7.3)$$

Based on Darcy's law and Eqn.(3.3), t_0 should be normalized for temperature:

$$t_0 \text{ at } 20^\circ\text{C} = \left(\frac{T + 42.5}{T_0 + 42.5} \right)^{-1.5} \times t_0 \quad (7.4)$$

Where, T is the measured temperature [$^\circ\text{C}$].

The charts can be presented in two ways: as a line chart or slide wheel chart. The following two examples show how these charts can be applied to normalize the measured SDI:

1- Line charts to correct for T , dP and R_M

Figure 7.4 contains three charts (T , dP and R_M) within one framework. Based on the model in Eqn. (4.5) and the reference conditions in Table 2.3, each chart is calculated one-by-one by varying the target parameter within a range of T (10 – 60 °C), dP (1 – 3 bar) and t_0 (4.51 – 72.26 s) for different fouling potential indexes I , corresponding to the SDI range 0 – 6.66. The

suggested range of t_0 is corresponding to the 0.45 μm MF membrane resistance range available in the market ($0.39 \times 10^{10} - 2.65 \times 10^{10} \text{ m}^{-2}$) [2]. The fouling potential index $I = 1.056 \times 10^9 \text{ m}^{-2}$ corresponds to the reference conditions in Table 2.3.

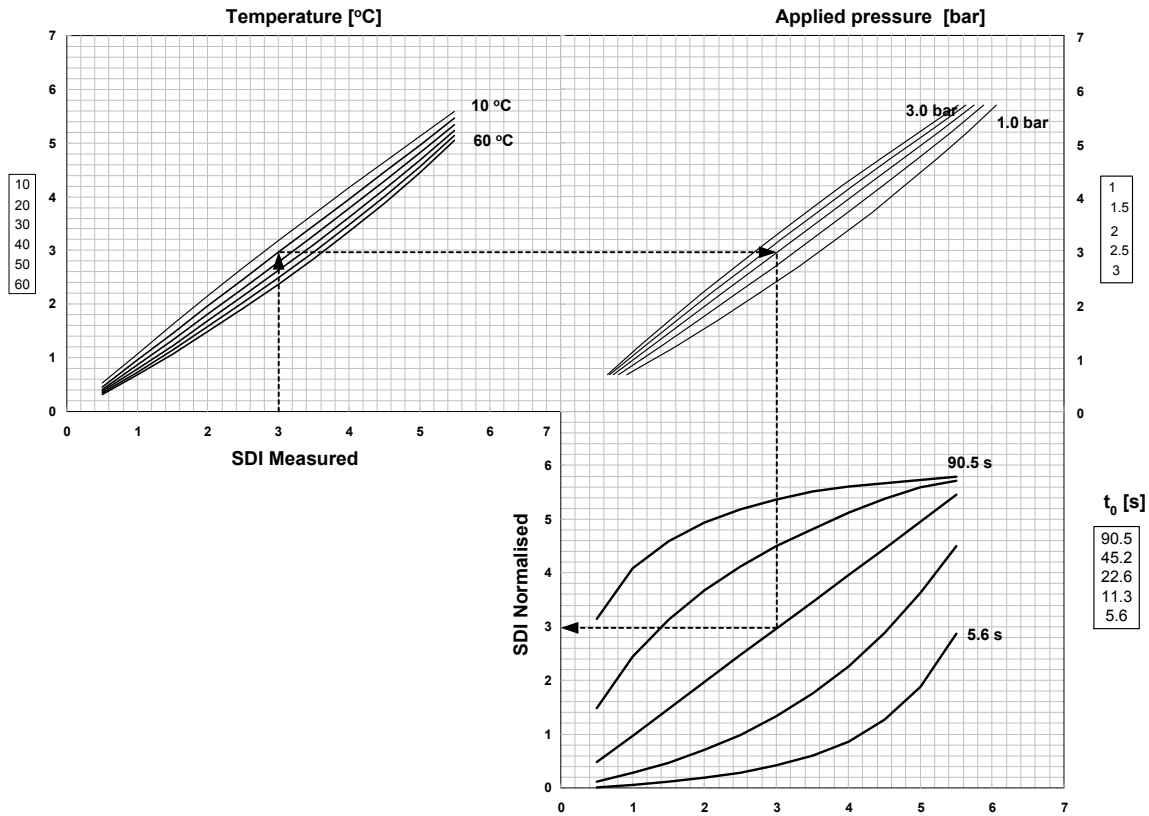


Figure 7.4. Line chart to normalize the SDI value to the reference testing conditions: T [°C], dP [bar], t_0 [s] assuming cake filtration and 100 % particle rejection.

Figure 7.4 presents the line chart to normalize the SDI for T , dP and R_M . The line chart contains three sub-charts: temperature, pressure and membrane resistance (as t_0). Starting with the measured SDI value on the x-axis in the left corner, a target line starts to vertically reach the actual temperature. The target line then moves to the right in direction of the pressure lines reaching the actual applied pressure. The next step for the target line is to move down in the resistance chart represented by t_0 (the time needed to collect the sample volume of RO production under pressure 207 kPa). After reaching the actual membrane resistance (measured t_0), the target line then moves horizontally to the left side and the SDI normalized value can be read on the Y-axis.

2- Slide wheel charts for T , dP and R_M

Three slide wheel charts for normalizing the SDI for T , dP and R_M are presented in Figure 7.5, Figure 7.6 and Figure 7.7, respectively. Similarly to the line chart, the slide wheel charts are

calculated with the model in Eqn. (4.5). Each chart for each parameter was calculated for different fouling potential indexes I corresponding to the SDI range 0 – 6.66 and for a proposed range T (6 – 58 °C), dP (1.5 – 2.8 bar) and t_0 (1 – 43 s).

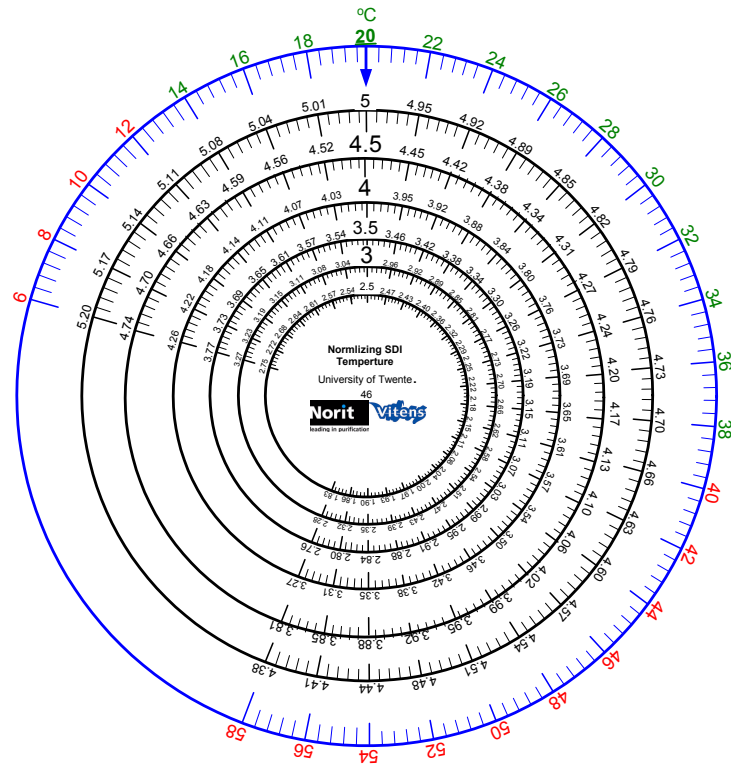


Figure 7.5. Slide wheel chart to normalize the SDI value to the reference testing conditions T [°C] assuming cake filtration and 100% particle rejection.

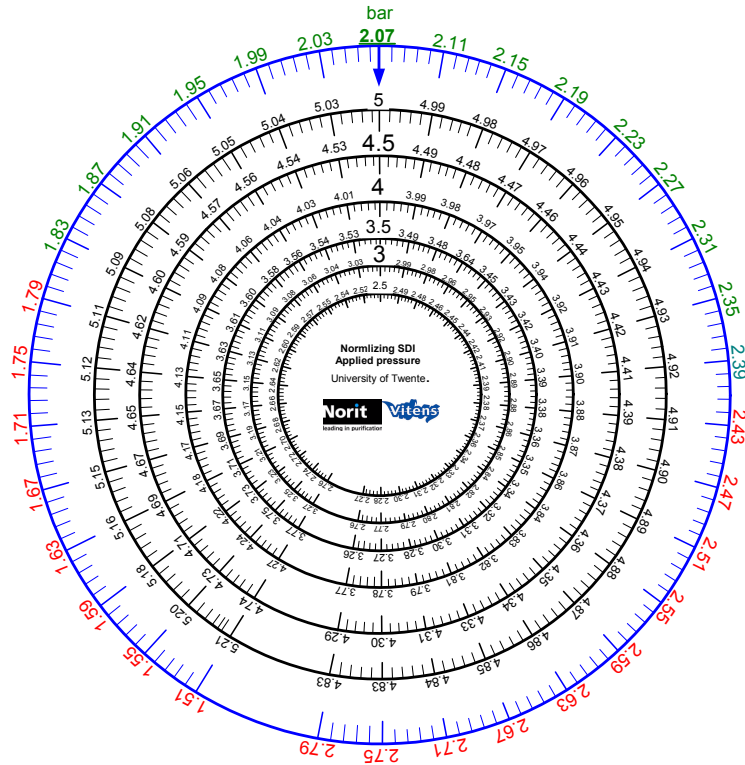


Figure 7.6. Slide wheel chart to normalize the SDI value to the reference testing conditions dP [bar] assuming cake filtration and 100% particle rejection.

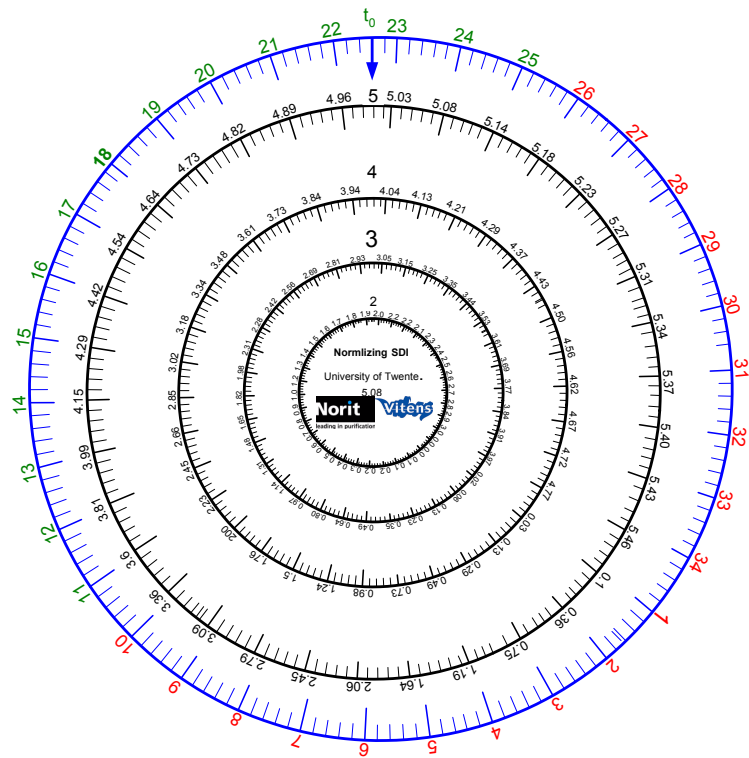


Figure 7.7. Slide wheel chart to normalize the SDI value to the reference testing conditions as t_0 assuming cake filtration and 100% particle rejection.

Figure 7.8 shows an example of the slide wheel chart implementation when a membrane resistance is assumed different from the reference value. $t_0=22.6$ s corresponds to the reference testing conditions in Table 2.3. (T_0 , dP_0 , R_{M0} and A_{M0}).

The wheel chart contains two wheels: an external-fixed wheel and internal slide wheel. Take as example as starting situation the wheel shown in Figure 7.5. Initially in Figure 7.6, the fixed-external wheel indicates $t_0=22.6$ s, while the internal slide wheel indicates the SDI values for different fouling potentials (SDI=5, 4, and 3). Let's assume that we perform SDI test with a membrane which has lower resistance than the reference membrane. With this membrane, 500 mL of clean water was collected in 18 s instead of 22.6 s for the reference membrane. The SDI measured for this specific membrane was 5. To normalized the SDI measured for the membrane resistance, the internal slide wheel will be turned to in the direction of the measured t_0 (counter-clock wise) until the SDI measured =5 faces $t_0=18$ s as shown in Figure 7.8. The normalized SDI value (SDI^+) then can be read in the internal slide wheel, as the SDI value which faces $t_0=22.6$ s and on the same slide as SDI=5, hence $SDI^+=5.25$ (indicated in Figure 7.8 with the red lines).

Due to the proportional relation between t_0 and R_M , the internal wheel in Figure 7.8 will be turned counter-clock wise when the measured membrane resistance R_M is smaller than the reference membrane resistance R_{M0} ($1.29 \times 10^{10} \text{ m}^{-1}$). On the other hand, the internal wheel will be turned clock wise if the measured R_M is larger than R_{M0} .

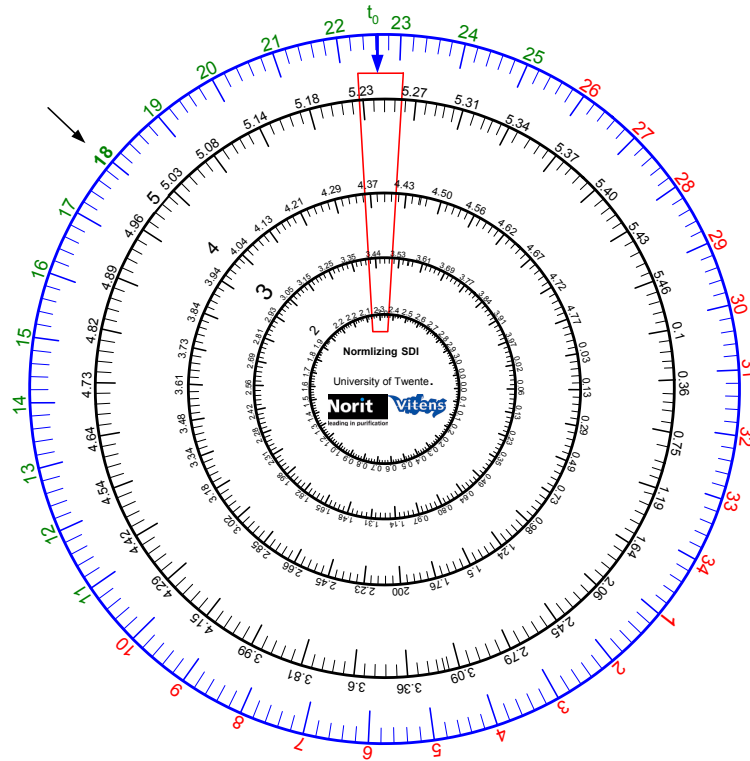


Figure 7.8. An example of using the slide wheel chart to normalize the SDI value to the reference testing conditions: R_M [m^{-1}] assuming cake filtration and 100% particle rejection.

7.2.4. Normalizing SDI under different fouling mechanisms (SDI^+)

The filtration laws for constant pressure and the parameters C and m were defined in Table 2.2. [3]. The constant C is proportional to the particle concentration, whereas the exponent m is defined by the fouling mechanism resulting in m values 0, 1, 1.5 and 2 but can in fact be any other real value. By using equations (5.8) & (5.9) for assumed m and C values, the SDI can be calculated. The relation between the constant C and the membrane resistance can be generalized as follow:

$$C \approx \frac{R_M^{1-m}}{W_{(R,A,V)}} \quad (7.5)$$

For exact m values of 0, 1, 1.5 and 2, Figure 7.9 shows the normalized SDI (SDI^+) values for different $\log(C)$ values for the four fouling mechanisms calculated using Eqns. (5.8) & (5.9). Based on m (0, 1, 1.5 and 2) the parameter $\log(C)$ was varied (2 – 12, -4 – 2, -10 – -4 and -15 – -10) respectively. The reference testing conditions of Table 2.3 were assumed.

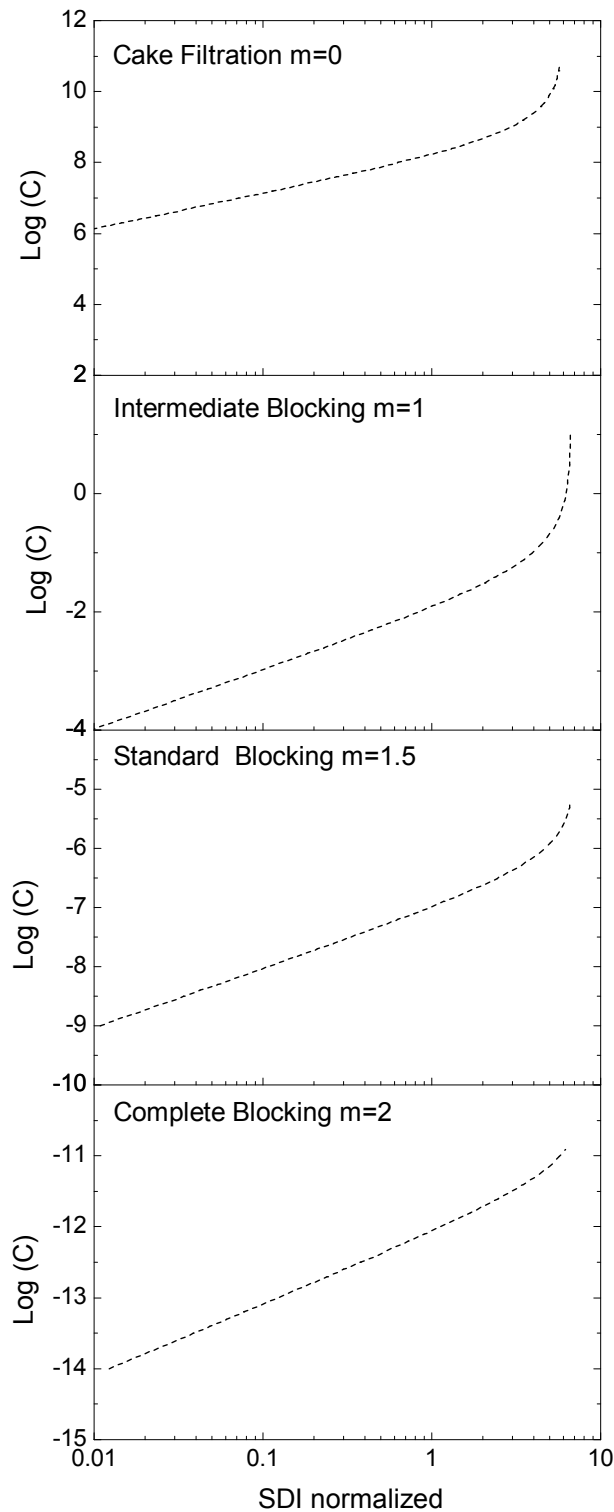


Figure 7.9. The normalized SDI values for measured C and m values. By assuming the reference conditions (Table 3), C and m , Eqns. (5.8) & (5.9) were used to calculate SDI.

When an SDI test is performed the filtration data t and V can be used to determine the parameters C and m using Eqn. (2.6). For the main four m values (corresponding to the four

fouling mechanisms) the normalized SDI value (SDI^+) for T , dP and R_M can be obtained by crossing the C value with the correct dotted line in Figure 7.9.

Figure 7.9 can be used for normalizing the SDI for the testing condition parameters and the membrane resistance when only single fouling mechanism occurs during the SDI test, (i.e. the m value is exactly 0, 1, 1.5 or 2) and the particle rejection is 100 %.

7.2.5. Alternatives for SDI

A new volume based SDI ("SDI_v") will be defined. The SDI_v will be compared to the standard SDI and SDI^+ results. The sensitivity of SDI_v for errors in the measurements and variation in the testing parameters will be calculated.

7.2.5.1. Definition of the volume based SDI_v

In the SDI test, the time between the two measurements t_f is fixed (5, 10 or 15 min) and the total volume that is filtered in that time depends on the flow rate. Thus, any effect that increases the flow through the membrane will increase the fouling load of the membrane and consequently the measured SDI will be higher. This explains our observation that the SDI increases with increasing temperature (decreasing viscosity implies increased flow), increasing pressure and decreasing membrane resistance [4]. To assure the same fouling load is provided to all the membranes under any testing condition, it is much more logical that the second sample should be collected after a fixed filtrated volume V_{f0} instead of fixed time t_f . In that way, the fouling load will be the same for all SDI determinations. Consequently, the volume based SDI test will overcome the effects of the testing condition parameters and will decrease the effect of the membrane resistance.

Definition 1

To determine the SDI_v [%/m], the volume-based plugging ratio per specific unit volume [m^3/m^2] of a membrane filter with pores of $0.45 \mu\text{m}$ and diameter 47 mm at 30 psi (207 kPa) is measured. The measurement is done as follows:

- The time t_1 is defined as the time required to filter the first V_1 500 mL.
- After a standard volume V_{f0} is filtered since from the start of this measurement, t_2 is defined as the time required to filter another V_2 500 mL.
- The index is calculated using the following formula.

$$SDI_{-v} = \frac{100\%}{\frac{V_{f0}}{A_{MO}}} \left(1 - \frac{t_1}{t_2} \right) = \frac{\%P_{-v}}{\frac{V_{f0}}{A_{MO}}} \quad (7.6)$$

Where t_1 [s] is the time to collect the first sample V_1 , t_2 [s] is the time to collect the second sample V_2 after filtrating the standard volume V_{f0} , A_{MO} is the reference membrane area [m²] and $\%P_{-v}$ is the volume-based plugging ratio [%].

Definition 2

SDI_v [%m] also can be defined as the plugging ratio after a fixed filtrated volume V_{f0} divided by 15 of a membrane filter with pores of 0.45 μm and diameter 47 mm at 30 psi (207 kPa), where 15 is a dimensionless number to scale SDI_v down to the standard (time-based) SDI values between 0 and 6.66.

$$SDI_{-v} = \frac{100\%}{15} \left(1 - \frac{t_1}{t_2} \right) = \frac{\%P_{-v}}{15} \quad (7.7)$$

Where t_1 [s] is the time to collect the first sample V_1 , t_2 [s] is the time to collect the second sample V_2 after filtering the standard volume V_{f0} . Both definitions can be used as the new fouling index. The volume of the first sample V_1 (500 mL), the second sample V_2 (500 mL) and the standard volume V_{f0} should be adjusted in direct proportion to the membrane area. In this study mainly definition 1 is used unless otherwise mentioned.

7.2.5.2. Calculation of SDI_v

Eqns.(5.8) and (5.9) can be combined to give the analytical expressions for the SDI_v for different fouling mechanisms based on C and m . The reference filtrated volume V_{f0} is arbitrarily defined as the average accumulated volume collected in 15 minutes (V_{15}) of the four fouling mechanisms with the reference testing parameters defined in Table 2.3:

$$V_{f0} = \frac{V_{f0}(cake) + V_{f0}(Inter) + V_{f0}(Stan) + V_{f0}(Comp)}{4} = 14.58 \text{ L.}$$

Where (*cake*) stands for cake filtration (14.1 L), (*Inter*) for intermediate blocking (14.5 L), (*Stan*) for standard blocking (14.7 L) and (*Comp*) for complete blocking (15.0 L).

The sample volumes V_1 and V_2 (500 mL) are based on a 47 mm filter diameter. When a different filter diameter is used, the sample volumes V_1 and V_2 are adjusted in direct proportion to the filter diameter as described in Eqn.(7.1).

With the functions $t(V)$ and $V(t)$, t_1 and t_2 can be determined which are required to calculate the SDI_v in Eqn.(7.3). These parameters are derived from Eqns. (5.8) & (5.9) using the following steps:

1. t_1 follows from Eqn. (5.9);
2. t_2 can not be determined directly and, as a consequence, a couple of steps are needed;
3. by substituting V_{f0} for V in Eqn. (5.9) one obtains t_f ;
4. $V_{total} = V_{f0} + V_2$ (V_{total} , V_{f0} and V_2 are the volumes filtered in t_{total} , t_f and t_2 respectively);
5. substitution of V_{tot} for V in Eqn. (5.9) gives t_{total} ;
6. t_2 follows from $t_2 = t_{total} - t_f$;
7. the SDI_v finally is calculated by substitution of t_1 and t_2 in Eqn.(7.6).

The filtrated volume as function of time (V vs. t) can plotted in a typical fouling curve as schematically presented in Figure 7.10, illustrating schematically the determination steps for SDI_v from a time-volume curve.

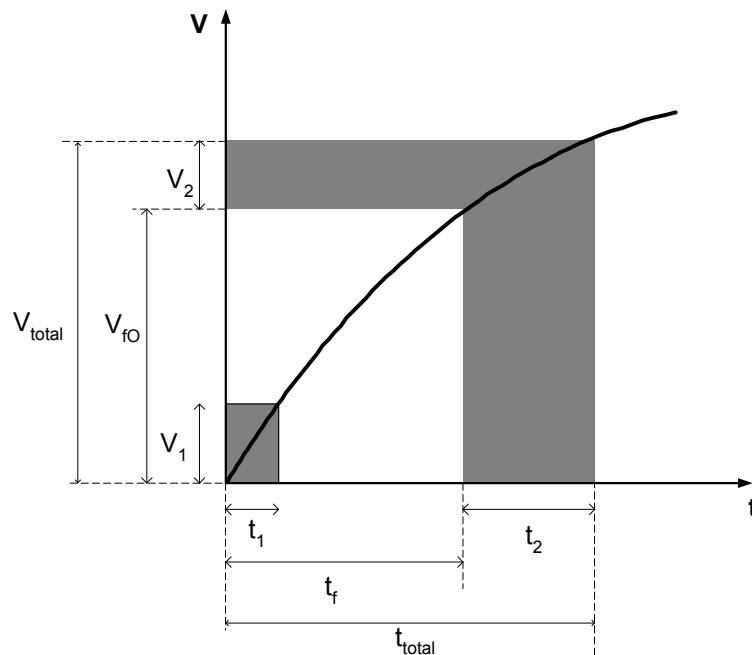


Figure 7.10. Theoretical diagram showing the filtrated volume as function of time and the variables used to determine SDI_v. $V_{f0}=14.58$ L.

7.2.5.3. SDI_v sensitivity for particle concentration and fouling mechanism

The sensitivity of SDI_v for the particle concentration was studied using the SDI_v model described in section 7.2.5.2. The relative particle concentration was varied, where a relative concentration of 1 corresponds to SDI_v=4.36. SDI_v values were plotted vs. the particle concentration in Figure 7.11. The reference testing conditions mentioned in Table 2.3 were assumed, and a standard filtrated volume V_{f0} of 14.58 L was used.

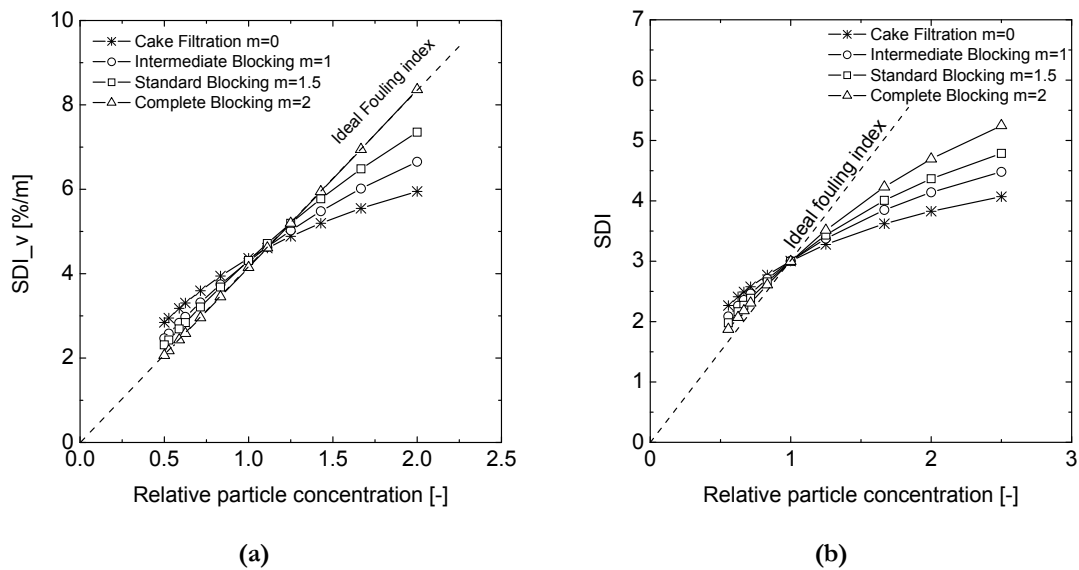


Figure 7.11. The sensitivity of (a) SDI_v and (b) time-based SDI for the relative particle concentration, where a relative concentration of 1 is corresponding to SDI_v=4.36. The standard filtrated volume $V_f=14.58$ L and the reference testing conditions from Table 3 were assumed.

Figure 7.11 shows that the SDI_v sensitivity for the particle concentration is different for the four fouling mechanisms. The SDI_v has a linear relationship with particle concentration if complete blocking mechanism is dominant during the SDI_v test. In previous work, we studied the sensitivity of the standard (time-based) SDI for the particle concentration and different testing condition parameters [2]. By comparing the sensitivity of SDI_v in Figure 7.11 (a) and the sensitivity of the time-based SDI Figure 7.11 (b), we conclude that SDI_v has a more linear relationship with particle concentration than the time-based SDI.

7.2.5.4. SDI_v sensitivity for testing parameters and fouling mechanism

The sensitivity of SDI_v for variations in the testing condition parameters was studied as well. The fouling indices $w_{A,V}$ were assumed to be independent of the membrane resistance R_M , while the relation between w_R and R_M was described before [4, 5]. For that the effect of the R_M on SDI_v will be separately discussed for cake filtration and the three pore blocking mechanisms.

Assuming pore blocking (the three fouling mechanisms standard, intermediate and complete blocking), SDI_v was plotted in Figure 7.12 as function of R_M ($0.5 \times 10^{10} \text{ m}^{-1} < R_M < 3.0 \times 10^{10} \text{ m}^{-1}$). For four different mechanisms, SDI_v was plotted as a function of dP ($0.5 \text{ bar} < dP < 2.75 \text{ bar}$) and T ($10 \text{ }^\circ\text{C} < T < 50 \text{ }^\circ\text{C}$).

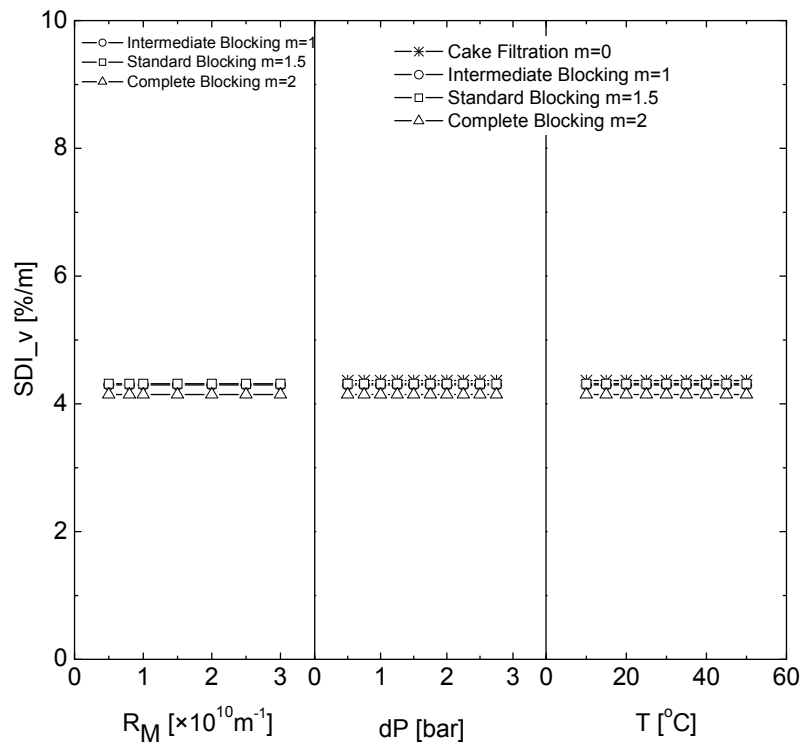


Figure 7.12. The sensitivity of SDI_v for membrane resistance, pressure difference and temperature for the standard filtrated volume of $V_f=14.58 \text{ L}$.

Figure 7.12 shows that the SDI_v is independent of the variation in the testing condition parameters dP and T for all four fouling mechanisms. SDI_v is independent of the membrane resistance R_M for intermediate, standard and complete blocking.

Assuming cake filtration is the only fouling mechanism, Figure 7.13 presents the effect of the membrane resistance R_M on the SDI_v results. In this graph, the SDI_v index was calculated based on the first as well as on the second definition given in section 7.2.5.1. The specific cake resistance R_C was assumed to be equal to $1.056 \times 10^9 \text{ m}^{-2}$, corresponding to the reference testing conditions and a time-based SDI equal to 3. The membrane resistance R_M was varied between 0.3 to $2.7 \times 10^{10} \text{ m}^{-1}$.

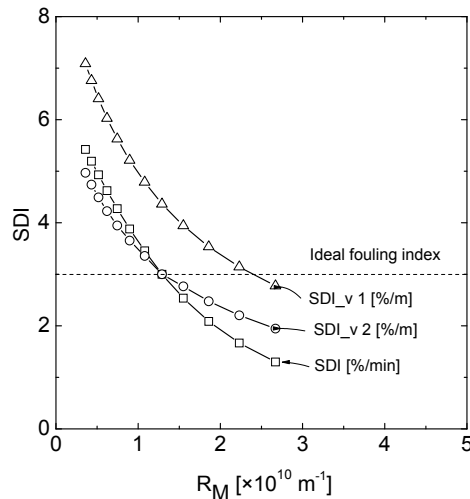


Figure 7.13. The sensitivity of the standard SDI and SDI_v based on definitions 1 (SDI_v1) and 2 (SDI_v2) in section 7.2.5.1 for the membrane resistance R_M . The standard filtrated volume V_f was 14.58 L, the cake resistance $1.055 \times 10^9 \text{ m}^{-1}$ with the assumed reference testing conditions of Table 3.

The SDI_v2 and SDI in Figure 7.13 have identical scale and they can be compared. From Figure 7.13 we can conclude that the new fouling index SDI_v2 is less sensitive for a variation in the membrane resistance than the time-based standard SDI. Thus, the influence of a variation in the membrane properties on SDI_v2 is smaller than the influence on the standard SDI. From Figure 7.11, Figure 7.12, and Figure 7.13, we conclude that the introduction of the SDI_v solves most of the time-based SDI problems and is closer to an ideal fouling index.

7.2.5.5. Experimental validation

The standard SDI and MFI0.45 indices were measured in the Evides RO/UF desalination plant in Jacobahaven, the Netherlands, described in Chapter 4 [6]. UF feed was diluted with RO permeate with different dilution ratios to investigate the influence of the foulant concentration on the SDI: 50 mL, 100 mL, 200 mL, 300 mL and 500 mL of UF feed were diluted in 25 L of

RO permeate. Three different membranes with different membrane resistances (M4, M5 and M7) were used to carry out the SDI tests. Table 3.1 shows the average membrane resistances of these membranes. SDI results were normalized for membrane resistance and temperature (SDI⁺).

The filtration data (V versus t) that were used to calculate the (time-based) SDI can be also used to calculate the SDI_v. However, filtration data for the time-based SDI were limited to a total filtration time of 20 minutes. Based on SDI_v definition 1, an accumulated filtrated volume V_{f0} of 3.65 L was suggested for the 25 mm diameter cell. In case of a high membrane resistance (M5), V_{f0} would need more than 20 minutes collection time. In order to compare the 3 membranes with the available data, a standard V_{f0} of 1.25 L instead of 3.65 L was assumed. To obtain a comparable fouling load for the time-based SDI and SDI_v, t_f was decreased to 5 min and the SDI₅ was calculated. The time-based SDI₅, normalized SDI⁺ and SDI_v results were plotted versus the fouling potential index I as shown in Figure 7.14 a-c.

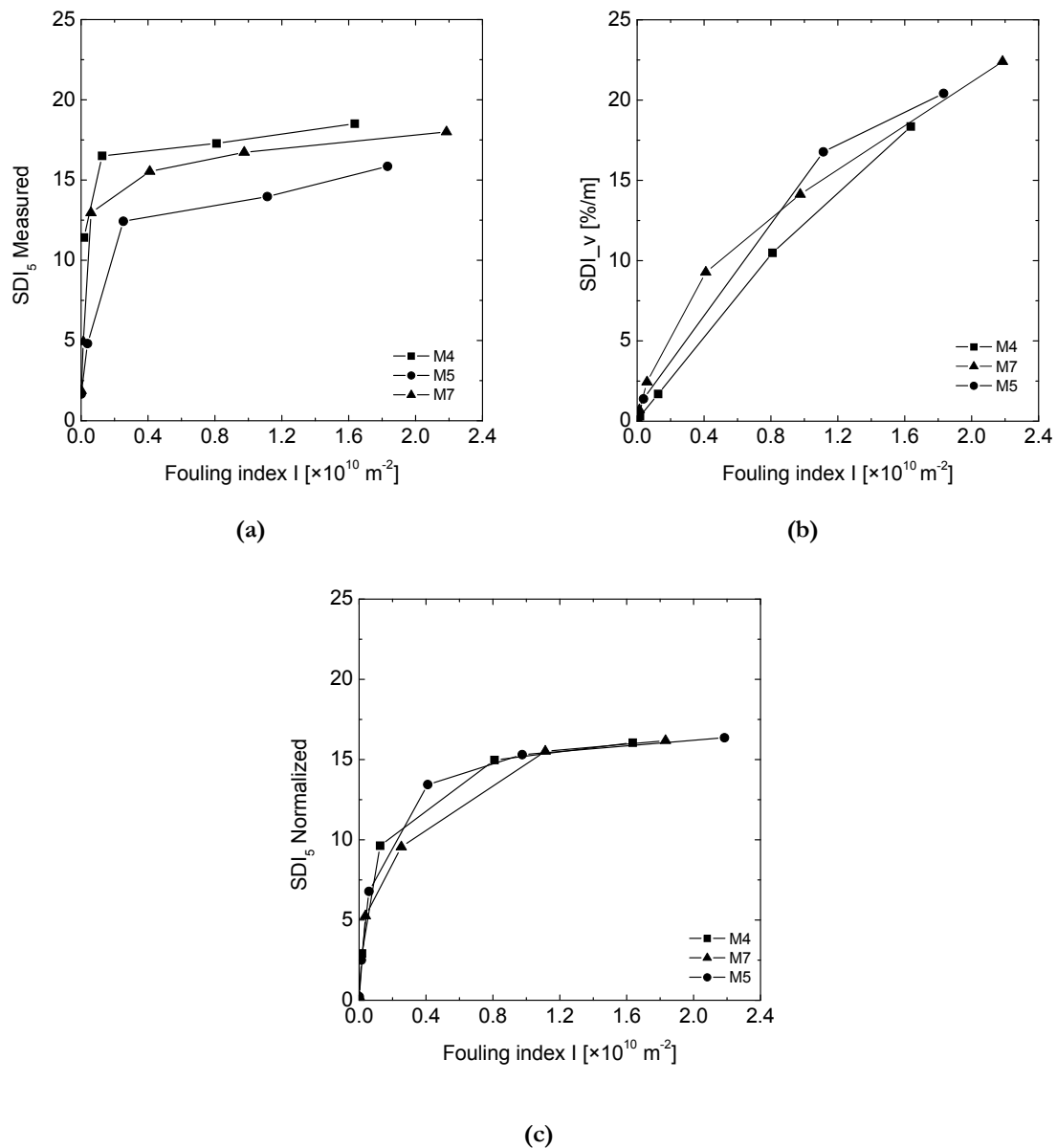


Figure 7.14. (a) standard time-based SDI for 5 minutes elapsed filtration time (b) SDI_v values (c) time-based SDI normalized for the membrane resistance and the testing condition parameters (SDI^+).

In Figure 7.14 (a) membrane M4 with the lowest membrane resistance shows in the highest SDI at a certain fouling load. Contrarily, M5 with the highest membrane resistance reveals the lowest SDI. SDI_v results based on $V_{f0} = 1.25$ L in Figure 7.14 (b) show a more linear relationship with the fouling index I. Besides that, the curves of the three membranes are closer to each other. Thus, SDI_v is less sensitive for differences in the membrane resistance compared to the time-based SDI. The standard SDI results were normalized to SDI^+ for the membrane resistance and temperature in Figure 7.14 (c). The curves of the three membranes are almost identical, especially

at higher fouling indexes. An ideal fouling index should not be affected by differences in the membrane resistance and should have a linear relationship with the particle concentration. However, the membrane resistance affects SDI_v , while SDI^+ has no linear relation with the particle concentration.

The fouling index SDI_v can be calculated through the $SDI_v/MFI_{0.45}$ relation following the steps in section 7.2.5.2 which results in Eqn.(7.8).

$$SDI_v = \frac{100}{\frac{V_{f0}}{A_M}} \left(1 - \frac{\frac{\mu \cdot R_M \cdot V_C + MFI \cdot V_C^2}{dP \cdot A_M}}{\frac{\mu \cdot R_M \cdot (V_{f0} + V_C) + MFI \cdot (V_{f0} + V_C)^2}{dP \cdot A_M} - \frac{\mu \cdot R_M \cdot V_{f0} + MFI \cdot V_{f0}^2}{dP \cdot A_M}} \right) \quad (7.8)$$

Where, V_C is the sample volume $V_C = V_1 = V_2$ and MFI is the modified fouling index. Another option is to determine SDI_v by measuring the fouling potential index I :

$$SDI_v = \frac{200 \cdot A_M \cdot I}{2 \cdot A_M \cdot R_M + 2 \cdot I \cdot V_f + V_C \cdot I} \quad (7.9)$$

Normalizing SDI_v can be done by measuring the fouling potential index I and substituting it and the reference testing conditions from Table 2.3 in Eqn.(7.9).

SDI_v can be normalized using Figure 7.15 for target t_0 (4.5 – 72.3 s). Starting with the measured SDI_v value on the x-axis, a target line starts vertically to the resistance lines represented by t_0 (the time needed to collect the sample volume of RO production under pressure 207 kPa). After reaching the actual membrane resistance (measured t_0), the target line then moves horizontally to the left side and the SDI_v normalized value can be read on the Y-axis.

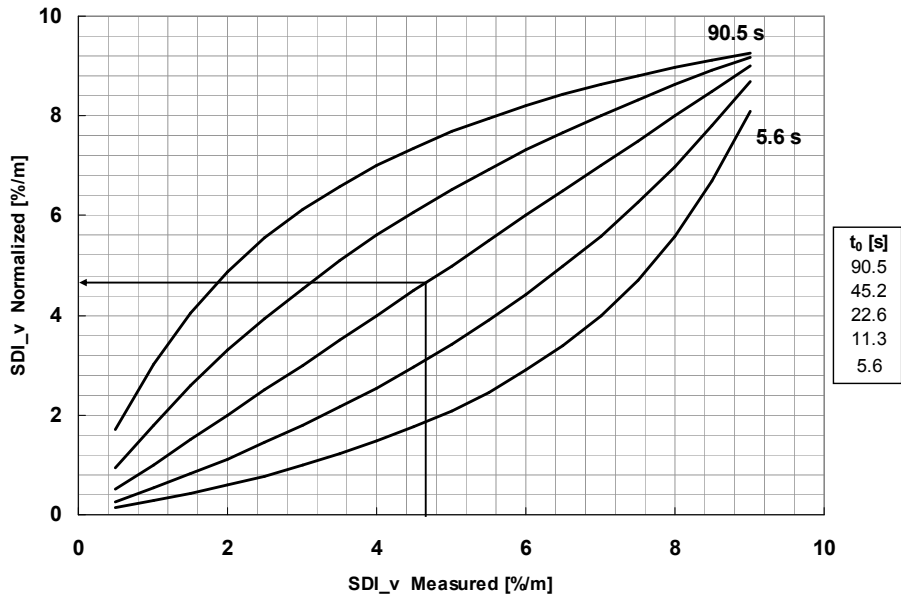


Figure 7.15. Line chart to normalize the SDI_v value to the membrane resistance represented by t_0 [s] assuming cake filtration and 100 % particle rejection.

7.2.5.6. Sensitivity of SDI_v for errors

By definition, the scale of the standard SDI is 0 – 6.66 (%P/15 min) while the scale of the SDI_v based on definition 1 is 0 – 9.5 (%P_v/ V_{JO} / A_M). Due to this difference in scale, the comparison between the sensitivities of both indices is presented as a percentage of the actual value. In this section, by assuming a cake filtration mechanism, the reference testing conditions (Table 2.3) and a fouling potential w_R of 12.22 (corresponding to a standard SDI value of 3), SDI_v was found to be equal to 4.36. The sensitivity of the SDI and SDI_v for errors in t_1 , t_2 , V_1 and V_2 was examined assuming variations of 1 s, 1 s, 50 mL and 50 mL, respectively. Table 7.1 shows the errors in SDI_v for these assumed variations which was calculated using the SDI_v definition in Eqn.(7.6).

Table 7.1 The effects of accuracy errors of the equipment on SDI=4.36.

Parameters	Error	Influence SDI _v =4.36±	% of SDI _v =4.36	% of SDI=3.00 *
T	1[°C]	0.00	0.00	1.00
dP	7[kPa]	0.00	0.00	1.67
R_M	$0.1 \times 10^{10}[\text{m}^{-1}]$	0.17-0.19	3.90-4.36	6.67
A_{MO}	2 mm	0.00	0.00	0.00
t_1	1[s]	0.22	5.14	1.00
t_2	1[s]	0.12	2.85	2.33
t_{15}	10[s]	0.00	0.00	0.67
V_1	50 mL/500 mL	0.52	11.95	12.33
V_2	50 mL/500 mL	+0.52, -0.58	11.95-13.20	12.33

* Calculated from Chapter 6 [7]

The results in Table 7.1 show that the SDI_v is not sensitive for a measurement error in T , dP and R_M . The SDI_v is more sensitive for errors in t_1 and t_2 than the time-based SDI. SDI_v is more sensitive for errors in measuring the time to collect the first sample t_1 than for the error in measuring the time to collect the second sample t_2 . From Table 7.1, we can conclude that the new fouling index SDI_v in general is less sensitive for errors.

7.3. Conclusions

Based on the SDI definition, a tool was developed to determine the required sample volumes $V_{1,2}$ based on the membrane diameter. The SDI value can also be calculated using Eqn. (2.1) along with a slide bar for a measured t_1 and t_2 when $t_f=15$ min. Based on the mathematical model that we developed in Chapter 4 [8], the standard SDI can be normalized to SDI^+ for the testing condition parameters T , dP and membrane resistance R_M using a developed line chart or slide wheel charts assuming cake filtration and 100 % particle retention. SDI can be normalized to SDI^+ for T , dP and R_M assuming different fouling mechanisms using a new line chart based on the measured parameters C and m .

A new fouling index, SDI_v , is the second fouling index developed at the University of Twente, 30 years after the MFI0.45. The SDI_v compares the initial flow rate to the flow rate after filtering a standard volume V_{f0} using MF membranes with an average pore size of $0.45 \mu\text{m}$. The SDI_v has a linear relationship with the particle concentration if the complete blocking mechanism is dominant during testing. SDI_v shows a more linear relationship to the particle concentration than the standard, time-based SDI. Furthermore, the mathematical model shows that SDI_v is independent of the testing parameters T and dP and less sensitive to variations in the membrane resistance. Experimentally, three membranes with different resistances were used to determine the standard SDI and SDI_v at a UF/RO desalination plant. $SDI/5\text{min}$ values were normalized to SDI^+ for the temperature and the membrane resistances. By normalizing the standard SDI values to SDI^+ , the effect of temperature and membrane type were eliminated. Moreover, the SDI_v is less susceptible for measurement errors and has a better linear relationship to the particle concentration compared to the standard SDI. To conclude, the SDI_v is a better index for determining the fouling potential of an RO feed than the standard SDI.

References

- [1] M. Mulder, Basic principles of membrane technology, 2 ed., Kluwer Academic Publishers, Dordrecht, The Netherlands, 2003.
- [2] A. Alhadidi, A.J.B. Kemperman, J.C. Schippers, M. Wessling, W.G.J. van der Meer, The influence of membrane properties on the Silt Density Index, Submitted to J. Membr. Sci., (2010).
- [3] J. Hermia, Constant pressure blocking filtration Laws - Application to power-low non-newtonian fluids, Trans IChemE, 60 (1982) 183-187.
- [4] A. Alhadidi, B. Blankert, A.J.B. Kemperman, J.C. Schippers, M. Wessling, W.G.J. van der Meer, Effect of testing conditions and filtration mechanisms on SDI, Submitted to J. Membr. Sci., (2010).
- [5] B. Blankert, B.H.L. Betlem, B. Roffel, Dynamic optimization of a dead-end filtration trajectory: Blocking filtration laws, J. Membr. Sci., 285 (2006) 90-95.
- [6] A. Alhadidi, A.J.B. Kemperman, J.C. Schippers, M. Wessling, W.G.J. van der Meer, Evaluate the fouling challenge in a RO/UF desalination plant using SDI, SDI⁺ and MFI, To be submitted (2010).
- [7] A. Alhadidi, B. Blankert, A.J.B. Kemperman, J.C. Schippers, M. Wessling, W.G.J. van der Meer, Sensitivity of SDI for the error in measuring the testing parameters, To be submitted (2010).
- [8] A. Alhadidi, A.J.B. Kemperman, J.C. Schippers, M. Wessling, W.G.J. van der Meer, Silt density index and modified fouling index relation, and effect of pressure, temperature and membrane resistance, Desalination, In press (2010).

CHAPTER 8

EVALUATING THE FOULING CHALLENGE IN A UF/RO DESALINATION PLANT USING THE SDI, SDI⁺ AND MFI

THIS CHAPTER HAS BEEN SUBMITTED TO PUBLICATION:

A. Alhadidi, A.J.B Kemperman, R. Schurer, J.C. Schippers, M. Wessling, and W.G.J. van der Meer, Evaluating the fouling challenge in a UF/RO desalination plant using the SDI, SDI⁺ and MFI, Desalination

SDI has no corrections for testing condition parameters such as the applied pressure, feed temperature and membrane resistance. Therefore, corrections were proposed for the SDI, resulting in a corrected fouling index SDI^+ . The new index SDI^+ was tested and the mathematical models were confirmed in this Chapter with a case study at the Evides UF/RO seawater desalination plant in the Netherlands.

The use of different membrane materials for the SDI test results in significantly different numerical values for the same water quality. The effects of the individual membrane resistance and the testing condition parameters on SDI were properly incorporated in the SDI^+ values according to practice experiments. Consequently, the SDI results of different membranes made from different materials could be compared. We have proven that the SDI results under different testing conditions can be normalized to the reference testing condition parameters and therefore developed a more reliable filtration index.

The plant was evaluated by performing the SDI, SDI^+ and MFIO.45 tests on-site under different operation regimes (coagulation, pH correction). It was found that the UF performance was good and SDI values were ~ 1 whereas MFIO.45 values were lower than 1 s/L^2 in general. The MFIO.45 shows the same tendency as the SDI in most cases. Storing the RO feed for one night in the feed tank increases the fouling potential of the RO feed.

8.1 Introduction

In this Chapter, the performance of an UF unit as RO pretreatment in removing the colloidal matter will be examined using the SDI test under different operation regimes. The effect of using different commercial membranes with a $0.45\ \mu\text{m}$ pore size for the SDI test will be studied as well. The SDI results will be normalized for the testing parameters and membrane resistance ("SDI⁺") using the developed model for the relation between the SDI and the MFI0.45 in Chapter 4 [1]. Besides that, the sensitivity of SDI for the particle concentration will be conformed experimentally.

8.1.1 Plant description

In the south-western part of the Netherlands, the seawater UF/RO demonstration plant is operated by Evides, a water supply company in the Netherlands. The site is located at the Oosterschelde as shown in Figure 8.1. The net desalinated water production capacity of the plant is $13.5\ \text{m}^3/\text{hr}$.

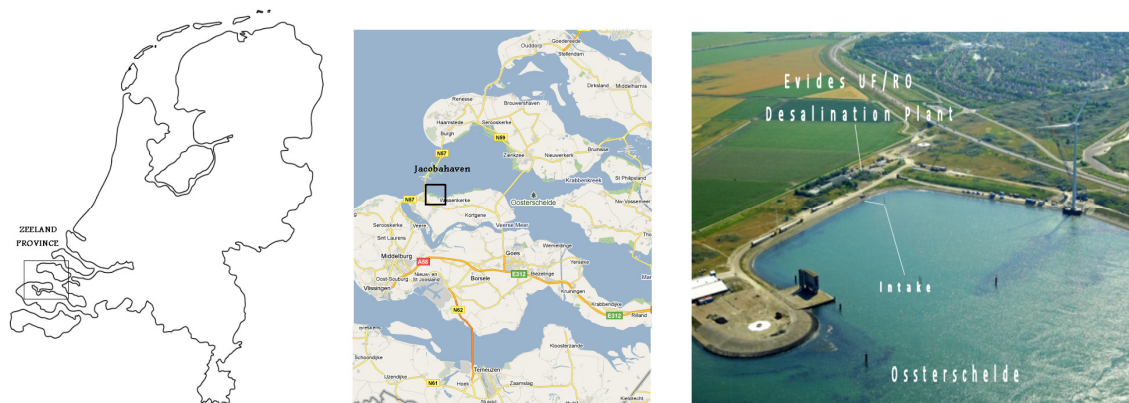


Figure 8.1. Location of Jacobahaven in Zeeland, the Netherlands.

Figure 8.2 shows the flowchart of the UF/RO demonstration plant. The seawater is pumped via an open intake to a buffer tank inside the plant. The raw water is filtered with a Micro-strainer $50\ \mu\text{m}$ followed by a optional coagulation and acidification process. The coagulant and the acid are added to the mixing tank. Both dosages are optional and to be applied according to actual raw water quality and resultant UF behavior. After the mixing step, the UF feed is collected in a buffer tank and then pumped to the UF. The UF unit contains Norit Seaguard UF membranes. UF permeate is collected in another buffer tank to be pumped to the RO unit. Part of the UF permeate is used for UF backwash (BW). Due to the BW discharge regulations, the BW water

should be treated through a sedimentation process after which it is partly recycled to the UF buffer tank.

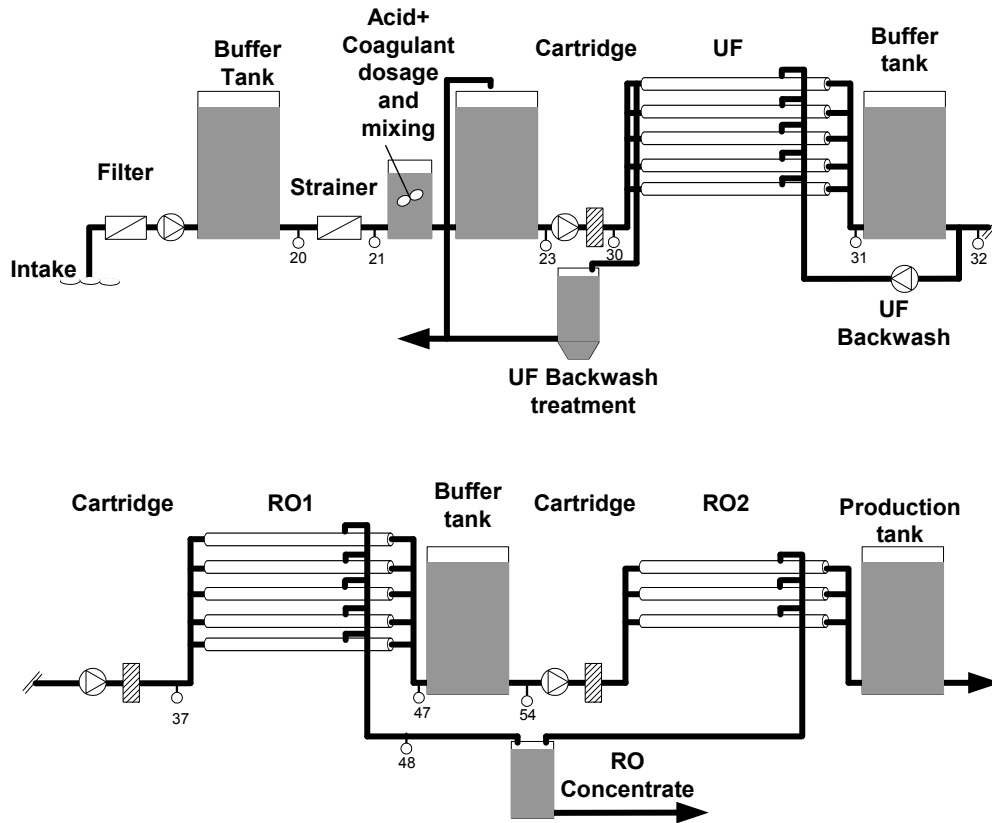


Figure 8.2. The flowchart of the Jacobahaven plant. The numbers indicate the sampling points used.

Two RO stages operate in the plant: one sea water RO for desalination and subsequently seasonally required additional brackish water RO for boron removal (Dow Filmtec). The RO permeate for the first RO stage is collected in a buffer tank in order to be pumped to the second stage. To secure the pumps and the membrane units, each feed tank is followed by cartridge filter.

For research and analysis purposes, more than 54 sampling points are fixed among the plant at different locations. The water samples for the SDI tests described here were collected in the sampling points shown in Figure 8.2.

8.1.2 Raw water characteristics

The plant faces a biological algae bloom challenge for three months during the spring season. During their active period, the algae produce a polymer material called Transparent Exopolymer Particles (TEP). TEP causes fouling and/or bio-fouling in UF and RO membrane

installations [2-5]. Figure 8.3 shows a large amount of foam generated by the algae close to the plant intake in May 2010.



Figure 8.3. Open intake of the Jacobahaven plant, showing the foam caused by algae.

8.2 Results and discussion

The Evides UF/RO plant operation will be described. The SDI test was performed at different locations in the plant using different membranes. The SDI results will be normalized for the testing condition parameters and the membrane resistance (resulting in the SDI^+ values). The performance of the UF unit in the Evides plant with regard to the permeability and transmembrane pressure will be discussed.

8.2.1 Evides UF/RO plant operation

The Evides UF/RO plant was operated with different regimes in terms of coagulation and pH due to the great variation in the raw water quality which will be discussed later on in this section. From experience, it is known that the spring period is the most critical operation period due to biological activity in the raw water. Several quality parameters are monitored among the plant such as turbidity, pH and temperature. This field work was carried out in the period 06/04/2010 to 12/05/2010. Figure 8.4 shows the raw water temperature for the periods 06-23/04/2010 and 11-12/05/2010 at sampling point 20 in Figure 8.2. The raw water temperature during the field work varied between 8 °C and 10 °C, with an average value of approximately 9 °C. The sharp fluctuations in the temperature are due to system start/stop sequences.

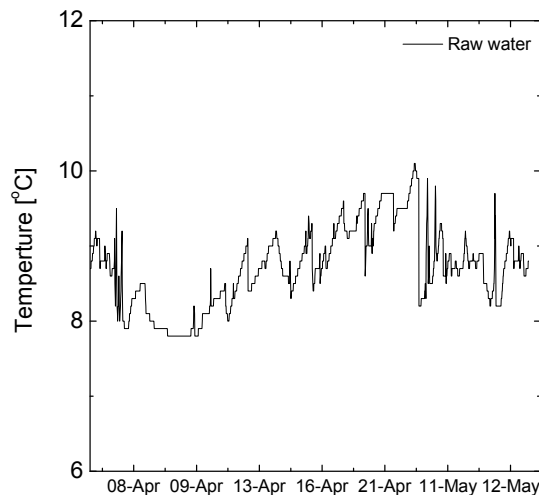


Figure 8.4. Jacobahaven raw water temperature in the period 06/04/2010 to 12/05/2010.

The raw water was filtered by a strainer to remove colloids larger than 50 μm . The turbidity of strained water was plotted in Figure 8.5. The turbidity varied between 30 FTU (Formazin

Turbidity Unit) and 5 FTU, with an average value over time of approximately 10 FTU. The fluctuations in turbidity are due to tidal currents (suspension), storm and system start/stop.

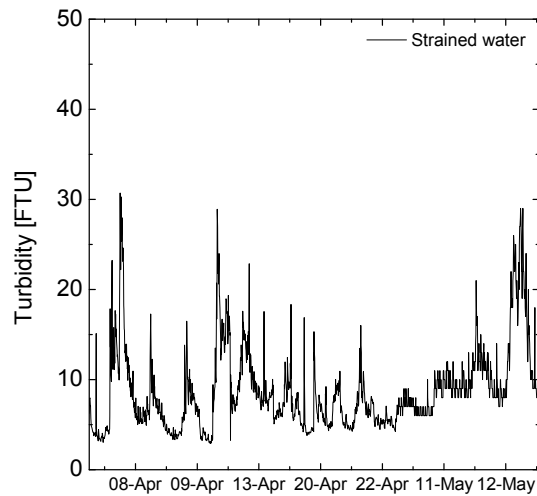


Figure 8.5. Strained water turbidity in the period 06/04/2010 to 12/05/2010.

If necessary, the water pH was adapted to the pH required for the coagulation process (Ferric pH 8) or to prevent RO scaling (pH 6.6) [6]. The plant was operated with Ferric during the field work. The raw water had a stable pH of 8 to 8.4 during the field work period. Nevertheless the water pH has been changed in order to study the effect of the pH on UF operation. The measured pH of the UF permeate was plotted in Figure 8.6.

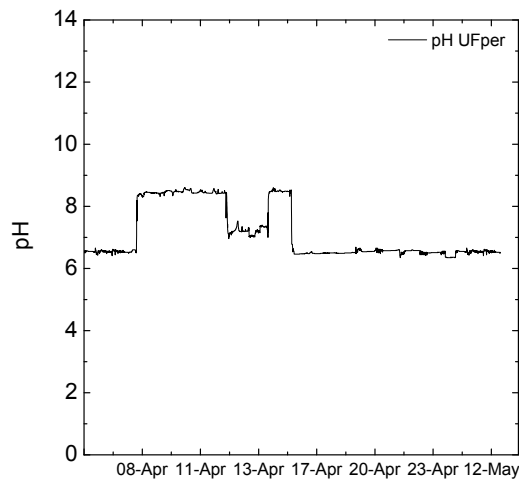


Figure 8.6. pH of the UF permeate in the period 06/04/2010 to 12/05/2010.

Figure 8.7 shows the coagulant and acid dosages (HCl) in the period 06/04/2010 to 12/05/2010. The operation regime was unstable during the field work period for several reasons: algae bloom resulting in extreme UF fouling, and accidental damages in some of the plant equipment. Different acid corrections and coagulant dosing were necessary to get to the optimum operation due to this variation in the raw water quality. The coagulant dosage was varied between 3.5, 2 and 1.5 g Fe/m³ depending on the UF fouling.

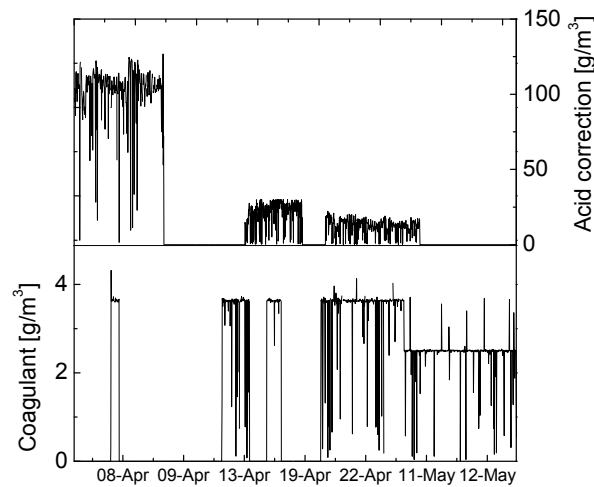


Figure 8.7. Coagulation and acid correction dosage in the period 06/04/2010 to 12/05/2010.

After the coagulant/acid mixing tank, the water was collected in the UF feed tank. The UF unit was operated in nearly constant flux mode. The UF performance was monitored continuously as permeability, transmembrane pressure (TMP) and flux, plotted in Figure 8.8.

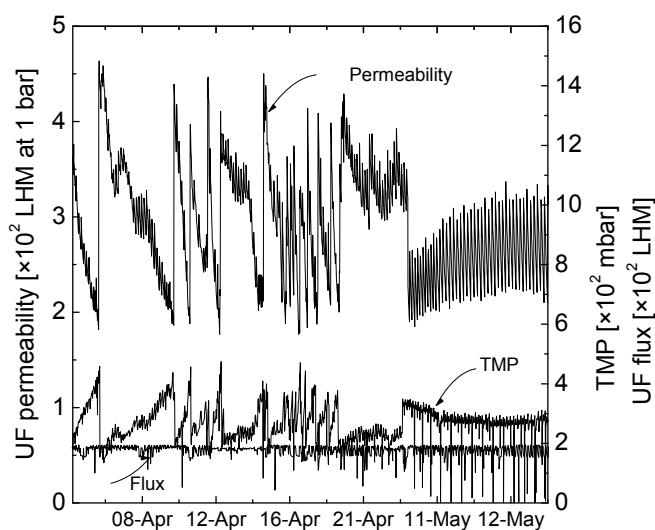


Figure 8.8. UF performance: permeability, transmembrane pressure (TMP) and flux in the period 06/04/2010 to 12/05/2010.

A Chemical Enhanced Backwash (CEB) cleaning using regular chemicals (HCl, NaOH and NaClO) was performed regularly to maintain a constant UF permeability. The CEB was performed at 200 LHM and 1 bar. During filtration, the UF transmembrane pressure starts at 120 mbar and ends at 400 mbar whereas the UF flux was maintained around 50-60 LHM.

8.2.2 SDI determination using different membranes

In the latest version of the ASTM standard, cellulose acetate/cellulose nitrate membranes are considered as the standard membranes to be used in an SDI test. However, 0.45 μm MF membranes can be obtained from several manufacturers, all with different properties and prepared out of various membrane materials. Table 2.1 listed the different membranes used in this study. These membranes differ in properties such as pore size distribution, porosity, surface charge, roughness, hydrophilicity and the cross-sectional morphology (depth filter, tracked-edge, spongy, or reinforced). The influence of membrane properties on the SDI was discussed in Chapter 3 [7]. It was suggested to use the membrane resistance as a “lump sum” parameter representative for the physical properties of the membrane.

For a comparison between the SDI values as obtained with the different membranes, a constant feed quality is necessary for all the SDI tests. For each SDI test with a 25 mm diameter membrane, around 6-7 L of feed water is consumed. In total 60 L is required for comparing the

full set of experiments. In order to assure a constant feed water quality, a feed tank (60 L) was batchwise filled with UF permeate within a short time (several minutes).

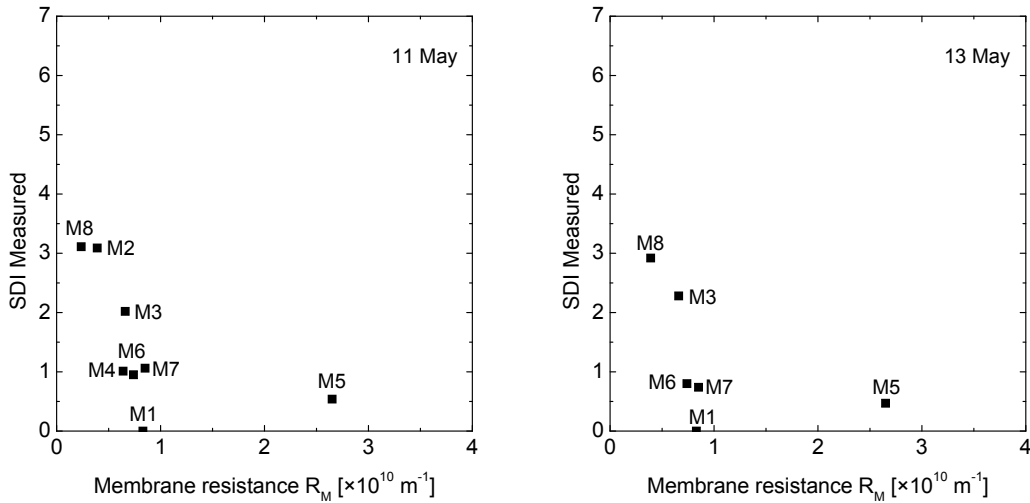


Figure 8.9. SDI of UF permeate with different membrane materials as measured on 11 May 2010 (left) and 13 May 2010 (right).

The SDI values for the UF permeate using different membranes on two different days were plotted versus the membrane resistance in Figure 8.9. It shows that an increase in membrane resistance results in a lower measured SDI value. During the 15 minutes an SDI test is lasting, the total volume that is filtered through the membrane depends on the flow rate. A higher specific membrane resistance decreases the flow through the membrane and as a result the accumulated fouling load on the membrane decreases. This results in a lower and distorted SDI value. One exception is the PVDF membrane (M1), which gives an SDI value of zero. This can be due to the hydrophilization of M1 by the membrane manufacturer, which decreases the membrane fouling rate and consequently lowers the obtained SDI value excessively [8]. Main conclusion from these experiments is that the measured SDI value is way too dependent on the chosen test membrane, and as such is an unreliable parameter to judge the fouling potential of an RO feed water.

8.2.3 Model validation

8.2.3.1 UF_{feed} diluted with UF_{permeate}

In this set of experiments, the UF feed was diluted with UF permeate in different ratios to obtain a range of different particle concentrations without affecting the initial water salinity. The

following UF feed volumes were diluted in 25 L of UF permeate: 25 mL, 50 mL, 100 mL, 200 mL and 500 mL. The SDI/MFI0.45 tests were performed with three different membranes (M4, M7 and M5) in parallel in order to compare the SDI values for different membrane resistances (low, average and high membrane resistance, respectively).

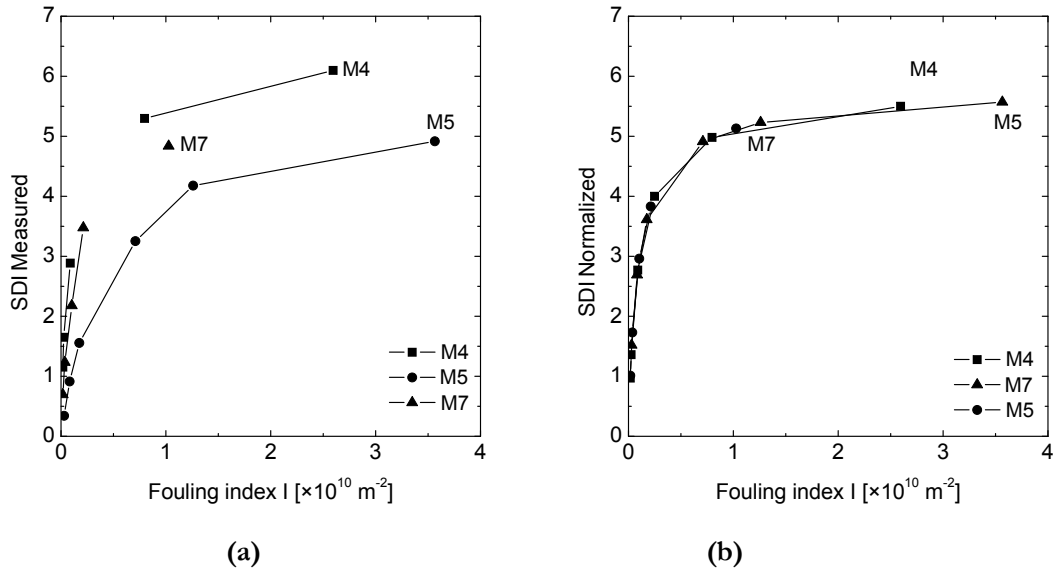


Figure 8.10. a: Measured SDI values b: SDI normalized for membrane resistance and testing condition parameters $T=10^\circ\text{C}$ and $\kappa=53600\mu\text{S}/\text{cm}$ (SDI^+).

Membranes M4, M7 and M5 have different membrane resistances (0.64×10^{10} , 8.50×10^{10} and $2.65 \times 10^{10} \text{ m}^{-1}$ respectively) which results in different SDI values as shown in Figure 8.10 (a). The measured SDI values for M4 are the highest whereas the measured SDI values for M5 are the lowest. Figure 8.10 (b) shows the SDI values when normalized for the membrane resistance and the testing condition parameters, using the SDI/MFI0.45 theoretical relationship and assuming a cake filtration mechanism. Normalizing the SDI helps in neutralizing the effects of the testing condition parameters and the membrane resistance. The normalized SDI values (SDI^+) were calculated using the reference testing conditions and membrane resistances in Table 3.1.

8.2.3.2 UF feed diluted with RO permeate

Another way for having a broad range of different colloidal concentration is by diluting the UF feed with RO permeate in different ratios. However, unlike with UF permeate dilution, this simultaneously decreases dramatically the salinity of the SDI feed water. SDI as a fouling index is related to the interaction between particles and the membrane, which is influenced by the water salinity and acidity. A high ionic strength of the test water may result in increasing SDI values [9].

Different UF feed volumes (25 mL, 50 mL, 100 mL, 200 mL, 300 mL and 1000 mL) were diluted in 25 l of RO permeate. The measured and normalized SDI values are plotted in Figure 8.11 a and b.

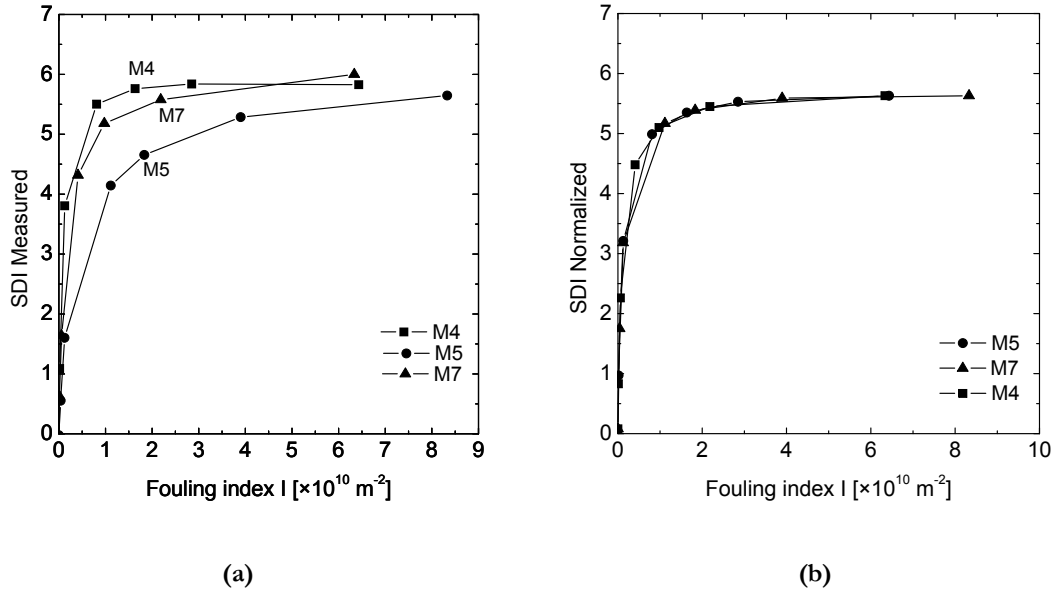


Figure 8.11. (a) Measured SDI values (b) SDI normalized for membrane resistance and testing condition parameters $T=10^\circ\text{C}$ (SDI^+).

Increasing the colloidal concentration leads to a higher SDI. Membrane M4 gives higher SDI values comparing to M7 and M5 because of the larger membrane resistance. Normalizing the SDI results for the membrane resistance and the condition testing parameters show less variations in the results in Figure 8.11(b).

Both Figure 8.10 and Figure 8.11 show that the use of different membrane materials results in different SDI values for the same water quality. The effects of the membrane resistance and the testing condition parameters on SDI were eliminated in the SDI^+ values. Consequently, the SDI results for different membranes made from different materials could be compared. We have proven that the SDI results under different testing conditions can be normalized to the reference testing conditions and consequently developed a more reliable filtration index, the SDI^+ .

8.2.4 UF performance under different operation regimes

The performance of the UF unit in removing particles was investigated by measuring the SDI and the MFI0.45. The tests were performed for UF permeate samples under different

operation conditions such as acid and coagulant dosing. Each result in this section is measured in triplicate using cellulose acetate membrane M7.

8.2.4.1 Influence of coagulation

The SDI and MFI0.45 results for the UF permeate under both conditions (with and without adding coagulant) were plotted in Figure 8.12 (a) and (b).

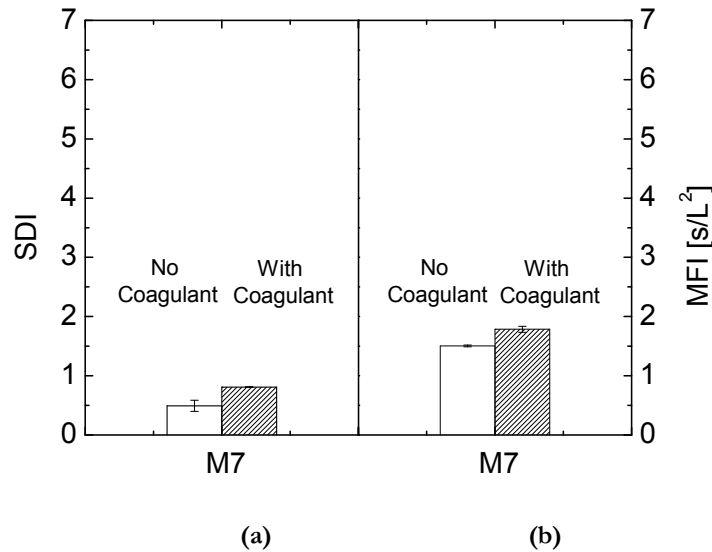


Figure 8.12. (a) SDI and (b) MFI0.45 values at 10 °C after the UF unit using cellulose acetate membrane M7 without and with coagulant dosing. Fe⁺³ 1 mg/L. 14 and 15 April.

Figure 8.12 (a) shows that dosing 1.5 mg/L coagulant to the UF feed leads to a slight increase in the SDI value of the UF permeate. Both SDI values are lower than 1 which indicates a good performance of the UF step in removing the particles. The MFI0.45 numbers shows same tendency as the SDI values. The increase of SDI and MFI0.45 values by adding coagulant can be due to residual coagulant which can pass the UF (TEP post coagulation). TEP post coagulation after the UF permeate can increase the particle size, which can lead to fouling of the MF membrane during the SDI measurement.

A number of parameters can reduce the removal efficiency of the coagulation step, such as the type of coagulant, coagulant concentration, water pH, residual time and the mixing efficiency [10-14]. In the following sections this will be assessed by additional SDI, MFI, and SDI+ measurements under several conditions of coagulation and pH (mixing regime, dosing point, dose).

8.2.4.2 Influence of acid addition

In this operation regime, only acid was added and no coagulant. The UF particle removal efficiency was examined with the SDI/MFI0.45 test. The pH of the UF feed dropped to 6.5 after adding the HCl in the mixing unit. In Figure 8.13 the results of the SDI and MFI0.45 measurements without and with acid dosing are given.

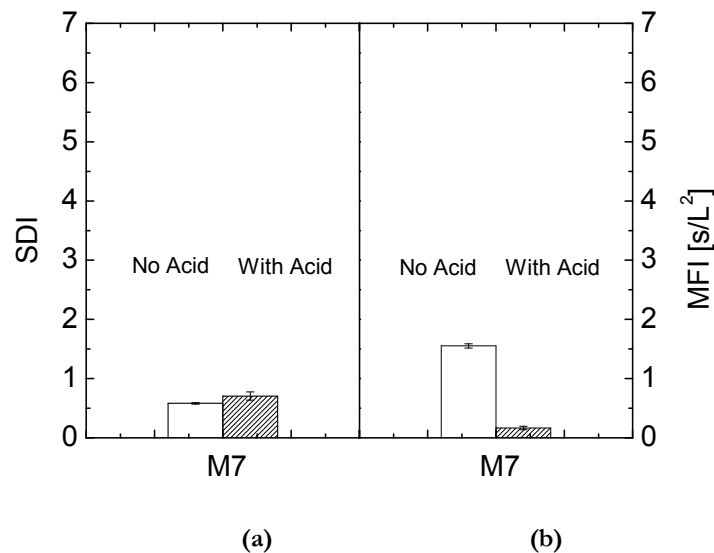


Figure 8.13. (a) SDI and (b) MFI0.45 values at 10 °C after the UF unit using cellulose acetate membrane M7 without and with acid dosing. pH 8.3, 6.3. Samples taken on 14 April 2010.

In general, the UF unit shows good performance and both SDI and MFI0.45 values were low. The minor decrease in the observed MFI0.45 values indicate an increase in the UF efficiency concerning particle removal when acid is added.

8.2.4.3 Influence of simultaneous coagulation and acid dosing

The raw water has a pH of 8.4 which is close to the optimum pH for Ferric as coagulant. The influence of the pH and the coagulation on the UF performance was examined by performing SDI/MFI0.45 tests. The results are plotted in Figure 8.14.

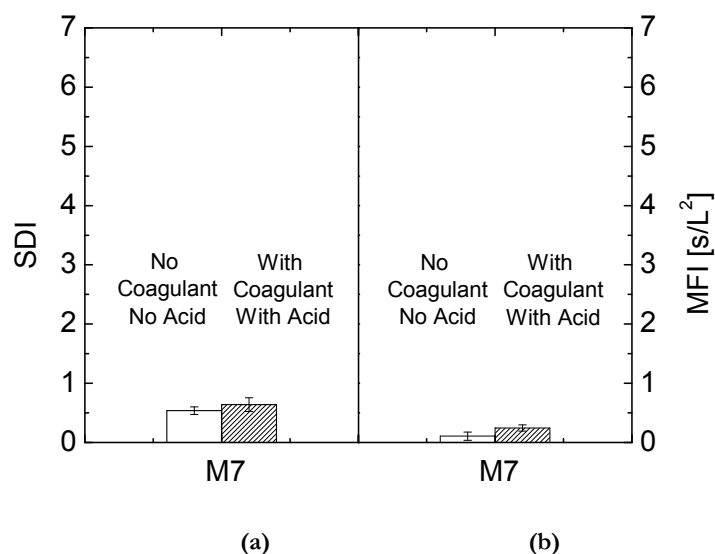


Figure 8.14. (a) SDI and (b) MFI0.45 values at 10 °C after the UF unit using cellulose acetate membrane M7 when both acid and coagulant are added. pH 8.5, Fe⁺³ 1mg/L. 14, 15 and 16 April.

Both the SDI and the MFI0.45 were below 1 in both cases. Due to the error margin of the data presented in Figure 8.12, Figure 8.13 and Figure 8.14, we can not draw a clear conclusion which regime can result in better UF performance.

8.2.4.4 Influence of the RO feed tank on the water fouling potential

The UF permeate is collected in the RO feed tank. The plant was not working continuously during the field work. The plant was not operated during the night, the weekend and during maintenance. Therefore, at such occasions the RO feed was stored for 14 hr during the night (from 6 pm to 8 am) in the buffer tank before pumping to the RO installation next morning. Two SDI/MFI0.45 tests were performed. The first test was performed for the fresh water in the tank at 6 pm. The second SDI test was performed the next morning at 7:30 am, just before operation of the plant started. The results are shown in Figure 8.15.

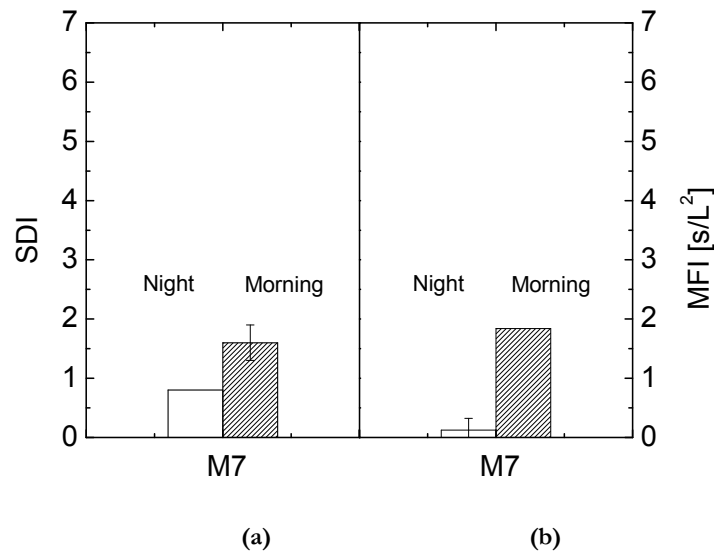


Figure 8.15. (a) SDI and (b) MFI0.45 values of the RO feed tank at 10 °C using cellulose acetate membrane M7 as measured at 6 pm ('night') and 7.30 am next morning ('morning') i.e. after being stagnant for 14 hours.

Both the SDI as well as the MFI0.45 results shows that storing the water in the RO feed tank for 14 hr results in an increase of the water fouling potential. Several factors influence the efficiency in removing the colloidal matter of the in-line coagulation such as pH, coagulant dosage, and mixing intensity [15, 16]. Coagulant passage through the UF is mainly a function of the solubility of the coagulant which is determined by pH and temperature [17]. Therefore, some residual coagulant can be present in the UF permeate and the coagulation might continue after passing the membrane [18]. Villacorte et al. investigated TEP removal across the Evides UF/RO plant. These TEP measurement showed that 60-80 % of the initial amount of TEP was present in the UF permeate [19]. This TEP and the coagulant stored in the RO feed tank for one night (14 hr) might result in post-coagulation of TEP after UF.

The effect of the TEP post-coagulation is temporary and only after a system restart, in regular operation the residence time in the RO feed tank is only ~0.5 hr.

8.2.5 Fouling potential at different locations in the plant

In this section, the Evides UF/RO plant will be scanned with SDI and MFI0.45 tests using the 0.45 µm cellulose acetate membrane M7. The measured SDI and MFI0.45 values at the different locations in the plant are shown in Figure 8.16. The fouling indices SDI and MFI0.45

were measured on two different days, May 11 and May 12, 2010. Due to the time constraints SDI and MFI tests for the UF and RO permeate were not carried out on May 12.

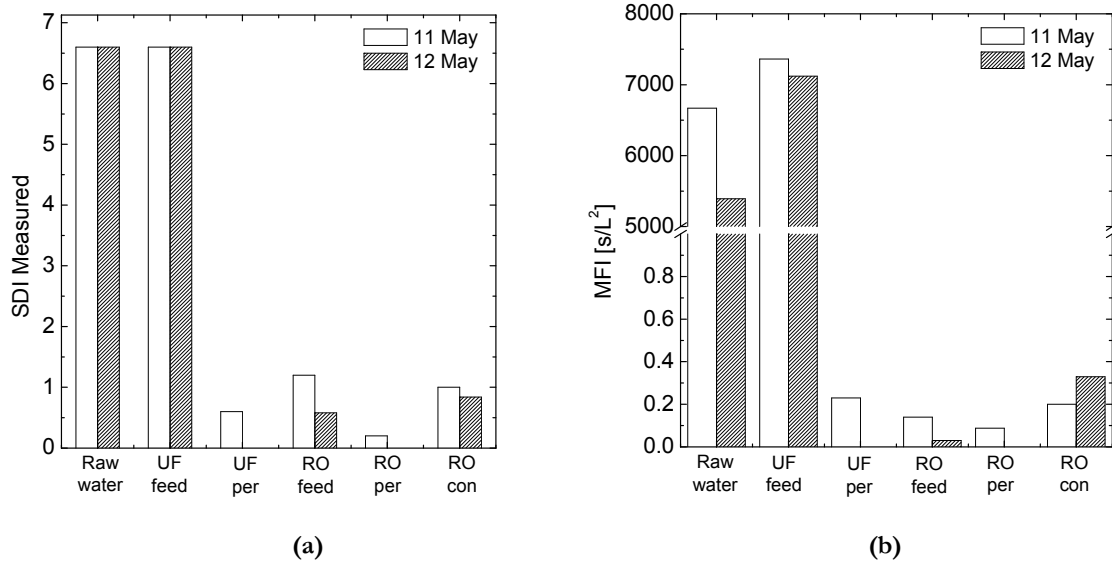


Figure 8.16. SDI (a) and MFI0.45 (b) values in the Evides UF/RO plant on 11 and 12 May 2010 using cellulose acetate membrane M7. The feed samples were taken at sampling points 20, 30, 31, 37, 47 and 48 in Figure 8.2. Per = permeate; con = concentrate.

Both the raw water as well as the UF feed samples have a high fouling potential ($SDI > 5$), and the plugging ratio (%P) was exceeding the 75 % limit during the measurement. The XIGA UF membrane has an MWCO of 150 kDa and can remove particles larger than 20 nm [20]. This results in a drop in the SDI to values below 1. The slight increase in SDI values in the RO feed can be explained by the effect of ongoing coagulation in the RO feed tank as discussed before (TEP post-coagulation). Due to the sensitivity of the SDI for errors at small values (< 1), drawing detailed conclusions from the individual SDI values of the UF permeate, RO feed, RO permeate and RO concentrate is not possible, except that the obtained range is in line with expectations and targets (< 3).

The MFI0.45 values show the same trend as the SDI. MFI0.45 values for raw water as given in Figure 8.16 (b) are 5000-6600 s/L². The MFI0.45 value increases to around 7500 s/L² due to addition of the coagulant to the UF feed. The UF membrane removes the particles and consequently the MFI0.45 value dropped down to values below 1. RO feed, concentrate and permeate have MFI0.45 values below 1 as well.

Figure 8.17 shows water samples from different locations in the UF/RO plant. The raw water has a high turbidity due to the algae bloom presents in the seawater. Adding the Ferric to the UF feed increases the turbidity and changes the sample color to more yellowish. It is impossible to see any particles in the RO feed due to the UF filtration step.

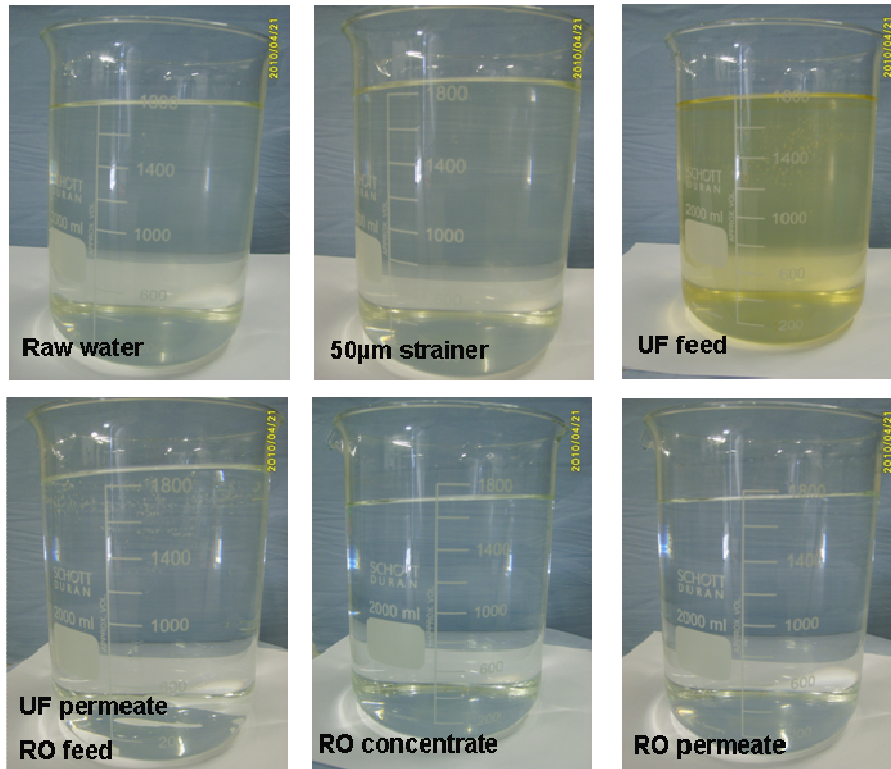


Figure 8.17. Water samples from different locations in the plant: raw water, after the 50 µm strainer, UF feed, RO feed, RO concentrate and RO permeate. Sampling points 20, 21, 30, 37, 48 and 47 in Figure 8.2, respectively.

8.2.6 Reduction in SDI values and MFI0.45

The results presented in Figure 8.16 (a) and (b) in section 4.4 were used to calculate the average reduction in the fouling potential of the UF permeate compared to the UF feed. The reduction in SDI and MFI 0.45 values is defined as the ratio of those values in permeate and feed $(UF_{feed} - UF_{permeate}) / UF_{feed}$. The particle removal values based on the average SDI was $90.86 \pm 5\%$ and that based on MFI0.45 $99.947 \pm 0.053\%$. The MFI0.45 shows higher particle reduction due to the sensitivity of the SDI for errors at these low values.

8.2.7 Total resistance at different sampling points

The SDI is defined as the change in the flow after 15 minutes during the constant pressure filtration test. The SDI can be considered as the change in the total resistance after 15 min. It may be useful to compare not only two slopes but to compare the whole resistance curves for a better understanding of the fouling behavior. The total resistance curve describes the history of the filtration test. The total resistance during the SDI and MFI0.45 tests were determined and plotted in Figure 8.18 for different sampling points (RO permeate, RO concentrate, RO feed and UF permeate).

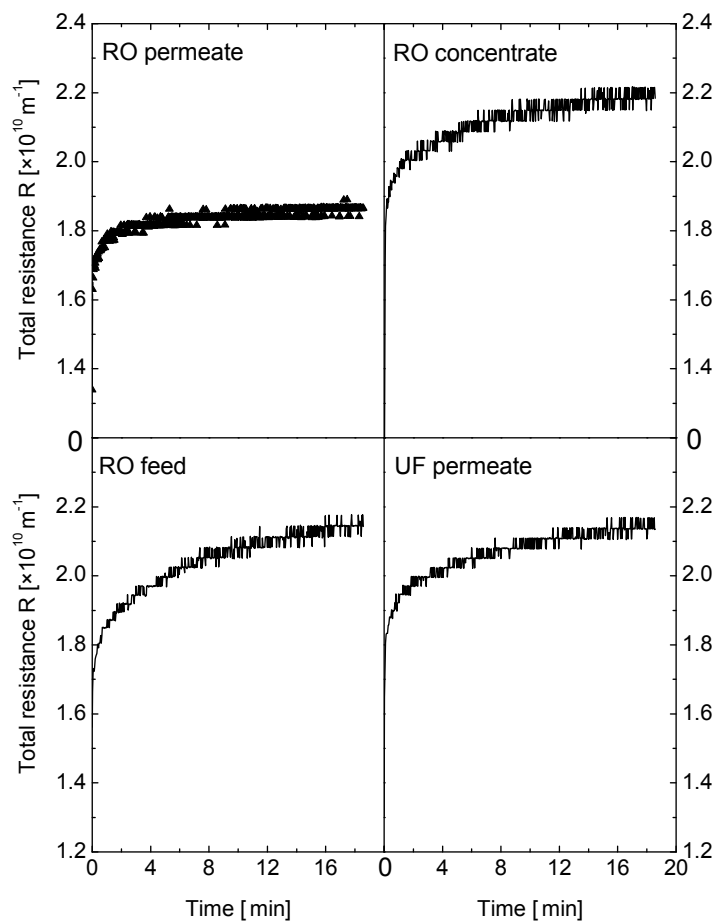


Figure 8.18. Total resistance (R) at different sampling points in the plant using cellulose acetate membrane M7 at 9-10 °C.

Figure 8.18 shows that the RO permeate has a small and constant slope after 1.5 min, which is an indication of a low fouling potential. Furthermore, the RO concentrate results in the highest total resistance ($2.2 \times 10^{10} \text{ m}^{-1}$ after 17 minutes). Some differences can be observed between the

resistance curves of the RO feed and UF permeate. The UF permeate curve has a more constant slope after 2 minutes compared to the RO feed curve. Moreover, the UF permeate reveals a higher total resistance in the first 2 minutes than the RO feed water. This difference can be explained by the additional coagulation due to remaining coagulant in the RO feed tank as was explained in 8.2.4.4.

In Figure 8.19, resistance curves of RO feed and RO concentrate are plotted for two different days. A difference in the fouling potential of RO feed and RO concentrate was observed between May 11 and May 12, 2010. This difference can be due to the effect of the high turbidity peak in the raw water on May 12. The RO unit is operated at a recovery of 40 %. Therefore, the particle concentration in the RO concentrate is 67 % higher than in the RO feed assuming 100 % particle retention. The resistance curves in Figure 8.19 (a) and (b) confirm that the RO concentrate has a higher fouling potential than the RO feed.

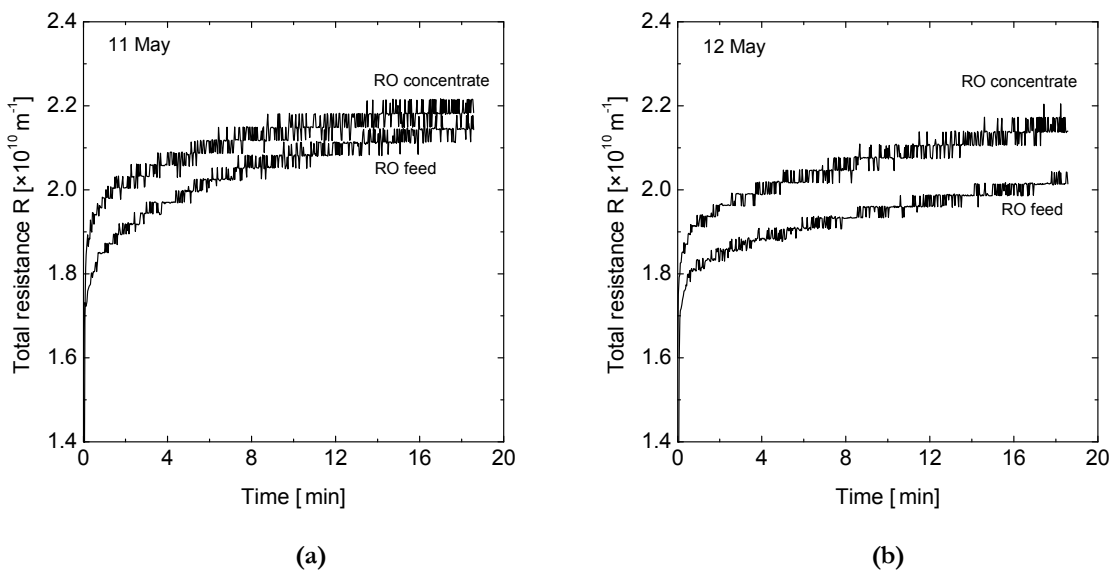


Figure 8.19. Total resistance (R) for RO feed and RO concentrate at different days using cellulose acetate membrane M7. (a) 11 May 2010; (b) 12 May 2010.

8.3 Conclusions

The results of this work show that when the SDI tests were carried out with different membranes, this resulted in a large variation in SDI values. This makes the standard SDI test an unreliable test. The effects of the membrane resistance and the testing condition parameters on SDI were eliminated in the SDI^+ values using the previously developed mathematical model. All SDI^+ values were established in practice and turned out to be independent of the type of membrane used for the SDI test. Consequently, the SDI results measured for different membranes made from different materials could be compared. We have proven that the SDI results under different testing conditions can be normalized to the reference testing conditions and consequently developed a more reliable filtration index, the SDI^+ .

In this work both the SDI as well as the MFI0.45 fouling tests were used to evaluate the performance of the Evides UF/RO sweater desalination demonstration plant in the Netherlands. This plant receives raw water from an open intake with great variation in the water quality. In the spring the plant faces an algae bloom challenge. As a result, the operation regime was unstable having its effect on the acid/coagulant dosage and the necessity of a CEB to deal with the high UF fouling.

The UF performance, concerning removal of the particles and the preparation of a high-quality RO feed water, was good. SDI values were lower than 1 when the tests were carried out with an ASTM standard membrane. The MFI0.45 results show the same tendency as the SDI in most cases, and were in general lower than 1 s/L^2 . The reduction in SDI and MFI0.45 values due to the UF pretreatment was $90.860 \pm 5\%$ and $99.947 \pm 0.053 \%$, respectively. Storing the water for 14 hours during the night in the RO feed tank, increased the fouling potential of the RO feed., most likely due to a post coagulation of TEP.

References

- [1] A. Alhadidi, A.J.B. Kemperman, J.C. Schippers, M. Wessling, W.G.J. van der Meer, Silt density index and modified fouling index relation, and effect of pressure, temperature and membrane resistance, *Desalination*, In press (2010).
- [2] T. Berman, Biofouling: TEP - a major challenge for water filtration, *Filtration & Separation*, 47 (2010) 20-22.
- [3] T. Berman, M. Holenberg, Don't fall foul of biofilm through high TEP levels, *Filtration & Separation*, 42 (2005) 30-32.
- [4] U. Passow, Transparent exopolymer particles (TEP) in aquatic environments, *Progress In Oceanography*, 55 (2002) 287-333.
- [5] E. Bar-Zeev, I. Berman-Frank, B. Liberman, E. Rahav, U. Passow, T. Berman, Transparent exopolymer particles: Potential agents for organic fouling and biofilm formation in desalination and water treatment plants, *Desalination*, 3 (2009) 136-142.
- [6] C.J. Gabelich, T.I. Yun, B.M. Coffey, I.H.M. Suffet, Effects of aluminum sulfate and Ferric chloride coagulant residuals on polyamide membrane performance, *Desalination*, 150 (2002) 15-30.
- [7] A. Alhadidi, A.J.B. Kemperman, J.C. Schippers, M. Wessling, W.G.J. van der Meer, The influence of membrane properties on the Silt Density Index, Submitted to *J. Membr. Sci.*, (2010).
- [8] N.A. Hashim, F. Liu, K. Li, A simplified method for preparation of hydrophilic PVDF membranes from an amphiphilic graft copolymer, *J. Membr. Sci.*, 345 (2009) 134-141.
- [9] A. Alhadidi, B. Blankert, A.J.B. Kemperman, J.C. Schippers, M. Wessling, W.G.J. van der Meer, Sensitivity of SDI for the error in measuring the testing parameters, To be submitted (2010).
- [10] S.G. Salinas Rodriguez, M.D. Kennedy, A. Diepeveen, H. Prummel, J.C. Schippers, Optimization of PACl dose to reduce RO cleaning in an IMS, *Desalination*, 220 (2008) 239-251.
- [11] A. de la Rubia, M. Rodriguez, V.M. Leon, D. Prats, Removal of natural organic matter and THM formation potential by ultra- and nanofiltration of surface water, *Water Research*, 42 (2008) 714-722.
- [12] H.-H. Cheng, S.-S. Chen, S.-R. Yang, In-line coagulation/ultrafiltration for silica removal from brackish water as RO membrane pretreatment, *Separation and Purification Technology*, 70 (2009) 112-117.
- [13] K. Konieczny, M. Bodzek, A. Kopec, A. Szczepanek, Coagulation-submerge membrane system for NOM removal from water, *Desalination*, 200 (2006) 578-580.
- [14] K. Konieczny, D. Sakol, J. Plonka, M. Rajca, M. Bodzek, Coagulation-ultrafiltration system for river water treatment, *Desalination*, 240 (2009) 151-159.
- [15] M.E. Walsh, N. Zhao, S.L. Gora, G.A. Gagnon, Effect of coagulation and flocculation conditions on water quality in an immersed ultrafiltration process, *Environmental Technology*, 30 (2009) 927-938.
- [16] C. Guigui, J.C. Rouch, L. Durand-Bourlier, V. Bonnelye, P. Aptel, Impact of coagulation conditions on the in-line coagulation/UF process for drinking water production, *Desalination*, 147 (2002) 95-100.
- [17] S.A.A. Tabatabai, S.I. Gaulinger, M.D. Kennedy, G.L. Amy, J.C. Schippers, Optimization of inline coagulation in integrated membrane systems: A study of FeCl₃, *Desalination and Water Treatment*, 10 (2009) 121-127.
- [18] N.N. Li, A.G. Fane, W.S.W. Ho, T. Matsuura, *Advanced Membrane Technology and Applications*, Wiley & Sons, Inc., New Jersey, 2008.
- [19] L.O. Villacorte, M.D. Kennedy, G.L. Amy, J.C. Schippers, The fate of transparent exopolymer particles (TEP) in seawater UF-RO system: A pilot plant study in Zeeland, The Netherlands, *Desalination and Water Treatment*, 13 (2010) 109-119.

[20] G. Pearce, Introduction to membranes: Manufacturers' comparison: part 2, Filtration & Separation, 44 (2007) 28-31.

CHAPTER 9

SUMMARY AND OUTLOOK

9.1. Summary

Reverse osmosis (RO) and nanofiltration (NF) membrane systems are widely used in the desalination of water. However, fouling phenomena in these systems remains a challenge. Four main different fouling types are identified: 1) Particulate fouling due to suspended and colloidal matter, 2) Biofouling due to adhesion and subsequent growth of bacteria, 3) Organic fouling due to organic compounds and 4) Scaling due to precipitation of sparingly soluble compounds. Silt Density Index (SDI) testing is a widely-accepted method for estimating the rate at which colloidal and particle fouling will occur in water purification systems when using RO or NF.

During the SDI test the time required to filter a fixed volume of water through a standard microfiltration membrane at a constant given pressure is measured. The difference between the initial time and the time of a second measurement after 15 minutes (after silt built-up) results in the SDI value. The ASTM describes this test as a standard test for RO fouling potential due to particles. According to the standard, the applied pressure is $207 \pm 7 \text{ kPa}$ ($30 \pm 1 \text{ psi}$). The water temperature must remain constant ($\pm 1^\circ \text{C}$) throughout the test.

In practice, the SDI is used most often and has been applied worldwide for decades. From a practical point of view, the SDI for fine hollow fiber RO feed water preferably must be lower than 3. A pretreatment method such as UF therefore has to guarantee an RO feed water with an $\text{SDI} < 3$. An SDI test is one of the criteria in designing new desalination plants and has to be performed on the RO feed water. SDI is a useful tool to monitor the efficiency of the RO pretreatment in removing the particles presents in the raw water. The main advantage of the SDI test is that the test is simple to execute even by non-professionals. The SDI test is used to choose and design RO pretreatment processes. The SDI has an economical value since it is mentioned as a condition in the pretreatment process contract.

Although the SDI test is widely used, there is growing doubt about the value of the SDI test as a predictive tool for RO membrane fouling. These doubts consist of two factors: 1) the relation between the SDI value and the performance of the RO unit, and 2) the reproducibility and accuracy of the SDI test.

Limitations: In chapter 3, the influence of membrane properties on the SDI value is investigated. Eight commercial '0.45 μm ' membrane types made of different materials and by different manufactures (PVDF, PTFE, Acrylic copolymer, Nitro Cellulose, Cellulose Acetate, Nylon 6,6, and Polycarbonate) were used to measure the SDI.

Three samples were randomly chosen from each membrane type (same lot), and several membrane properties were studied (pore size distribution, pore shape, surface and bulk porosity, thickness, surface charge, contact angle and surface roughness). SDI values for an artificial feed, composed of a solution of α – alumina particles 0.6 μm , were determined. The characterization of these membranes shows variation between the membranes used in this study (M1-M8), and within a batch of one membrane type. Substantial differences were found in SDI values for different types of membrane filters used.

The variations are attributed to differences in properties of the membranes used.

Improvements: In chapter 4 a mathematical relation between SDI and MFI_{0.45} has been developed, assuming that cake filtration is the dominant filtration mechanism during the tests. Based on the developed mathematical relation and experiments with a model feed water of α -aluminum particles (0.6 μm), it could be demonstrated that the SDI depends on pressure, temperature and membrane resistance. The effect of temperature and membrane resistance explains to a large extend the erratic results from the field. In chapter 5, mathematical models were developed to study the effect of temperature and applied pressure on the SDI value under different fouling mechanisms. The fouling mechanisms are described by the relationship between the specific filtrated volume w and the total resistance R . A significant variation in the SDI value was observed mathematically as a result of differences in temperature and membrane resistance for the same water quality. The sensitivity of the SDI for variations in the testing parameters theoretically increases when the relation between w and R is stronger.

The SDI increases with an increase in the feed temperature and the applied pressure. The SDI value decreases when membranes with a high resistance are used. These effects were confirmed experimentally. In chapter 6, the in chapter 4 and 5 developed mathematical models were used to investigate the sensitivity of SDI for the following types of errors: errors due to inaccurate lab or

field equipment, systematic errors, and errors resulting from artifacts and personal observations and experience. The mathematical results were also verified experimentally.

The allowable ASTM variation in the membrane resistance (R_M) is responsible for a deviation in SDI between 2.29 and 3.98 at a level of $SDI_O=3$. Besides that, a 1 second error in measuring the time to collect the second sample t_2 results in a ± 0.07 variation at $SDI_O=3$. The artifacts and personal experience also influence the SDI results. The total error in measuring SDI can be equal to ± 2.11 in the field and only ± 0.4 in the lab at the level of $SDI_O=3$. Furthermore, several recommendations are proposed based on these theoretical results and our personal experience.

This study demonstrates the sensitivity of the SDI for errors in R_M and the accuracy of the equipments, and explains the difficulties in reproducing SDI results for the same water.

A **lternatives:** Assuming cake filtration and 100% particle rejection, the SDI can be normalized to the SDI^+ based on a mathematical model developed in chapter 4 and 5. In chapter 7 and based on these the mathematical relations, a line chart and slide wheel charts are developed to normalize SDI to SDI^+ for the testing conditions and the membrane resistance. Reference membrane resistance and reference testing conditions were proposed.

A new fouling index was developed to estimate the RO feed fouling potential. The SDI_v compares the initial flow rate to the flow rate after filtering the standard volume V_f using MF membranes with an average pore size of $0.45 \mu m$. SDI_v has a linear relationship to the particle concentration if complete blocking is the dominant fouling mechanism during the test. The mathematical model shows that SDI_v is independent of the testing parameters and membrane resistance. The mathematical model and the experimental results show that SDI_v eliminates most of the above mentioned SDI disadvantages. SDI_v is the second fouling index developed at the University of Twente, 30 years after the MFI0.45.

In chapter 8, the new index SDI^+ was tested and the mathematical models were confirmed in a case study at the Evides UF/RO seawater desalination plant in the Netherlands. The use of different membrane materials for the SDI test results in significantly different numerical values for the same water quality. The effects of the individual membrane resistance and the testing condition parameters on SDI were properly incorporated in the SDI^+ values according to practice experiments. Consequently, the SDI results of different membranes made from different

materials could be compared. We have proven that the SDI results under different testing conditions can be normalized to the reference parameters and therefore developed a more reliable filtration index. The plant was evaluated by performing the SDI, SDI⁺ and MFI0.45 tests on-site under different operation regimes (coagulation, pH correction). It was found that the UF performance was good and SDI values were ~ 1 whereas MFI0.45 values were lower than 1 s/L^2 in general. The MFI0.45 shows the same tendency as the SDI in most cases. Storing the RO feed for one night in the feed tank increases the fouling potential of the RO feed water.

9.2. Outlook

The characterization of MF 0.45 μm membranes shows variation between the membranes used in this study (M1-M8), and within a batch of one membrane type. Substantial differences were found in the SDI values for the different types of membrane filters used. The differences in the SDI results for the same feed water are attributed to differences in properties of the membranes used. By taking the right membrane any desired SDI value can be get (i.e. the tests determined the outcome). For a reliable SDI determination in the field, there is a very strong need for standardized membrane filters having uniform and constant properties.

A higher membrane resistance results in dramatically lower SDI values. The indirectly formulated guideline by ASTM for an acceptable range for membrane resistance R_M (between $0.86 \times 10^{10} < R_M < 1.72 \times 10^{10} \text{ m}^{-1}$) is far from adequate. The allowable variations in membrane resistance are responsible for values of the SDI between 2.29 and 3.98 at a level of SDI=3.

It is therefore recommended:

- to narrow the resistance range to e.g. $1.29 \times 10^{10} \text{ m}^{-1} \pm 10 \%$ ($1.16 \times 10^{10} < R_M < 1.42 \times 10^{10}$); this range results in deviations of ± 0.25 in SDI value (at SDI₀ =3);
- to correct the SDI for temperature and membrane resistance.

The effects of temperature and variations in membrane resistance on SDI explain to a large extend the erratic results reported in practice. Reference testing condition and reference membrane resistance were defined, and proposed line and wheel charts are recommended to be used for normalizing SDI to SDI⁺.

The following advices and recommendations based on the theoretical results and personal experience can be provided. Besides the ASTM protocol, we believe that these recommendations are important for reliable and reproducible SDI results.

It is strongly recommended to use fresh SDI feed water. The SDI feed water should not be stored close to a heat source. The SDI setup should be cleaned and flushed well with clean water (RO production) before the test. After that, the SDI setup should be flushed with the SDI feed water to remove the residual clean water and guarantee a constant feed water quality from $t=0$ on. The pressure gauge and the filter holder should be positioned at the same level. Accurate equipment is needed for reliable SDI results. The membrane should not be touched with the experimenter's hands; tweezers should be used. The support plate has to be with fine bulge and low resistance. It is recommended to use an adjusted filter holder with a relief air valve. It is recommended to place filter paper under the membrane. t_0 should be between 25-50 s, where t_0 is the time to collect 500 mL of clean water under a pressure difference of 91.4-94.7 kPa. Preferably, new membranes should be used which are stored in a dry and covered place.

The mathematical model shows that SDI_v is independent of the testing parameters and membrane resistance. The mathematical model and the experimental results show that SDI_v eliminates most of the above mentioned SDI disadvantages

The new volume-based SDI_v test forms a new platform for further investigation on the reliability of the fouling index SDI_v. Furthermore, the need for standardized membrane filters having uniform and constant properties is another gate for further developments.

خلاصة

محددات وتطوير و بدائل لمؤشر كثافة الطمي SDI في انظمة التحلية بالتناضح العكسي RO تعتبر تقنية التناضح العكسي RO احد اهم واحداث الطرق لتحلية المياه المالحة. اغشية التناضح العكسي البلومرية المستخدمة لها القدرة على انتاج ماء تقارن نقاوته بنقاوة الماء المقطر وبقدرة على احتجاز مانسبته 99% من الاملاح وخالي من الاحياء المجهرية والفيروسات. تمتاز هذه التقنية بقله استهلاكها للطاقة مقارنة مع الطرق التقليدية للتقطير وكونها صديقة للبيئة. يقابل هذه المميزات بعض العيوب اهمها قابلية الاغشية للانسداد Fouling. يمكن تصنيف انواع الانسدادات الى: انسدادات بيولوجية Bio-fouling و انسدادات ملحية وتكلس Scaling و انسدادات بالعوالق Particulate fouling. وعلية يجب ان تمر المياه قبل ضخها الى اغشية التناضح العكسي بعمليات معالجة Pre-treatment لغرض خفض قابلية هذه المياه على الحاق الضرر باغشية التناضح العكسي وخفض انتاجيتها.

لاختبار كفاءة عملية المعالجة السابقة للاغشية يتم تنفيذ اختبارات القدرة على السداد. من هذه الاختبارات ووسعها انتشارا مؤشر كثافة الطمي (SDI) Silt density index. هذا المؤشر اعتمد بواسطة هيئة المقاييس الامريكية ASTM-4189-07 كاختبار معياري لقياس قدة الماء على سد انظمة التناضح العكسي من اغشية Membrane وعوازل Spacers. يتم حساب هذا المؤشر من التغير في الجريان ويعتمد على ضخ عينة الماء تحت ضغط ثابت dP مقداره 207 kPa خلال غشاء ذو مسامات متوسط حجمها $0.45 \mu m$. حيث يتم حساب الوقت لجمع العينة الاولى 500 ml ثم حساب الوقت لجمع العينة الثانية 500 ml بعد 15 دقيقة من بدء الاختبار. يمتاز هذا المؤشر بسهولته وامكانية تنفيذه من قبل الاشخاص الغير محترفين. وبالرغم من اعتماد هذا الاختبار عالميا كمؤشر لقدرة الماء على سد انظمة التناضح العكسي RO الا ان به بعض العيوب تم رصدها منها عدم كفاءة المؤشر في توقع الانسداد في انظمة التناضح العكسي RO نتيجة الفوارق بين الاغشية المستخدمة في المؤشر MF membrane وفي انظمة التناضح العكسي RO membrane. كذلك فان المؤشر ينفذ تحت ضغط ثابت عمودي على سطح الاغشية فيما انظمة التناضح العكسي تعمل بنظام هيدروليكي مختلف يعتمد الجريان الثابت الموازي لسطح الاغشية. علاقة مؤشر كثافة الطمي SDI مع تركيز العوالق Particle concentration في الماء ليست خطية ولا يوجد عوامل تصحيح للمؤشر للحرارة T. كما ويتأثر المؤشر باختلاف خواص اغشية الاختبار باختلاف موادها وتصنيعها. وعلية في هذا العمل تم مايلي:

دراسة الاختلاف في خصائص الاغشية المستخدمة في المؤشر باختيار اغشية مصنعة من مواد مختلفة ومن مصانع مختلفة ودراستها من حيث: حجم وشكل المسامات المسامية وكثافة مادة البوليمر والسماكة و خشونة السطح الشحنة المتراكمة على السطح واخيرا الممانعة لجريان الماء النظيف. تم اعتماد ممانعة الاغشية R_M كمؤشر عمومي على بقية الخواص. كما تم دراسة التغيرات على مستوى العلبه من نفس المصنع باختيار ثلاثة عينات من نفس العلبه اعلى-وسط-اسفل وداسة الاختلافات بينها ومن ثم ربط ممانعة الاغشية R_M بنتائج المؤشر المستنبطة من اختبارات مخبرية لمياه صناعه معده لهذا الغرض في المختبر. تتكون المياه الصناعية من ماء مقطر وحببيبات المنيوم بحجم متوسط $Alumina \text{ particles } \alpha _0.6 \mu m$ اوضحة النتائج وجود اختلافات تصل الى 50% بين خواص الاغشية المصنعة من مواد مختلفة وكذلك اختلافات تصل الى 20% بين الاغشية في نفس العلبه. كما تم ملاحظة علاقة قوية بين قيمة المؤشر SDI وممانعة الغشاء R_M المستخدم للاختبار.

ربط مؤشر كثافة الطمي SDI بمؤشر اخر يعرف بالمؤشر المعدل لقياس قابلية الماء لسد الاغشية Modified Fouling Index (MFI) من خلال علاقة رياضية فرض فيها آلية ترسب العوالق وتكوين طبقة رغويات على سطح الغشاء Cake filtration. استخدمت العلاقة الرياضية في دراسة تاثير درجة حرارة الماء والضغط وممانعة الاغشية على مؤشر كثافة الطمي. كما تم معمليا اثبات هذه العلاقات الرياضية من خلال عدد من التجارب باستخدام الماء الصناعي. اثبت في الجزء عليما ان مؤشر كثافة الطمي SDI يتاثر باضطراد بارتفاع الضغط dp ودرجة الحرارة T كما يتاثر عكسيا بارتفاع ممانعة الاغشية R_M . توضح هذه العلاقة من خلال تاثير عوامل ظروف الاختبار على كمية العوالق الواصلة الى سطح الاغشية Fouling load في زمن ثابت قدرة 15 دقيقة. بناء على العلاقات الرياضية المستنبطة تم اقتراح معادلات رياضية تم ترجمتها الى ادوات تستخدم يدويا لغرض تصحيح مؤشر كثافة الطمي SDI^+ واستخدامه تحت حرارة وضغط وممانعة اغشية مختلفة ومقارنة النتائج.

كما تمت دراسة تاثير آليات مختلفة لتموضع العوالق على وفي الاغشية Fouling mechanisms. حيث تم دراسة اربع حالات مختلفة. وتم بناء نموذج رياضي محاكي لدراسة تاثير الآليات المختلفة على نتيجة مؤشر كثافة الطمي SDI. كما تم دراسة تاثير عوامل الاختبار من حرارة T وضغط dp وممانعة الاغشية R_M على نتائج مؤشر الطمي SDI تحت آليات التموضع المختلفة كلا على حده. كما تم ايضا اقتراح وسائل لتصحيح الانحراف في قراءة مؤشر كثافة الطمي SDI^+ الناتج من تاثير عوامل الاختبار وممانعة الاغشية تحت كل الية.

في جزء اخر من هذا العمل تم دراسة حساسية مؤشر الطمي للاخطاء الشائعة عند تنفيذ الاختبار في المختبر وفي الحقل Error analysis. كما تم افتراض معدلات لدقة الادوات المستخدمة Accuracy ودراسة تاثير هذا التغير في نتائج مؤشر كثافة الطمي SDI. كما تم سرد امثله على الاخطاء البشرية الناتجة عن الاستنباط من خلال الخبره في المختبر ومن خلال تجارب اخرين مذكوره في المراجع Personal experience. الاخطاء الغير منضوره Artifacts والاطفاء الممنهجه Systematic error تم دراستها وحصر جوانب منها.

اقترح بديل لمؤشر كثافة الطمي سمي بمؤشر كثافة الطمي المبني على فلتره حجم ماء ثابت SDI_v . حيث تم تعريفه بالفارق في الجريان بين عينة تؤخذ في بداية الاختبار وعينة ثانية تؤخذ بعد فلتره كمية ماء تقدر بـ 14.58 في حالة استخدام غشاء بقطر 47 mm تعدل كمية الماء بناء على قطر الغشاء المستخدم. يحل المؤشر الجديد كثير من مشاكل المؤشر السابق من خلال: عدم تاثيره باعوامل الاختبار من حرارة وضغط وقله تاثيره بتغير خواص الاغشية المستخدمة في الاختبار. يأمل بان يعتمد هذا التحديث في مؤشر كثافة الطمي وان يستخدم كبديل فعلي في الحقل.

اعتمدت محطة التخلية المختبرية الواقعه في جنوب غرب هولندا بمنطقة ياكوباهافن Jacobahaven RO/UF كمحطة للدراسة الحقلية للبحث. حيث تم اختبار فعالية عمليات المعالجة السابقة لاغشية التناضح العكسي RO من خلال تنفيذ اختبار مؤشر كثافة الطمي SDI في عدة مواقع في المحطة وتحت ظروف تشغيل مختلفة. كما تم اختبار ادوات التصحيح لنتائج المؤشر لعوامل الاختبار المختلفة وممانعة الاغشية SDI^+ . حيث وجد ان عمليات المعالجة UF السابقة لاغشية التناضح العكسي تعمل بكفاءة كما تم اثبات صحة التوقعات بتاثير ممانعة الاغشية على نتائج مؤشر الطمي. كما اثبتت طرق التصحيح فعالية كبيره في تعديل الانحراف في النتائج الناتجة عن استخدام اغشية في الاختبار بممانعات مختلفة وتحت درجة حرارة مختلفة.

Nederlandse samenvatting

Omgekeerde osmose (RO) en nanofiltratie systemen worden vaak gebruikt voor de ontziltling van water. Vervuiling van de membranen bij deze processen is echter een probleem. Er wordt daarbij onderscheid gemaakt in vier verschillende vervuilingsmechanismen: 1) Deeltjesvervuiling door opgeloste deeltjes en colloïdale stoffen, 2) Bio-vervuiling door adhesie en groei van bacteriën, 3) Organische vervuiling door organische componenten en 4) Scaling door precipitatie van slecht oplosbare stoffen.

De 'Silt Density Index' (SDI) test is een veelgebruikte test om te voorspellen hoe snel colloïdale- en deeltjesvervuiling optreedt bij waterzuivering met RO en NF. De SDI meet de benodigde tijd voor de filtratie van een vast volume water door een standaard microfiltratiemembraan bij een constante druk. Het verschil tussen de initiële tijd en de tijd na 15 minuten resulteert in de SDI waarde. De ASTM beschrijft deze test als standaard test voor potentiële vervuiling bij RO door deeltjes. Volgens de standaard is de opgelegde druk 207 ± 7 kPa (30 ± 1 psi). De watertemperatuur moet gedurende de test constant (± 1 °C) blijven.

In de praktijk wordt de SDI wereldwijd al decennia gebruikt. Om praktische redenen moet de SDI van RO voedingswater voor kleine holle vezels lager zijn dan 3. Een voorbehandeling van het RO water met bijvoorbeeld UF moet dus water opleveren met een SDI lager dan 3. De SDI test is een van de criteria voor RO voedingswater als een nieuwe ontziltingsinstallatie ontworpen wordt. Bij de verwijdering van deeltjes in het water voor de RO stap is de SDI is een goede indicator voor om de efficiëntie van de voorbehandeling van het voedingswater voor de RO te monitoren. Het grote voordeel van de SDI test is dat het makkelijk uit te voeren is, ook door niet professionals. De test wordt gebruikt om een RO voorbehandeling te kiezen en te ontwikkelen. Economisch heeft de SDI ook waarde, aangezien deze als conditie genoemd wordt in het contract over het voorbehandelingsproces. Alhoewel de test wereldwijd gebruikt wordt, is er toenemende twijfel over de waarde van de SDI test als voorspellende waarde voor de vervuiling van RO membranen. De twijfel bestaat uit twee factoren: 1) De relatie tussen de SDI waarde en de prestatie van de RO unit, 2) de reproduceerbaarheid and betrouwbaarheid van de SDI test.

Beperkingen: In hoofdstuk 3 wordt de invloed van de membraaneigenschappen op de SDI waarden onderzocht. Acht verschillende commerciële $0.45 \mu\text{m}$ membranen van verschillende

materialen en van verschillende fabrikanten (PVDF, PTFE, Acrylisch copolymeer, nitrocellulose, cellulose acetaat, nylon 6.6, en polycarbonaat) zijn gebruikt om de SDI te bepalen.

Van elk membraan zijn drie willekeurige monsters gekozen waarvan verschillende membraan eigenschappen zijn bestudeerd (poriegrootteverdeling, porievorm, oppervlakte- en bulkporositeit, dikte, oppervlaktelading, contacthoek en oppervlakteruwheid). De SDI is bepaald voor een artificiele voeding bestaand uit $0.6 \mu\text{m}$ α -aluminium deeltjes. De karakterisering van de membranen laat verschil zien tussen de type membranen die gebruikt zijn tijdens deze studie (M1-M8) maar laat ook verschil zien in één batch van één membraan type. Grote verschillen in de SDI waarden zijn gevonden voor de verschillende typen membranen die gebruikt zijn. De variatie is toe te schrijven aan de verschillende eigenschappen van de gebruikte membranen.

Verbeteringen: In hoofdstuk 4 wordt een wiskundige relatie gelegd tussen de SDI en MFI_{0.45} ervan uitgaande dat de koekfiltratie het dominante filtratiemechanisme is. Met behulp van deze mathematische relatie en experimenten met de model oplossing met α -aluminium deeltjes kan aangetoond worden dat de SDI afhankelijk is van druk, temperatuur en membraanweerstand. Het effect van de temperatuur en membraanweerstand op de SDI kan voor een groot deel de afwijkende resultaten in de praktijk verklaren.

In hoofdstuk 5 zijn mathematische modellen ontwikkeld om het effect van temperatuur en druk bij verschillende vervuilingmechanismen te bekijken. De vervuilingmechanismen worden beschreven door het specifiek gefiltreerde volume, w , en de totale weerstand, R . Een significant verschil in de SDI waarde is waargenomen als resultaat van het verschil in temperatuur en membraanweerstand bij dezelfde waterkwaliteit. De gevoeligheid van de SDI voor variaties bij test parameters is theoretisch groter als de relatie tussen w en R groter is.

Uit het model volgt dat de SDI hoger wordt bij hogere voedingstemperatuur en druk terwijl de SDI waarde lager wordt als de membranen een hogere weerstand hebben. Deze resultaten zijn experimenteel bevestigd.

In hoofdstuk 6 zijn de theoretische modellen uit hoofdstuk 4 en 5 gebruikt om de gevoeligheid van de SDI voor fouten te onderzoeken. De volgende fouten zijn onderzocht: fouten door gebruik van verkeerde lab- of veldapparatuur, systematische fouten en fouten die ontstaan door artefacten en persoonlijke observatie en ervaring. Deze theoretische resultaten zijn eveneens experimenteel bevestigd.

De toelaatbare ASTM variatie in de membraanweerstand, R_M is verantwoordelijk is voor de variatie in de SDI van 2.29 tot 3.98 bij een SDI_0 van 3. Daarnaast heeft een fout in de filtratietijd van 1 seconde bij de tweede filtratie, t_2 , een fout van ± 0.07 tot gevolg bij een SDI van 3. De artefacten en de persoonlijke ervaring van de onderzoeker hebben ook invloed op de SDI. De totale fout kan oplopen tot ± 2.11 in het veld en ± 0.4 in het laboratorium bij een SDI van 3. Gebaseerd op de theoretische resultaten, alsmede op persoonlijke ervaringen worden enkele aanbevelingen gegeven.

Dit onderzoek laat zien dat de SDI gevoelig is voor fouten in de R_m en de betrouwbaarheid van de apparatuur. Het verklaart ook de moeilijkheid met de reproduceerbaarheid van de SDI voor hetzelfde water.

Alternatieven: Als koekfiltratie en 100% deeltjes reëctie verondersteld worden, kan de SDI genormaliseerd worden naar de SDI^+ . De SDI^+ is gebaseerd op het ontwikkelde model in hoofdstuk 4 en 5. In hoofdstuk 7 wordt vanuit de mathematische relaties een ‘line chart’ en ‘slide wheel chart’ ontwikkeld om de SDI te normaliseren naar SDI^+ voor de gegeven testcondities en de membraanweerstand. De referentieweerstand en referentie testcondities worden hier ook geïntroduceerd.

Een nieuwe vervuilingindex is ontwikkeld om de vervuilingspotentie van voedingswater op RO te voorspellen. Dit is de SDI_v , welke de initiële stroomsnelheid vergelijkt met de stroomsnelheid na filtratie van het standaard volume V_f met MF membranen met een gemiddelde poriegrootte van $0.45 \mu\text{m}$. SDI_v is lineair afhankelijk van de deeltjesconcentratie als volledige blokkering het dominante vervuilingmechanisme is. Het mathematisch model laat zien dat de SDI_v onafhankelijk is van de testomstandigheden en de membraanweerstand. Zowel het mathematisch model alsmede de uitgevoerde experimenten laten zien dat de SDI_v de meeste bij de SDI optredende nadelen niet heeft. Dertig jaar na de ontwikkeling van de MFI0.45 is de SDI_v de tweede vervuilingindex die aan de Universiteit Twente is ontwikkeld.

In hoofdstuk 8 worden correcties voor de SDI voorgesteld resulterende in een gecorrigeerde vervuilingindex SDI^+ . Het mathematische model van deze index is bevestigd door een praktijkstudie uitgevoerd bij de Evides UF/RO zeewater ontziltingsfabriek in Nederland. Het gebruik van verschillende membraanmaterialen voor de SDI test resulteert in significant verschillende waarden bij dezelfde waterkwaliteit. De effecten van de variatie in individuele

membraanweerstand van de membranen en de variatie in testomstandigheden op de SDI waarden zijn eenduidig verwerkt in de SDI⁺. Als zodanig konden de SDI resultaten van verschillende resultaten vergeleken worden. Wij hebben bewezen dat de SDI resultaten bij verschillende testomstandigheden genormaliseerd kunnen worden naar de referentie parameters, en daarmee is de index een betrouwbaardere en flexibelere index geworden. De ontziltingsfabriek is geëvalueerd door ter plaatse SDI, SDI⁺ en MFI0.45 metingen uit te voeren onder verschillende omstandigheden (coagulatie, pH correctie). De UF prestatie was goed en de SDI waarden waren ~ 1 terwijl de MFI0.45 waarden lager dan 1 s/L^2 waren. In de meeste gevallen laat de MFI0.45 dezelfde trend zien als de SDI. Opslag van de RO voeding gedurende de nacht in de voedingstank verhoogt de vervuilingspotentie van het RO voedingswater.

Nomenclature

A_M	Membrane area [m ²]
A_{M0}	Reference membrane area 13.4×10^{-4} [m ²]
C	Scaling factor proportional to the foulants concentration
dP	Applied pressure [Pa]
dP_o	Reference applied pressure 207 [kPa]
I	Fouling potential index (Cake filtration constant) [m ⁻²]
J	Flux [m ³ /m ² s bar]
J_o	Initial flux [m ³ /m ² s bar]
m	Fouling mechanism parameter (0, 1, 1.5 and 2)
MFI	Modified Fouling Index [s/m ⁶] or [s/L ²]
n	Number of data points
$\%P$	Plugging ratio [%]
$\%P_v$	Volume-based plugging ratio [%]
R	Total Resistance [m ⁻¹]
R_c	Specific cake resistance (Cake filtration constant) [m ⁻²]
R_M	Membrane resistance [m ⁻¹]
R_{M0}	Reference membrane resistance 1.29×10^{10} [m ⁻¹]
R_i	Total resistance at data point i
SDI	Silt Density Index [%/min]
SDI_o	Reference Silt Density Index=3 [%/min]
SDI_5	Silt Density Index for $t_f=5$ min [%/min]
SDI_v	Volume based Silt Density Index [%/m]
SDI^+	Normalized Silt Density Index [%/min]
s	Operating strategy parameter (0, 1 and 0.5)
t_f	Elapsed filtration time 15 [min] or 900 [s]
t_{ga}	Minimum slope in the relation t/V versus V [s/m ⁶]
t_o	Time to collect V_o of RO product [s]
$t_{1,2}$	Time to collect the first and second sample [s]
T	Temperature [°C]
T_o	Reference temperature 20 [°C]
V	Filtered volume [m ³]
V_{f0}	Average standard filtrated volume [m ³]
$V_{1,2,C}$	Sample Volume [m ³]
$w_{R,A,V}$	Fouling potential [m]
w	Filtrated state [m]
w_i	Local accumulated filtrated volume at data point i

Greek letters

μ	Viscosity, [Pa.s]
μ_{20}	Water viscosity at T_o °C [Pa.s]
K	Conductivity [S.m ⁻¹]
γ	Difficulty of operation due to fouling

Acknowledgements

(وَوَصَّيْنَا الْإِنْسَانَ بِوَالِدَيْهِ إِحْسَانًا حَمَلَتْهُ أُمُّهُ كُرْهًا وَوَضَعَتْهُ كُرْهًا وَحَمَلُهُ وَفِصَالُهُ ثَلَاثُونَ شَهْرًا ۖ حَتَّىٰ إِذَا بَلَغَ أَشُدَّهُ وَبَلَغَ أَرْبَعِينَ سَنَةً قَالَ رَبِّ أَوْزِعْنِي أَنْ أَشْكُرَ نِعْمَتَكَ الَّتِي أَنْعَمْتَ عَلَيَّ وَعَلَىٰ وَالِدَيَّ وَأَنْ أَعْمَلَ صَالِحًا تَرْضَاهُ وَأَصْلِحْ لِي فِي دُرِّيَّتِي ۖ إِنَِّّي كُنْتُ مِنَ الْمُسْلِمِينَ) الاحقاف آية 14

الحمد لله اولا واخيرا. اشكر نعمته علي بان فتح لي طريق العلم استقي من انهاره بفضلله وجود كرمه واستغفره ان انا قصرت في الاخلاص بعلمي لوجهه الكريم.

أهدي عملي المتواضع الى روح من أدين له بكل الفضل بعد الله سبحانه وتعالى والدي. كما اتقدم بعظيم الشكر والامتنان لوالدتي التي ألمتها كثيرا بغربتي وأقلقتها بهمومي واحوالي. كما اشكر دعم اخي محمد و زوجتي واولادي داعيا الله سبحانه ان يعينني على رد الجميل لهم جميعا. كما اشكر من اعماق قلبي اصدقائي في انسخدي (وسيم السقاف, مهند علوان, ماجد العماد, ابوجاسم محمد واخوه احمد) كما واشكر زملائي في الدكتوراه (اشرف حدوش, محمد مرسى, وسام أسعد) وكل من لم اذكره بالاسم.

I would like to express my deep and sincere gratitude to my promoter, Prof. W.G.J. van der Meer, Head of Membrane Process Technology group, Faculty of Science and Technology, University of Twente for believing in me. His wide knowledge and his logical way of thinking have been of great value for me. His understanding, encouraging and personal guidance have provided a good basis for the present thesis.

I am deeply grateful to my supervisor, Dr. A.J.B. Kemperman of the Membrane Process Technology group, Faculty of Science and Technology, University of Twente, for his detailed and constructive comments, and for his important support throughout this work.

I would like to express my sincere gratitude to Prof M. Wessling, Head of the Membrane Technology Group, Faculty of Science and Technology, University of Twente, for the support of my Ph.D study and research, for his patience, motivation, enthusiasm, and immense knowledge.

I wish to express my warm and sincere thanks to Prof. J. Schippers, Prof. in Water Technology, who gave me important guidance during my first steps into desalination studies. His ideals and concepts have had a remarkable influence on my entire career.

My sincere thanks also goes to Dr. B. Blankert, Norit-X-Flow B.V., for his valuable advice and friendly help. His extensive discussions around my work and interesting ideas and explorations have been very helpful for this study.

My warm thanks are due to Ir. L. Broens, Dr. H. Futselaar, Ir. F. Spenkelink (Norit, X-Flow), Prof. M. Kennedy (UNESCO-IHE) and R. Schurer (Evides) for all their scientifically and technical support.

My great thanks to my English teacher Mrs Catherine Ann Lombard for her kind help during the writing of my thesis. I would like to acknowledge Alexander Bismarck of the Polymers and Composites Engineering Group at Imperial College London (Great Britain) for his technical support on the zeta potential measurements, as well as the Physics of Complex Fluids Group at the University of Twente (Enschede, the Netherlands) for there technical assistance on the AFM. During this work I have collaborated with many colleagues for whom I have great regard, and I wish to extend my warmest thanks to all those in the Membrane Technology Group who have helped me with my work.

This work was scientifically and financially supported of Vitens and Norit Process Technology B.V./X-Flow B.V. Part of this work is carried out in the framework of the InnoWATOR subsidy regulation of the Dutch Ministry of Economic Affairs (project IWA08006 ‘Zero Chemical UF/RO System for Desalination’).

To the spring of my life.

Abdulsalam